

NIST NCSTAR 1-6

Federal Building and Fire Safety Investigation of  
the World Trade Center Disaster

# Structural Fire Response and Probable Collapse Sequence of the World Trade Center Towers

(Chapter 7- Appendix B)

John L. Gross  
Therese P. McAllister



# Chapter 7

## STRUCTURAL RESPONSE OF MAJOR TOWER SUBSYSTEMS TO AIRCRAFT IMPACT DAMAGE AND FIRE

---

### 7.1 INTRODUCTION

Prior to conducting the analysis of the global structural response of each tower, major structural subsystems were analyzed to provide insight into their behavior within the WTC global system<sup>1</sup>. The three major structural subsystems, the core framing, a single exterior wall, and full tenant floors, were analyzed separately for their response to impact damage and fire. The hat truss was not analyzed separately as its structural behavior did not require significant reductions in model complexity for the global analysis. The component analyses provided a foundation for these large, nonlinear analyses with highly redundant load paths by determining component behavior and failure modes and enabling a significant reduction in finite element model complexity and size. While the component models used preliminary estimates of elevated temperatures, the major subsystem models used final estimates of impact damage and elevated temperatures determined from the aircraft impact analysis and the fire dynamics and thermal analyses.

The capacity of each subsystem to sustain loads for the imposed damage and elevated temperatures was evaluated. The isolated subsystem models lacked the restraint and load paths to other subsystems found in the global analysis. Even so, the isolated subsystem response was useful for refining the global models and interpreting subsystem behavior in the global system. For instance, when a column buckled in the isolated core subsystem model, the only load path available to carry that column's load was the floor system within the core structure. However, in the global structure, the hat truss at the top of the core would transfer loads to other core columns or the exterior walls, assuming the connections between the core columns and hat truss remained intact.

### 7.2 CORE SUBSYSTEM

The core subsystem in the WTC towers was designed to carry gravity loads, which included the weight of the structure, equipment, furnishings, and occupants. The core system was not designed to carry lateral wind loads. The core columns were 3 stories in length (36 ft) and were either box columns or wide flange columns. At the aircraft impact floors, box columns transitioned to wide flange columns as loads and member sizes decreased with height. Column connections used either welded or bolted splice plates and were designed for compressive loads only; tensile, shear, or moment load transfer between columns was not intended. The core floor slab was typically 4.5 in. normal weight concrete that was composite with the floor beams through shear studs. The core floor was supported by wide flange beams with either a simple shear connection or a moment connection to the core columns.

---

<sup>1</sup> All information and data related to the design and construction of the WTC towers were obtained from contract drawings provided to NIST by The Port Authority of New York and New Jersey. Refer to NIST NCSTAR 1-2A for a complete description of the WTC structural system and an index of all structural drawings.

It is important to note that in the global structure, the core floors provided a secondary load path for load redistribution between the core columns. The primary load path for load redistribution was through the hat truss to adjacent columns. If columns were severed or a column or hat truss connection failed under tensile loads, the floors above the damage area provided the load redistribution between columns.

The isolated core models provided insight into expected behavior for situations where the hat truss was not able to redistribute loads. It also provided insight into the effects of impact damage and thermal weakening over time of affected areas of the core structure.

### 7.2.1 Model and Method of Analysis

Isolated core models extended from Floor 89 to Floor 106 for WTC 1 and from Floor 73 to Floor 106 for WTC 2, shown in Figs. 7-1(a) and (b), and did not include the hat truss, which extended from Floor 107 to the top of each building. The models included core columns and floor beams and slabs. Floor slabs were modeled as membrane elements with a relatively coarse mesh, which resulted in approximate slab openings for elevators and mechanical shafts. The meshing did not affect the floor's ability to provide a load path between columns. For the purposes of the isolated core model, only the floor beams with partial moment connections were included. It was assumed that simple shear connections were not capable of transferring significant loads between columns. At the base of the models, vertical springs were provided to represent the stiffness of columns below the model. The core subsystem model included large deflection, temperature-dependent material properties with plasticity and creep for all structural framing and plastic buckling behavior for columns.

The core subsystem was first analyzed for stability under gravity loads. The structural impact damage and gravity loads were applied to the core subsystem for all four damage cases, WTC 1 Cases A and B and WTC 2 Cases C and D (see Chapter 5). Impact damage was modeled by removing severed core columns and damaged floor areas. The gravity loads included dead load, superimposed dead load, and service live load (25 percent of design live load). The use of 25 percent of design live load as the service live load is discussed in NIST NCSTAR 1-2.

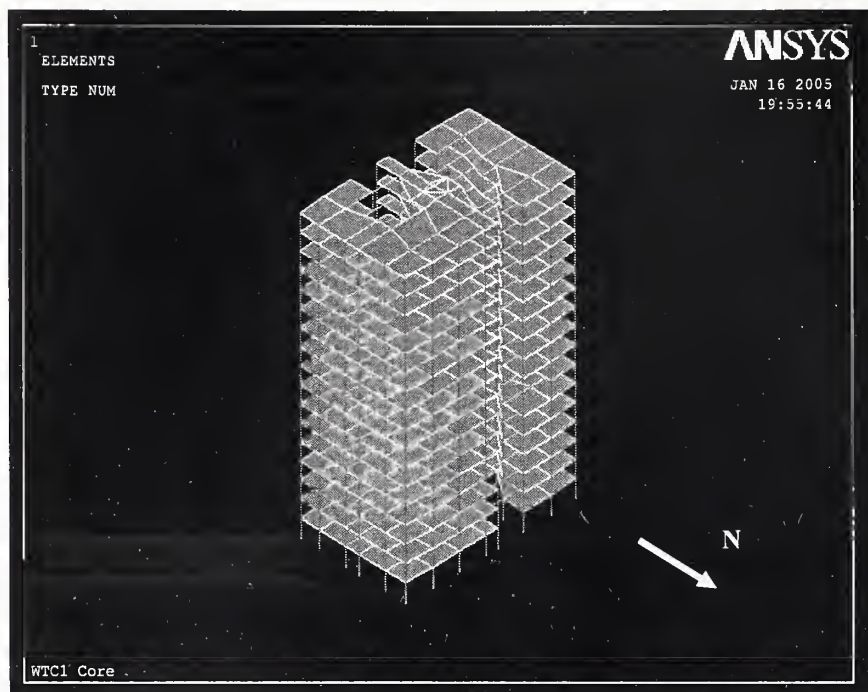
The WTC 1 isolated core model was stable for Case A structural damage and applied gravity loads. The isolated core model solution did not converge for WTC 1 Case B structural impact damage, which had more severed columns than Case A. The core structure was not able to tolerate the imposed damage without shedding some load to the exterior walls. For the WTC 2 isolated core model to reach a stable solution under Case C structural damage and gravity loads, horizontal restraints were required in the east and south directions at each floor to represent the lateral restraint provided by the office area floors and the exterior framed tube. Without the horizontal restraints, the WTC2 core model tilted significantly to the southeast due to the severed columns in that corner of the core. The isolated core model did not converge for WTC 2 Case D structural impact damage, which had more severed columns than Case C.

Each isolated core model was subjected to two temperature conditions as follows:

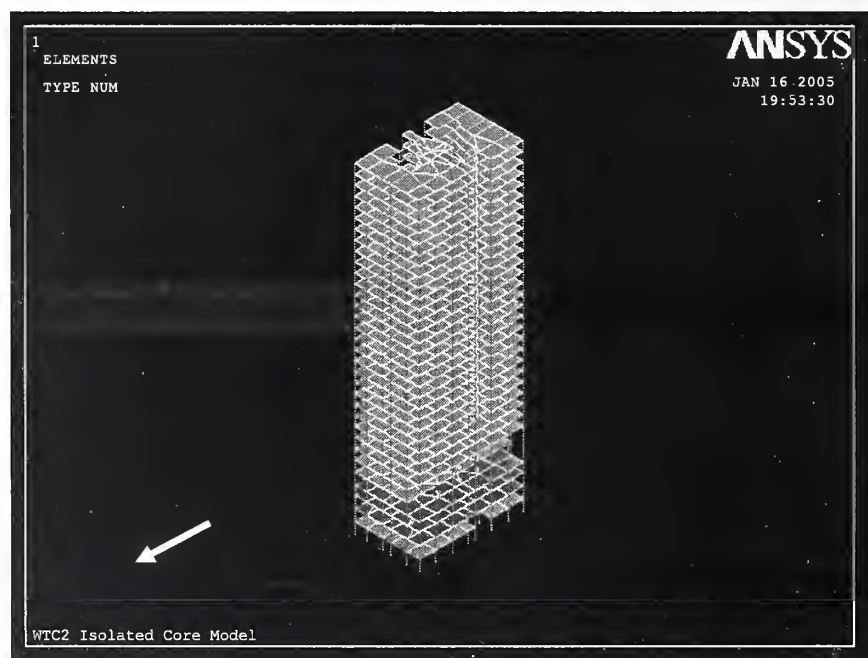
- WTC 1 (Case A impact damage) was subjected to Case A and Case B temperature histories
- WTC 2 (Case C impact damage) was subjected to Case C and Case D temperature histories

Case B and Case D impact damage could not be used for the isolated core models as no stable solution was obtained. Instead, for WTC 1, Case A impact damage was used for both Case A and Case B temperature histories and, for WTC 2, Case C impact damage was used for both Case C and Case D temperature histories. This approach allowed for comparison of the differences between Case thermal loads for the same impact damage for each tower.

Temperature histories were input as nodal temperatures at each node in the structural model that was subject to heating. The temperatures predicted in the structural members depended on the extent of insulation assumed to be in place and on the material properties and geometry of the structural members. In each tower, the temperature in the structural members varied through the length and cross section and changed with time. The temperature at every node in the global models was calculated by interpolation of temperatures from the thermal analysis, which had a much finer mesh than the global structural models. A linear temperature gradient was assumed across column cross sections and along the length of members. To reduce data handling, the continuous temperature time histories were replaced with piecewise linear time-histories without significant loss of accuracy. Elevated temperatures were applied to the damaged core structure in 10 min intervals, where a temperature state was given for all structural components at a given time and linearly ramped to the next temperature state. Examination of temperature histories indicated that no significant fluctuations between temperature states occurred for the 10 min intervals selected for analysis. Temperature data were provided at 10 min intervals up to 100 min for WTC 1 and up to 60 min for WTC 2 (see NIST NCSTAR 1-5G for more discussion of the 10 min intervals).



(a) WTC 1



(b) WTC 2

Figure 7–1. Isolated core models.

### 7.2.2 WTC 1 Core Analysis Results

Figure 7–2 shows the vertical displacement of the WTC 1 isolated core model with impact damage (prior to applying thermal loading) for Case A, where the colors represent the magnitude of vertical displacement. The maximum vertical displacement was approximately 5 in. along the north side of the

core where core columns were severed. Figures 7-3 and 7-4 show the WTC 1 core structural response to Case A and Case B temperature histories, respectively. Case A resulted in column buckling at the northwest corner and the center of the south side between Floors 94 and 97. There was a 21 in. vertical displacement at the northwest corner and a 12 in. vertical displacement at the center of the south side of the core. Case B resulted in column buckling between Floors 94 and 98 and a 44 in. vertical displacement at the center of the south side of the core.

For Case A temperatures, the core structure was first weakened on the northeast side as fires started in that area after the aircraft impact and then on the south side as the fires spread. For Case B temperatures, the core structure weakened at the center of the north side and then the south side. The core structural responses to these two temperature conditions illustrate the slight difference in core areas that were weakened by the elevated temperatures (northeast versus center of north side). When the results of each isolated core model were compared to the observed behavior of WTC 1, the weakening on the south side of the core was best matched by Case A impact damage and Case B temperatures (Case A impact damage and Case A temperatures showed core weakening at the northwest corner of the core).

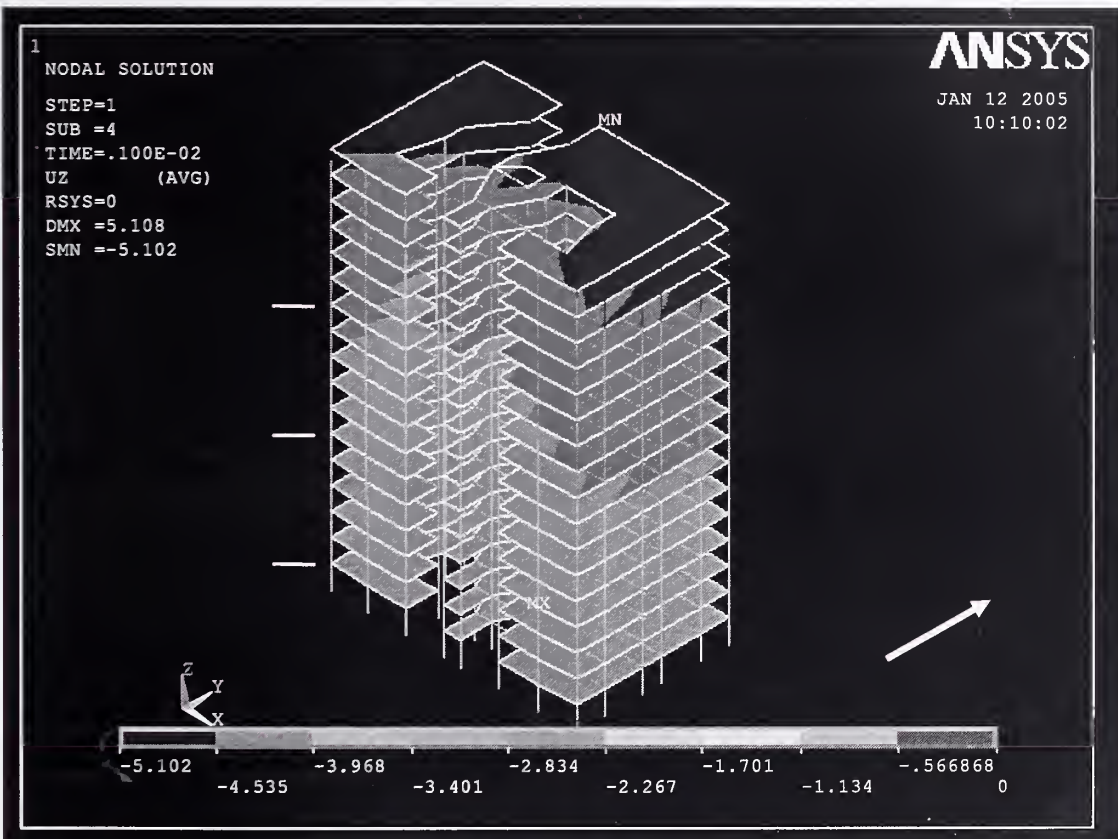
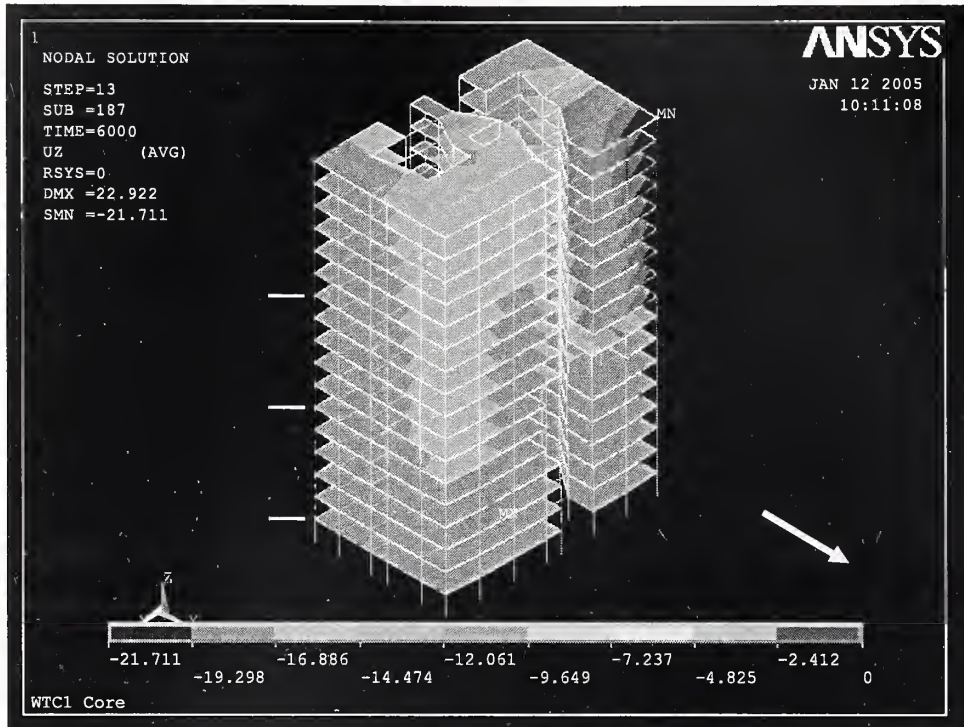
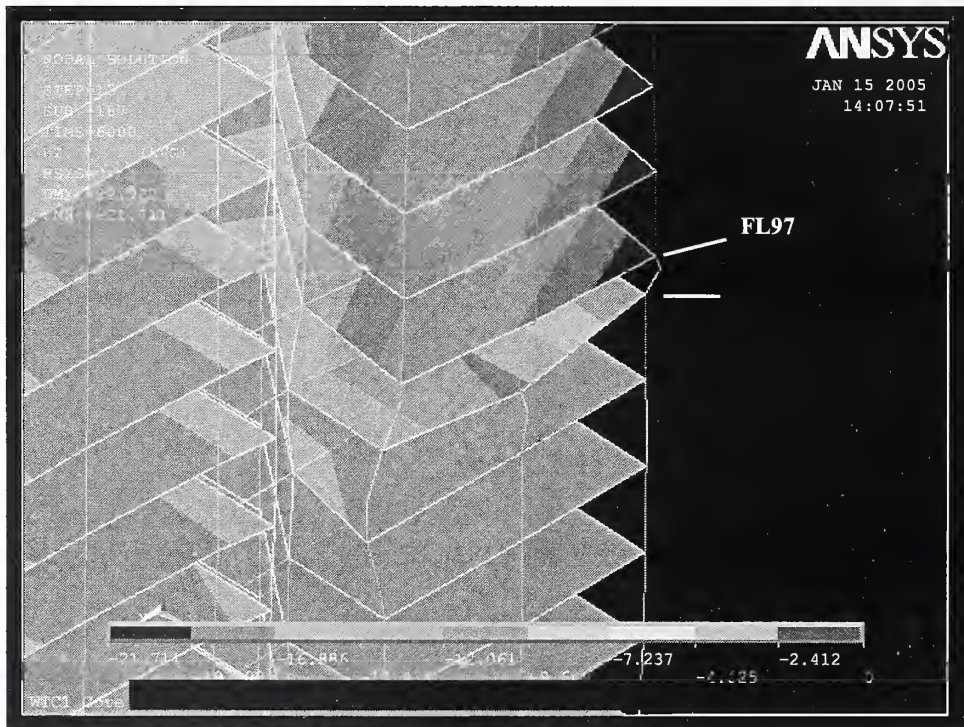


Figure 7-2. Vertical displacement of WTC 1 isolated core model with impact damage and gravity loads.

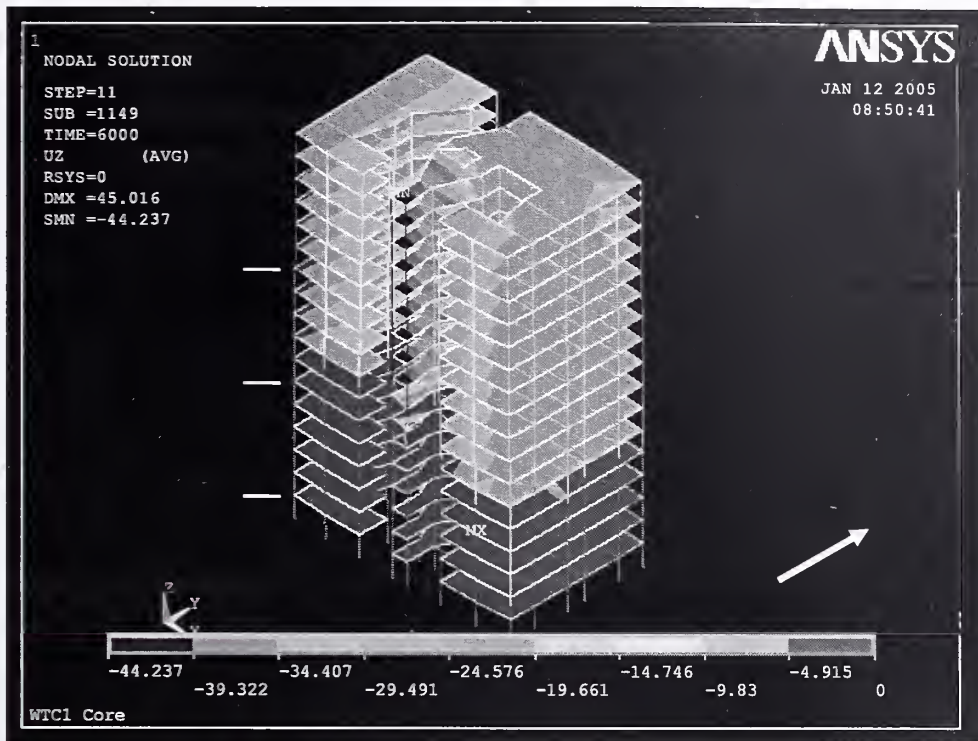


(a) North and east sides

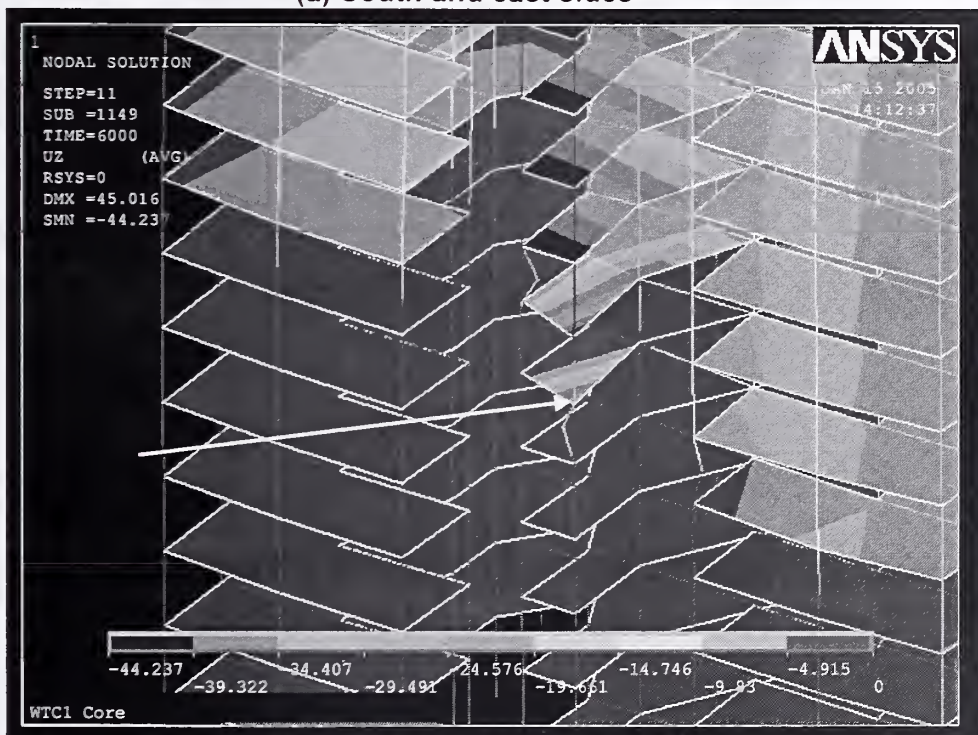


(b) Northwest corner (5X magnification)

Figure 7-3. North side vertical displacement of the WTC 1 core model at 100 min for Case A temperatures.



(a) South and east sides



(b) South side (10X magnification)

Figure 7-4. South side vertical displacement of the WTC 1 core model at 100 min for Case B temperatures.

### 7.2.3 WTC 2 Analysis Results

Figure 7–5 shows the vertical displacement of the WTC 2 isolated core model with impact damage for Case C. The maximum vertical displacement was approximately 5.6 in. at the southeast corner of the core where core columns were severed. Figures 7–6 and 7–7 show the response (vertical displacement) of the WTC 2 core model to Case C and Case D temperature histories, respectively. Case C resulted in a 6.1 in. vertical displacement at the southeast corner. Case D resulted in an 8.1 in. vertical displacement at the southeast corner. Without horizontal restraints, the core would have tilted more toward the southeast corner, and the vertical displacement would have been larger. No columns buckled in either Case C or Case D.

For both Case C and Case D temperatures, the core structure was weakened at the southeast corner and along the east side of the core. The core structural responses to these two temperature conditions illustrate the slight difference in core weakening by the larger deflection in the southeast corner for Case D, which had more column damage. The WTC 2 response for Case C and Case D temperatures was similar, with a 2 in. increase for Case D. When the results of each isolated core model were compared to the observed behavior of WTC 2, both Cases provided a reasonable match.

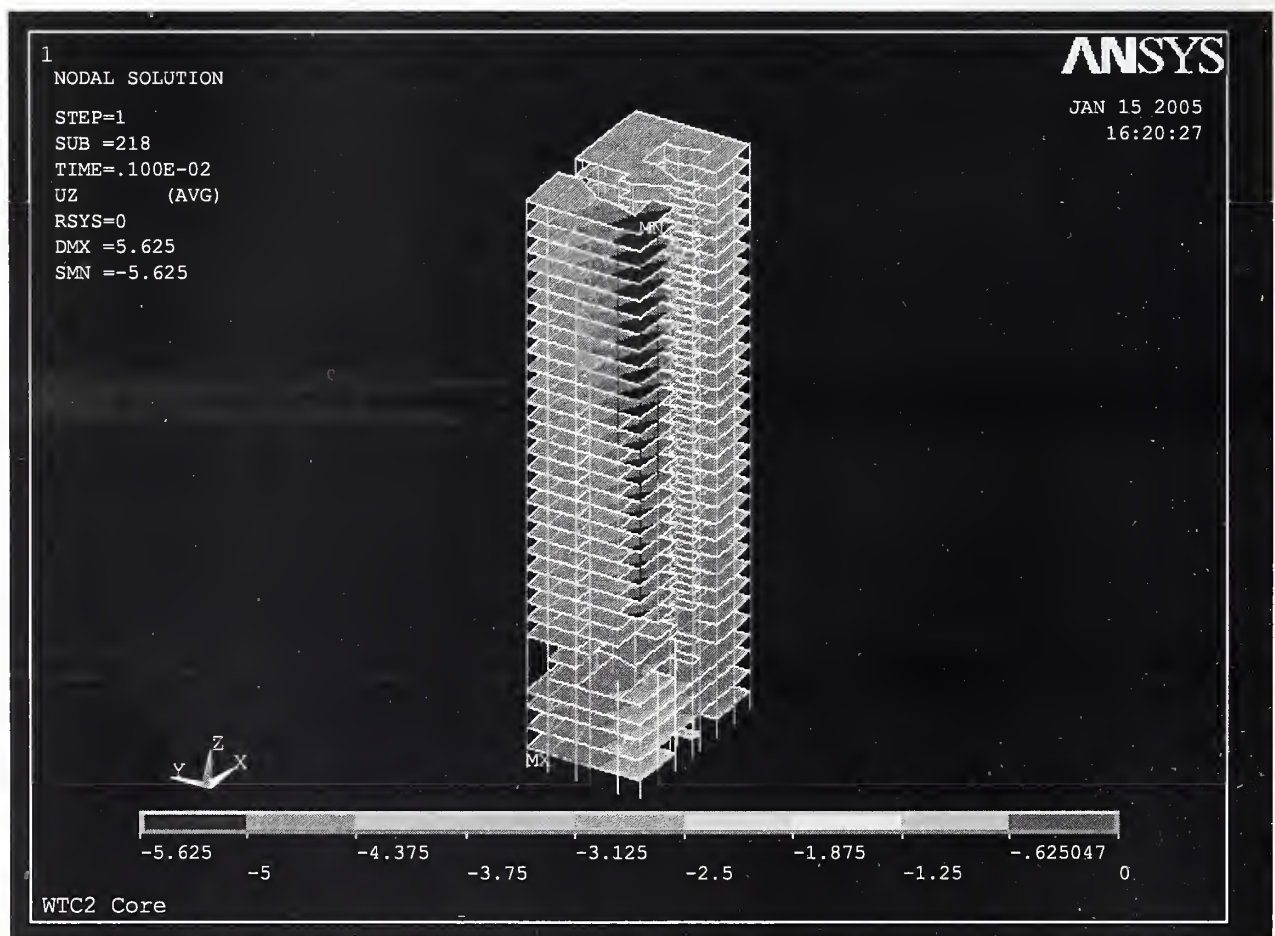


Figure 7–5. Vertical displacement of the WTC 2 isolated core model with impact damage and gravity loads (south and east faces).

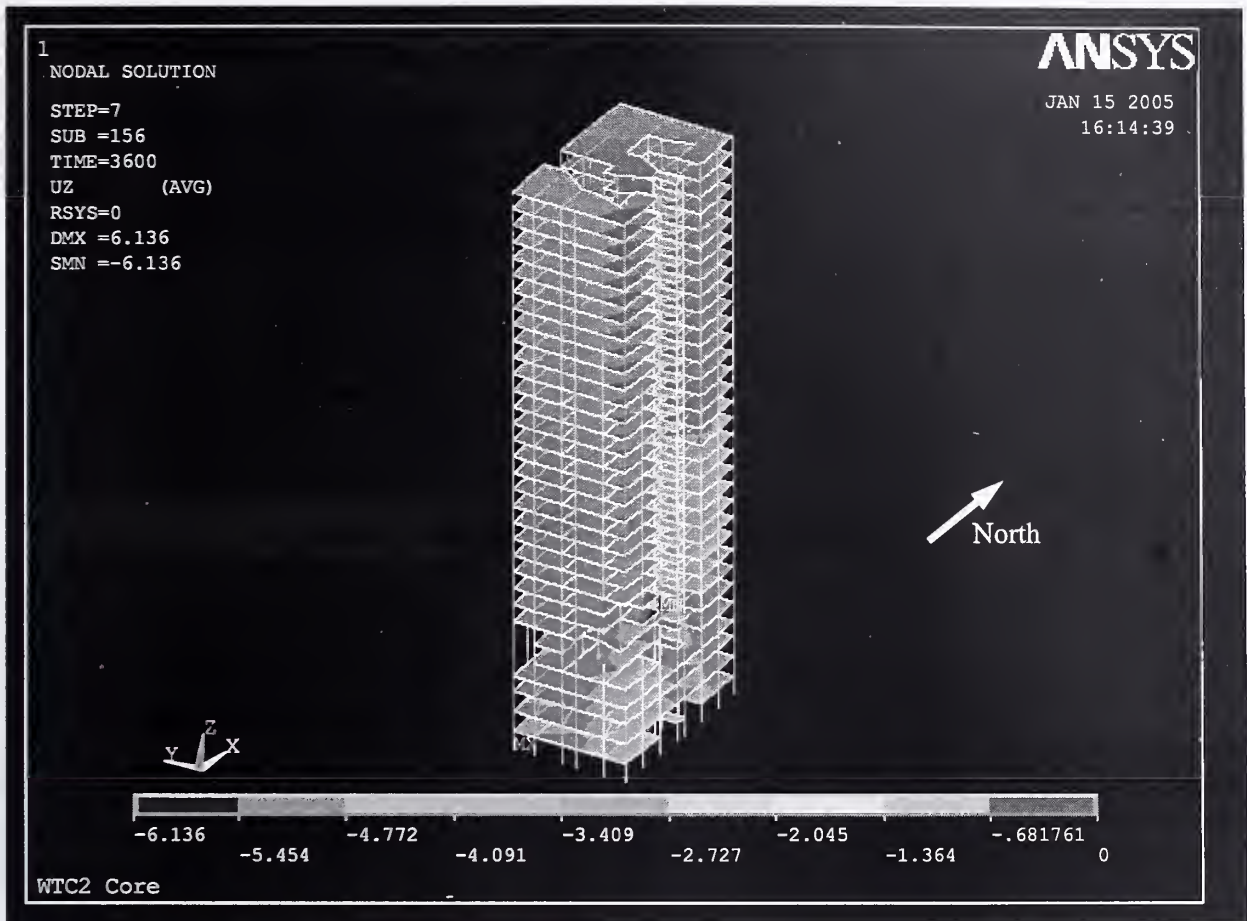


Figure 7-6. Vertical displacement of the WTC 2 core model at 60 min for Case C temperatures (south and east faces).

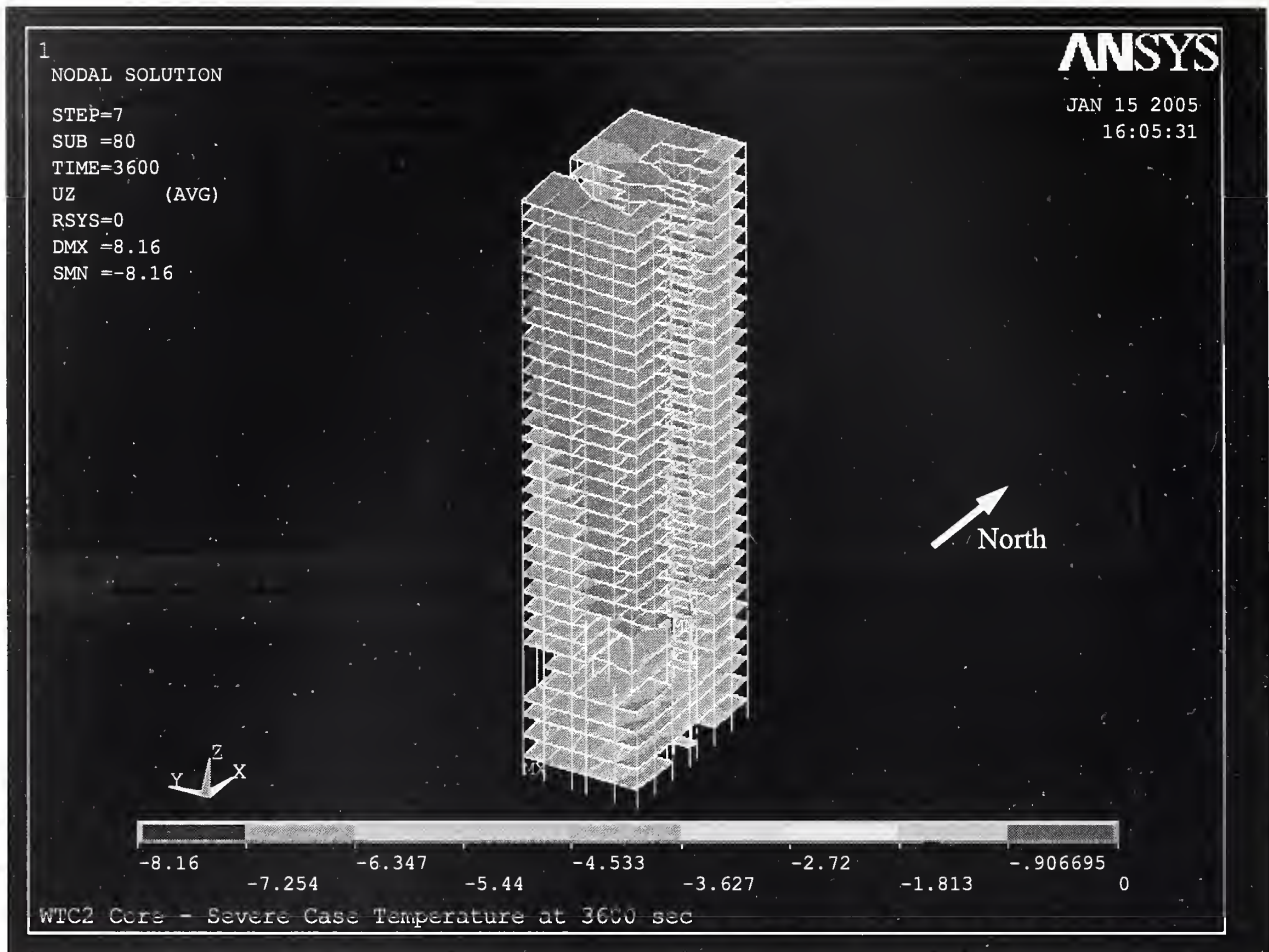


Figure 7–7. South and east side vertical displacement of the WTC 2 core model at 60 min for Case D temperatures.

## 7.3 FULL FLOOR SUBSYSTEM

### 7.3.1 Model and Method of Analysis

Figure 7–8 shows the full floor model (described in Chapter 4), which included 1) exterior and core columns extending one story below and one story above the floor model, 2) spandrels, 3) floor slab, 4) floor trusses (bridging trusses were retained only in the two-way floor areas), 5) strap anchors, 6) core beams, 7) deck support angles, and 8) break elements to capture failure modes. Both core and exterior columns were fixed against vertical movement at the lower ends and free to displace at the upper ends. Exterior columns were restrained from out of plane displacement and all three components of rotation at the both column ends. The core columns were free to displace horizontally. Note that the two-way zones shown in Fig. 7–8 extended only to the corners of the core rather than beyond the corners as shown in Fig. 4–7. The extent of two-way action shown in Fig. 7–8 was believed to better represent actual structural boundary conditions.

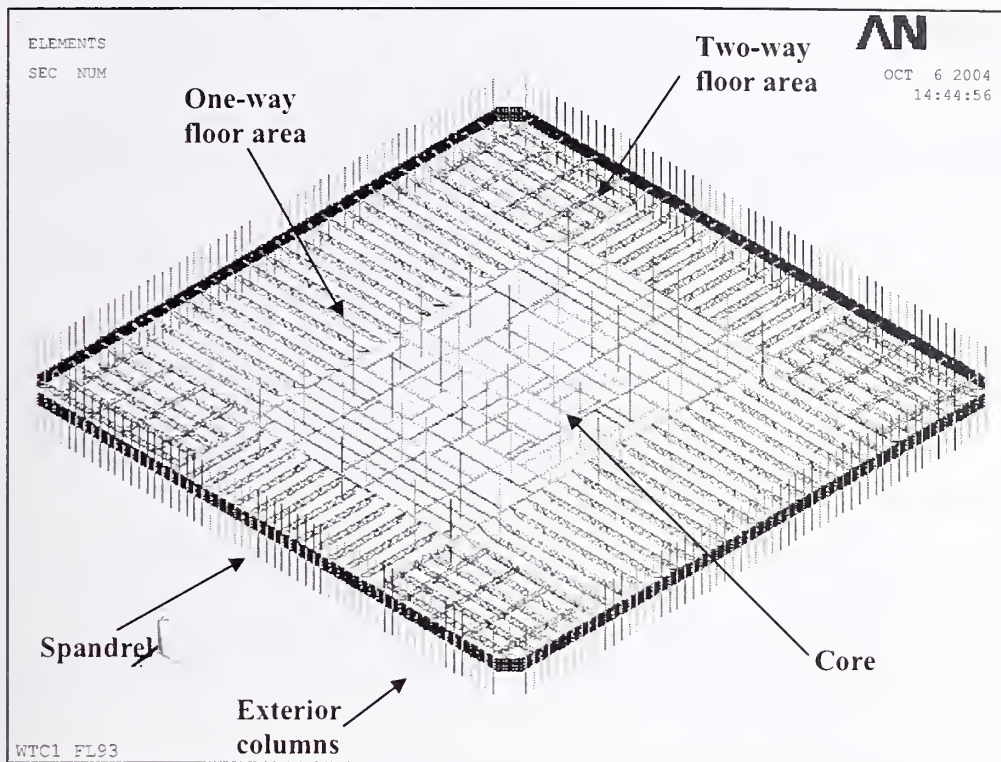


Figure 7-8. Full floor model.

The full floor subsystem models included large deflection and temperature-dependent material properties with plasticity for all steel components. The model was used to evaluate structural response under dead and live loads and elevated temperatures, identify failure modes and associated temperatures and times to failure, and identify reductions in modeling complexity for global models and analyses. The structural response included thermal expansion of steel and concrete members, temperature-dependent properties of steel and concrete that affected material stiffness and strength, and bowing or buckling of structural members. Creep was not included in the full floor models, as this analysis feature did not work with the BEAM 188/189 elements in version 8.0 of ANSYS (the detailed truss model had 3D finite strain elements that were changed to beam elements in the full floor model). Creep was included for beam elements in ANSYS 8.1, and subsequent analyses of the core and exterior wall subsystems included creep deformation.

The floor slab was modeled as lightweight concrete across the entire floor (tenant and core floor areas) with a bilinear stress-strain constitutive model that did not account for cracking or crushing. The concrete material model used the compressive strength as the yield point, with the same yield strength in both tension and compression (the reinforcing steel was assumed to provide the tensile capacity in the composite floor). With this material model, tensile strength of the concrete slab was not represented accurately, and the actual floor stiffness was overestimated. In the full floor models, bending stresses in the concrete slab that exceeded the actual tensile strength of concrete were found in few locations. This phenomenon was typically observed when the temperature of the top of the slab was higher than the temperature at the bottom of the slab, and the concrete slab still deflected down due to large thermal expansion of the truss. However, when the temperature is higher at the bottom, the simplified truss model

with this material model showed a very similar behavior to the detailed truss model, and the key failure modes of the floors were not significantly affected.

Failure modes of the full floor model included truss diagonal buckling and weld failure, exterior and interior truss seat failure, stud failure, strap anchor weld failure, connection failure between primary and bridging trusses, and connection failure between long-span and transfer trusses.

Separate floor models were created from the Floor 96 structural model by imposing the different damage and temperature conditions for WTC 1 Floors 93 to 99 and WTC 2 Floors 79 to 83. Structural components that were severed due to the aircraft impact were removed from each floor model, based upon four initial damage cases, WTC 1 Case A<sub>i</sub> and Case B<sub>i</sub> and WTC 2 Case C<sub>i</sub> and Case D<sub>i</sub>. Each full floor model was analyzed for stability under gravity loads consisting of dead load, superimposed dead load, and service live load (25 percent of design live load), which varied from 55 psf to 85 psf. No column loads were applied.

Each floor model was then subjected to the corresponding temperature conditions for each Case in 10 min intervals, as described previously. Temperatures were assigned at structural component nodes. A uniform distribution of temperatures through a cross section was assumed for truss members and spandrels. For columns, a linear gradient in two directions was assumed, and the slabs had temperatures defined at 5 nodes through the slab depth.

Some members were removed from the model to improve computational performance. They were found to fail in the early stages of thermal loading and caused convergence problems. Removal of the following members did not affect the stability and ultimate failure mode of the full floor system under fire:

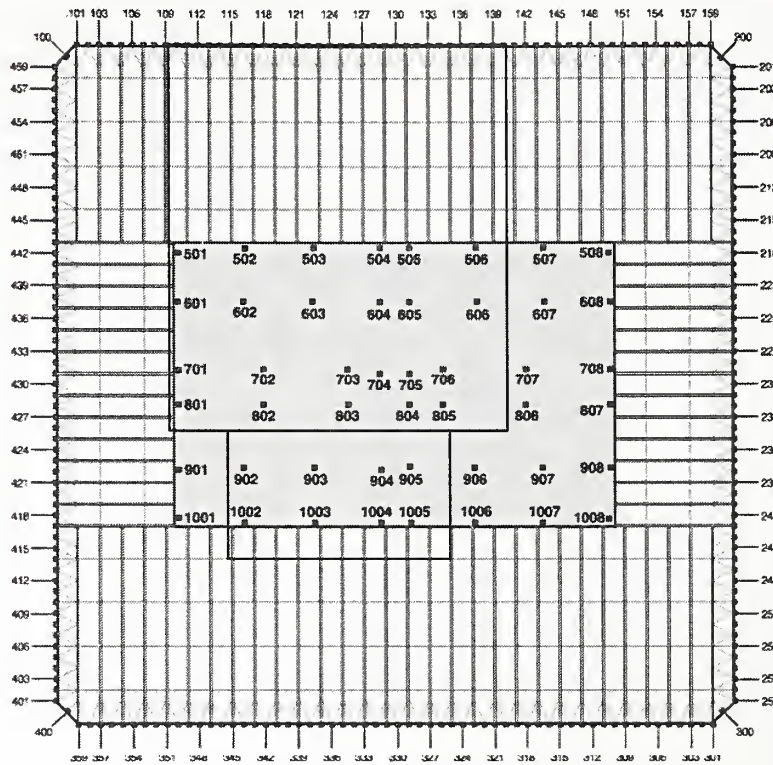
- Deck support angles and bridging trusses, which buckled due to thermal expansion.
- Shear studs and welds between strap anchors and truss top chords, which failed due to shear force caused by differential thermal expansion between the floor and the exterior wall.

Final damage Cases A, B, C, and D were completed after the initial set of floor analyses were conducted, as described above. The fire simulations did not change between initial Cases A<sub>i</sub> to D<sub>i</sub> and final Cases A to D, which resulted in the same concrete slab temperatures for the initial and final Cases. The truss temperatures differed as a result of the different estimates of dislodged fireproofing. The full floor models were not rerun for Cases A through D as comparisons showed that the structural temperature histories of the floors were nearly identical for most floors and only slightly different for a few floors. The floor analysis results for Cases A<sub>i</sub> to D<sub>i</sub> were used for Cases A to D in the exterior wall subsystem (Section 7.4) and global analyses (Chapter 8).

For WTC 1, only Floor 97 showed a significant increase in damage to truss fireproofing on the south side between Case A<sub>i</sub> and Case A, where the fireproofing damage over 11 trusses increased from just beyond the core to two thirds of the floor span, as shown in Fig. 7–9. Figure 7–10 shows the temperature distributions for WTC 1 Floor 97 trusses for Case A<sub>i</sub> and Case A. Analysis of Floor 97 for Case A damage and temperature histories showed little difference in the floor behavior. Case B<sub>i</sub> and Case B structural and fireproofing damage were similar for all floors.

A review of WTC 2 Cases showed that the differences in truss fireproofing damage between Cases C<sub>i</sub> and C and Cases D<sub>i</sub> and D (mostly on the east side) would cause little difference in the floor temperatures or in the structural behavior. The exception was Floor 83 for Cases C<sub>i</sub> and C, where the fireproofing damage increased from half to three quarters of the floor area. However, observations from photographs suggested that the floor was disconnected immediately after the aircraft impact and fireball in this area. Since Floor 83 was assumed to be disconnected at the exterior wall over the area that would be heated in Case C, the analysis was not rerun for this case.

Case A<sub>i</sub>



Case A

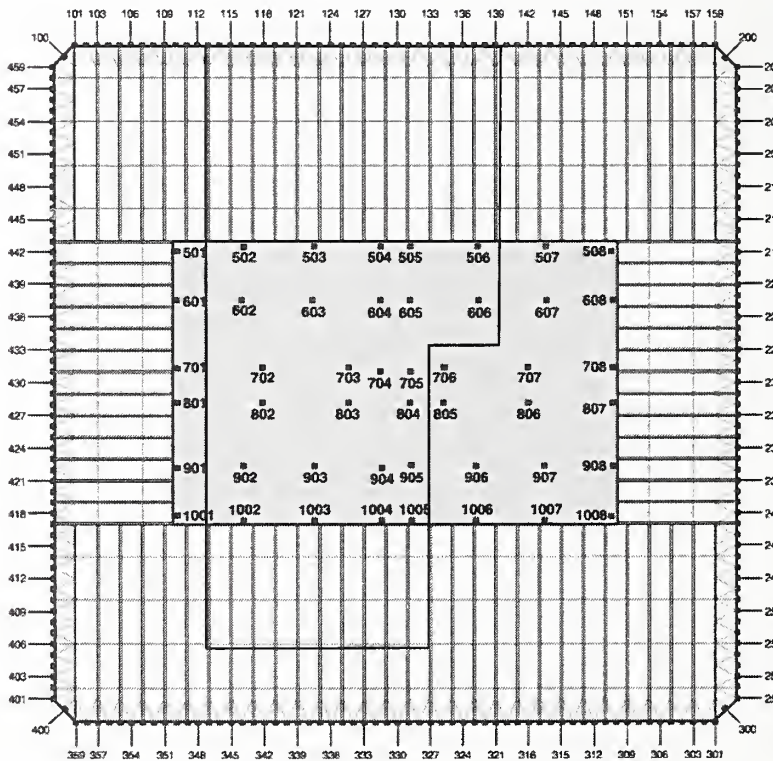
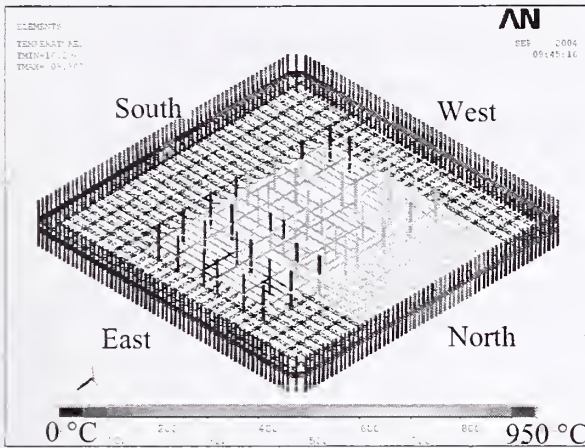
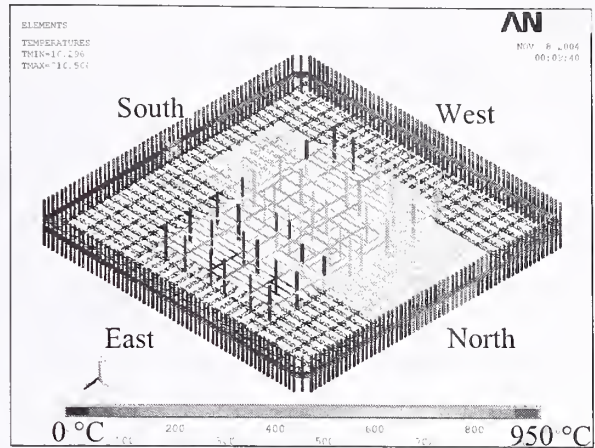


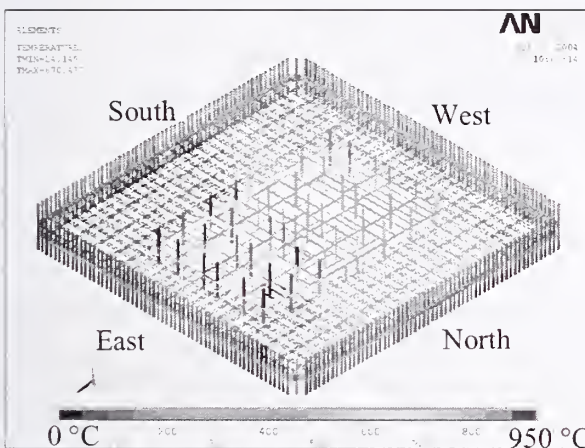
Figure 7-9. Fireproofing damage to WTC 1 Floor 97 for Case A<sub>i</sub> and Case A.



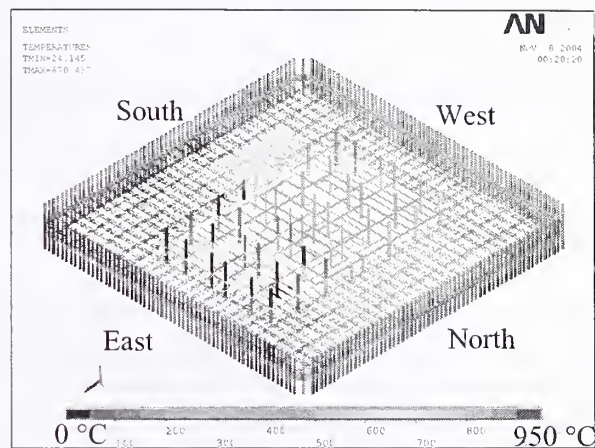
(a) Case A<sub>1</sub> top view at 10 min



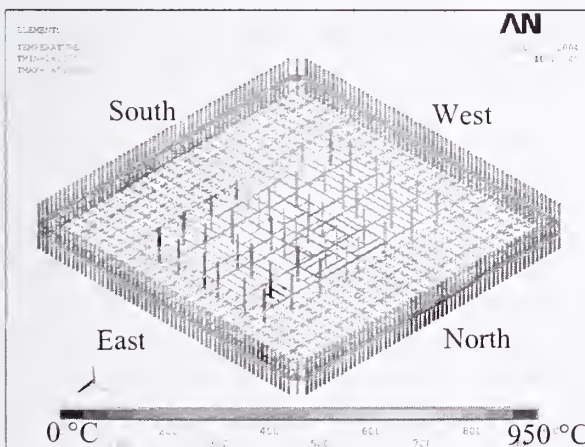
(b) Case A top view at 10 min



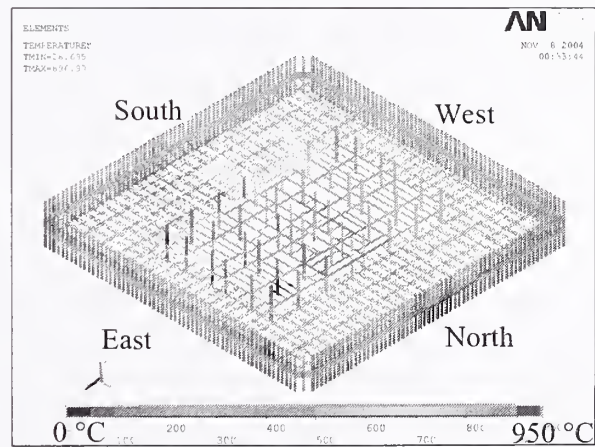
(c) Case A<sub>1</sub> top view at 50 min



(d) Case A top view at 50 min



(e) Case A<sub>1</sub> top view at 100 min



(f) Case A top view at 100 min

Figure 7-10. WTC 1 Floor 97 comparison of truss temperatures for Case A<sub>1</sub> and Case A.

### 7.3.2 WTC 1 Analysis Results

Areas of the floors that were subject to the combined effects of dislodged fireproofing and exposure to fire were found to have two primary failure mechanisms: buckling of diagonal web members and associated sagging of the floor or disconnection of exterior truss seat connections. When the vertical support of truss seat connections failed, the floor would hang or sag between the remaining intact supports. The following descriptions of floor responses to structural impact damage and temperature histories for Cases A<sub>i</sub>, B<sub>i</sub>, C<sub>i</sub>, and D<sub>i</sub> present the time, locations, and maximum vertical displacements of the sagging predicted in the floors.

#### Case A<sub>i</sub>

As shown in Fig. 7–9, the intact fireproofing on the south floor trusses resulted in delayed heating of the trusses. The WTC 1 floors in the impact zone had upgraded fireproofing thickness of 2.5 in. (modeled as a thermally equivalent 2.2 in. to account for variability in thickness, Chapter 2). The maximum temperatures shown for Floor 97 trusses on the south side ranged from 300 °C to 400 °C at 100 min. At these temperatures, the steel expanded thermally but had only a modest reduction in stiffness and strength (see Chapter 4).

The maximum vertical displacements of WTC 1 floors are listed in Table 7–1. Floor 95 to Floor 98 showed a significant vertical deflection (sag) in the north office area near the impact damage. The vertical deflection in the south office area was found to be insignificant for all floors. Many diagonals of Floor 95 to Floor 98 buckled in the hottest zones of the north office area. Although gusset plates fractured at several locations, a complete disconnection of the floor from the exterior wall was not predicted. Slab thermal expansion at 100 min (across the entire floor) ranged between 4 in. and 8 in. Since the floors did not sag except in areas adjacent to the impact zone on the north side, almost all the exterior columns were pushed out by the floors. The high level of restraint imposed on the slab expansion by the exterior columns, due to their fixed boundary conditions at column ends, resulted in compressive forces developing in the slab. These compressive forces would likely have been smaller in the towers, as the exterior columns would have expanded outward over the four to five floors subject to fires and provided minimal restraint against thermal expansion of the slab.

#### Case B<sub>i</sub>

Table 7–2 gives the maximum vertical displacement of WTC 1 floors for Case B<sub>i</sub>, and Figs. 7–11 through 7–15 show the vertical displacement contours at time of maximum displacement for Floors 95 to 99. Floors 93 and 94 had no fireproofing damage to the south floor trusses. The maximum deflection of Floors 95 and 96 occurred just after the aircraft impact on the north side next to the damage area. Floors 97 and 98 maximum deflection occurred at 100 min on the south side. The time and location of maximum floor deflections illustrate the movement of the fires from the north side just after impact to the south and the effect of the truss fireproofing. The large deflections on the south side of Floors 97 and 98 were caused by the exterior seat failures that began at 90 min, due to reduction of vertical shear strength under the elevated temperatures. Figure 7–16 shows the extent of truss seat failures for Floor 97 and Floor 98, which was a loss of 18 percent to 25 percent of exterior connections for the two floors on the south face. The average slab expansion across the entire floor ranged from 5 in. to 8.5 in. The interaction of the floor slab and exterior columns was the same as described for Case A<sub>i</sub>.

**Table 7-1. Maximum vertical displacement of WTC 1 floors for Case A<sub>i</sub>.**

Floor	Maximum Displacement (in.)	Location of Displacement on WTC 1 floor	Time after Aircraft Impact (min)
93	5.4	North side	30
94	13.5	North side	100
95	30.9	North side	10
96	23.3	North side	10
97	31.5	North side	60
98	26.4	North side	30
99	7.0	North side	50

**Table 7-2. Maximum vertical displacement of WTC 1 floors for Case B<sub>i</sub>.**

Floor	Maximum Displacement (in.)	Location of Displacement on WTC 1 floor	Time after Aircraft Impact (min)
93	-5.8	South side	100
94	12.7	South side	100
95	29.2	North side	10
96	28.6	North side	10
97	37.4	South side	100
98	49.0	South side	100
99	6.8	North side	100

Note: Negative value represents upward displacement.

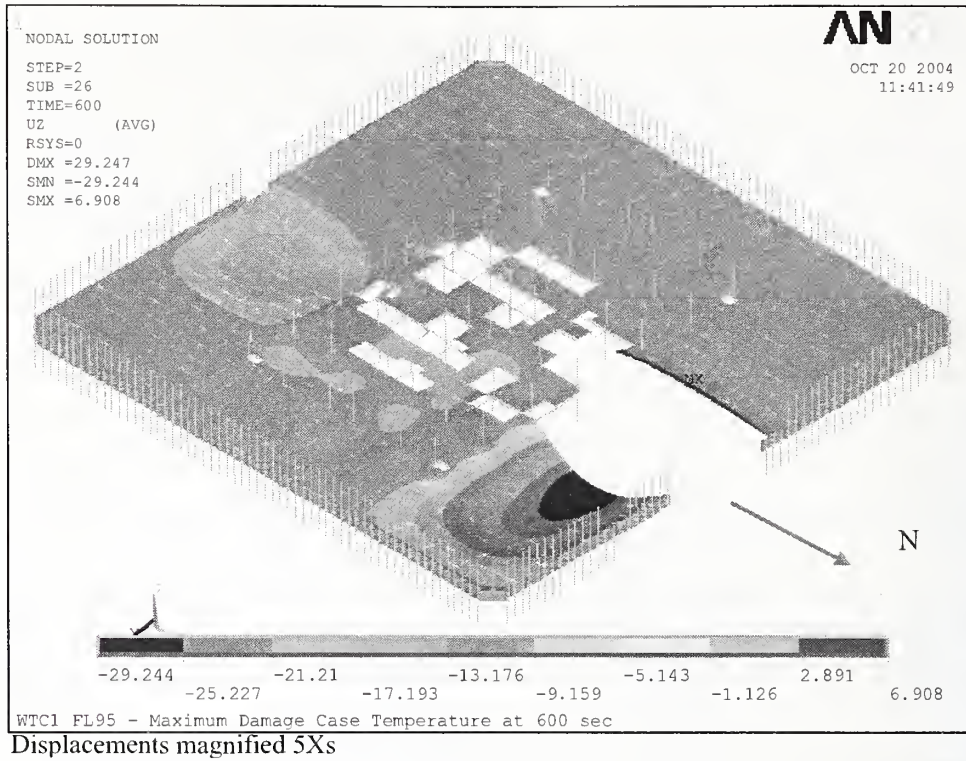


Figure 7-11. Vertical deflection of WTC 1 Floor 95 for Case B; at 10 min.

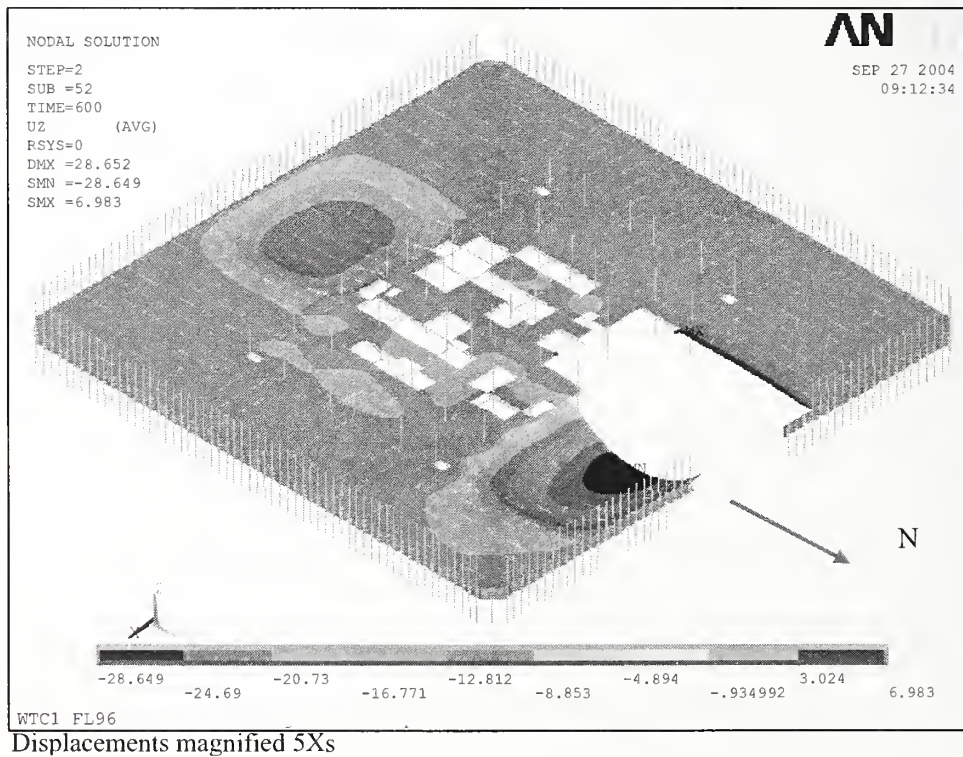


Figure 7-12. Vertical deflection of WTC 1 Floor 96 for Case B; at 10 min.

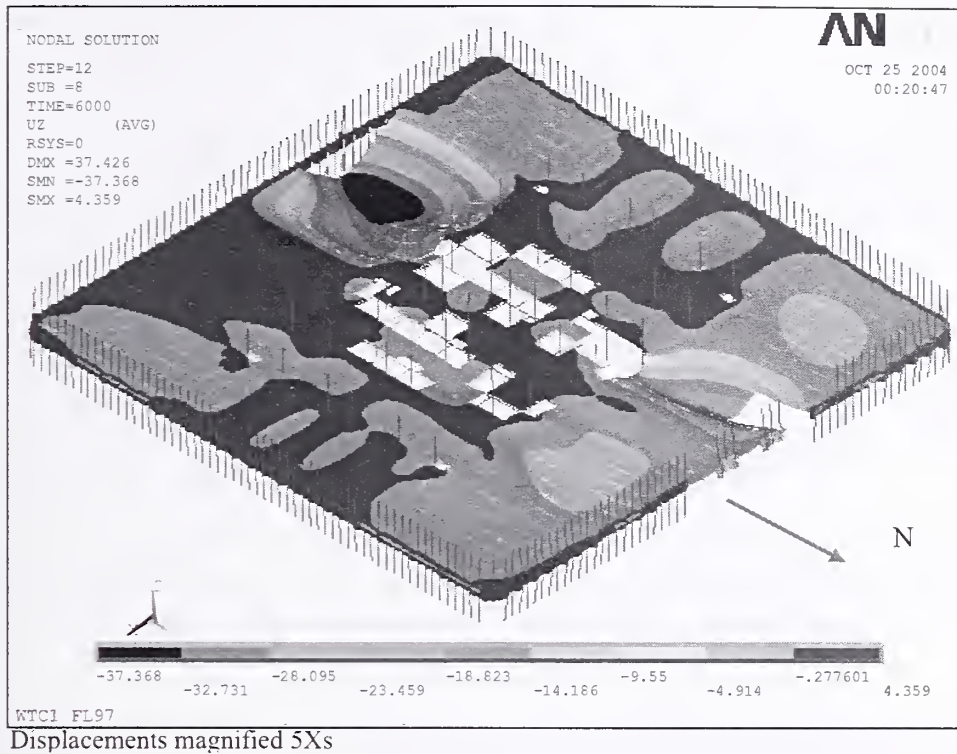


Figure 7-13. Vertical deflection of WTC 1 Floor 97 for Case B<sub>i</sub> at 100 min.

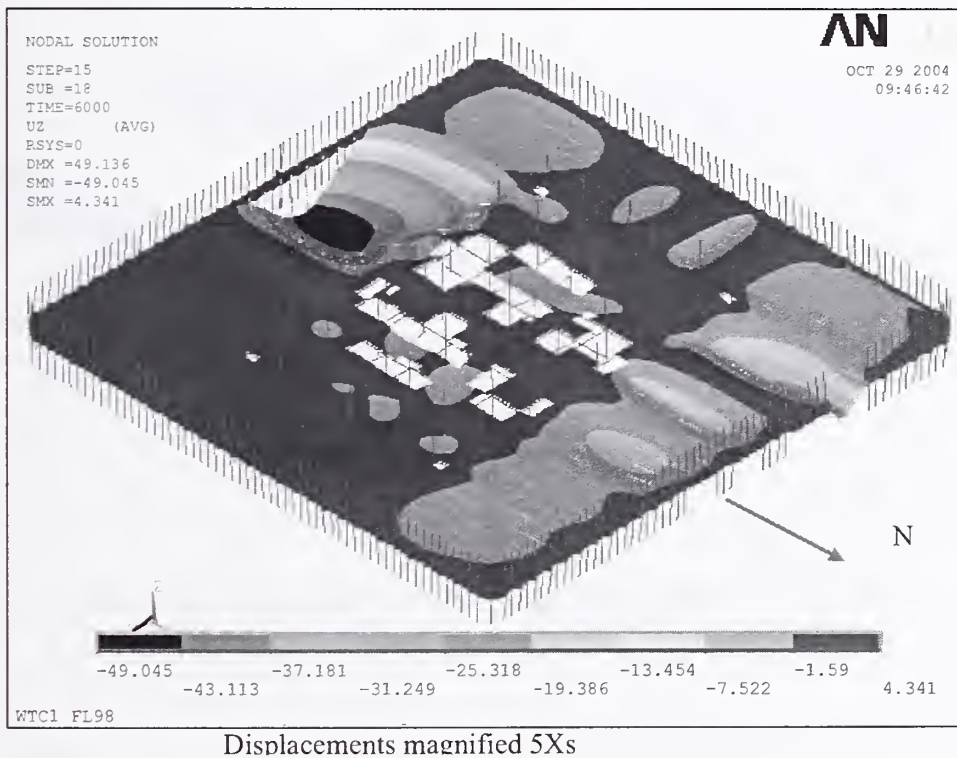


Figure 7-14. Vertical deflection of WTC 1 Floor 98 for Case B<sub>i</sub> at 100 min.

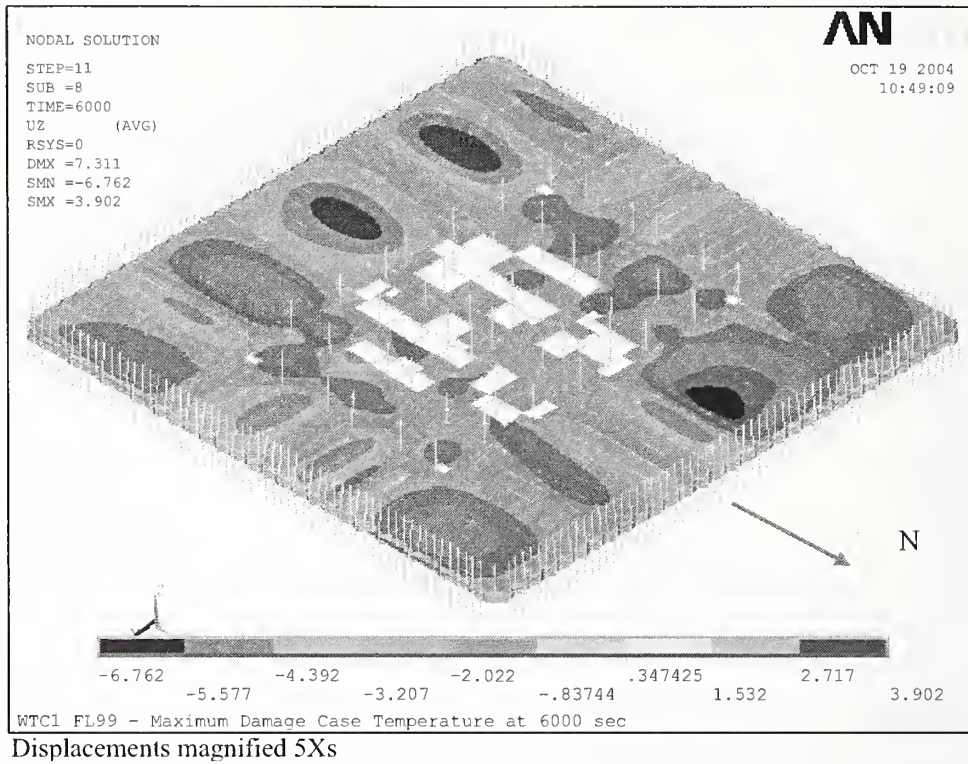
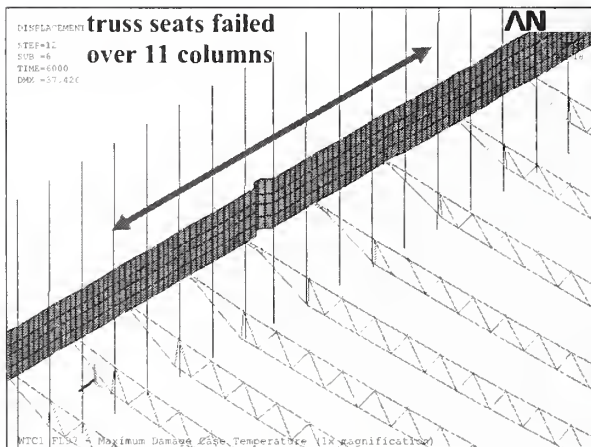
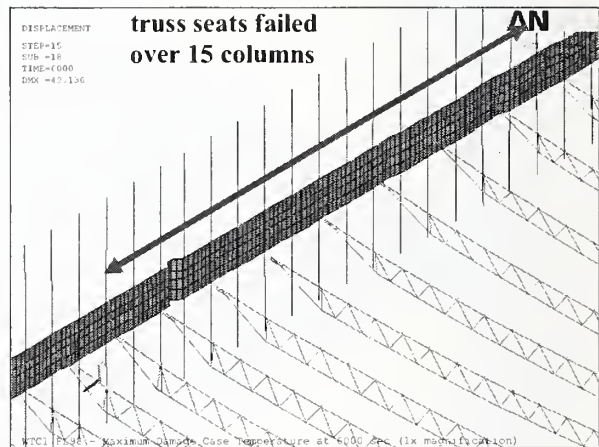


Figure 7-15. Vertical deflection of WTC 1 Floor 99 for Case B<sub>i</sub> at 100 min.



(a) Floor 97



(b) Floor 98

Figure 7-16. Loss of vertical supports in WTC 1 Floor 97 and Floor 98 for Case B<sub>i</sub>.

### 7.3.3 WTC 2 Analysis Results

#### Case C<sub>i</sub>

Table 7-3 lists the maximum vertical displacement of WTC 2 floors for Case C<sub>i</sub>, and Figs. 7-17 through 7-21 show the vertical displacement contours at time of maximum displacement for Floors 79 to 83. Floors 79 to 83 had impact damage at the south side of the east floor area, but Floors 80 and 81 had many interior truss seats severed from the south exterior wall to the east side of the core perimeter. The maximum vertical deflection occurred in the southeast floor area near the impact damage for all floors, with the exception of Floor 82, which had a maximum deflection in the northeast floor area. The maximum deflection occurred at 60 min for all floors. The location of the maximum deflection was primarily due to the combined effects of impact damage and elevated temperatures. Floor 82 had a large span of unsupported floor along the exterior wall resulting from heat-induced truss seat failures, which led to floor sagging in the northeast corner (see Fig. 7-20).

The west office area of Floors 79 to 83 had vertical deflections ranging from 12 in. to 18 in. at 60 min, due to the combined effect of hot gases that spread throughout the floors and the 0.75 in. fireproofing on the trusses. The average thermal expansion of slabs across the entire floor ranged from 2.5 in. to 5.5 in. at 60 min.

A significant number of truss web diagonals buckled in the east floor area of Floor 81 to Floor 83. Truss seat failures were not observed on Floor 79 to Floor 81. Figure 7-22 shows the truss seat failures for Floor 82 and Floor 83, which extended over 15 percent to 30 percent of the exterior wall width.

**Table 7-3. Maximum vertical displacement of WTC 2 floors for Case C<sub>i</sub>.**

Floor	Max. Displacement (in)	Location of Displacement On East Floor	Time After Aircraft Impact (min)
79	19.0	South side	60
80	30.1	South side	60
81	31.0	South side	60
82	45.2	North side	60
83	38.9	South side	60

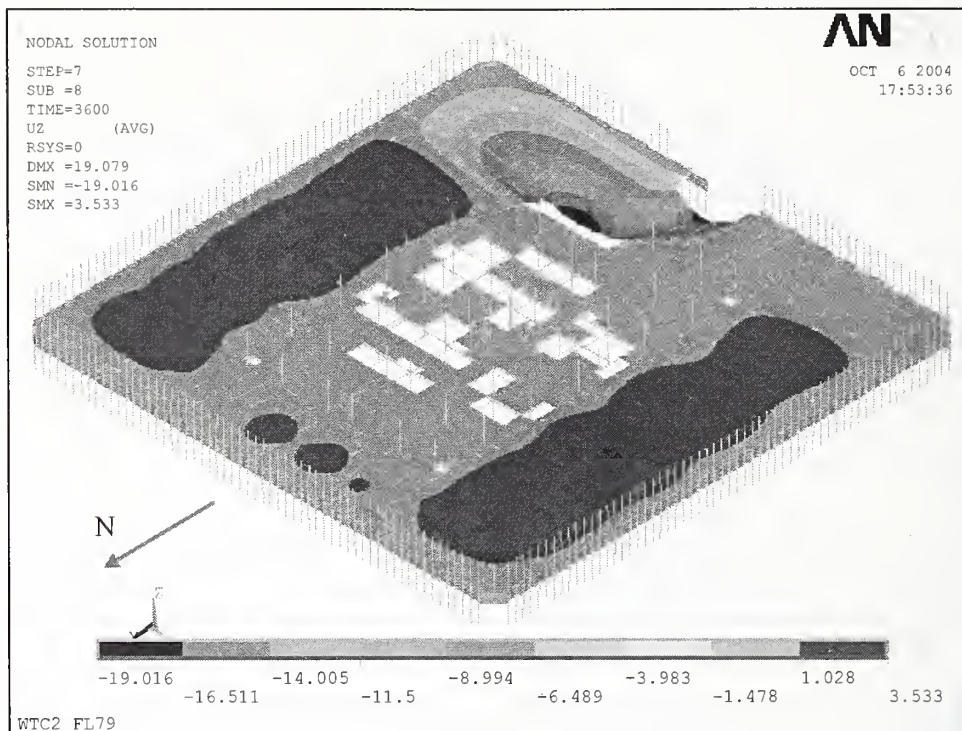


Figure 7-17. Vertical deflection of WTC 2 Floor 79 for Case C<sub>i</sub> at 60 min.

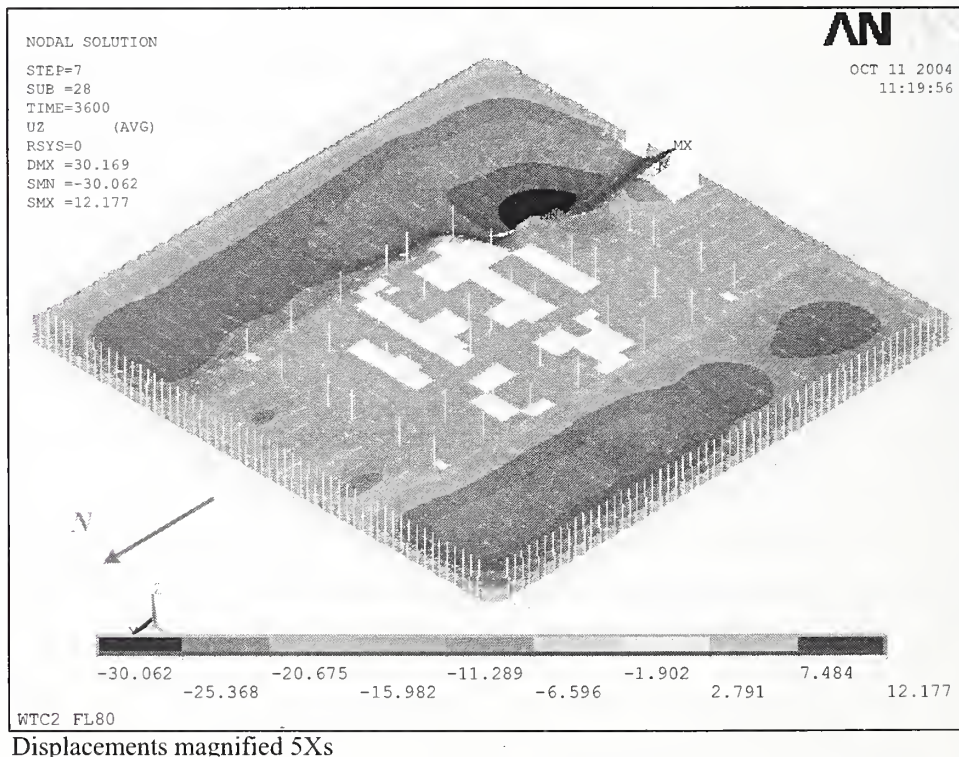


Figure 7-18. Vertical deflection of WTC 2 Floor 80 for Case C<sub>i</sub> at 60 min.

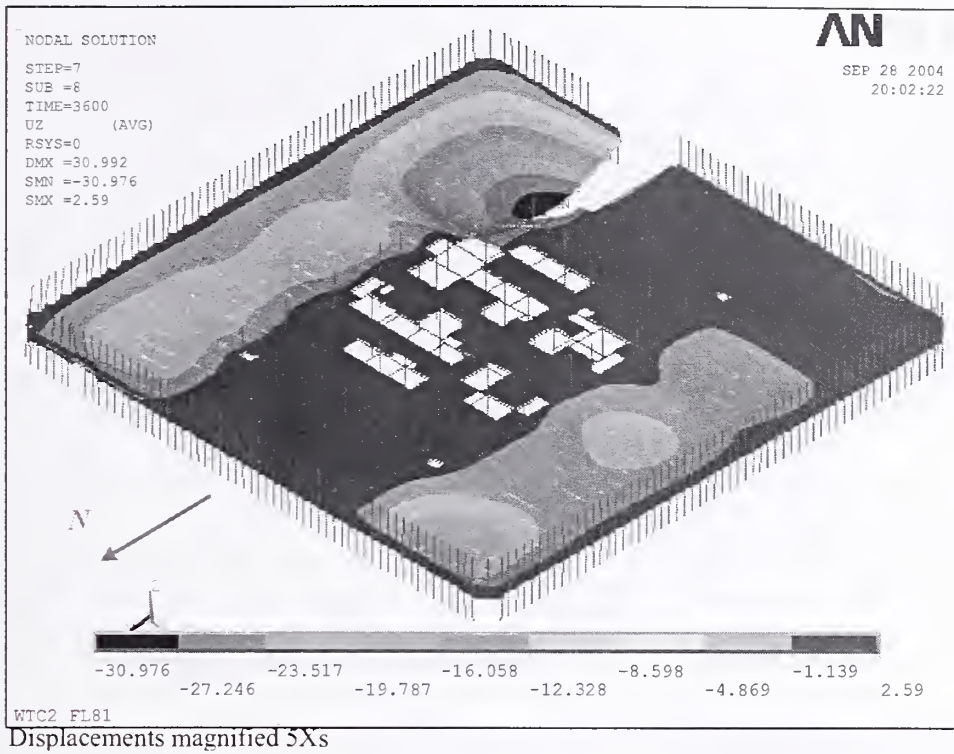


Figure 7-19. Vertical deflection of WTC 2 Floor 81 for Case C<sub>i</sub> at 60 min.

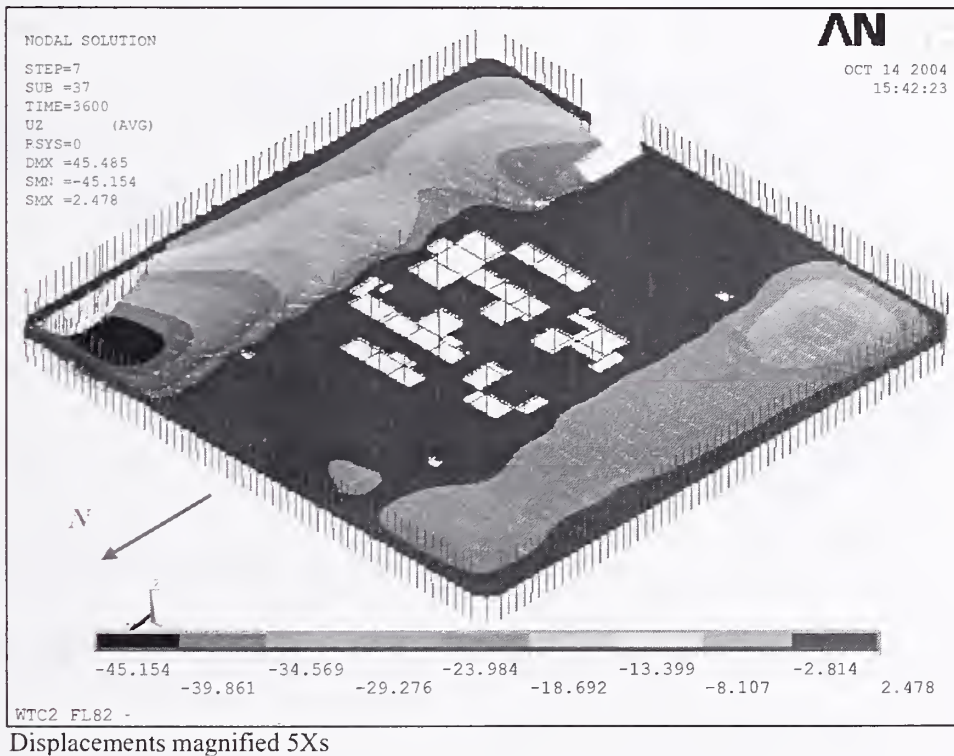


Figure 7-20. Vertical deflection of WTC 2 Floor 82 for Case C<sub>i</sub> at 60 min.

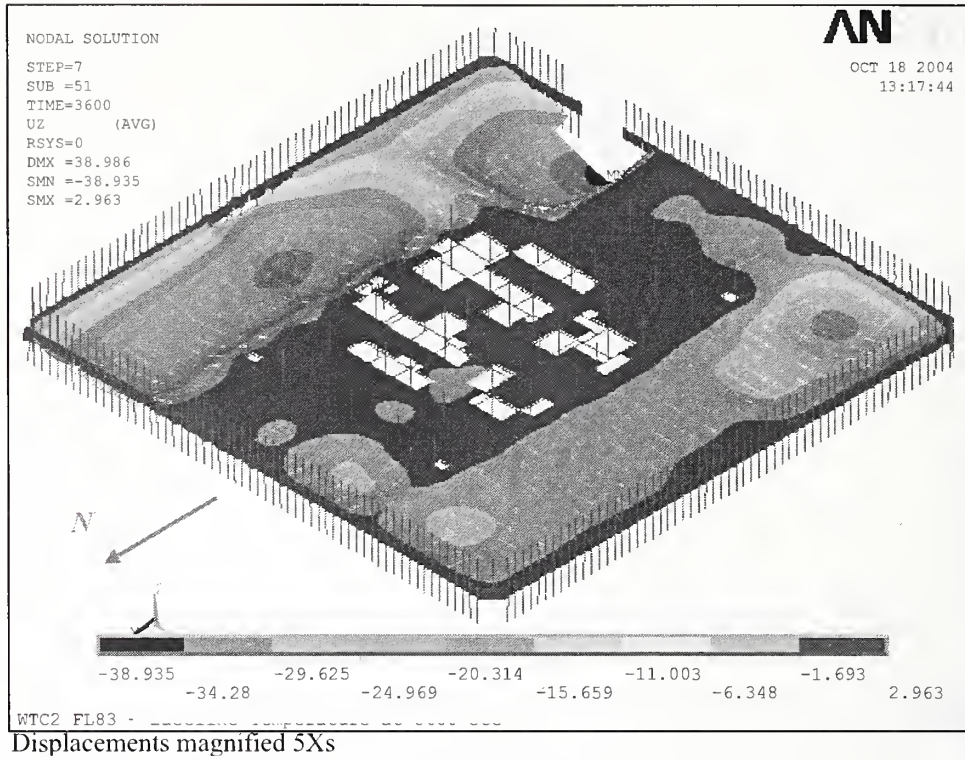


Figure 7–21. Vertical deflection of WTC 2 Floor 83 for Case C<sub>i</sub> at 60 min.

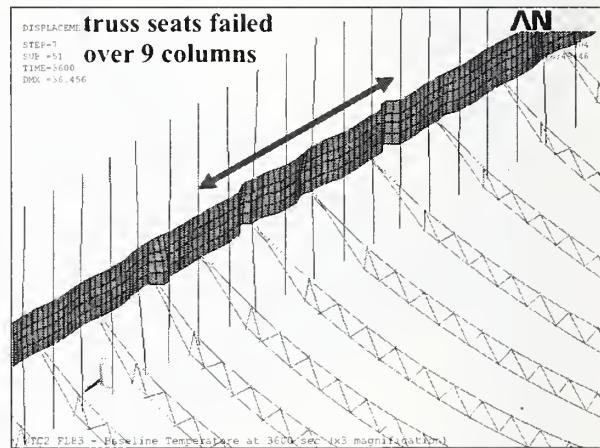
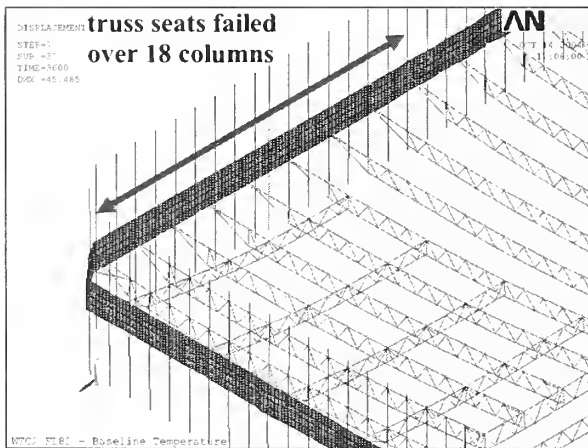


Figure 7–22. Loss of vertical supports in WTC 2 Floor 82 and Floor 83 for Case C<sub>i</sub>.

## Case D<sub>i</sub>

Table 7–4 lists the maximum vertical displacement of WTC 2 floors for Case D<sub>i</sub>, and Figs. 7–23 through 7–27 show the vertical displacement contours at time of maximum displacement for Floors 79 to 83. Floors 79 to 83 had impact damage at the southeast floor area, but Floors 80 and 81 had many interior truss seats severed from the south exterior wall to the east side of the core perimeter. As Case D<sub>i</sub> had more impact damage near the southeast corner of the core than did Case C<sub>i</sub>, Floors 80 and 81 had much greater vertical deflections. At 50 min they were 66 in. and 97 in., respectively, in the southeast floor area. The maximum temperatures were similar for Case C<sub>i</sub> and Case D<sub>i</sub>, but differences in times and locations of maximum temperatures led to differences in locations of maximum vertical displacements. Bridging trusses that had been removed in Case C<sub>i</sub> were replaced in Floors 80 and 81 to provide support to the primary trusses in the single-span (one-way) floor area during greater vertical deflections.

The slab expansion across the entire floor ranged from 1 in. to 5 in. Gusset plates and bolts at more than 75 percent of all the exterior seats along the east face of Floors 82 and 83 failed. These connection failures were due to horizontal shear, parallel to the exterior wall, which was caused by differential thermal expansion between the floor framing, the floor slab, and the exterior wall. The truss at Column 357 of Floor 81 was the only one that lost its vertical support at the exterior seat among all the floors. This truss walked off the truss seat.

Several columns along the east and west sides of Floor 80 were pulled inward by the floor sagging in the southeast area. (The inward pull on the west face was due to the lack of horizontal restraint for the core columns in the floor model; in the global model, the inward pull would be resisted by the core. The west face inward pull was not applied in the global model). Floor 79 and Floor 81 showed similar behaviors to Floor 80 in terms of column horizontal reaction forces. Many columns of the west face of Floor 82 were pulled inward, while reaction forces at many columns of the east face were close to zero. As described above, gusset plates and seat bolts failed at a number trusses on the east face of Floor 82. Because columns at these locations were not supported in the horizontal direction by the floor, the reaction force became zero at these columns.

**Table 7–4. Maximum vertical displacement of WTC 2 floors for Case D<sub>i</sub>.**

Floor	Maximum Displacement (in)	Location of Displacement on East Floor	Time After Aircraft Impact (min)
79	35.8	South side	60
80	65.6	South side	40
81	96.7	South side	50
82	49.4	South side	60
83	44.6	South side	60

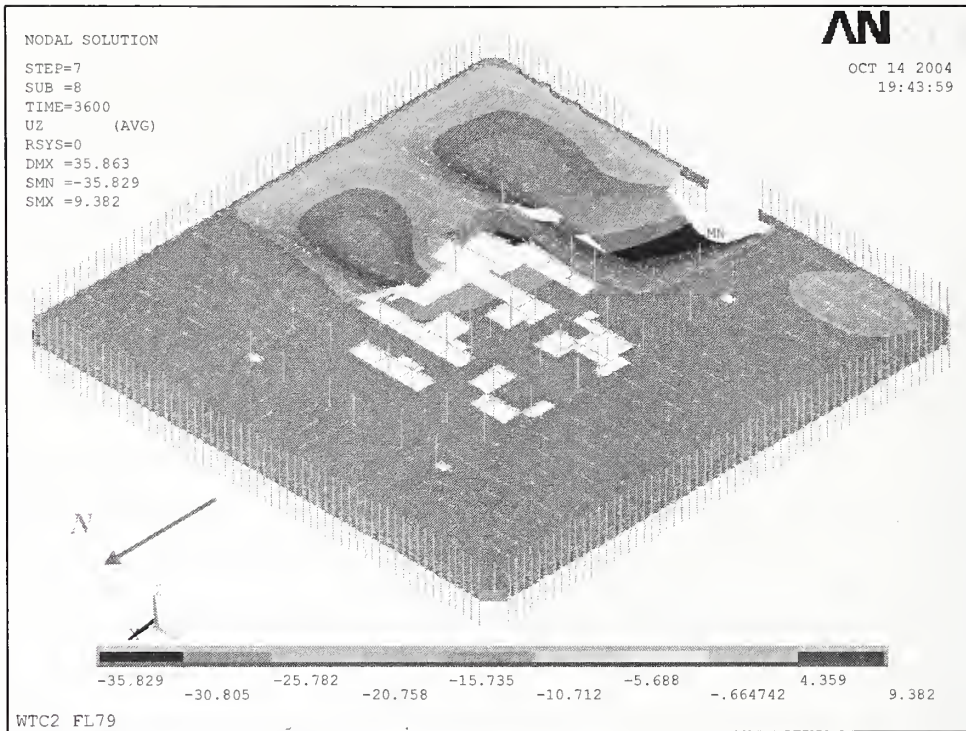


Figure 7-23. Vertical deflection of WTC 2 Floor 79 for Case D<sub>i</sub>.

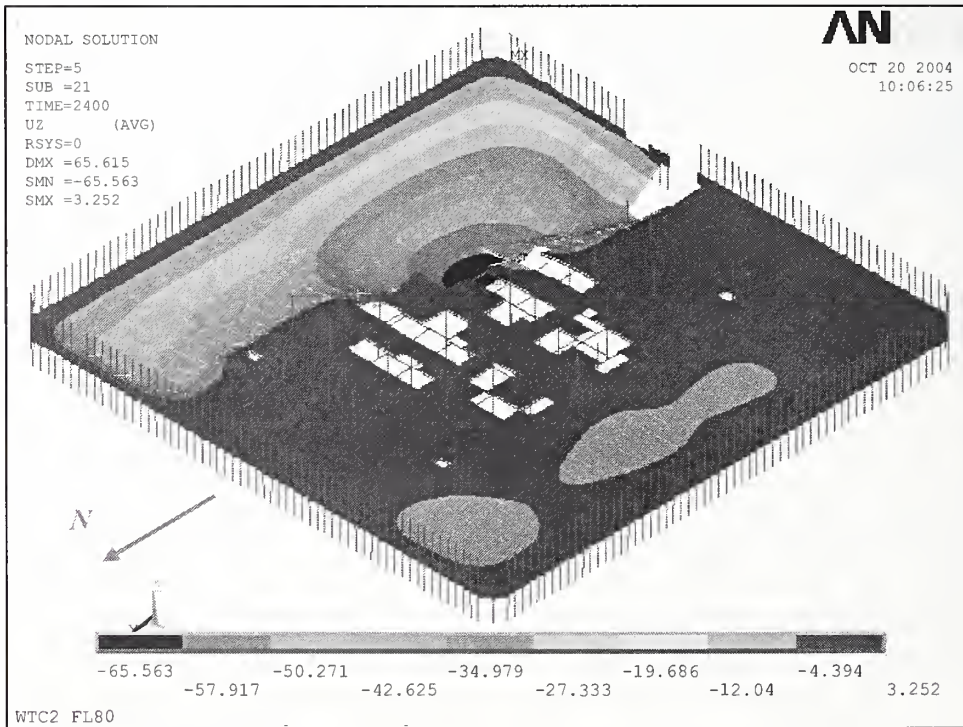


Figure 7-24. Vertical deflection of WTC 2 Floor 80 for Case D<sub>i</sub>.

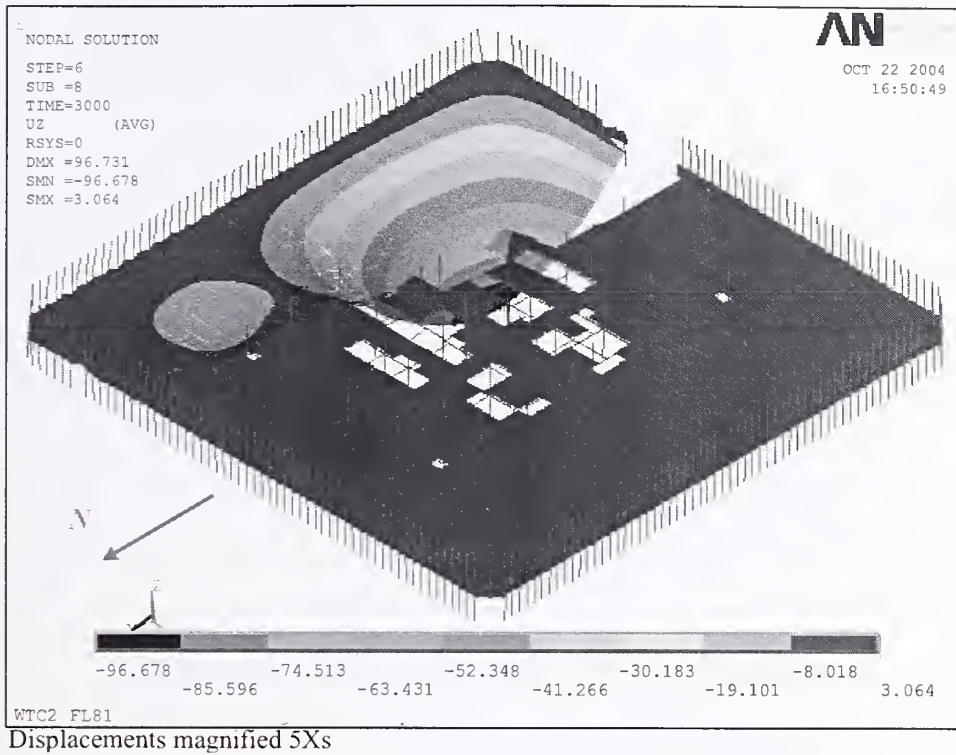


Figure 7–25. Vertical deflection of WTC 2 Floor 81 for Case D<sub>i</sub>.

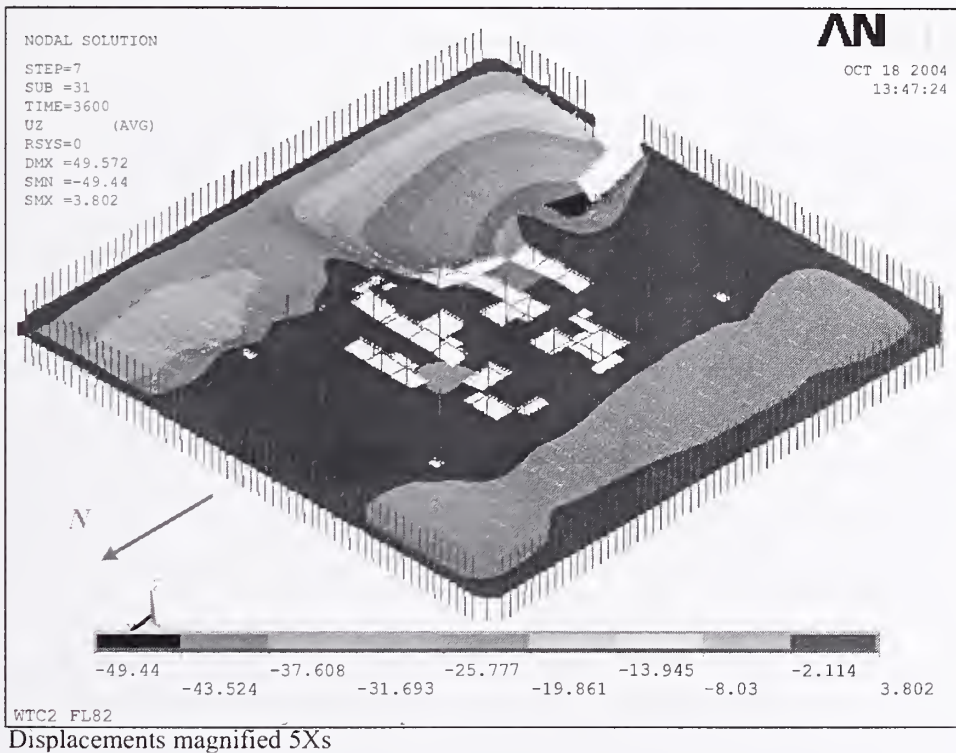


Figure 7–26. Vertical deflection of WTC 2 Floor 82 for Case D<sub>i</sub>.

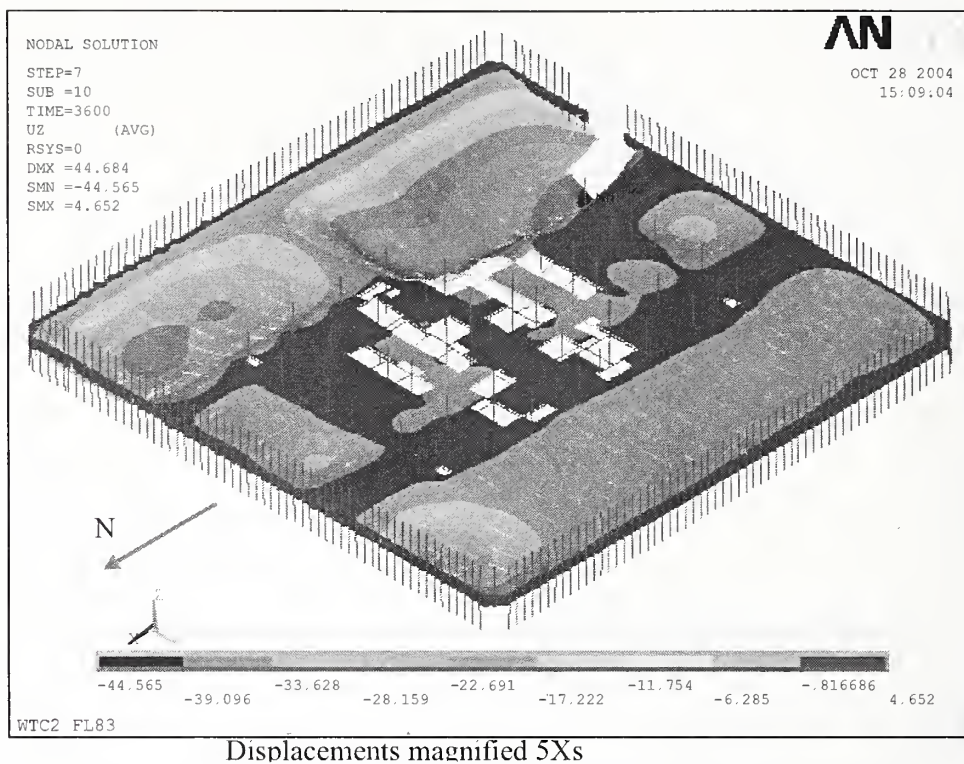


Figure 7–27. Vertical deflection of WTC 2 Floor 83 for Case D<sub>i</sub>.

## 7.4 EXTERIOR WALL SUBSYSTEM

The primary function of the exterior walls of the WTC towers was to resist wind loads, but they also carried approximately 50 percent of the building gravity loads. For the WTC tower response to impact damage and ensuing fires, the performance of the exterior wall under gravity loads was of interest and is addressed in this section. NIST NCSTAR 1-2 addresses the performance of the exterior wall under gravity and wind loads.

The exterior wall was assembled with panels that were 3 stories high and 3 columns wide with spandrel beams at each floor level. Adjacent panels were staggered by one floor to avoid alignment of the bolted panel connections across a given floor level. Panel geometry was generally uniform at the upper stories of the towers, but the steel grade and plate thickness varied within and between panels, depending upon a panel's location in the tower face. Examination of structural drawings showed that the plates at the impact floors had the same yield strength. Therefore, in the translation process, all plates in the same column cross section were considered to be of the same material. Panel connections were designed for compressive and tensile loads.

Floor trusses were attached to every other column, with the same set of columns loaded at every floor. The exterior columns and deep spandrel beams resulted in a rigid frame that was efficient at redistributing loads in the plane of the wall. The columns redistributed their loads within three to four floors. The floors and spandrels provided lateral support to the exterior columns. Loss of lateral support through failed floor connections increases the possibility of column instability (buckling), depending upon a column's load and temperatures. The hat truss was connected to each exterior wall at Floor 108 with four

truss members extending from the core perimeter. The hat truss provided a load path between the core and exterior walls. As discussed previously, the hat truss was the primary load path between the core and exterior walls, and the floors provided a secondary load path.

The analysis of a single exterior face provided insight into the conditions that would result in the inward bowing of the south wall of WTC 1 and the east wall of WTC 2 observed in photographs (see Chapter 6). Conditions examined included pull-in forces resulting from sagging floors, disconnected floors resulting from truss seat failure, additional vertical loads simulating load transfer to the exterior wall, and elevated temperatures.

#### 7.4.1 Finite Element Model and Methods of Analysis

The exterior wall models extended over 18 floors for the full width of a single face and were centered around the areas of impact and fire damage. The south face of WTC 1 extended from Floor 89 to Floor 106, and the east face of WTC 2 extended from Floor 73 to Floor 90, as shown in Fig. 7–28. The exterior panel that was severed during the aircraft impact and found south of the tower was removed from the south face of WTC 1. No structural damage to the panels was observed on the east wall of WTC 2. The same boundary conditions were applied for both exterior wall models, shown in Fig. 7–29. Springs were included at the base of the global models to represent the response of the exterior wall below the model. The exterior wall models included temperature-dependent plasticity, creep, and plastic buckling behavior.

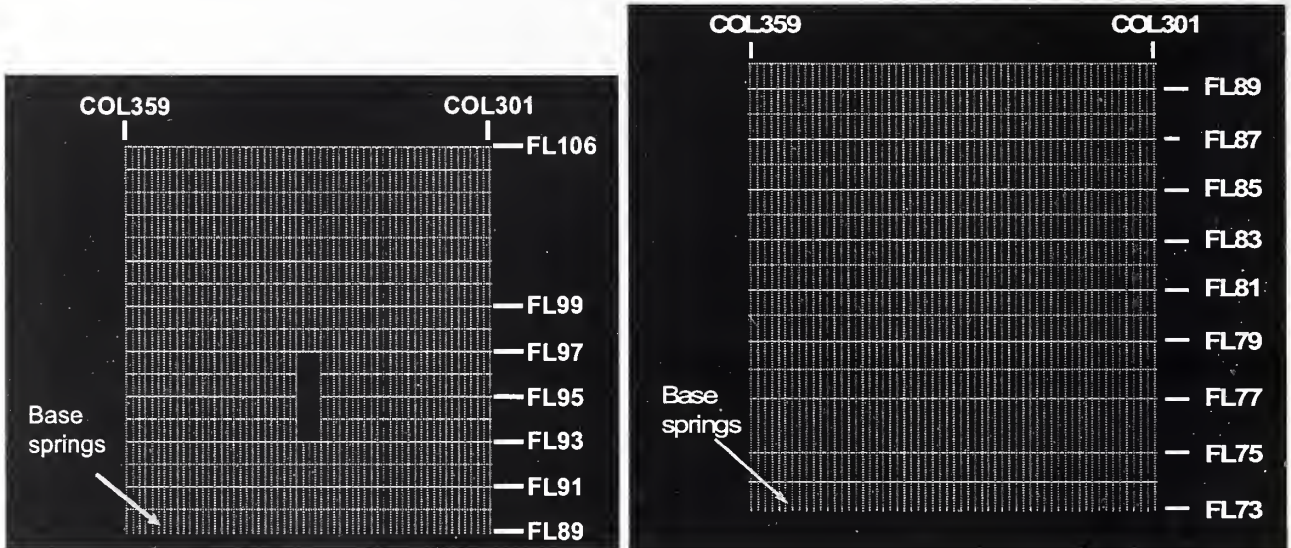
The exterior wall models were first analyzed for gravity loads with aircraft impact damage. The loads in the columns right after aircraft impact included a set of axial forces at the top of the isolated wall model that accounted for the columns above the top of the model. These loads were taken from an initial global model that did not include creep or column buckling. This global model is further described in NIST NCSTAR 1-6C. Floor gravity loads were also applied at each column with a floor connection.

The exterior wall models were then subjected to two temperature conditions for each tower: Case A and Case B for WTC 1 and Case C and Case D for WTC 2. Elevated temperatures were applied to the wall structure in 10 min intervals, as described previously. At the beginning of each 10 min interval, floor connections were either (1) disconnected where observed in photographs and videos or computed in the full floor analyses, or (2) loaded with an inward force where inward bowing was observed during that time interval. At later stages of the WTC 2 analysis, where additional floor disconnection occurred, the inward pull at that connection was removed.

Temperatures of structural components were based upon the combined effects of member size, fireproofing damage, and fire size and duration. For the exterior columns and spandrels, the interior face was heated directly by fires through radiation and convection and the adjacent faces were heated through conduction and cooled by convection. Elevated temperatures caused thermal expansion of heated columns and modified the stresses in affected and adjacent structural members. Elevated temperatures above 400 °C to 500 °C resulted in a reduction of load-carrying capacity and an increase in plastic and creep deformations.

Inward pulling forces were estimated through a trial and error procedure. In each trial, a magnitude of inward pull force was assumed and the model results were checked. The magnitude was kept constant until the end of the analyses unless a floor connection became disconnected (see Section 7.3), at which point the inward pulling force was set to zero. The inward bowing displacements were compared to the

displacements measured from photographs at the same time points. The wall response was significantly affected by accumulated plastic and creep strains, which were themselves functions of temperature and inward pull over time.



Model of WTC 1 south wall

Model of WTC 2 east wall

Figure 7–28. Isolated exterior wall segments from WTC 1 and WTC 2.

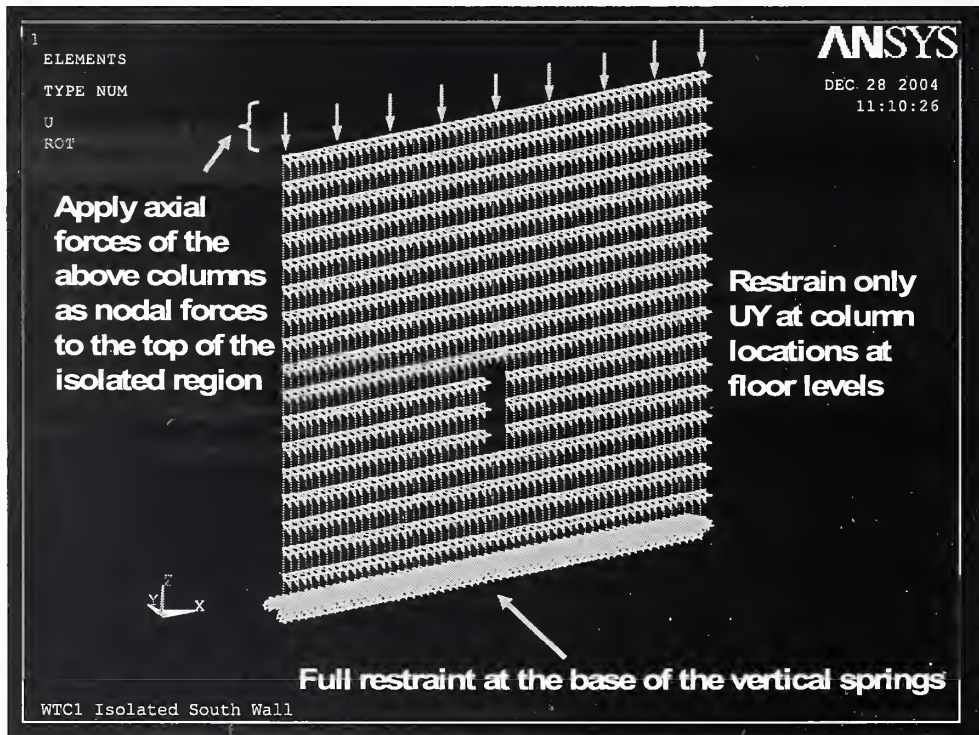


Figure 7–29. Boundary conditions applied on the isolated exterior wall segment.

## 7.4.2 WTC 1 Analysis Results

The magnitude and distribution of inward pull forces on the south wall, which resulted in inward bowing similar to that observed in photographs, were estimated from the WTC 1 exterior wall subsystem analyses. The final magnitude thus obtained was used in the WTC 1 global analysis.

Initial trials with Case A and Case B damage and temperatures limited pull-in forces to areas with floor sagging sufficient in the full floor models to cause pull-in forces. However, such limited areas of pull-in forces did not produce results that were consistent with the observed inward bowing. This was primarily due to the lack of fireproofing damage to the south exterior wall and floor truss on the south side in Case A impact damage estimates. With the thermally equivalent 2.2 in. of fireproofing intact on the south trusses, these trusses did not heat appreciably, and the floors did not sag.

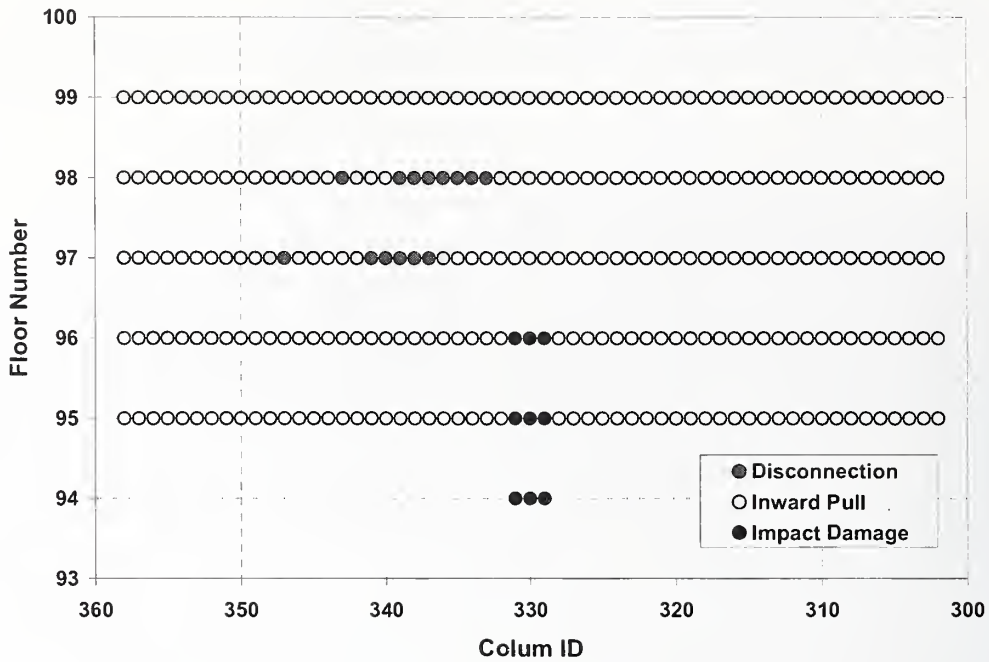
Case B had elevated temperatures for the south floor trusses and exterior columns where fireproofing was damaged between Floors 94 and 98. A second set of trials applied a pull-in force uniformly across Floors 95 to 99, except where the floor connections had failed. This extent of pull-in forces from floor sagging was greater than that shown by the full floor analyses, but produced a better estimate of the inward bowing as evidenced from the photographs. The smaller extent of floor sagging in Floors 95 to 99 that was predicted by the full floor analyses was likely due to the conservative estimates of fireproofing damage. This assumption produced a lower bound on the bare steel surface area, thereby making it more difficult to heat the steel to the point of failure. Greater fireproofing damage from structural accelerations caused by the aircraft impact and subsequent vibrations as well as possible damage to the concrete slab from high thermal gradients near the slab surface may have contributed to the more extensive inward bowing of the exterior wall that was observed.

In one trial, the magnitude of the pull-in force was increased over time until the wall became unstable at 90 min. When the magnitude of the pull-in force reached 9.37 kip per column, the analysis stopped due to non-convergence. At the end of analysis, the maximum inward bowing was 24.7 in.

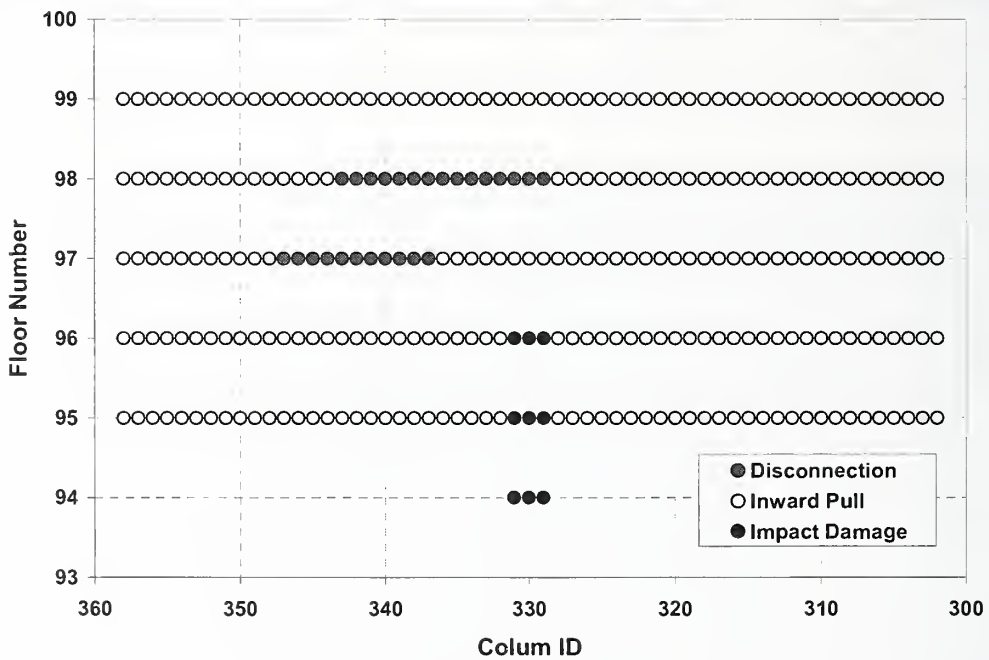
In another trial, the effect of thermal loading in combination with pull-in forces was examined. Pull-in forces were applied at 80 min, since temperatures on the south side began to increase around that time, and the thermal loading was continued to 100 min. In this analysis, the magnitude of the pull-in force was set to 6 kip per column so that the wall would not become unstable as a result of pull-in forces alone.

Figure 7-30 shows the locations of floor disconnections and pull-in forces. After applying a 6 kip pull-in force per column from 80 min to 100 min, the maximum inward bowing increased from 12.2 in. to 31.3 in., as shown in Figs. 7-31 and 7-32. This analysis demonstrated that the thermal softening increased existing inward bowing. Analysis results also showed that, at 100 min, Columns 320 to 346 had reached their load capacity for their plastically buckled shape and steel temperatures and were shedding their loads to adjacent columns.

The maximum inward bowing of 31 in. was smaller than the observed maximum bowing of 55 in., and the bowed wall was still stable in the analysis at 100 min. The magnitude of pull-in forces was expected to be less than 6 kip in the global analysis with the addition of gravity loads from the core subsystem as it also weakened; therefore, pull-in forces of 4 kip to 5 kip were used in the global model analyses.



(a) Between 80 min and 90 min



(b) Between 90 min and 100 min

Figure 7–30. Locations of WTC 1 disconnections and pull-in forces over five floors for Case B.

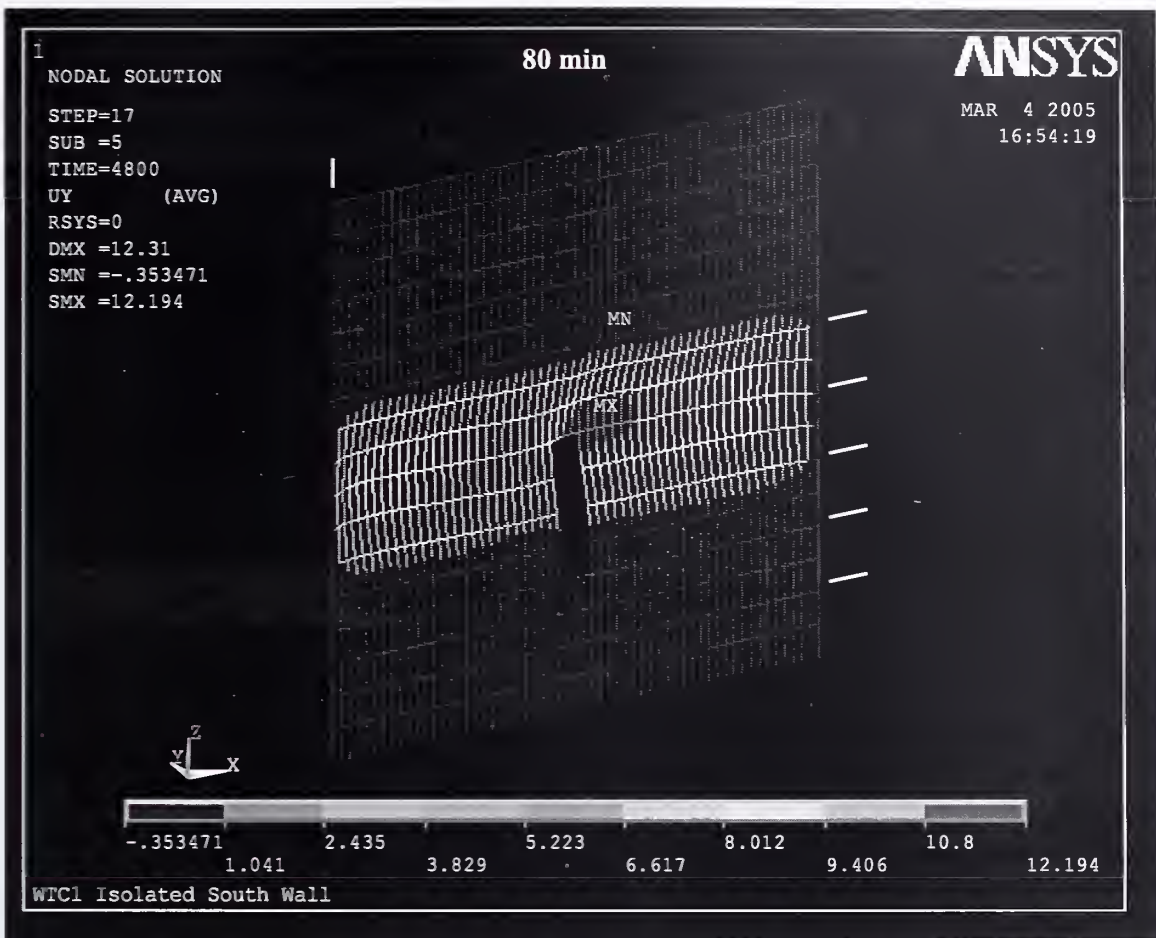
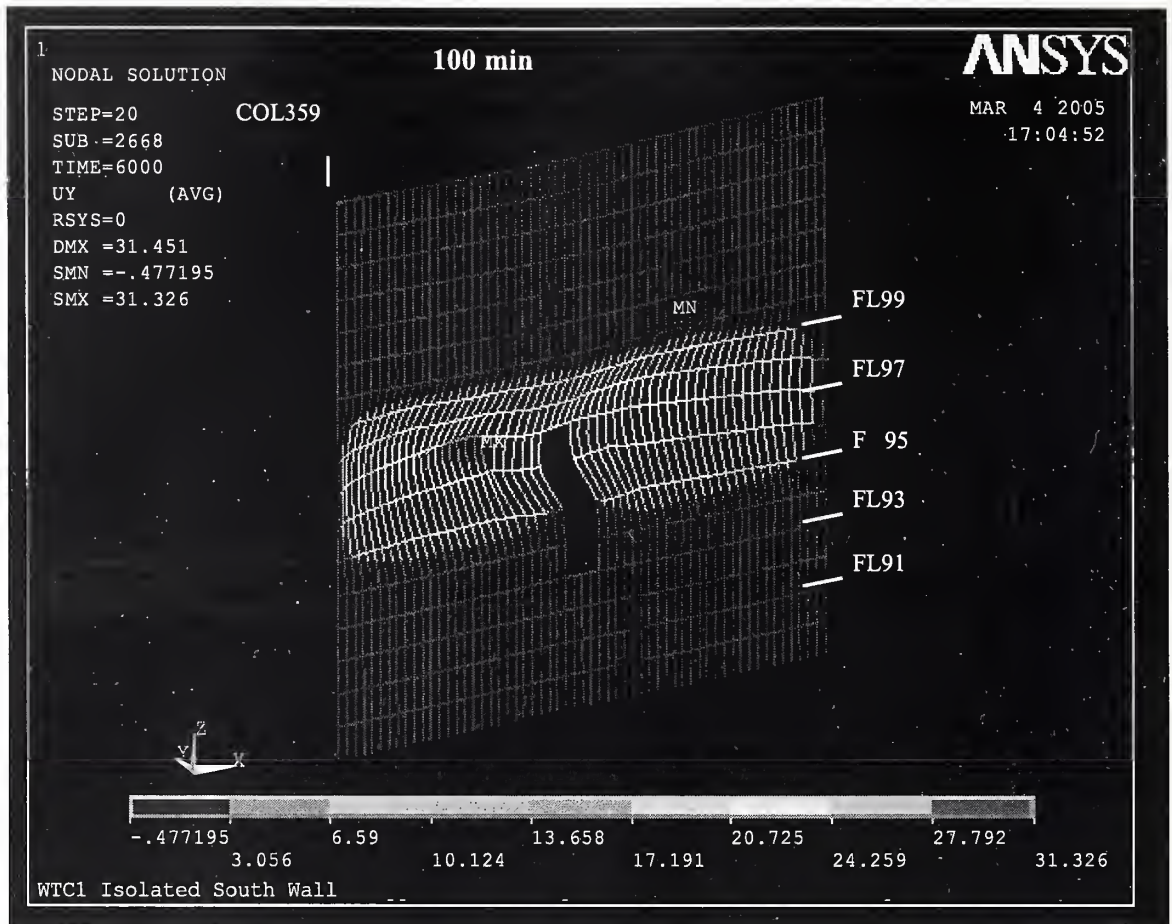


Figure 7-31. Inward displacement of the WTC 1 south wall at 80 min of the Case B temperatures with floor disconnections and 6 kip pull-in forces over five floors.



**Figure 7–32. Inward displacement of the WTC 1 south wall at 100 min of the Case B temperatures with floor disconnections and 6 kip pull-in forces over five floors.**

### 7.4.3 WTC 2 Analysis Results

The magnitude and distribution of inward pull forces on the east wall, which resulted in inward bowing similar to that observed in photographs at approximately 20 min and 50 min after the aircraft impact, were estimated with these analyses. The final estimated magnitude and distribution was used in the WTC 2 global analysis.

Initial trials with Case C and Case D damage and elevated temperatures limited pull-in forces to areas with floor sagging sufficient in the full floor models to cause pull-in forces. However, such limited areas of pull-in forces did not produce results that were compatible with the observed inward bowing. While damage to truss and exterior column fireproofing was similar for Cases C and D, the fire spread and growth was not the same and produced different temperature histories for structural elements. Case C full floor models sagged and had pull-in forces at the north side of the east wall, whereas Case D had floor sagging and pull-in forces at the south side of the east wall. Review of full floor model results showed that Case D temperature histories more closely matched the observed inward bowing of the east face. Case D was used for the global analyses.

A second set of trials with Case D elevated temperatures applied a pull-in force uniformly across Floors 79 to 83 of the east wall, except where the floor connections had failed. In two separate analyses, pull-in forces of 0.5 kip and 5 kip were held constant as the temperature histories were applied until the analysis failed to converge. The analysis with the 0.5 kip pull-in force failed to converge at 32 min. As shown in Fig. 7-33, the wall bowed primarily outward (positive displacement direction is inward) as the pull-in force was insufficient to cause inward bowing. The analysis with the 5.0 kip pull-in force failed to converge at 18 min. The inward bowing of the exterior wall had reached 31 in., as shown in Fig. 7-34. This value is about three times larger than the 10 in. displacement measured in photographs at this time, indicating that the assumed value of pull-in force was too large. Based on these two analyses, it was concluded that the magnitude of the pull-in force for a uniform distribution was bounded by 0.5 kip and 5.0 kip. This range for the pull-in force is of the same order of magnitude as the tension calculated from the detailed truss model (see Chapter 4).

The out-of-plane displacements shown in Fig. 7-33 at 20 min were inward on the south side and outward in the middle and north section of the wall. This difference in behavior was due to the combined effects of column temperatures and column loads across the east wall. Temperatures were higher at the middle and north half of the wall compared to the area near the southeast corner. The primary reasons for the outward bowing on the north side of the east wall are as follows: (1) the higher temperatures in the north side of the wall resulted in restrained thermal expansion and larger column loads; (2) the higher temperatures of the inside face of the columns, relative to the outside, caused higher plastic and creep strains and resulted in differential shortening of the inside relative to the outside; and (3) the plastic softening and creep of the inside caused an outward shift in the neutral axis, and a resulting outward bow of the columns.

This observation formed the basis for the next set of trials, where a step function was used to represent the distribution of pull-in forces along the east wall. In each trial, the magnitude of pull-in force for each half of the wall was assigned independently, with a higher magnitude on the north half of the east wall.

Two additional trials were analyzed. In the first trial, the magnitude of the pull-in forces was set to 1.0 kip and 4.0 kip for the south and north halves of the east wall, respectively. Figure 7-35 shows the out-of-plane displacements at 20 min and 50 min. As can be seen, the maximum inward bow calculated at 20 min was 7.5 in. and located near the middle of Floor 81. This agreed well with the measured displacements, which showed a maximum inward displacement of 10 in. near the middle of Floor 81.

The inward bowing started to decrease with time after 20 min and at around 40 min changed to outward bowing. The bowing at 50 min was mostly outward and did not agree with the measured displacements at this time. This indicated that the assumed magnitudes of the applied pull-in force were smaller than the actual pull-in force on the east wall.

In the second trial, the magnitude of the pull-in force was increased to 1.5 kip and 5.0 kip on the south and north portions of the east wall, respectively. Temperature histories were applied up to 50 min, at which point the analysis failed to converge. Figure 7-36 shows the magnitude of inward bowing at 20 min and at 50 min. The maximum inward bowing calculated at 20 min was 9.5 in. near the middle of Floor 81. This observation agreed well with the 10 in. measured displacements at that time. The inward bowing continued to increase with increasing time and reached a maximum of 37 in. at 50 min. As seen in Fig. 7-30, the location of the maximum displacements agreed well with the observations, but the calculated magnitude of 37 in. was twice as large as the measured inward displacement of 20 in.

This indicated that the magnitude of the applied pull-in force was close to the two sets of values assumed for the step function distribution, 1.0 kip to 1.5 kip and 4.0 kip to 5.0 kip on the south and north portions of the east wall, respectively. Considering the possible increase in column loads after impact for Case D conditions, a pull-in force of 1.0 kip on the south half and 4.0 kip on the north half of the east wall was selected as the initial estimate for the WTC 2 global model analysis.

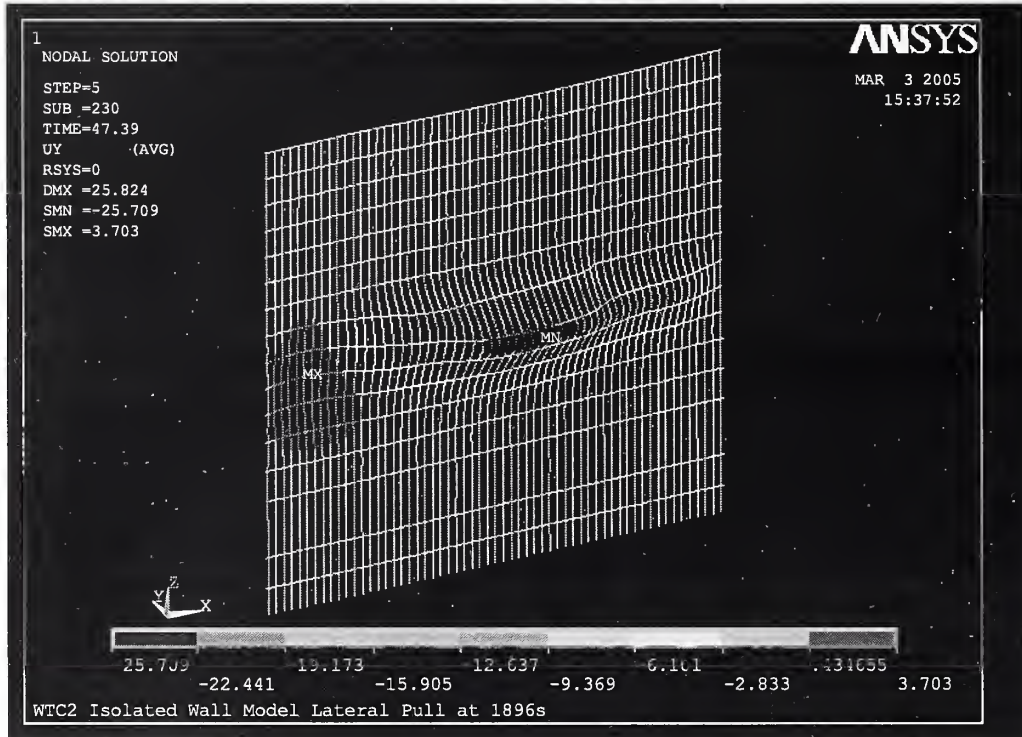


Figure 7–33. Out-of-plane displacements of the WTC 2 east wall calculated with 0.5 kip pull-in force with uniform magnitude distribution at 32 min.

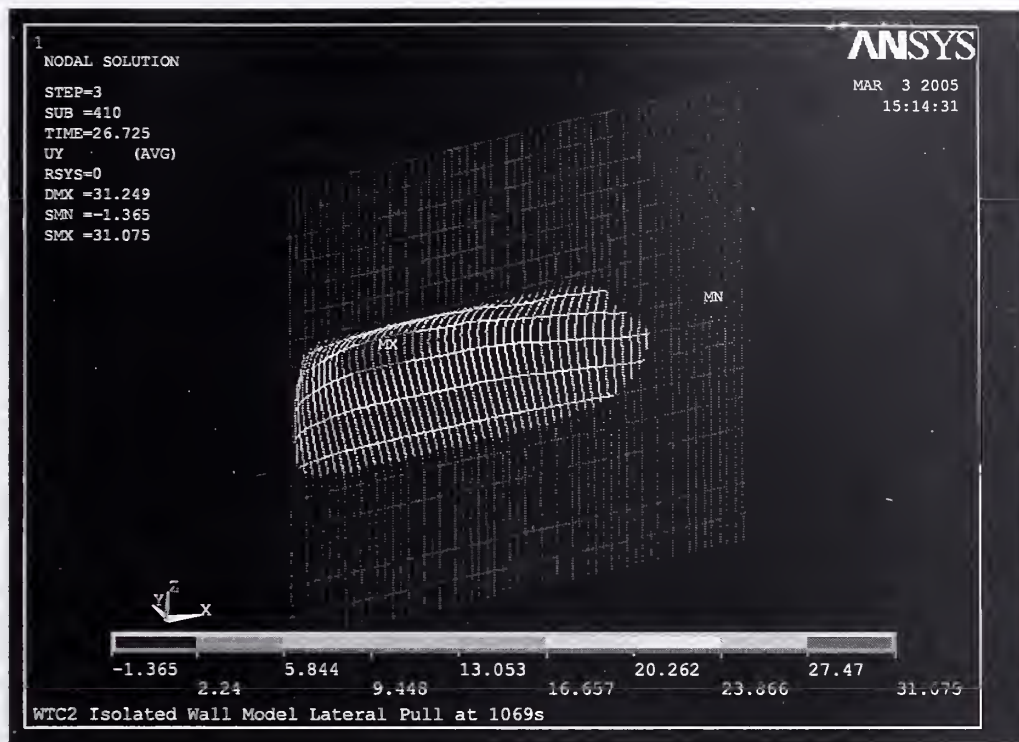
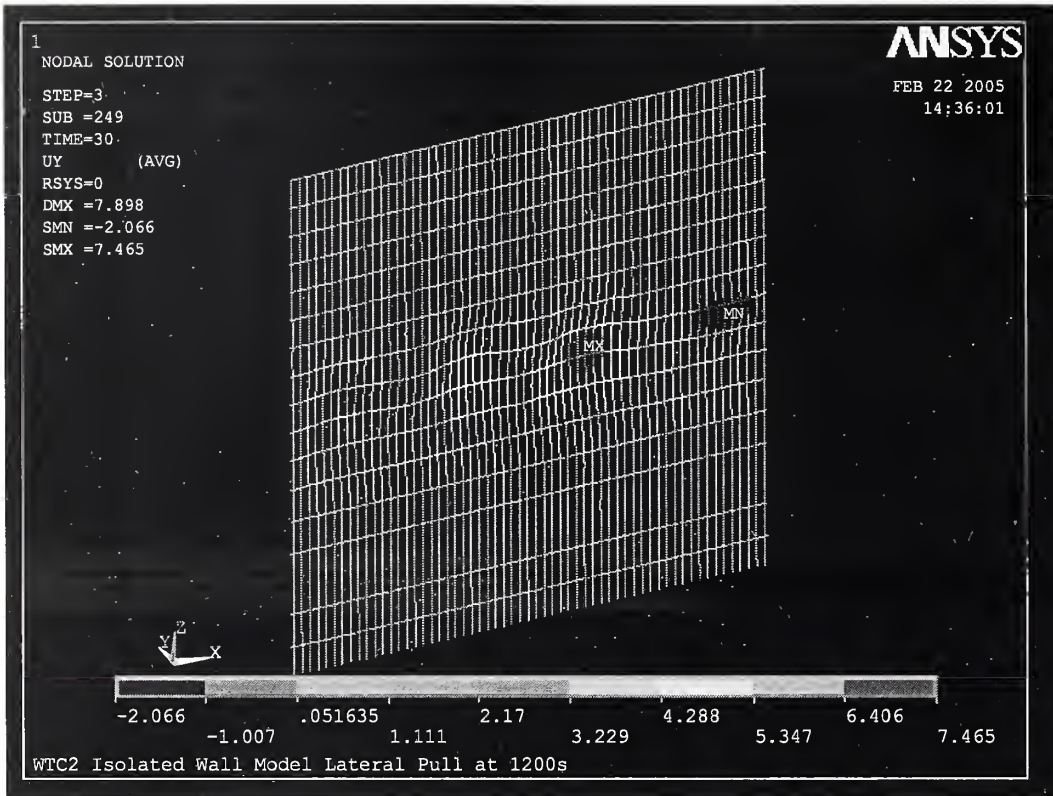
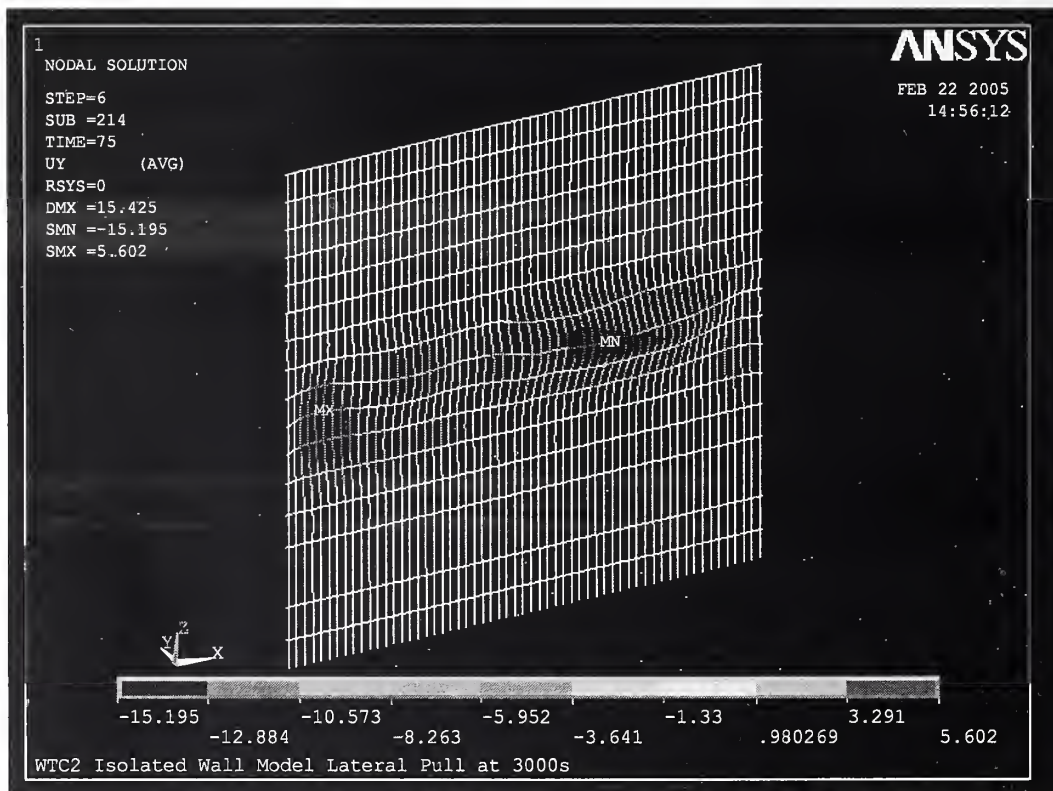


Figure 7-34. Out-of-plane displacements of the WTC 2 east wall calculated with 5.0 kip pull-in force with uniform magnitude distribution at 18 min.



At 20 min



At 50 min

Figure 7-35. Out-of-plane displacements of east wall calculated with pull-in force of 1.0 kip on the south half and 4.0 kip on the north half of the WTC 2 east wall.

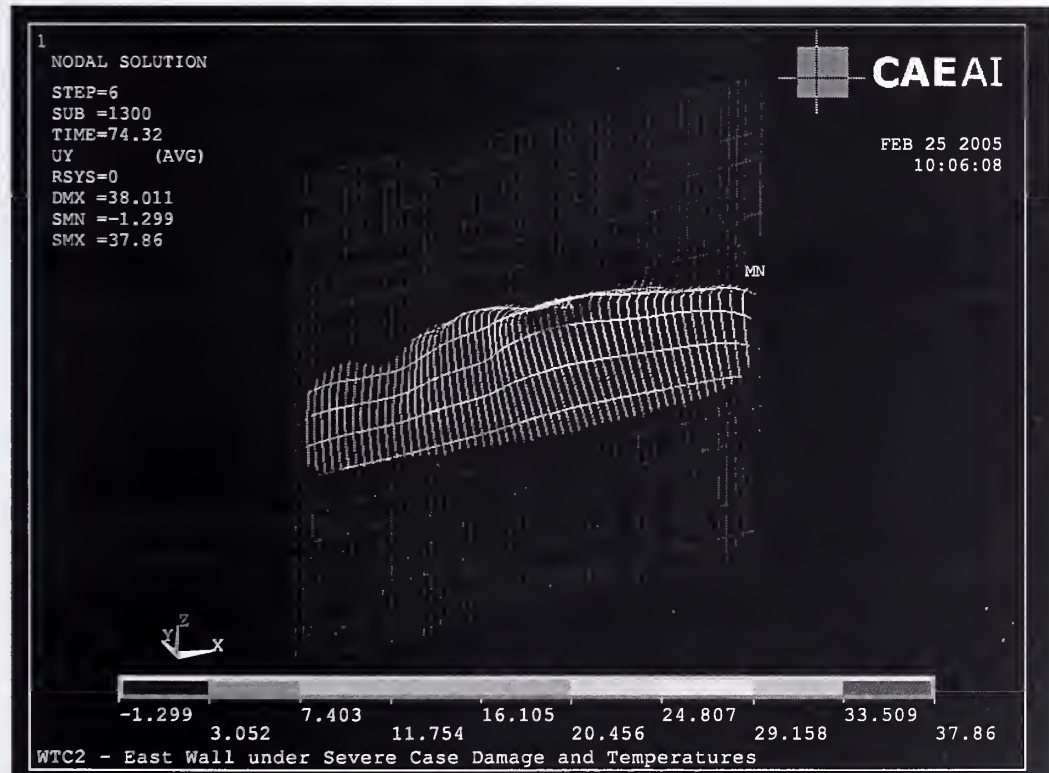
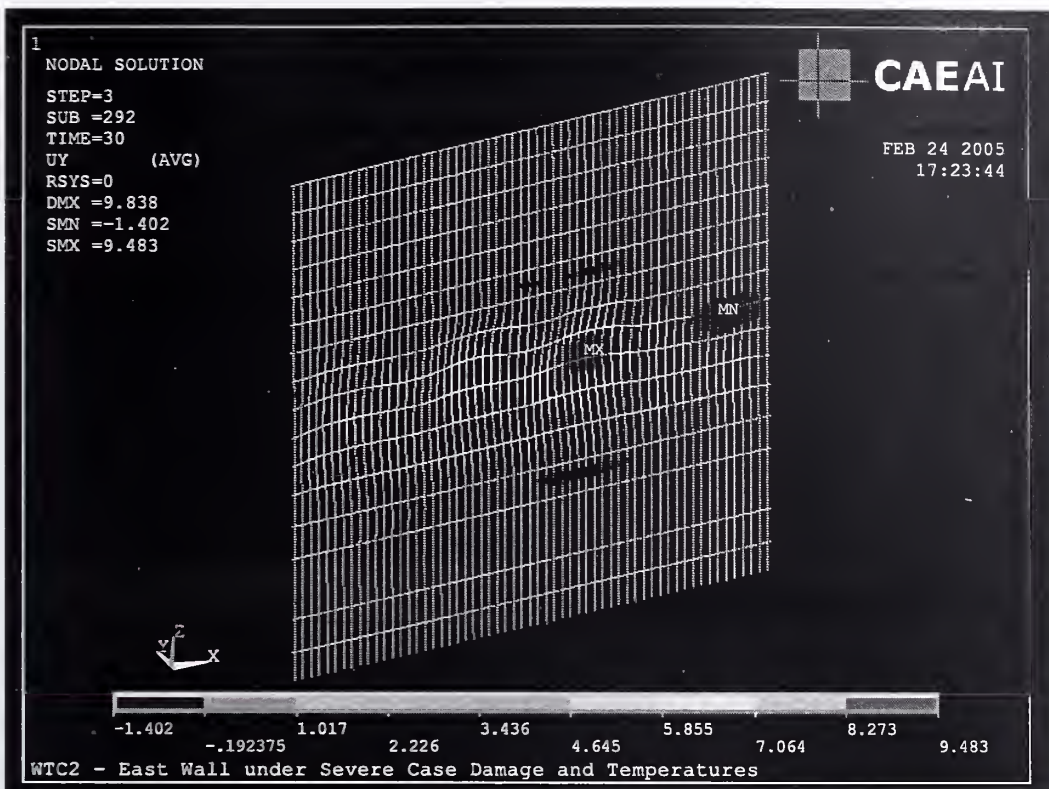


Figure 7-36. Out-of-plane displacements of east wall of WTC 2 calculated with pull-in forces of 1.5 kip on the south half and 5.0 kip on the north half.

## 7.5 SUMMARY OF SUBSYSTEM ANALYSES

The structural response of the isolated major subsystems (core, full floor, and exterior wall) to aircraft impact damage and fire are summarized here. These responses provided insight for the global model and results analysis.

### Core Subsystem

- If core column connections to the hat truss failed, the core subsystem may have experienced large vertical deflections in the local area of the connection failure due to loss of the primary load path for the redistribution of loads and subsequent column plastic buckling and/or plastic and creep deformations.
- The WTC 1 isolated core subsystem was stable with Case A aircraft impact damage and gravity loads.
- To reach a stable solution for Case C structural damage and gravity loads, the WTC 2 isolated core model required horizontal restraints to be added in the east and south directions at each floor representing the lateral restraint provided by the office area floors. Without the horizontal restraints, the WTC 2 core model tilted significantly due to the severed columns in the southeast corner of the core.
- The isolated core models did not converge for WTC 1 Case B and WTC 2 Case D structural impact damage, which had more severed columns than Case A and Case C, respectively. The core needed to redistribute loads to other areas in the global system for a stable solution with Case B and Case D damage.
- The WTC 1 isolated core subsystem with Case A impact damage and Case B temperature histories resulted in column buckling between Floors 94 and 98 and a 44 in. vertical displacement at the center of the south side of the core. The core structure was most weakened from impact and thermal effects at the center of the south side of the core. Smaller displacements occurred in the global model due to the constraints of the hat truss and floors.
- The WTC 2 isolated core subsystem with Case C impact damage and Case D temperature histories resulted in an 8.1 in. vertical displacement at the southeast corner. Without the horizontal restraints, the core would have tilted more toward the southeast corner, and the vertical displacement would have been larger. No columns buckled. The core structure was weakened from impact and thermal effects at the southeast corner and along the east side of the core.

### Full Floor Subsystem

- Final damage Cases A, B, C, and D were completed after the initial set of floor analyses were conducted with Cases A<sub>i</sub>, B<sub>i</sub>, C<sub>i</sub>, and D<sub>i</sub>. The fires did not change between initial Cases A<sub>i</sub> to D<sub>i</sub> and final Cases A to D. The concrete slab temperatures were the same for the initial and final Cases. The truss temperatures changed where the fireproofing damage changed. The full floor models were not rerun for Cases A through D as comparisons showed that the

structural temperature histories of the floors were nearly identical for most floors and only slightly different for a few floors. The floor analysis results for Cases A<sub>i</sub> to D<sub>i</sub> were used for Cases A to D in the exterior wall subsystem and global analyses.

- The full floor model boundary conditions for the exterior columns constrained thermal expansion of the concrete slab, which led to high compressive forces in the slabs, even with sagging of floors.
- At lower elevated temperatures (approximately 100 °C to 400 °C), the floors thermally expanded and displaced the exterior columns outward by a few inches; horizontal displacement of the core columns was insignificant. None of the floors buckled as they thermally expanded, even with the exterior columns restrained so that no horizontal movement was allowed at the floors above and below the heated floor, which maximized column resistance to floor expansion. Even with level of column restraint, the exterior columns did not develop a sufficient reaction force (push inward to resist the expansion outward) to buckle any of the floors.
- At higher elevated temperatures (above 400 °C), the floors began to sag as the floors' stiffness and strength were reduced with increasing temperature and the difference in thermal expansion between the trusses and the concrete slab became larger. As the floor sagging increased, the outward displacement of the exterior columns was overcome, and the floors exerted an inward pull force on the exterior columns.
- The floors began to exert inward pull forces when floor sagging exceeded approximately 25 in. for the 60 ft floor span. This is based upon analysis results of both the detailed truss model and the full floor models (which showed a reduction in compression instead of tension at the truss connections).
- Floor sagging was primarily caused by either buckling of truss web diagonals or disconnection of truss seats at the exterior wall or the core perimeter. Except for the truss seat failures near the southeast corner of the core in WTC 2 following the aircraft impact, web buckling or truss seat failure was caused primarily by elevated temperatures of the structural components.
- Sagging at the floor edge was due to loss of vertical support at the truss seats. The loss of vertical support was caused by the reduction in vertical shear capacity of the truss seats due to elevated steel temperatures in most cases.
- When the gusset plates and bolts of the truss seat failed in the floor models due to horizontal loads, it was rare that the truss also walked-off of the seats because the thermal expansion of the floor was restrained by the exterior columns. The straps and studs at the exterior wall had been removed from the floor models, which provided additional resistance to horizontal loads; if the floor slab expansion had not been restrained by the exterior columns, the horizontal loads between the slab and gusset plate and bolt would have been reduced.
- The high surface temperatures in the concrete slabs of fire affected floors could have resulted in delamination by spalling of the slab. This would possibly compromise knuckle strength,

crack the slab, or cause loss of integrity of the floor system, contributing to greater floor sagging.

- Case B impact damage and thermal loads for WTC 1 floors resulted in floor sagging on the south side of the tower over floors that reasonably matched the location of inward bowing observed on the south face. Case A impact damage and thermal loads did not result in sagging on the south side of the floors.
- Case C and Case D impact damage and thermal loads for WTC 2 both resulted in floor sagging on the east side of the tower over floors that reasonably matched the location of inward bowing observed on the east face. However, Case D provided a better match.

### Exterior Wall Subsystem

- Inward forces were required to produce inward bowing that was consistent with displacements measured from photographs. The inward pull was caused by sagging of the floors. Heating of the inside face of the perimeter columns also contributed to inward bowing. Thermal expansion occurred as soon as steel temperatures began to rise; column shortening occurred when creep and plastic strains overcame thermal expansion strains, typically at temperatures greater than 500 °C to 600 °C with accompanying high stresses and duration of temperatures and stress levels.
- Models of exterior wall sections bowed outward in a pushdown analysis when several consecutive floors were disconnected, the interior face of the columns was heated, and column gravity loads increased (e.g., due to load redistribution from the core and hat truss). At lower temperatures, thermal expansion of the inside face was insufficient to result in inward bowing of the entire exterior column. At higher temperatures, outward bowing resulted from the combined effects of reduced steel strength on the heated inside face, which shortened first under column gravity loads, and the lack of lateral restraint from the floors.
- The observed inward bowing of the exterior wall indicated that most of the floor connections must be intact to cause the observed bowing.
- The floor levels predicted to have damaged fireproofing in the aircraft impact analysis matched well with the floors that were identified from photographic and video analysis to have participated in the inward bowing of the exterior walls.
- The extent of floor sagging required at each floor was greater than that predicted by the full floor models. The estimates of the extent of sagging at each floor were governed by the combined effects of fireproofing damage and fire; fireproofing damage was limited to areas subject to direct debris impact. Other sources of floor damage from the aircraft impact and fires (e.g., fireproofing damage from structural accelerations at impact and subsequent strong vibrations or floor damage from concrete cracking and spalling from thermal effects) were not included in the floor models.
- The exterior wall models were used to estimate the pull-in force magnitude and locations for each tower that would produce the observed bowing of the exterior wall.

- The WTC 1 isolated exterior wall analysis found that an inward pull force of 6 kip at each column at Floors 95 to 99, starting 80 min after the aircraft impact, caused a maximum inward bowing of 31 in. This inward deflection was smaller than the observed maximum bowing of 55 in., and the bowed wall was stable at 100 min. The magnitude of pull-in forces was expected to be less than 6 kip in the global analysis with the addition of gravity loads from the core subsystem as it also weakened; therefore, pull-in forces of 4 kip to 5 kip were used in the global model analyses.
- The WTC 2 isolated exterior wall analysis found that an inward pull force of 1.0 kip to 1.5 kip and 4.0 kip to 5.0 kip on the south and north portions of the east wall, respectively, over Floors 79 to 83, caused a maximum inward bowing of 9.5 in. at 20 min and 37 in. at 50 min. The observed deflections were 10 in. and 20 in., respectively. Considering the possible increase in column loads after impact for Case D conditions, a pull-in force of 1.0 kip on the south half and 4.0 kip on the north half of the east wall was selected for the initial estimate for the WTC 2 global model analysis.

This page intentionally left blank.

# Chapter 8

## STRUCTURAL RESPONSE OF THE WTC TOWERS TO AIRCRAFT IMPACT DAMAGE AND FIRE

---

### 8.1 INTRODUCTION

Prior to conducting global analysis of the structural response of each World Trade Center (WTC) tower, a tremendous amount of input data was obtained<sup>2</sup> and developed. Input data required for the structural response models included:

- Reference model of each WTC tower before the aircraft impact, based upon design and construction documents (NIST NCSTAR 1-2)
- Steel and concrete material properties for room and elevated temperatures (NIST NCSTAR 1-3 and Chapter 4)
- Structural damage to columns and floors from the aircraft impact (NIST NCSTAR 1-2 and Chapter 5)
- Passive fire protection conditions before and after impact (NIST NCSTAR 1-6A and Chapter 5)
- Temperature histories for all structural elements in the impact zone (NIST NCSTAR 1-5)
- Observed structural conditions and events from photographic and videographic records (NIST NCSTAR 1-5A and Chapter 6)

Input data was based on available records. For data that were not directly available, analytical and experimental results were used to develop the required information. The tower design and construction and the supplied structural materials were well documented. The passive fire protection conditions before impact were less well documented, but review of Port Authority of New York and New Jersey (PANYNJ) records and interpretation of photographs (from several sources throughout the life of the structure) provided a documented basis for determining the likely conditions that existed in both towers before September 11, 2001. Steel and concrete temperature-dependent properties were developed from available technical literature and from tests of samples recovered from the collapse site (steel tests were conducted at National Institute of Standards and Technology (NIST) and concrete tests were conducted at Simpson Gumpertz & Heger, Inc. (SGH) under contract to NIST) to assess conformance with specified properties. Temperature histories were developed from fire dynamics simulations and thermal analyses conducted at NIST. The observed structural conditions and events defined the known events that occurred that day. The structural response analyses helped determine the probable collapse sequence for each tower. These sequences were validated using the observed structural events.

---

<sup>2</sup> All information and data related to the design and construction of the WTC towers were obtained from contract drawings provided to NIST by The Port Authority of New York and New Jersey. Refer to NIST NCSTAR 1-2A for a complete description of the WTC structural system and an index of all structural drawings.

The global analyses of WTC 1 and WTC 2 used final estimates of impact damage and elevated temperatures to determine the structural response and sequence of component and subsystem failures that led to collapse initiation. Case B was used for WTC 1 and Case D was used for WTC 2 used, as described in previous chapters.

The global models and required input data are discussed in Section 8.2. The analysis methodology is presented in Section 8.3, and the results of the global analyses for WTC 1 and WTC 2 are presented in Sections 8.4 and 8.5, respectively. To better understand the relative contributions of impact damage and fire to each tower collapse initiation, the hypothetical condition of the towers subjected to the same fires without aircraft impact damage is discussed in Section 8.6.

## **8.2 GLOBAL MODEL OF TOWERS**

### **8.2.1 Model Description**

The global model of each tower, which was used to determine the structural collapse sequence, was based on the reference structural models developed for baseline structural analyses of the towers (NIST NCSTAR 1-2). The reference models were developed with SAP2000 and were used as a common basis for the aircraft impact analysis, using LS-DYNA, and the structural response analysis, using ANSYS.

The SAP2000 global models were more detailed than models typically used for structural design purposes. The models included exterior and core columns, the hat truss, and mechanical floors, but did not explicitly model the tenant floors due to model size limitations. The tenant floors were accounted for with constraint equations and concentrated floor loads at floor-to-column connection nodes.

The reference global models for WTC 1 and WTC 2 were translated into ANSYS models using an automated translator developed specifically for this effort by Computer Aided Engineering Associates, Inc. (CAEA), as a subcontractor under the NIST contract to SGH. The coordinates of the nodes, cross-sectional properties of members including orientation and offset of the cross-section, nodal loads, material properties, and member end releases were automatically converted from the SAP2000 format to the ANSYS format as described in NIST NCSTAR 1-6C.

The ANSYS models were truncated several floors below the impact floors, as previous analyses showed that the structural response below the impact area remained elastic. WTC 1 was truncated at Floor 91, and WTC 2 was truncated at Floor 77. The axial stiffness of the remaining structure below the line of truncation was replaced with equivalent elastic springs. The global models of the two towers are shown in Fig. 8-1.

The truncated ANSYS global models were validated against the SAP2000 baseline global analyses for gravity loads. The results from the translated ANSYS global models showed good agreement with the baseline analyses: displacements were within 1.4 percent for WTC 1 and 0.7 percent for WTC 2, and base reactions were within 1.2 percent for WTC 1 and 0.3 percent for WTC 2. Based on these comparisons, it was concluded that the translation of the global models from SAP2000 to ANSYS was correct, and the ANSYS models and their derivatives were used for the global analyses. Details of the translation and validation are found in NIST NCSTAR 1-6C.

The core columns and exterior columns and spandrels were modeled with elements and features similar to those used in the isolated core and exterior wall analyses. Column analysis features included the effects of thermal expansion, plastic, and creep strains on column behavior within the global structural system. When thermally-induced strains were sufficiently large, column loads increased if they were restrained. Columns shortened and shed loads if either plastic or creep strains were large enough or if they buckled plastically. Plastic (or inelastic) buckling describes the condition where a column becomes bowed (displaced laterally between its ends) by plastic or creep strains, but continues to support a reduced axial load. As the bowing becomes larger, the column's capacity to carry load diminishes further (see Fig. 435) until the column no longer participates in carrying load in the global structure.

Floors in the global model were modeled by shell elements, which have their membrane stiffness equal to that of the full floor system. Floors in the global model functioned as diaphragms and transferred loads between the exterior wall system and the core. Office area and core floors were modeled with an equivalent floor slab thickness and modulus calculated to match the in-plane stiffness of the composite floor system, including the concrete slab, floor trusses, and the floor seats. Bending stiffness of the floor system was not matched because the floor loads were applied at the columns. Both core and office area floor slabs were modeled with linear-elastic material properties for lightweight concrete.

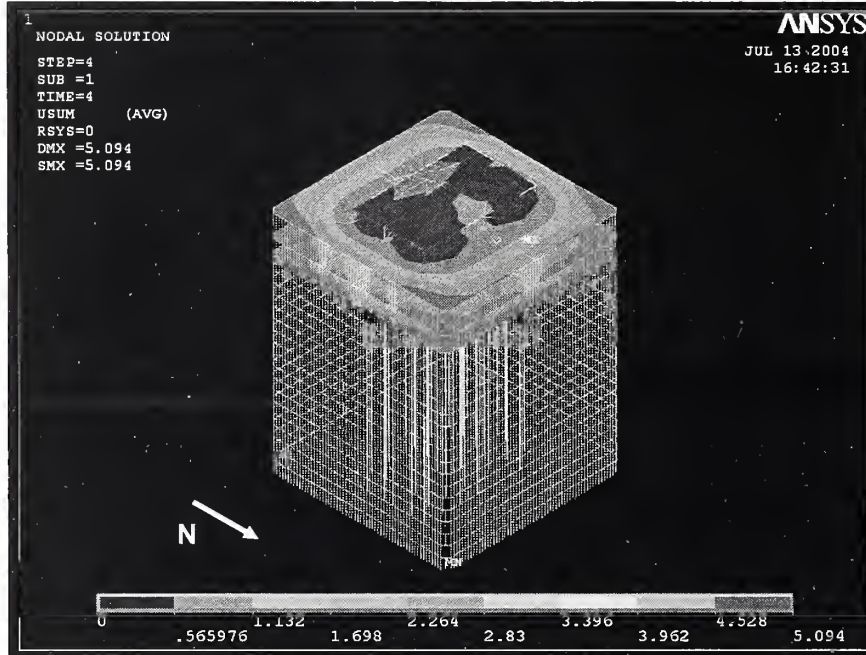
Figure 8–2 shows the model of the core and tenant floors and the core beams that had moment connections. Beams without moment connections cannot effectively transfer shear between columns without significant relative displacement and, thus, were not modeled individually. The stiffness of simply connected beams was smeared into that of the slab to capture the in-plane stiffness of the floor in the core. Inclusion of the core and office area floors was necessary for modeling force redistribution within the core and between the core and the exterior columns. The core was effective in redistributing loads from damaged core columns to adjacent core columns when the load path through the hat truss could not be developed due to either severed columns or column splices.

Floors in the global models were not intended to capture floor response and failure modes during fires. It was not practical, or in some cases not possible, to create computationally efficient global models that included all details of the floor system. The BEAM188/189 elements used in the full floor model caused severe convergence problems when creep was included and those elements experience thermally-induced buckling. Also, the extent of pull-in forces from sagging floors in the full floor models was less than estimated from the observed bowing of the exterior walls in photographs and videos because the aircraft impact damage to thermal insulation of the floors was conservatively estimated by limiting the dislodged thermal insulation to regions of direct debris impact.

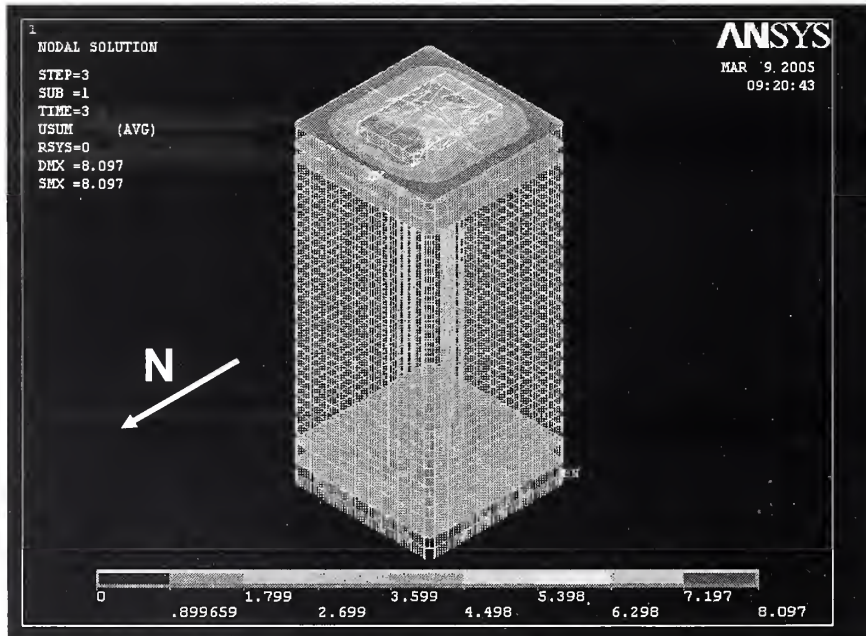
Important failure modes were identified in the truss and full floor analyses and incorporated into the global models as floor/wall disconnections and pull-in forces at appropriate time intervals. Since the full floor models did not accurately estimate the pull-in forces at floor/wall connections, the fire-induced damage obtained from the full floor model analyses were modified by observations obtained from the examination of photographs and videos performed by NIST (NIST NCSTAR 1-5A). See Chapter 7 in NIST NCSTAR 1-6C and Chapter 2 in NIST NCSTAR 1-6D for more details.

The global model included the hat truss at the top of each tower. The hat truss was designed to support an antenna on top of the towers and transmitted loads to both the core and exterior columns. The loads were distributed primarily to the core columns. There were four outriggers to each exterior wall that provided rotational restraint for the antenna under wind loads. In addition, the outriggers provided a secondary

load path between the core and exterior walls as determined from the structural response of the towers to impact damage and fires. Figure 8–3 shows the hat truss, with the outriggers labeled A through P. During the global structural response to impact and fire, the hat truss provided a primary path for transferring loads between the core columns and between the core and exterior walls.



(a) WTC 1 ANSYS Model Vertical Displacements



(b) WTC 2 ANSYS Model Vertical Displacements

Figure 8–1. Displaced shape of WTC 1 and WTC 2 at the end of gravity load analysis.

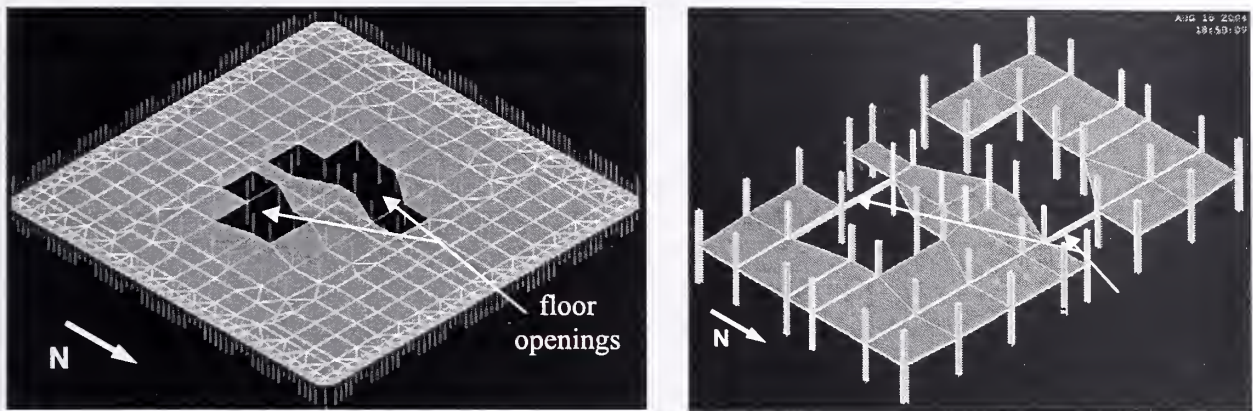


Figure 8-2. Office area and core floors and core beams.

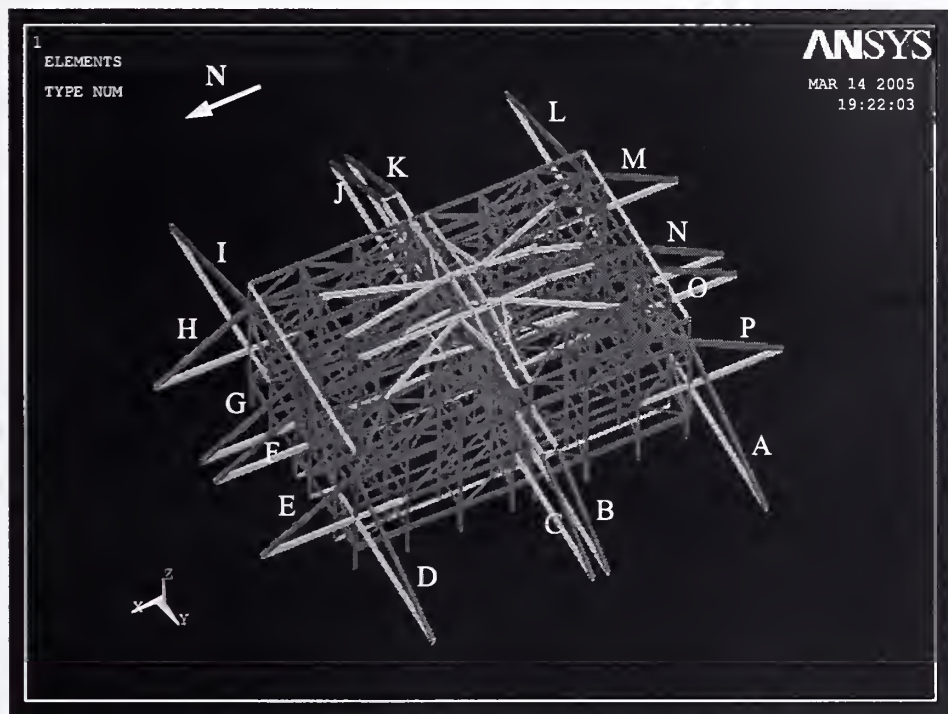


Figure 8-3. Hat truss with labeled outriggers.

### 8.2.2 Model Modifications

The validated ANSYS models were modified to incorporate nonlinear material and geometric behaviors required in areas subject to impact and fire. Modifications incorporated modeling enhancements and refined input data based on numerous component and subsystem analyses. Temperature-dependent modifications included material properties, coefficients of thermal expansion, plastic and creep strains. Nonlinear geometric behavior modifications included large displacements, plastic buckling and post-buckling of columns. Break elements were not included, based on the behaviors shown in the major subsystem analyses of the isolated core, exterior wall, and full floors. Break elements for knuckles, exterior wall bolted connections, and spandrel connections did not fail in the full floor and exterior wall

analyses. Truss seat connection failures were imposed during analyses according to the time they were calculated or observed to have occurred, rather than through use of break elements.

Preliminary global analyses had unacceptably slow rates of computation, due to the size of the models and the computational effects of temperature-dependent material properties, especially creep. To reduce the size of the global models and to increase the speed of the solution without adversely affecting the analysis results, modifications were made to the models to improve computational efficiency.

The spandrels were modeled with BEAM 188 elements which experienced convergence problems when thermal expansion caused them to buckle since there were not enough elements between two columns to capture the buckling detail. The buckling of spandrels did not compromise their ability to transfer shear and bending moment. Based on visual evidence, buckling of spandrels did not play an important role in the collapse sequence, and increasing the number of spandrel elements would have unnecessarily increased the model size. Therefore, the coefficient of thermal expansion for spandrels was set to zero, and the axial degree of freedom was released.

Since trusses were not modeled individually, the equivalent floor slab buckled easily when thermal expansion was restrained by the exterior wall. Buckling of the equivalent floor slab often caused convergence problems in the global analysis. The coefficient of thermal expansion of the floor in the office area was set to zero to eliminate the unrealistic buckling problem. Neglecting the thermal expansion of the office area floors introduced errors in bending of exterior columns between a heated floor and a cool floor. The effect of this modeling assumption was small for columns extending between two heated floors.

Neglecting the thermal expansion of the office area slabs did introduce small errors in the out-of-plane bending of columns extending between a hot floor and a cool floor, but such errors were small for columns extending between two hot floors. The error introduced by this modification was not expected to change failure modes or collapse sequence in the global analysis, because thermal expansion of floors was limited to less than a few inches (see Appendix A). The full floor models thermally expanded and pushed outward on the columns until the thermal expansion was overcome by the floor sagging and the floors pulled inward on the exterior columns.

Construction sequence was not included in the global models with creep. The effect of neglecting construction sequence was examined for both buildings. When construction sequence was not included in the analysis, the total axial loads in columns along the exterior walls increased by 7 percent to 15 percent. Similarly, the total column loads supported by the core columns decreased by about 10 percent.

The calculations showed that the outriggers in the WTC 1 simulations were more highly stressed when the construction sequence was not considered. Since it was believed that the hat truss played an important role in transferring loads in WTC 1, the yield strengths of the materials for these outriggers in WTC 1 were artificially increased to account for the incorrect increase in compressive stresses when construction sequence was not considered.

The term “super-element” in ANSYS is used for sub-structuring in an analysis, where a portion of the model with elastic behavior is condensed into a single element with a representative stiffness, damping and mass matrix. The WTC 2 model was suitable for such a simplification as the section of the building

above Floor 86 was expected to remain elastic, based on the results of the isolated core analyses and preliminary global analyses without creep strains or plastic buckling (see NIST NCTAR 1-6D).

The use of super-elements reduced the time to complete a single iteration by a factor of three. However, if at later stages of the analysis the hat truss members became inelastic, the nonlinearities associated with such inelastic behavior were not captured. A super-element cannot determine individual component behavior as the group of components is represented by a single 'super' element. Moreover, the effects of construction sequence on the load distribution between the core and wall elements could not be represented, since the birth and death option could not be used in a super-element. (Birth and death refer to the addition or removal, respectively, of an element during an analysis.) The effect of not including construction sequence was evaluated and found to introduce an error of less than 12 percent for vertical displacement. To evaluate whether the hat truss exceeded elastic limits, a separate model that included the components at and above Floor 86 in the super-element was created. The stresses in all the components were calculated at the end of each 10 min time interval and compared with their capacities.

As the use of a super-element in the WTC 2 global model precluded the application of construction sequence, construction sequence was not included in either the WTC 1 or WTC 2 global analysis. Construction sequence refers to an analysis method where the self-weight loads are applied to the structural model in steps to simulate the sequential loading that takes place as a building is constructed. When construction sequence was not included, the total column loads in each exterior wall increased by 7 percent to 15 percent, and the total core columns loads decreased by about 10 percent for both models. It was also found that the outriggers of the hat truss were more highly stressed in the WTC 1 model without construction sequence than in the translated ANSYS model which included construction sequence (see Section 8.2.1). Since the hat truss played an important role in transferring loads, the yield strengths of these outriggers in WTC 1 were increased to account for the artificially higher compressive stresses that resulted without consideration of construction sequence. The difference in the maximum displacement between the models with and without construction sequence was within 12 percent for both WTC 1 and WTC 2.

### 8.3 ANALYSIS METHODOLOGY

WTC 1 and WTC 2 global models were subjected to Case B and Case D aircraft damage and fires, respectively. The results of the isolated wall, core, and full floor analyses indicated that structural responses to Case B and Case D more closely matched observed structural behavior in photographs and videos than did Case A or Case C, respectively. Thus, Case B and Case D were chosen for the global analysis of WTC 1 and WTC 2, respectively.

The global analysis was conducted in steps. Severed and heavily damaged core columns, floors, and exterior columns and spandrels were removed from the model, and gravity loads were applied as concentrated loads at each column-floor node. Then, dead load and 25 percent of the design live loads were applied to the model without considering construction sequence. The solution for the first step, which determined the structural condition of the tower after aircraft impact, provided the initial condition for the application of temperature histories and thermally-induced structural damage.

Wind forces were not included in the global analysis of the WTC towers. Wind speeds were recorded at three nearby airports, and are shown in Table 8-1. The average wind speed on September 11, 2001,

ranged from 7 knots to 11 knots (10 mph to 13 mph). In comparison, the design wind speed was 98 mph averaged over 20 minutes at a height of 1,500 ft above ground (see Chapter 3 of NIST NCSTAR 1-2). This speed is equivalent to a 3 s peak gust wind speed of about 81 mph to 90 mph at 33 ft above ground in open terrain. Wind force is proportional to the wind velocity squared, therefore, the wind force on the towers from the 13 mph winds on September 11, 2001, were approximately two percent of the average design wind speed of 86 mph, which were negligible.

**Table 8–1: Wind speeds recorded at airports near the WTC towers on September 11, 2001.**

Airport	Time (a.m.)	Direction	Speed <sup>1</sup> (knots)	Speed <sup>2</sup> (mph)
LaGuardia (NOAA 2001a)	8:51	320	9	13
	9:51	340	9	13
John F. Kennedy (NOAA 2001b)	8:51	310	11	16
	9:51	350	7	10
Newark, NJ (NOAA 2001c)	8:51	330	8	12
	9:51	No data	No data	No data
Average Wind Speed			9	13

1. Wind speed recorded as a 20 min average at a 33 ft elevation.

2. Wind speed converted to a 3 s peak gust at 33 ft (knots (20min) \* 1.4375 = mph (3 s))

Temperature data were provided for heated structural components at 10 min intervals up to 100 min for WTC 1 and up to 60 min for WTC 2. The temperature histories were based on the combined effects of impact damage to fireproofing and fire spread and growth. The structural analysis used time steps significantly less than 10 min, as a result the temperatures were linearly interpolated between the temperatures at 10 min intervals.

Column-floor disconnections and pull-in forces that occurred during a time step were imposed at the start of the time step. In the global models, nodal couplings tied the exterior columns to the floors. The nodal couplings were removed at locations of floor/wall disconnections. If disconnections were projected to occur or were observed in visual evidence at a time intermediate to the 10 min intervals used in the analyses, for example, between 10 min and 20 min, they were imposed starting at the earlier time point, in this example, at 10 min. Once a portion of a floor was disconnected from the exterior wall, it remained disconnected for the remainder of the analysis. Similarly, pull-in forces were also applied to the global models at the beginning of the 10 min time intervals in which they were predicted to occur or were observed, and they were maintained at a constant level for the 10 min time interval.

Thermal expansion of the floors was not included in the global models. Floor analyses showed that the floors initially pushed exterior column outward by a few inches. However, significant outward bowing was not observed and several inches of outward deflection of exterior columns would not affect the global stability of the towers.

## 8.4 RESULTS OF WTC 1 ANALYSIS

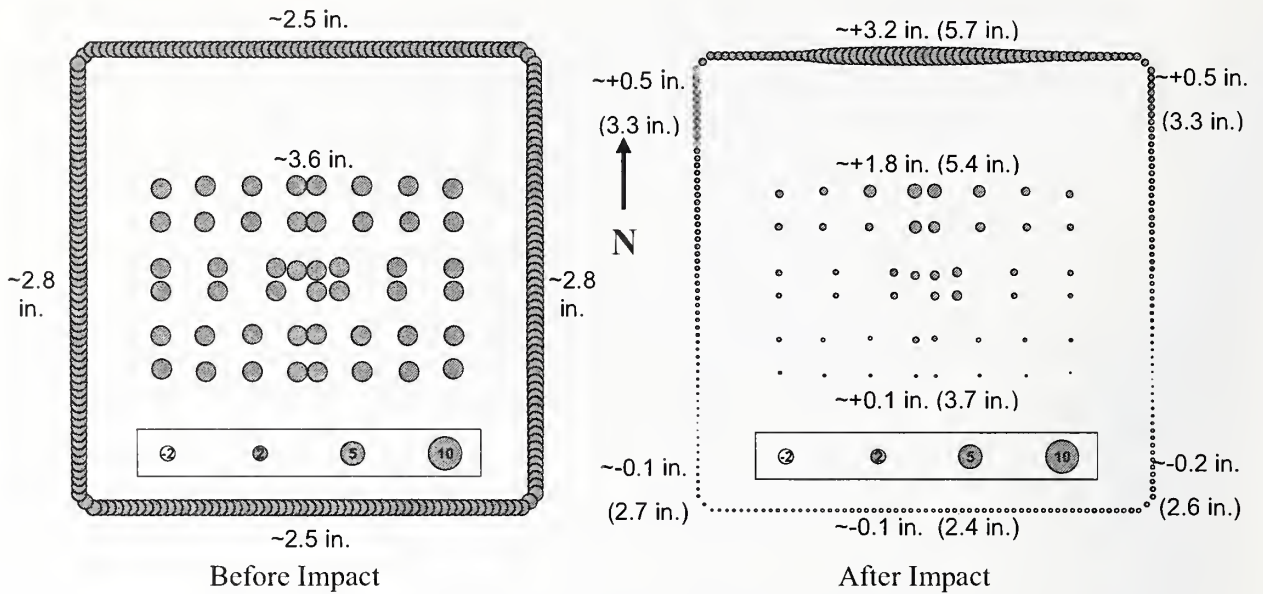
The global model of WTC 1 with creep, plastic buckling of columns, plasticity, and nonlinear geometry was analyzed with Case B structural damage and temperature histories.

### 8.4.1 WTC 1 Structural Response to Aircraft Impact Damage

Case B structural and passive fire protection damage after the aircraft impact was as follows:

- WTC 1 had 41 north exterior columns (Columns 112 to 151) severed, 9 core columns on the north central side of the core (Columns 503, 504, 505, 506, 604, 704, 706, 805, and 904), and one exterior panel of the south face (Columns 329 to 331 between Floors 93 and 96 ) severed or heavily damaged between Floors 93 and 98
- Floor slabs and framing were severed or heavily damaged in the north office floor area through to the central north region of the core on Floors 94 to 97
- WTC 1 fireproofing damage was centered primarily through the north face and floor area, the core, and into the south floor area between Floors 94 to 99.

Figure 8-4 shows the vertical displacements at Floor 99, just above the impact area, with total displacements before aircraft impact and incremental displacements after impact. Figures 8-5 through 8-8 show the vertical displacement contours of the exterior walls and the core area before and after the aircraft impact. Before the aircraft impact, the maximum vertical displacements of the exterior wall and the core at Floor 99 were 2.5 in. and 3.6 in., respectively. Due to severe impact damage on the north face and the north side of the core, WTC 1 tilted slightly to the north after the aircraft impact as can be seen in Fig. 8-4. The maximum displacement of the north wall increased from 2.5 in. to 5.7 in., and the maximum displacement of the south wall decreased from 2.5 in. to 2.4 in. The vertical displacement of the east and west wall slightly increased due to load redistribution.



Note: displacements are shown as positive downward

Figure 8-4. Vertical displacement at Floor 99 of WTC 1. Total displacements are shown before aircraft impact and incremental displacements, with total displacements in parentheses, are shown after impact.

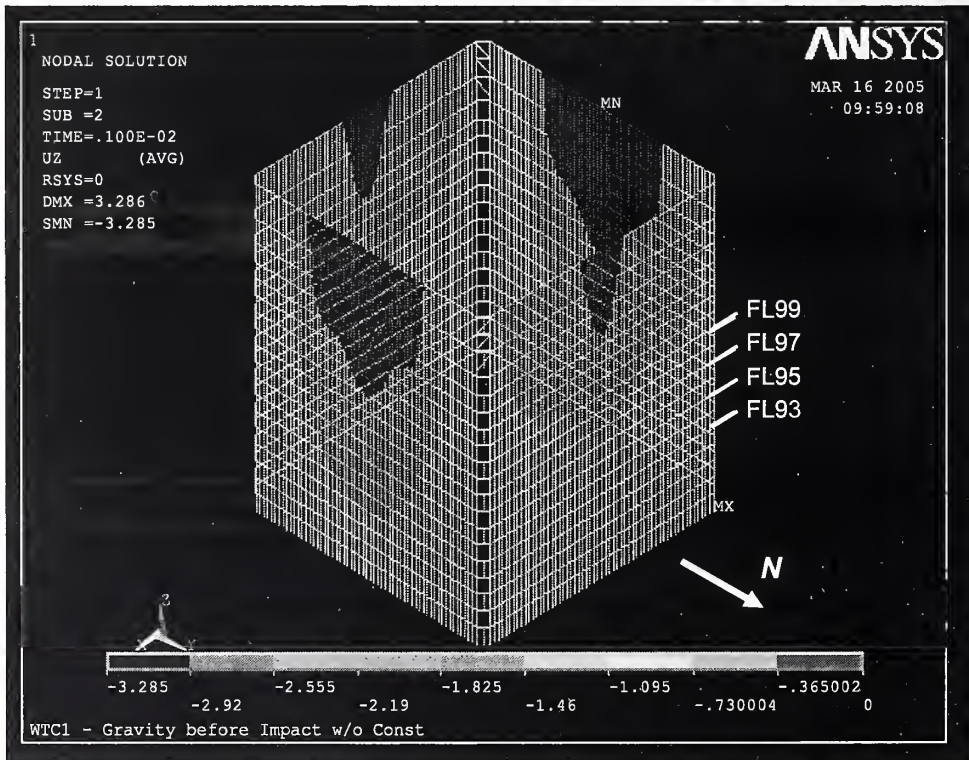


Figure 8-5. Vertical displacement of WTC 1 east and north exterior walls before aircraft impact.

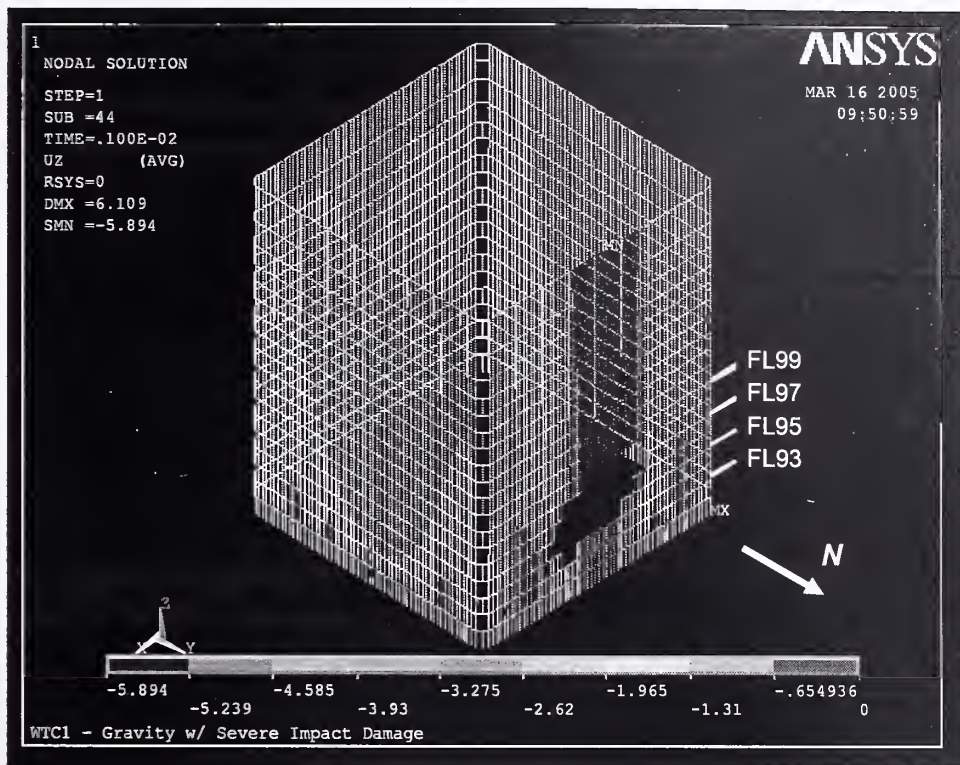


Figure 8-6. Vertical displacement of east and north exterior walls of WTC 1 after aircraft impact for Case B.

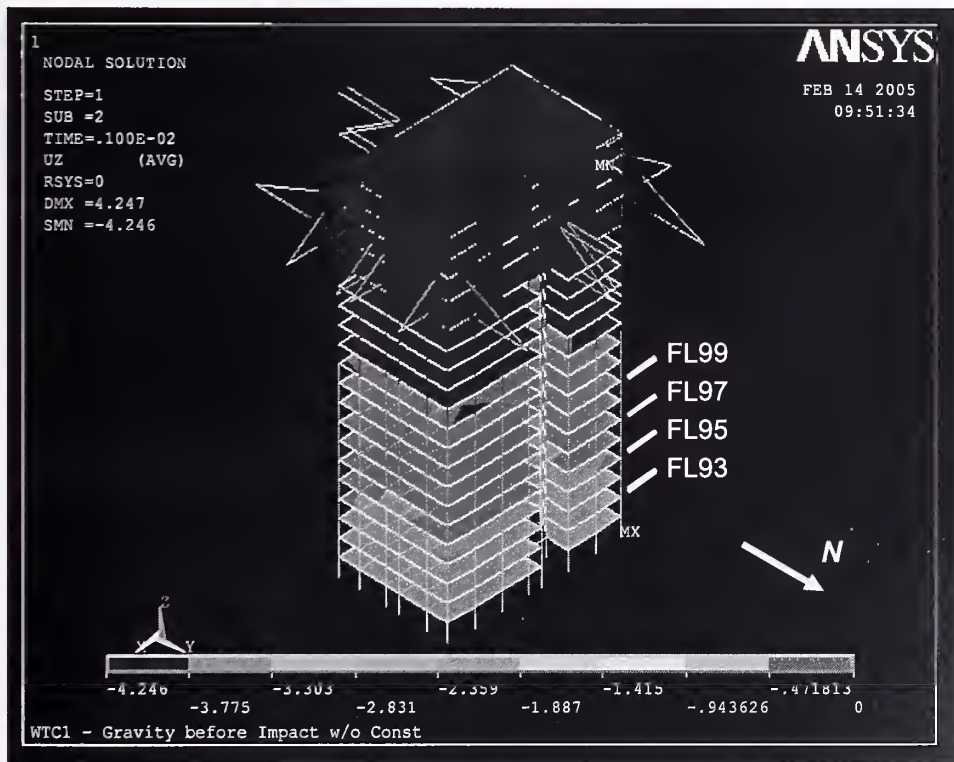
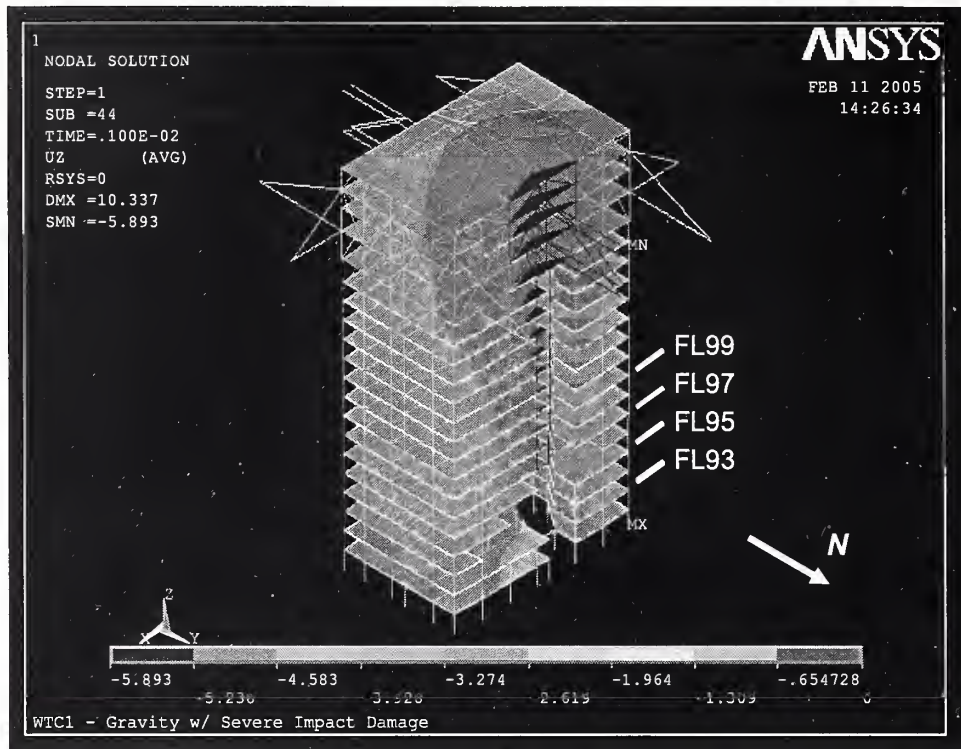


Figure 8-7. Vertical displacement of the east and north side of the WTC 1 core before aircraft impact.



**Figure 8–8. Vertical displacement of the east and north side of the WTC 1 core after aircraft impact for Case B.**

The global analysis results showed that WTC 1 did not collapse following aircraft impact, as was observed, and had considerable reserve capacity. The core columns were loaded to approximately 50 percent of their capacity prior to impact, and the exterior columns were loaded to approximately 20 percent of their capacity. The exterior columns were capable of large load transfers from the core columns.

Gravity loads were redistributed to adjacent core columns and the exterior walls, primarily through the hat truss. Figures 8–9 and 8–10 show the demand-to-capacity ratios for the core columns before and after impact. The capacity of core and exterior columns was computed as the plastic (or inelastic) buckling load according to the American Institute of Steel Construction (AISC) Load and Resistance Factor Design (LRFD) Specification procedures. Ratios less than 1.0 indicate that the column can carry additional gravity loads, whereas ratios greater than 1.0 indicate that the column is carrying more than its computed capacity and, therefore, has plastic strains. Figure 8–10 shows that only two columns had a demand-to-capacity ratio greater than 1.0, and they were adjacent to severed or heavily damaged core columns.

After the aircraft impact, gravity loads that were previously carried by severed columns were redistributed to other columns. Table 8–2 shows that the north wall at Floor 98 carried a total load of 10,974 kip before aircraft impact, and 10,137 kip after the impact. The total load lost due to aircraft impact was 837 kip, or about 7 percent of the total load. Table 8–3 shows that the north wall at Floor 105 lost 732 kip of axial force after impact. Therefore, most of the core loads (732 kip out of 837 kip) were transferred by the hat truss, and the rest were redistributed to the adjacent exterior walls by the spandrels. Due to the impact damage and the tilting of the building to the north after impact, the south wall also lost gravity loads, and about 7 percent (604 kip) was transferred by the hat truss. As a result, the east and west walls

each gained about 7 percent (466 kip and 472 kip, respectively) and the core gained about 1 percent (400 kip) through the hat truss.

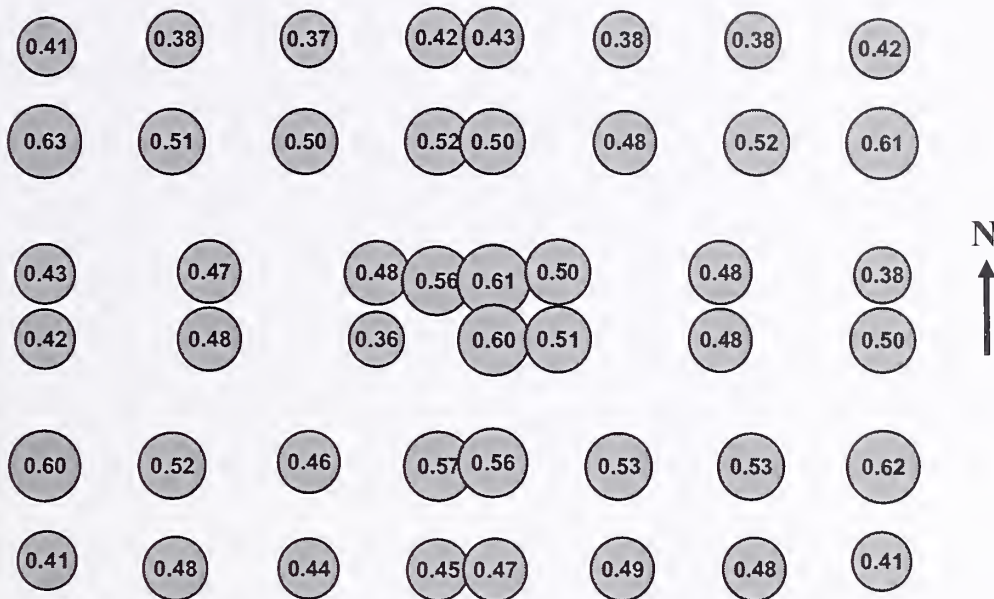


Figure 8-9. Maximum demand-to-capacity ratio for axial force in core columns between Floor 93 and Floor 99 of WTC 1 before aircraft impact.

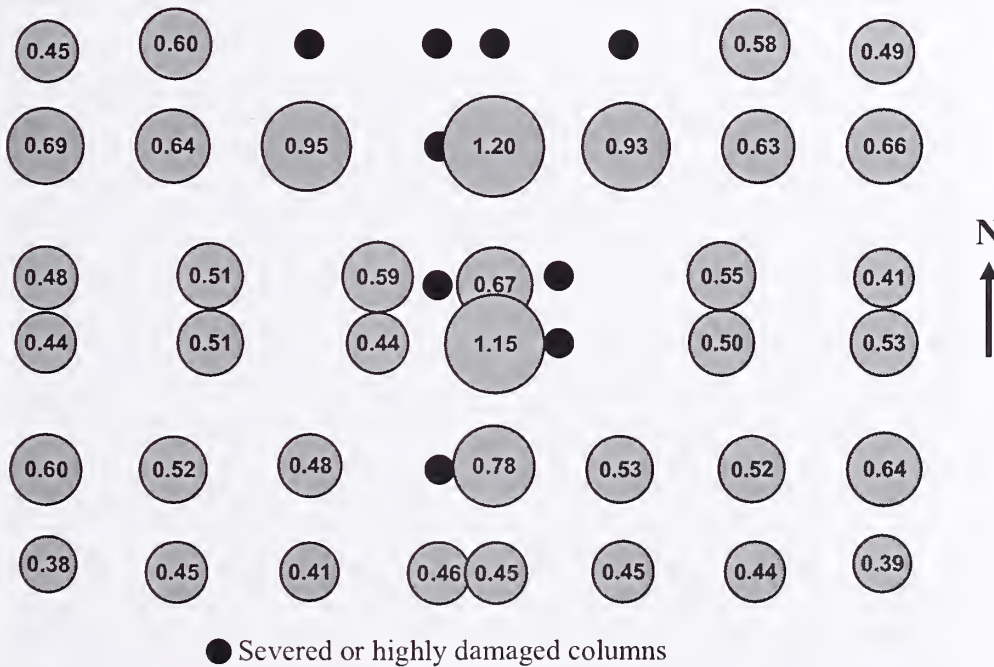


Figure 8-10. Maximum demand-to-capacity ratio for axial force in core columns between Floor 93 and Floor 99 of WTC 1 after aircraft impact for Case B.

**Table 8–2. Total column loads at Floor 98 of WTC 1 for Case B conditions.**

	North	East	South	West	Core	Total
(1) Before Impact	10,974	8,545	11,025	8,572	34,029	73,144
(2) After Impact	10,137	9,071	10,356	9,146	34,429	73,139
(3) 10 min	9,796	8,490	9,848	8,536	36,473	73,143
(4) 20 min	10,437	9,108	9,900	9,202	34,495	73,143
(5) 30 min	10,913	10,034	10,420	9,715	32,060	73,142
(6) 40 min	11,068	10,599	11,004	10,178	30,294	73,142
(7) 50 min	11,149	10,908	11,192	10,458	29,435	73,141
(8) 60 min	11,205	11,168	11,285	10,716	28,766	73,141
(9) 70 min	11,286	11,366	11,343	10,939	28,205	73,138
(10) 80 min	11,376	11,555	11,409	11,119	27,681	73,140
(11) 90 min	10,916	11,991	9,949	11,657	28,587	73,099
(12) 100 min	10,828	12,249	9,638	11,905	28,478	73,098
(13) (2) - (1)	-837	526	-668	574	400	-5
(14) (10) - (2)	1,239	2,484	1,052	1,973	-6,748	1
(15) (12) - (2)	692	3,178	-719	2,759	-5,951	-41
(16) (12) - (10)	-548	694	-1,771	786	797	-42

Note: Compression is positive. Units are in kip.

**Table 8–3. Total column loads at Floor 105 of WTC 1 for Case B conditions.**

	North	East	South	West	Core	Total
(1) Before Impact	8,026	6,562	8,092	6,604	20,361	49,645
(2) After Impact	7,294	7,028	7,488	7,076	20,761	49,646
(3) 10 min	6,944	6,461	6,981	6,469	22,790	49,646
(4) 20 min	7,551	7,075	7,057	7,158	20,806	49,647
(5) 30 min	8,020	7,998	7,569	7,685	18,377	49,648
(6) 40 min	8,193	8,571	8,129	8,147	16,608	49,649
(7) 50 min	8,285	8,878	8,315	8,428	15,743	49,650
(8) 60 min	8,351	9,130	8,414	8,687	15,069	49,650
(9) 70 min	8,435	9,319	8,481	8,914	14,502	49,651
(10) 80 min	8,528	9,497	8,551	9,097	13,978	49,651
(11) 90 min	8,096	9,847	7,327	9,506	14,876	49,652
(12) 100 min	8,023	10,076	7,066	9,720	14,767	49,653
(13) (2) - (1)	-732	466	-604	472	400	1
(14) (10) - (2)	1,234	2,470	1,063	2,021	-6,783	5
(15) (12) - (2)	730	3,048	-422	2,644	-5,993	7
(16) (12) - (10)	-504	579	-1,485	623	790	2

Note: Compression is positive. Units are in kip.

### 8.4.2 WTC 1 Structural Response to Elevated Temperatures

In the early stages of the fire, temperatures of structural components in the core rose between 500 °C and 700 °C over a 10 min to 20 min time interval (where fireproofing was damaged), and the thermal expansion of the core was greater than the thermal expansion of the exterior walls. The difference in the thermal expansion between the core and the exterior walls increased the loads in the core columns at 20 min. After 20 min, the core continued to lose gravity loads due to thermal weakening and shortening until the south wall started to bow inward. By 50 min, the core had displaced downward by 1.6 in on average at Floor 99 due to creep and buckling of core columns. About 20 percent (6,748 kip) of the gravity load was transferred by the hat truss to the exterior walls due to thermal weakening of the core at 80 min, as shown in Table 8–2; the north and south walls each carried about 10 percent more loads (1,239 kip and 1,052 kip, respectively) and the east and west walls each carried about 25 percent more loads (2,484 kip and 1,973 kip, respectively). Since the hat truss outriggers to the east and west walls were stiffer than the outriggers to the north and south walls, they transferred greater loads to the east and west exterior walls. At 100 min, the core displaced downward at Floor 99 by 2.0 in. on the south side of the core. As the core was weakened by creep and plastic buckling, gravity loads in the core were transferred to the exterior walls.

The full floor analyses for WTC 1 Case B showed that the floors on the south side in the impact zone did not begin to sag and apply a pull-in force at the column connections until approximately 80 min after impact. Based upon the full floor and isolated south wall subsystem analyses, 5 kip of pull-in force was applied to all columns across Floors 95 to 99 beginning at 80 min, as shown in Fig. 7–30. Figures 8–11 and 8–12 show the out-of-plane displacement contours of the south wall at 80 min and 100 min, respectively. Figure 8–13 shows the time history of the inward bowing of the south wall. Until the 5 kip pull-in forces were applied, no inward bowing had occurred. With the application of the 5 kip pull-in force, the maximum inward bow increased to 15.5 in.

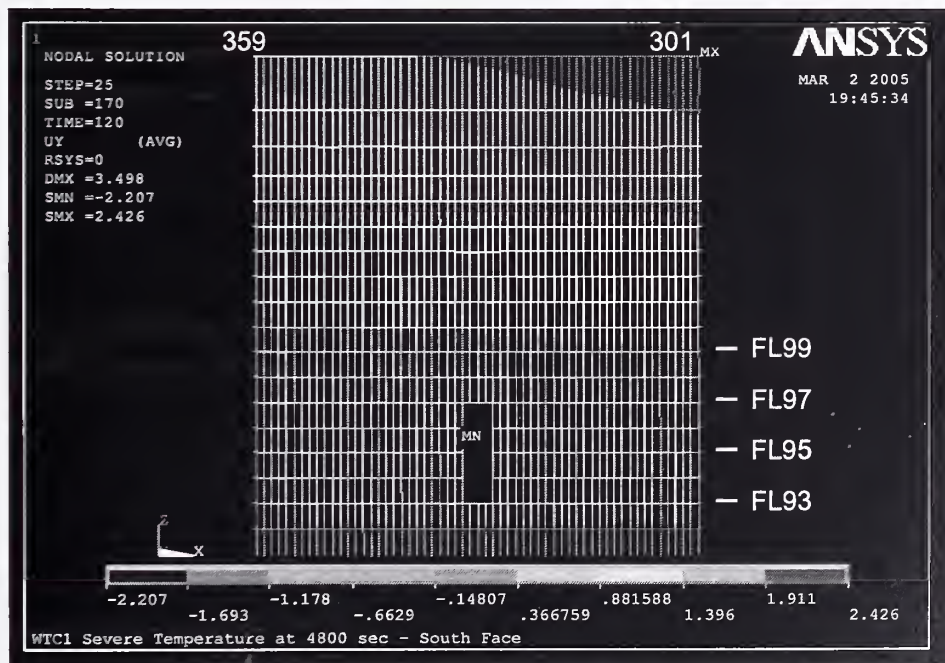


Figure 8–11. Out-of-plane displacement of south wall of WTC 1 at 80 min for Case B.

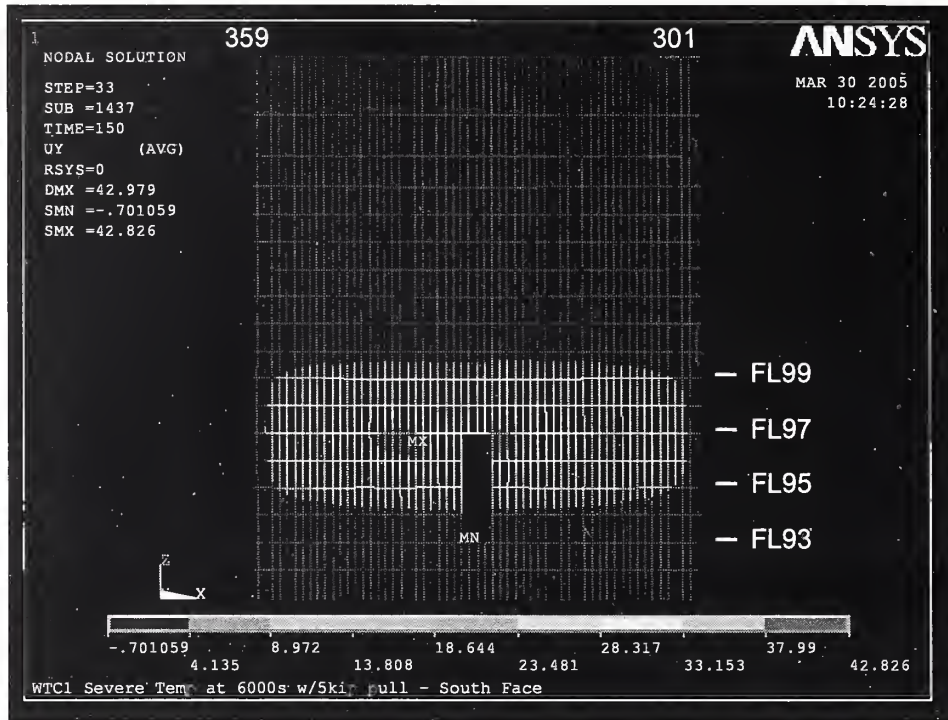


Figure 8–12. Out-of-plane displacement of south wall of WTC 1 at 100 min for Case B conditions with 5 kip pull-in forces.

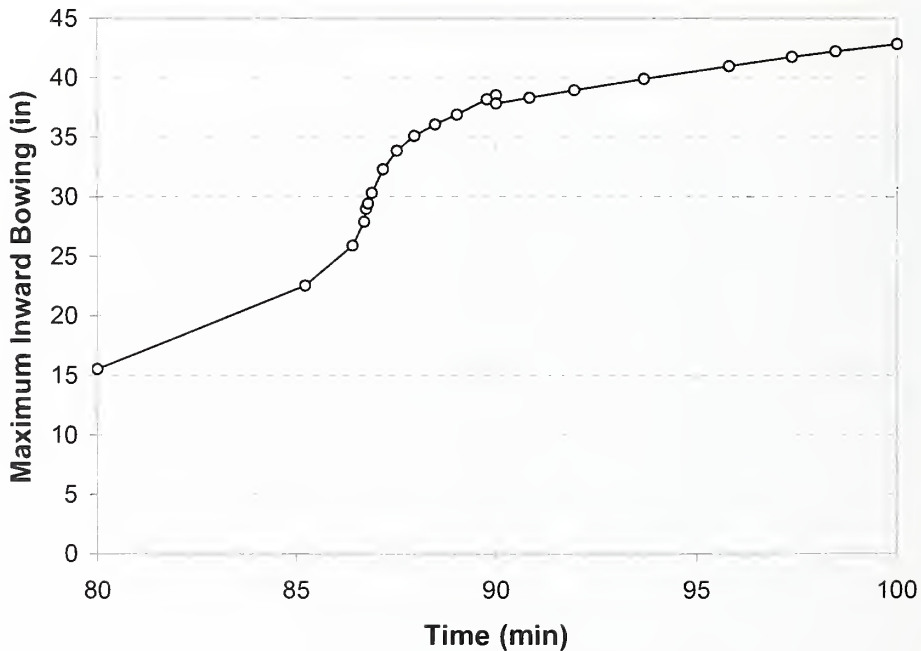


Figure 8–13. Time history of maximum out-of-plane displacement of WTC 1 south wall for Case B with 5 kip pull-in forces.

Figure 8–14 shows that Columns 318 to 346 on the south wall unloaded due to inward bowing after 80 min. The loads increased on the east and west walls. Figure 8–15 shows the load increase for the east

wall. Due to bowing of the south wall, the vertical displacement of the south wall increased as shown in Figs. 8–16 and 8–17, and the south wall lost about an additional 5 percent (1,771 kip) of load between 80 min and 100 min (see Table 8–2). As a result, the east and west walls and the core gained gravity loads.

By approximately 87 min, the inward bowing increased significantly. As the bowing of the south wall increased, a section of the south wall above the bowed-in area moved downward as can be seen in Fig. 8–18. By 90 min, the rate of increase in the inward bowing slowed down as the south wall redistributed the gravity loads to the east and west walls and to the core. The inward bowing increased to 42.8 in. at 100 min. However, the south wall remained stable (had not buckled) at 100 min.

Isolated exterior wall and global analyses showed that varying the inward pull force by a small amount caused a large difference in the amount of inward bowing. For a comparison, the inward bowing of the south wall at 100 min from the analysis with a 4 kip pull-in force was only 14.5 in. at 100 min. Given that the inward bowing increased from 14.5 in. to 42.8 in. when the inward pull force was increased from 4 kip to 5 kip, a slight increase in the pull-in force over 5 kip would have resulted in instability of the south wall.

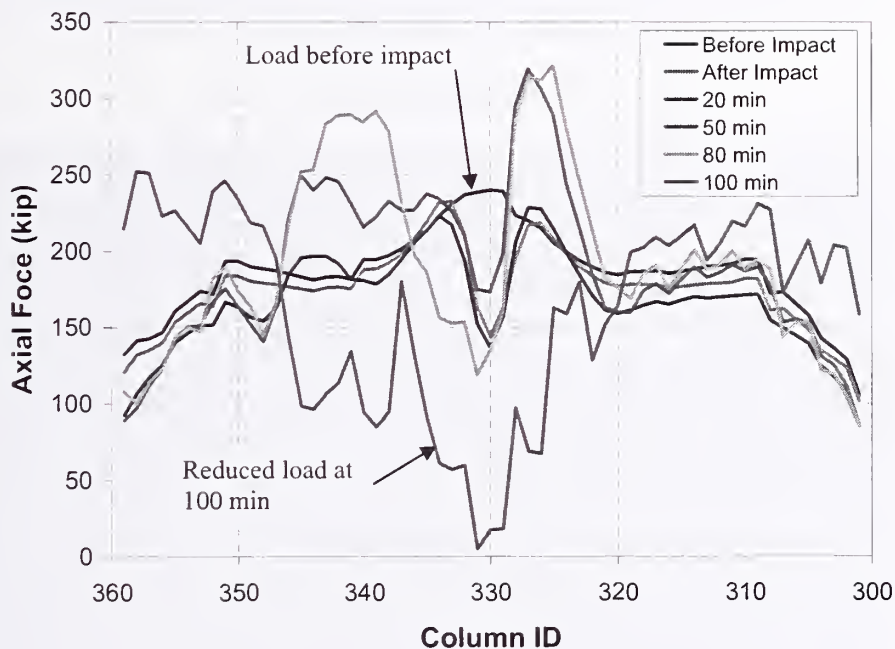


Figure 8–14. Distribution of axial force in exterior columns at Floor 98 of WTC 1 south wall for Case B with 5 kip pull-in forces.

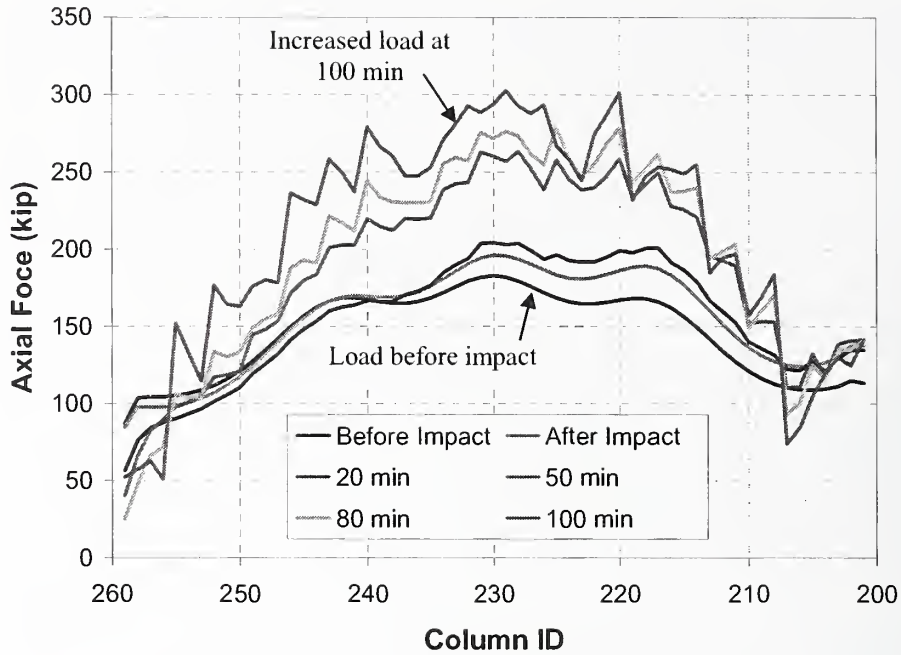


Figure 8–15. Distribution of axial force in exterior columns at Floor 98 of WTC 1 east wall for Case B with 5 kip pull-in forces.

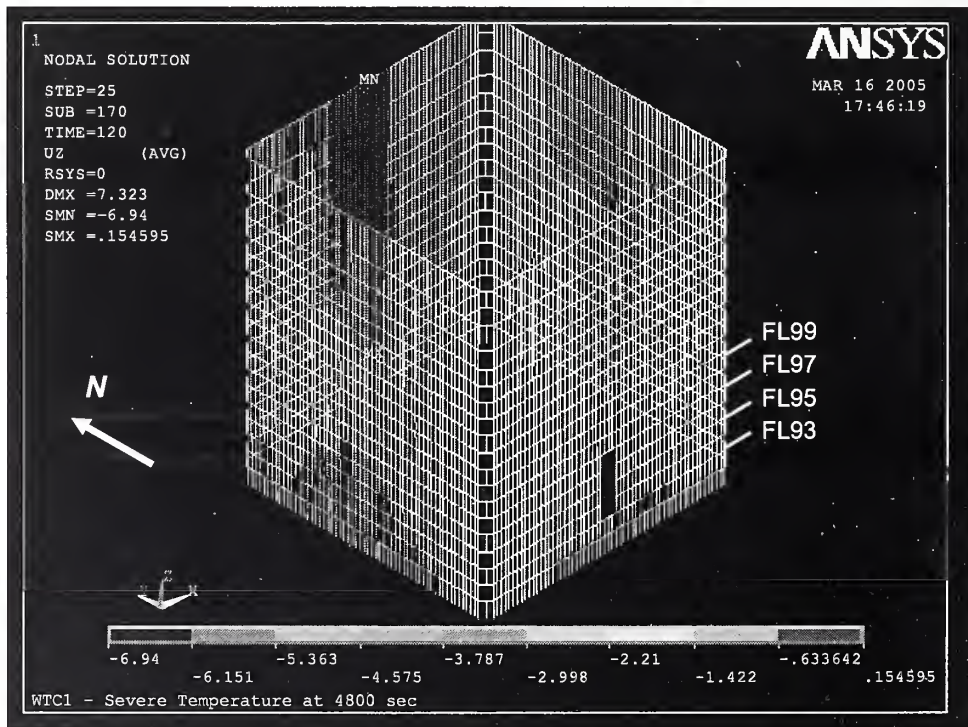


Figure 8–16. Vertical displacement of west and south exterior walls of WTC 1 at 80 min for Case B.

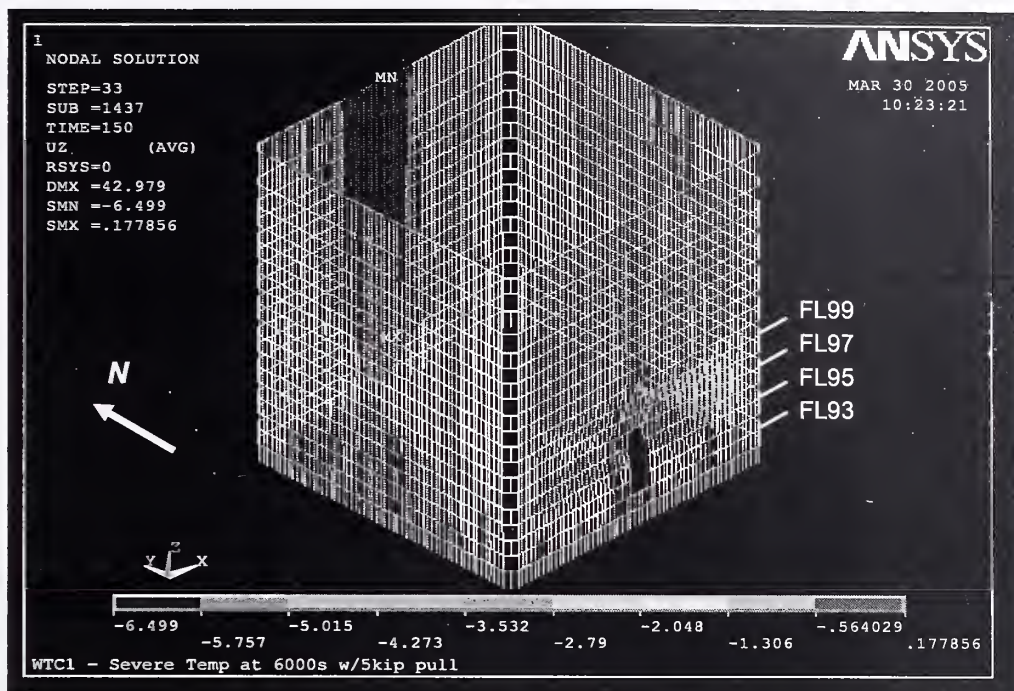
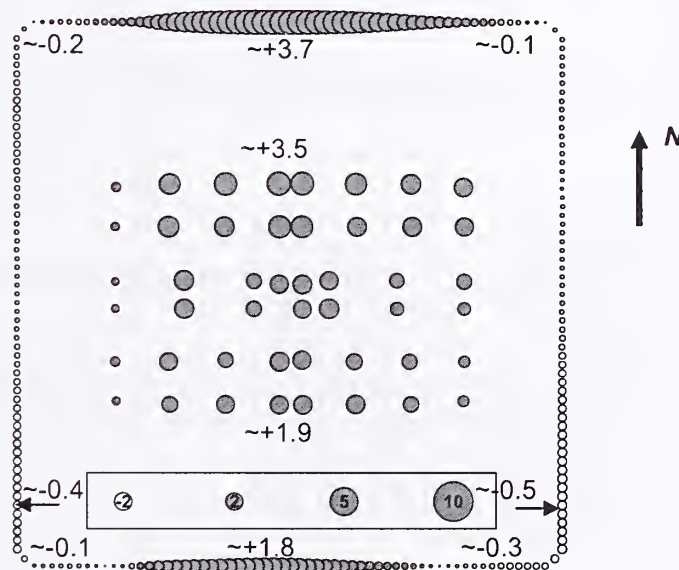


Figure 8–17. Vertical displacement of west and south exterior walls of WTC 1 at 100 min for Case B.



Note: downward displacement is shown as positive displacement

Figure 8–18. Change in vertical displacement at Floor 99 of WTC 1 from the state before impact to 100 min for Case B.

Plastic and creep strains played a significant role in the structural response of WTC 1 to the fires. Figures 8–19 to 8–21 show the maximum elastic-plus-plastic-plus-creep strain in each column between Floor 93 and Floor 99 at 10 min, 40 min, and 100 min, respectively. Before the aircraft impact, the columns had no plastic strain. After the aircraft impact, several columns that were close to severed and

highly damaged columns experienced plastic strains. Plastic strain of the core increased for the first 40 min, and then remained almost constant to 100 min. Plastic strain of the south exterior columns increased in almost all the bowed columns from 40 min to 100 min. However, creep strain was found to be far greater than plastic strain, especially in the core. At 40 min, 22 of 47 core columns had creep strain larger than 1.0 percent. After 40 min, creep strain in core columns on the south side had increased. The maximum elastic-plus-plastic-plus-creep strain at 100 min was 7.3 percent in Column 1006. As temperature increased on the south exterior wall in the later stages of the fire, creep strain also increased in about 20 columns on the south face. The maximum elastic-plus-plastic-plus-creep strain in the south exterior columns reached 2.9 percent.

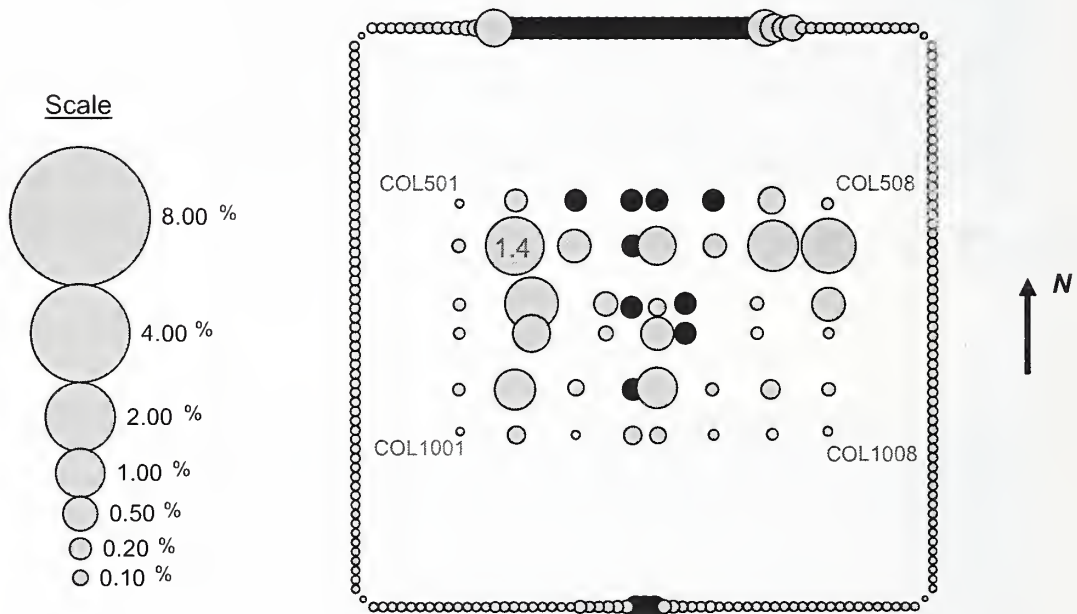


**Figure 8-19. Maximum elastic-plus-plastic-plus-creep strain for columns between Floor 93 and Floor 99 of WTC 1 at 10 min for Case B (strain values are in percent).**

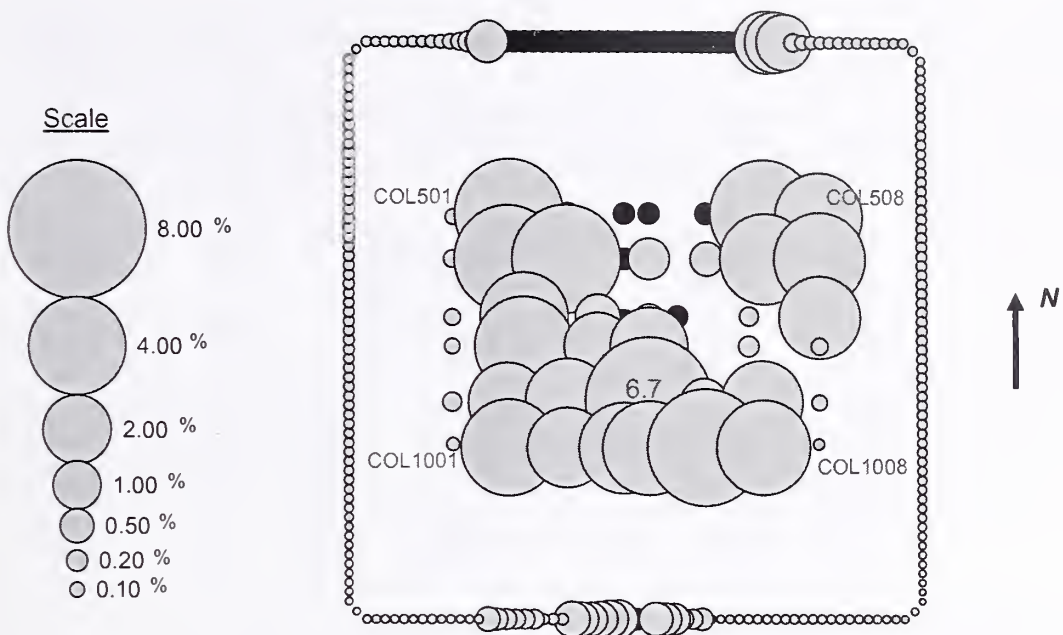


Figure 8-20. Maximum elastic-plus-plastic-plus-creep strain for columns between Floor 93 and Floor 99 of WTC 1 at 40 min for Case B (strain values are in percent).

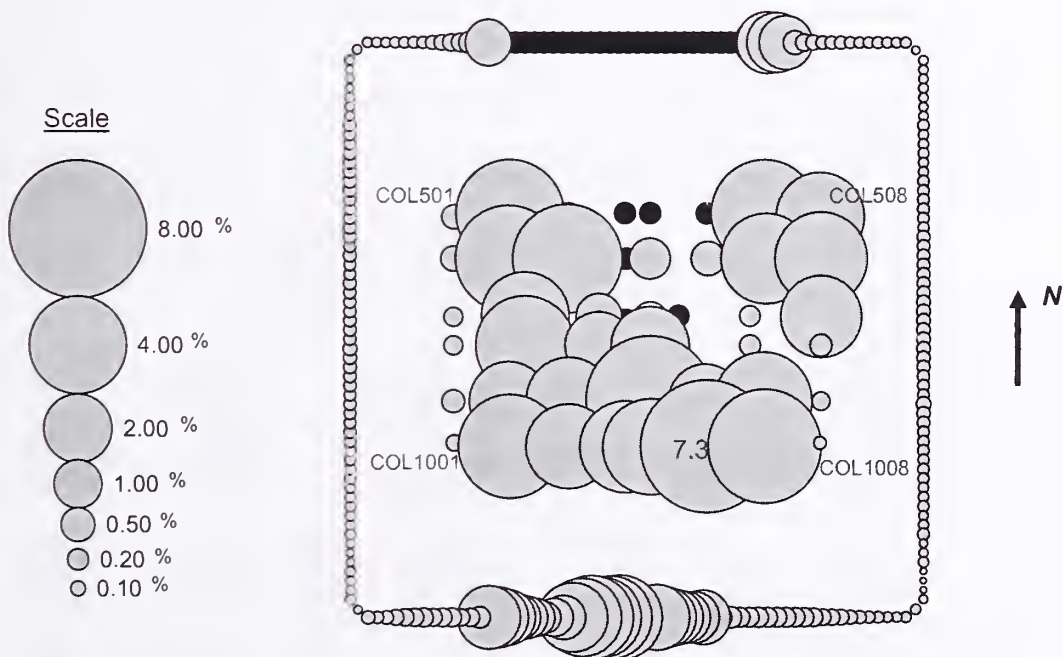


Figure 8-21. Maximum elastic-plus-plastic-plus-creep strain for columns between Floor 93 and Floor 99 of WTC 1 at 100 min for Case B with 5 kip pull-in forces (strain values are in percent).

Figures 8–22 and 8–23 show the axial force demand-to-capacity ratio for each core column at 80 min and 100 min, respectively. Compressive capacities of the core columns were calculated by AISC LRFD Eq. E2-1 for plastic buckling with effective length factor of  $K$  equal to 1.0 and a resistance factor of 1.0. Comparison of Figs. 8–10 and 8–23 shows that the demand-to-capacity ratio increased for core columns with relatively small elastic-plus-plastic-plus-creep strains and decreased for columns with high strains. Figure 8–21 shows that core columns with high creep strains had lower demand-to-capacity ratios. Columns with high compressive loads and large creep strains shortened and unloaded to stiffer columns with less creep.

At 100 min, the core had weakened on the south side and shortened by 1.6 in. The south wall had bowed inward approximately 43 in. and was unloading to the core and the adjacent east and west walls. As discussed previously, a small change in the magnitude of the inward pull force changed the rate at which the exterior wall bowed inward and reached a point of instability. Based upon observations and similar results for WTC 2 at collapse initiation (described in the next Section), the following sequence of events likely occurred as soon as the south wall reached instability and buckled.

The inward bowing of the south wall caused failure of exterior column splices and spandrels, and induced column instability. The instability progressed horizontally across the entire south face. The south wall unloaded and redistributed its gravity loads to the thermally weakened core through the hat truss and to the east and west walls through the spandrels. The beginning of this load redistribution is illustrated in Tables 8–1 and 8–2. The building section above the impact zone began tilting to the south as column instability progressed rapidly from the south wall along the adjacent east and west walls and increased the gravity load on the core columns. The change in potential energy due to downward movement of the building mass above the buckled columns exceeded the strain energy that could have been absorbed by the structure. Global collapse then ensued.

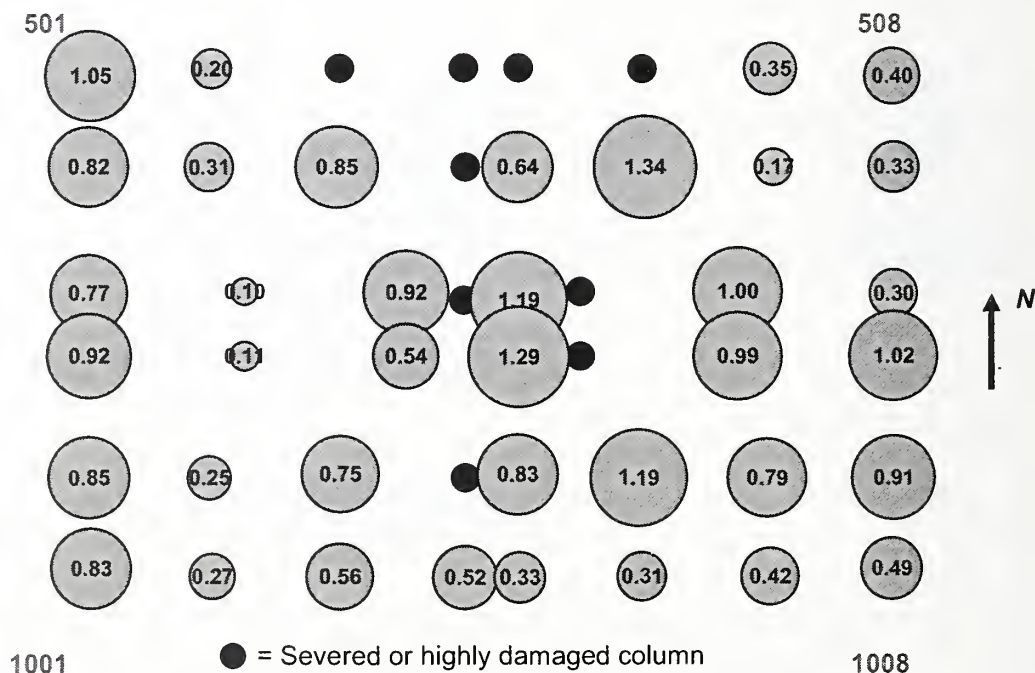


Figure 8–22. Maximum demand-to-capacity ratio for axial force in core columns between Floor 93 and Floor 99 of WTC 1 at 80 min for Case B conditions.

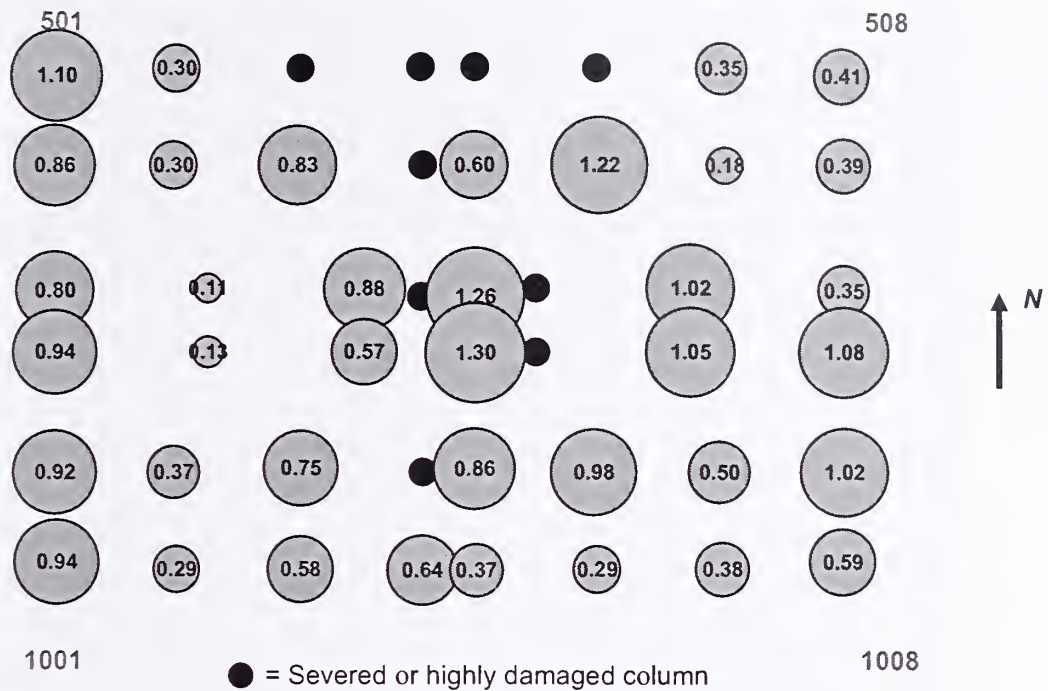


Figure 8–23. Maximum demand-to-capacity ratio for axial force in core columns between Floor 93 and Floor 99 of WTC 1 at 100 min for Case B with 5 kip pull-in forces.

#### 8.4.3 WTC 1 Hat Truss Members and Connections

The state of the hat truss members and the connections were checked since the global model did not include break elements to capture column and hat truss splice failures or sufficient beam elements to capture buckling of the hat truss outriggers. The condition of the connections and the members in the primary load path of the hat truss was evaluated at various time intervals. The evaluation included the core column splices for tension, outriggers and supporting columns for compression, and the hat truss connections that were in the primary load path for tension.

Core column splices had compressive forces before the aircraft impact. With the aircraft impact damage and increasing plastic and creep strains, the core weakened and shortened, and some core columns were supported from the hat truss. At 100 min, nine core columns (503, 504, 505, 602, 603, 604, 605, 702, and 802) were in tension at Floor 105 as shown in Fig. 8–24. To evaluate the condition of the core column splices at Floor 106, the tension capacity of these splices was compared to the tensile forces developed during each 10 min time interval. To calculate the connection tensile capacity, AISC-LRFD procedures were used. It was found that tensile forces in the core columns were less than the capacities of the splices.

There were sixteen outriggers (four on each face), as shown in Fig. 8–25, that transferred gravity loads between the core and the exterior walls. In the global model, each of these outriggers was modeled by only one BEAM 24 element; therefore, buckling of the member was not captured although material nonlinearity was included. Table 8–4 lists demand-to-capacity ratios for the outrigger members over time. Capacities of the outriggers were calculated using AISC LRFD procedures for plastic (inelastic) buckling with effective length factor  $K$  equal to 0.75 (the outrigger end connections were different from those used for the core columns) and a resistance factor of 1.0. As the outrigger members were not

modeled with sufficient elements to capture plastic buckling, they yielded when the outrigger reached its compressive capacity; therefore, force redistribution to other outriggers was underestimated.

The hat truss connections within the hat truss itself were also checked. The hat truss connections in the primary load path were identified, and their capacities were compared to their forces. The primary load path was identified by selecting hat truss members with an absolute axial stress of 25 ksi or more at 80 min, as this was when maximum forces occurred. Only the connections that were transferring tensile forces were evaluated. In calculating the capacity of the connections, the AISC-LRFD procedures were used. None of the hat truss connection capacities were exceeded. It was concluded that the hat truss redistributed loads between the core and the exterior wall columns as modeled in the global analysis.

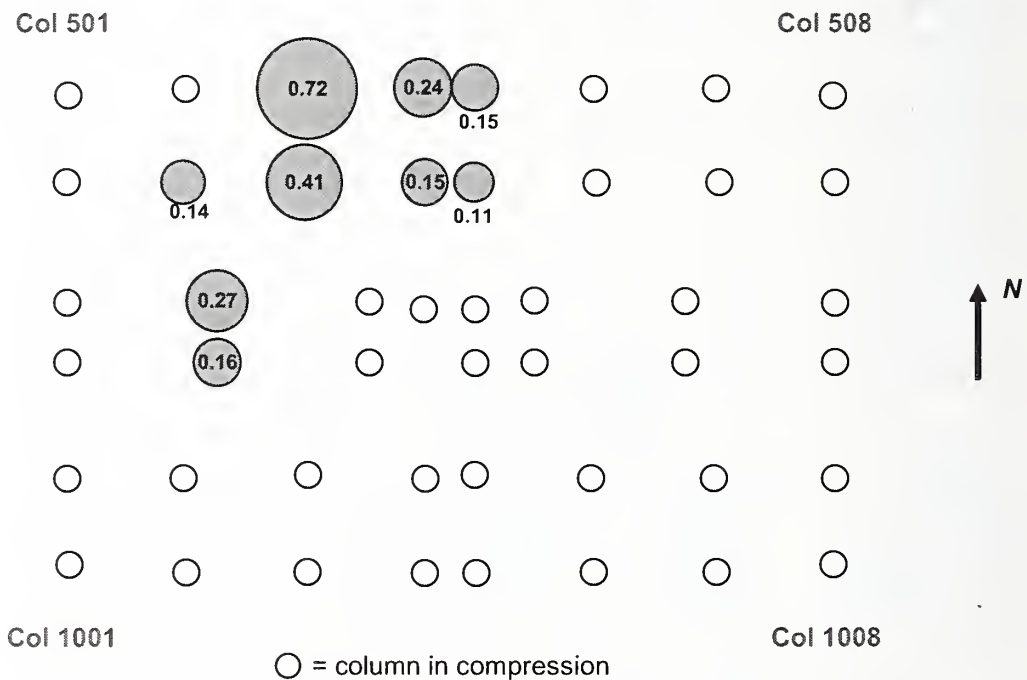


**Figure 8–24. Tension demand-to-capacity ratio for core column splices at WTC 1 Floor 106 at 100 min for Case B with 5 kip pull-in forces.**

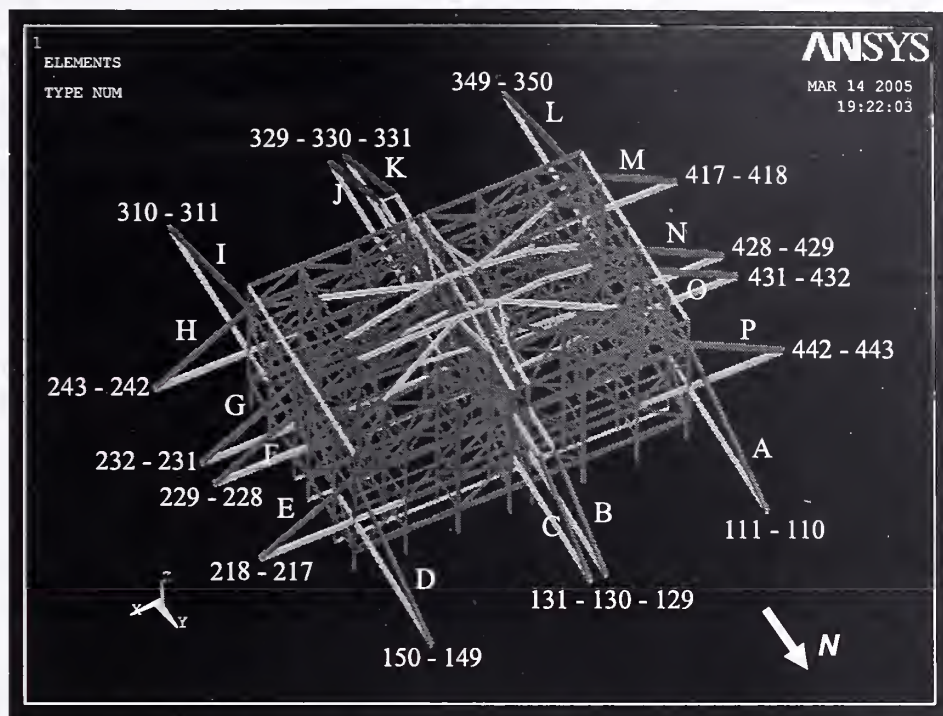


Figure 8-25. Location and label of outriggers and supporting columns for WTC 1.

Table 8-4. Demand-to-capacity ratio for axial force in outriggers of WTC 1 for Case B.

Outrigger ID	Bfr Imp	Afr Imp	10 min	20 min	30 min	40 min	50 min	60 min	70 min	80 min	90 min	100 min
<b>North</b>												
A	0.26	0.35	0.26	0.40	0.49	0.53	0.56	0.59	0.62	0.65	0.54	0.52
B	0.22	-0.07	-0.13	-0.04	0.02	0.04	0.06	0.07	0.08	0.09	0.03	0.03
C	0.21	-0.05	-0.11	-0.02	0.04	0.06	0.08	0.08	0.09	0.11	0.05	0.04
D	0.25	0.35	0.29	0.45	0.61	0.67	0.70	0.72	0.73	0.75	0.65	0.63
<b>East</b>												
E	0.32	0.48	0.38	0.56	0.75	0.83	0.88	0.92	0.94	0.97	0.95	0.96
F	0.23	0.28	0.21	0.30	0.41	0.48	0.52	0.55	0.57	0.59	0.62	0.64
G	0.23	0.26	0.20	0.26	0.35	0.42	0.46	0.49	0.51	0.54	0.58	0.61
H	0.33	0.31	0.23	0.25	0.36	0.46	0.51	0.55	0.58	0.60	0.72	0.77
<b>South</b>												
I	0.25	0.12	0.04	0.03	0.12	0.20	0.23	0.26	0.27	0.28	0.28	0.28
J	0.21	0.10	0.01	0.03	0.13	0.24	0.28	0.29	0.30	0.31	0.04	-0.02
K	0.21	0.10	0.01	0.03	0.13	0.24	0.27	0.28	0.30	0.31	0.02	-0.04
L	0.26	0.12	0.02	0.05	0.11	0.20	0.24	0.27	0.29	0.31	0.19	0.18
<b>West</b>												
M	0.33	0.33	0.22	0.29	0.36	0.44	0.49	0.53	0.56	0.58	0.69	0.73
N	0.24	0.27	0.20	0.28	0.34	0.40	0.44	0.47	0.50	0.52	0.56	0.58
O	0.24	0.29	0.22	0.31	0.38	0.43	0.47	0.50	0.53	0.55	0.59	0.61
P	0.33	0.48	0.39	0.54	0.64	0.71	0.75	0.79	0.83	0.87	0.88	0.90

## 8.5 RESULTS OF WTC 2 ANALYSIS

The global model of WTC 2 with creep, plastic buckling of columns, plasticity, and nonlinear geometry was analyzed with Case D structural damage and temperature histories.

### 8.5.1 WTC 2 Structural Response to Aircraft Impact Damage

Case D structural and passive fire protection damage after the aircraft impact was as follows:

- WTC 2 had 34 severed columns on the south wall (Columns 407 to 440) and 11 core columns on the south side of the core (Columns 701, 702, 801, 802, 803, 901, 903, 1001, 1002, 1003, and 1004) and 4 exterior columns on the north wall (Columns 253, 254, 257, and 258) that were severed or heavily damaged between Floors 78 to 84.
- Floor slabs and framing were severed or heavily damaged in the south office floor area through the east side of the core between Floors 78 and 84.
- WTC 2 fireproofing damage extended from the south exterior wall, through the east side of the core, to the east and north exterior walls between Floors 78 and 84.

The vertical displacements of the exterior wall before the aircraft impact were about 2.0 in. to 3.0 in. (Fig. 8–26). After aircraft impact, the vertical displacements increased to 7.4 in. on the south wall (Fig. 8–27). There was no horizontal (out-of-plane) displacement on the east wall before the aircraft impact. After aircraft impact, the south side of the east wall at Floor 86 displaced outward about 2.0 in.; whereas, the north side at the same floor did not displace.

In the core, the vertical displacements were about 3.5 in. to 4.2 in. before the aircraft impact, as shown in Fig. 8-28. After aircraft impact, the vertical displacements increased to 10 in. at the southeast corner of the core where the aircraft impact had severed columns, as shown in Fig. 8–29.

Figures 8–30 and 8-31 show the north-south and east-west lateral displacements of the exterior wall above Floor 86 after aircraft impact. Floor 110 moved toward the south about 5.1 in. and toward the east about 5.0 in. There was also a slight twist around the z-axis of the tower of about 0.07 percent at Floor 110. The twist around the z-axis was calculated by taking the difference between the average in-plane displacement of the two opposing exterior walls (such as the east and the west walls) at Floor 110 and dividing the result by the distance between these walls (~200 ft).

The global analysis showed that WTC 2 was stable following aircraft impact, as was observed, and had considerable reserve capacity. Similar to WTC 1, the core columns were loaded to approximately 50 percent of their capacity prior to impact, and the exterior columns were loaded to approximately 20 percent of their capacity. The exterior columns were capable of large load transfers from the core columns after impact.

The loads in the severed exterior columns were transferred to adjacent exterior columns through the spandrels and to the core through the hat truss. Several of the severed core columns at the southeast corner of the core were computed to have failed splice connections to the hat truss (discussed in Section 8.5.3). The loads from these columns were transferred through the core floors to adjacent core columns and then to the east and south exterior walls through the hat truss. Additionally, the severed core columns at the southeast corner resulted in the core leaning to the southeast. While the isolated WTC 2 core model was not stable with the structural impact damage, within the global system the core was supported by the floors and exterior walls.

The leaning of the core to the southeast contributed to the load redistribution in WTC 2, with a general pattern of increased loads on the south and east columns (core and exterior) and decreased loads on the north and west columns. Tables 8–5 and 8–6 show the total columns loads at Floors 83 and 105, respectively, for the analysis stages from before impact to collapse initiation at 43 min. After impact, as shown in Table 8–5, the core carried 6 percent less loads (4,007 kip), and the east wall carried 24 percent more gravity loads (4,368 kip). The north wall loads decreased by 10 percent (1,374 kip), and the south and west walls loads increased by 2 percent (227 kip) and 3 percent (604 kip), respectively.

The loads on the core columns before aircraft impact were distributed essentially symmetrically with respect to the center of the core. There was a slight difference between corner columns on the south side (501 and 1001) and north side (508 and 1008) due to slightly higher dead and live loads in the north side columns. Columns 506, 507, 508, and 1008 at the northeast and northwest corners unloaded; the other intact core columns increased in load (Figs. 8–32 and 8–33). The loads in Columns 904 and 1005, which were adjacent to the severed and heavily damaged columns, increased substantially at Floor 83 after impact. Column 904 increased from 660 kip to 1,506 kip and Column 1005 increased from 1,287 kip to 2,794 kip.

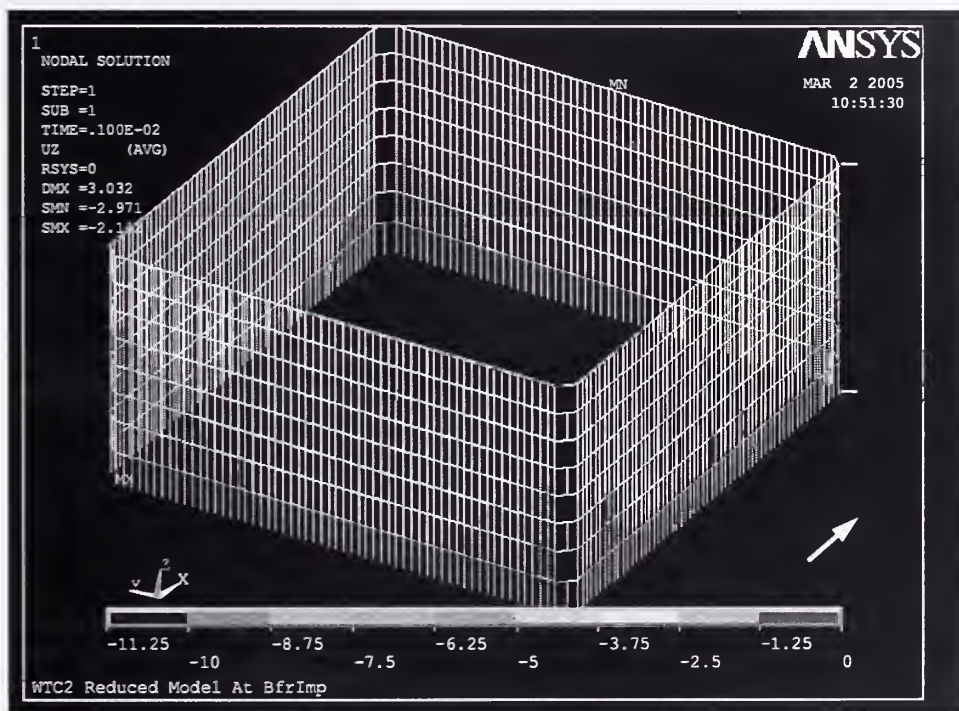


Figure 8–26. Vertical displacement before impact of WTC 2 exterior wall for Case D.

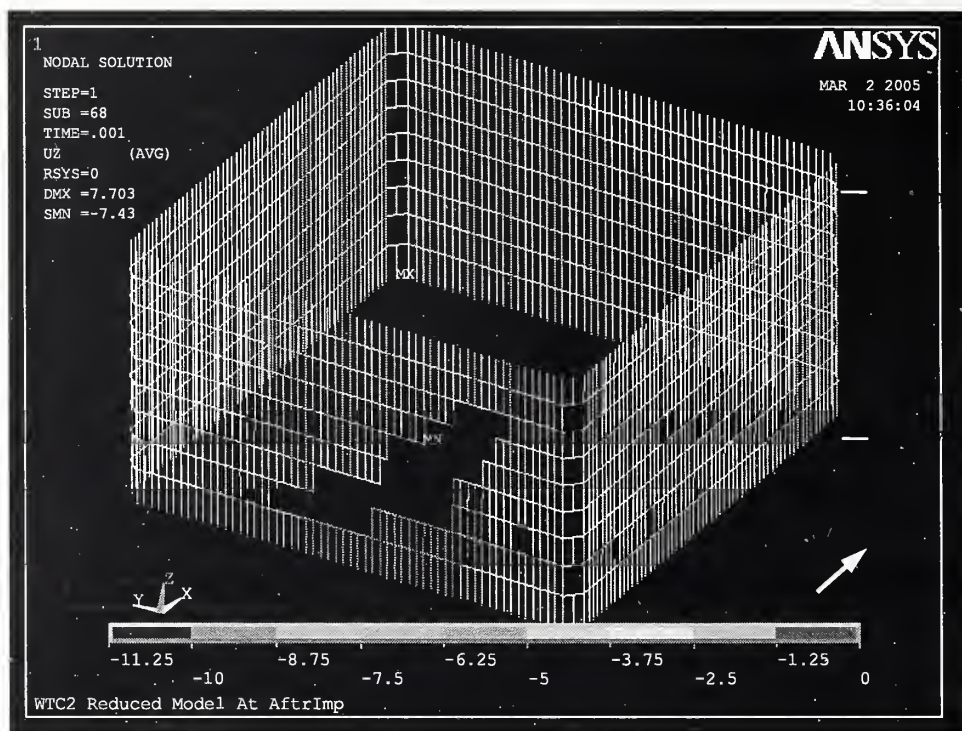


Figure 8–27. Vertical displacement after impact of WTC 2 exterior wall for Case D.

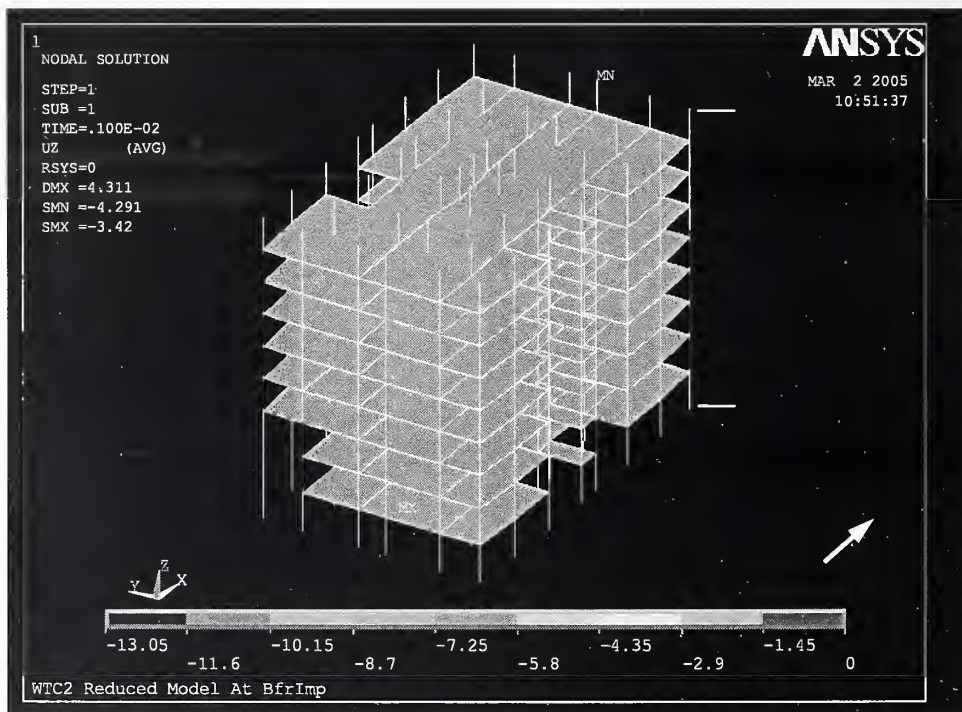


Figure 8–28. Vertical displacement before impact of WTC 2 core for Case D.

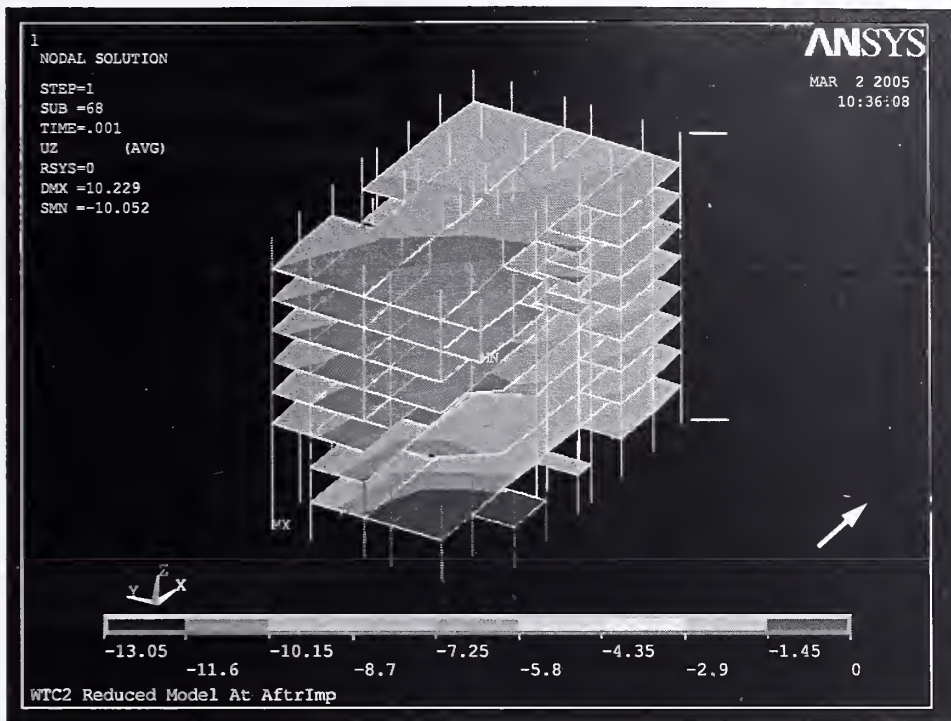


Figure 8–29. Vertical displacement after impact of WTC 2 core for Case D.

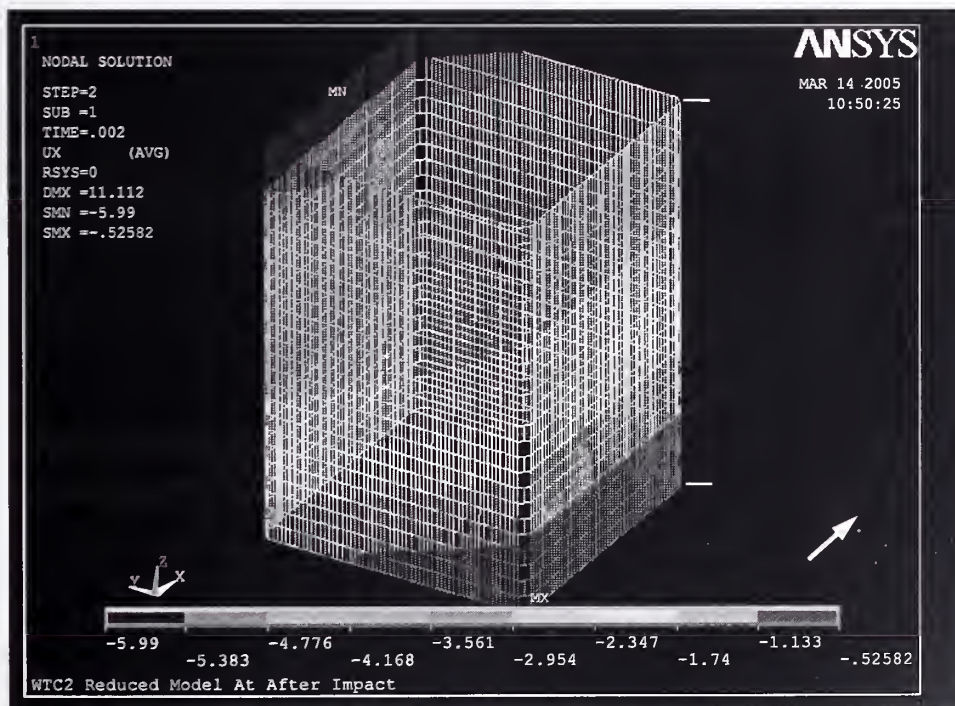


Figure 8–30. Lateral displacements after impact above WTC 2 Floor 86 in the x-direction (north-south) for Case D.

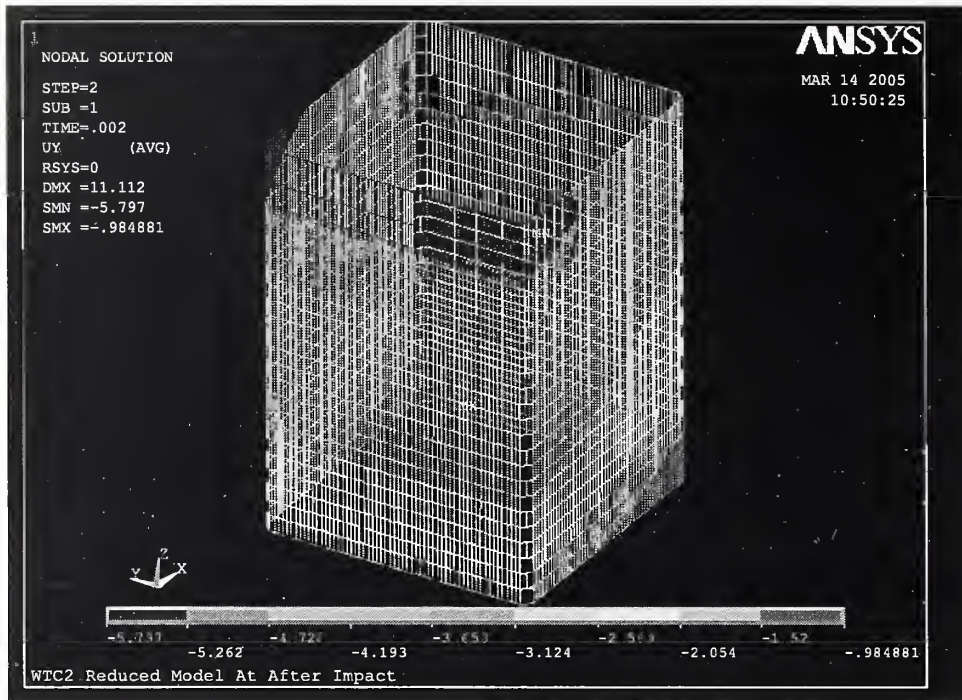


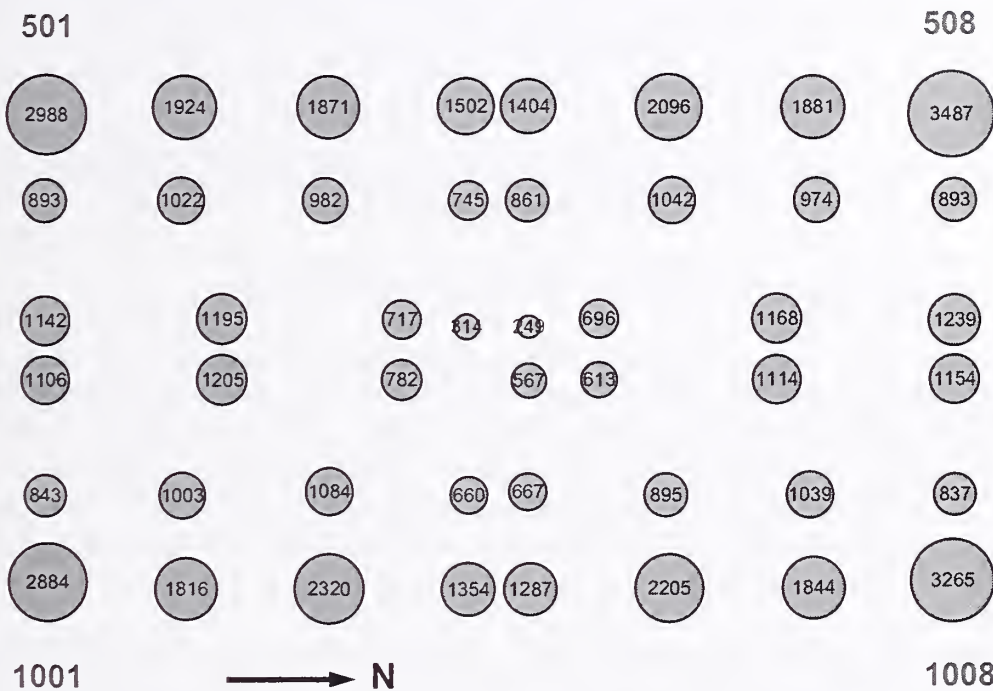
Figure 8–31. Lateral displacements after impact above WTC 2 Floor 86 in the y-direction (east-west) for Case D.

Table 8–5. Total column loads at WTC 2 Floor 83 for Case D (Compression is positive).

Row	Analysis Stage	West	East	North	South	Core	Sum
(1)	Before Impact	18065	18114	13567	13284	61828	124857
(2)	After Impact	18670	22481	12193	13511	57821	124676
(3)	10 min	18728	22226	11896	13358	58413	124621
(4)	20 min	18914	22208	12052	13318	58124	124616
(5)	30 min	18876	23681	11770	13365	56967	124659
(6)	40 min	18531	23682	11906	13473	56825	124418
(7)	43 min	15667	15143	14215	16292	62422	123738
(8)	(2)-(1)	604	4368	-1374	227	-4007	-181
(9)	(3)-(1)	662	4112	-1670	74	-3415	-236
(10)	(4)-(1)	849	4094	-1515	35	-3704	-241
(11)	(5)-(1)	811	5567	-1797	81	-4861	-199
(12)	(6)-(1)	466	5568	-1661	190	-5003	-439
(13)	(7)-(1)	-2398	-2971	648	3009	594	-1119

**Table 8-6. Total column loads at WTC 2 Floor 105 for Case D (Compression is positive).**

Row	Analysis Stage	West	East	North	South	Core	Sum
(1)	Before Impact	8497	8572	7382	7169	17123	48742
(2)	After Impact	9170	11272	6487	8432	13382	48742
(3)	10 min	9182	11061	6250	8275	13975	48742
(4)	20 min	9279	11120	6311	8351	13682	48742
(5)	30 min	9370	11859	6416	8553	12544	48742
(6)	40 min	9198	11927	6524	8691	12402	48742
(7)	43 min	7086	8026	6546	9169	17915	48742
(8)	(2)-(1)	674	2699	-895	1263	-3741	0
(9)	(3)-(1)	685	2489	-1132	1106	-3148	0
(10)	(4)-(1)	783	2547	-1071	1182	-3441	0
(11)	(5)-(1)	873	3287	-965	1384	-4579	0
(12)	(6)-(1)	702	3355	-858	1522	-4721	0
(13)	(7)-(1)	-1411	-547	-835	2000	792	0



**Figure 8-32. Core column loads (kip) before impact at WTC 2 Floor 83 for Case D (compression is positive).**

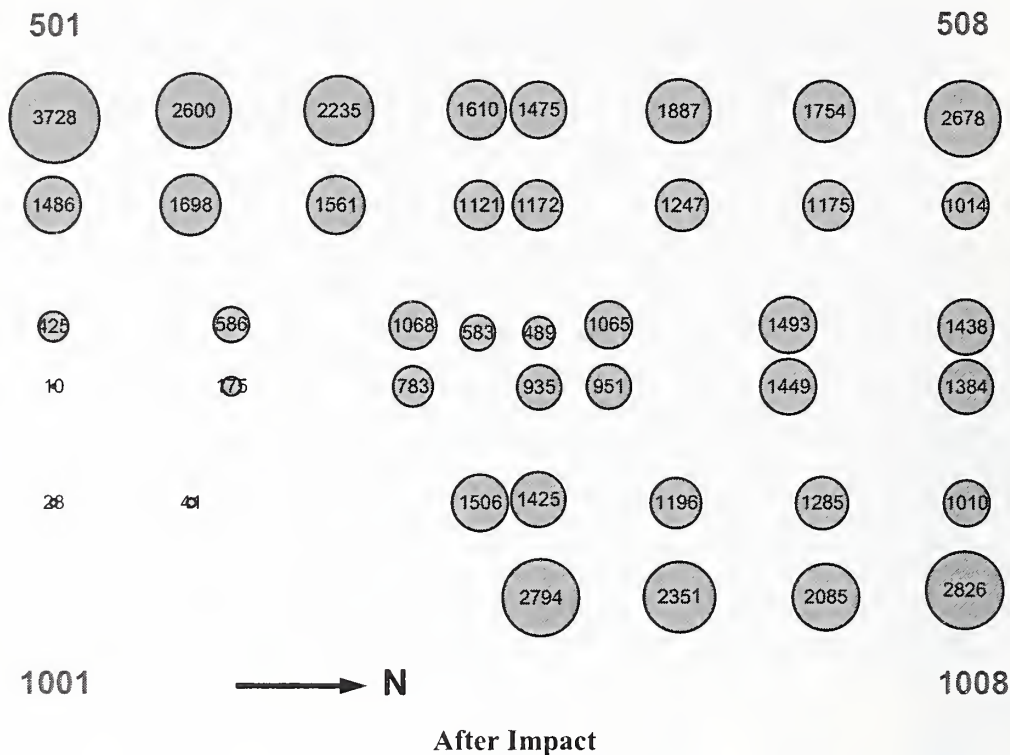


**Figure 8–33. Core column loads (kip) after impact at WTC 2 Floor 83 for Case D (compression is positive).**

### 8.5.2 WTC 2 Structural Response to Elevated Temperatures

In contrast to the fires in WTC 1, which generally progressed from the north side to the south side over approximately one hour, the fires in WTC 2 started and remained on the east side of the building until it collapsed, with the fires spreading from south to north. With fireproofing dislodged over much of the same area, the structural temperatures increased in the core, floors, and exterior walls at similar times. During the early stages of the fires, columns with dislodged fireproofing elongated due to thermal expansion. As the structural temperatures continued to rise beyond 500 °C, the thermal expansion was overcome by plastic and creep deformations under compressive loads.

Vertical displacement of the exterior walls before impact were 2.0 in. to 3.0 in. Vertical displacements of the south and east walls after impact were around 7.3 in. on the south face (over the severed columns) and about 3.5 in. on the east face, as shown in Figs. 8–34 and 8–35. These vertical displacements remained essentially constant after impact until the east wall became unstable at 43 min (Figs. 8–36 and 8–37).

After impact, the core and the north wall unloaded, and their load was redistributed to the south, west, and east walls. Table 8–7 shows that about 94 percent (3,740 kip/4,000 kip) of the load from the core was redistributed through the hat truss to the east, south, and west walls and 6 percent was redistributed through the floors to the east wall. A similar calculation for the east wall indicates that about 62 percent (2,699 kip/4,368 kip) of the load increase came through the hat truss and 38 percent was transferred through the spandrels to the north and south walls. Comparison of loads shown in Rows 8, 9, 10, and 11

in Tables 8-5 and 8-6 show that the column loads did not significantly change until the core unloaded at 30 min. Prior to this point, the thermal expansion of the core columns caused loads to increase. When the plastic and creep strains exceeded the thermal strains, the core columns shortened and unloaded. Loads in weakened core columns were redistributed to adjacent columns primarily through the hat truss.

Shortly after impact, Floors 79 to 83 began to sag and pull inward on the east wall (except where truss seat connections had failed). At 20 min, the east wall had bowed inward 9.5 in. near the center of the east wall, as shown in Fig. 8-38. The computed inward displacement agrees well with the observed inward displacement (~10 in.) that was measured from photographs at 9:21 a.m. (approximately 20 minutes after the aircraft impact). Inward displacements of the east wall steadily increased until collapse initiation.

At 30 min, the core unloaded about 850 kip (from 4,861 kip to 4,007 kip), the east wall increased about 1,200 kip (from 5,567 kip to 4,368 kip), and the north wall unloaded about 420 kip (from 1,797 kip to 1,374 kip) at Floor 83. Floor 105 column loads remained almost constant after aircraft impact until the east wall became unstable at 43 min. From 40 min to 43 min, the east wall suddenly unloaded about 8,540 kip, the west wall unloaded about 2,860 kip, the core load increased by about 5,600 kip, the north wall load increased by about 2,310 kip, and the south wall load increased about 2,820 kip at Floor 83 (Table 8-8). Comparison of the load redistribution that took place at Floor 105 with that at Floor 83 indicates that essentially all the additional core load from the east and west walls was transferred through the hat truss. For the east wall, about 46 percent (3,901 kip/8,539 kip) of the load shed was redistributed through the hat truss to the core and 54 percent was redistributed primarily through the spandrels to the south and north walls. After the load redistribution, the total load in the core columns increased to the same level as before the aircraft impact.

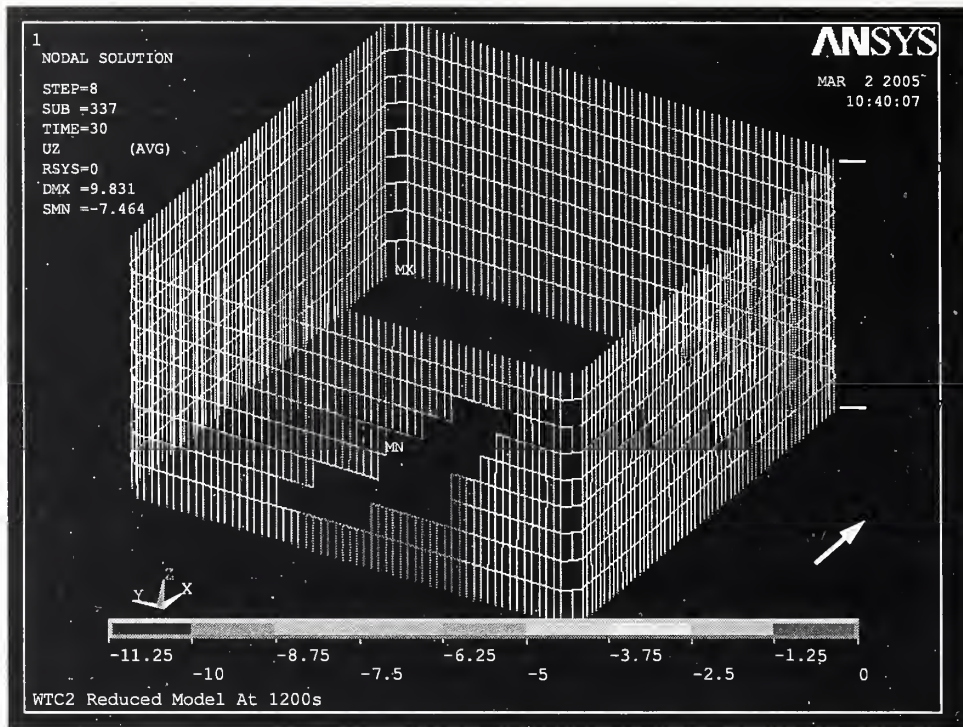


Figure 8–34. Vertical displacement of exterior wall of WTC 2 at 20 min for Case D.

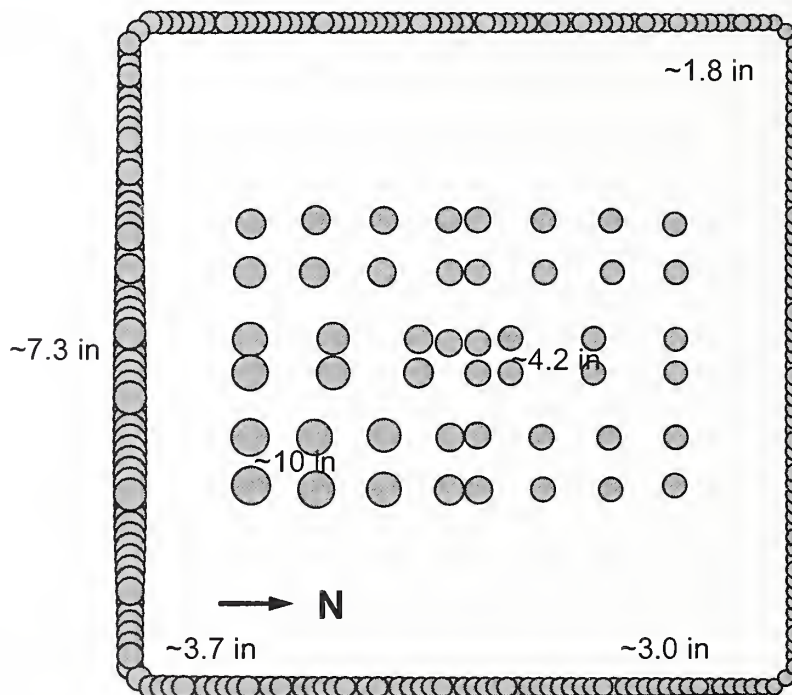


Figure 8–35. Vertical displacement at Floor 83 of WTC 2 at 20 min for Case D (note the tilt toward east and south).

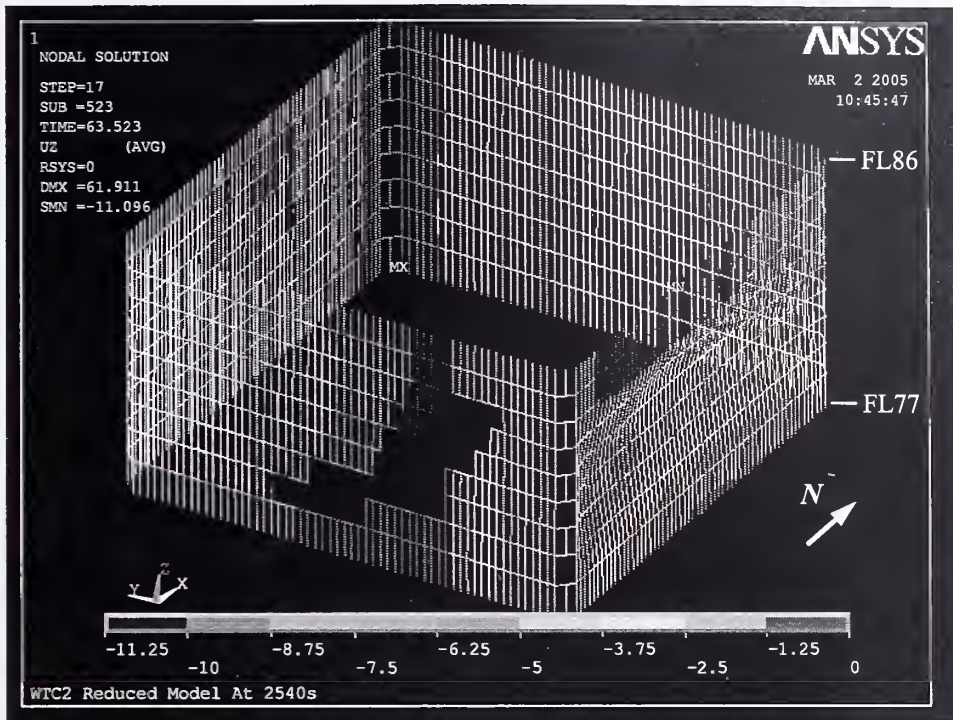


Figure 8–36. Vertical displacement of exterior wall of WTC 2 at 43 min for Case D.

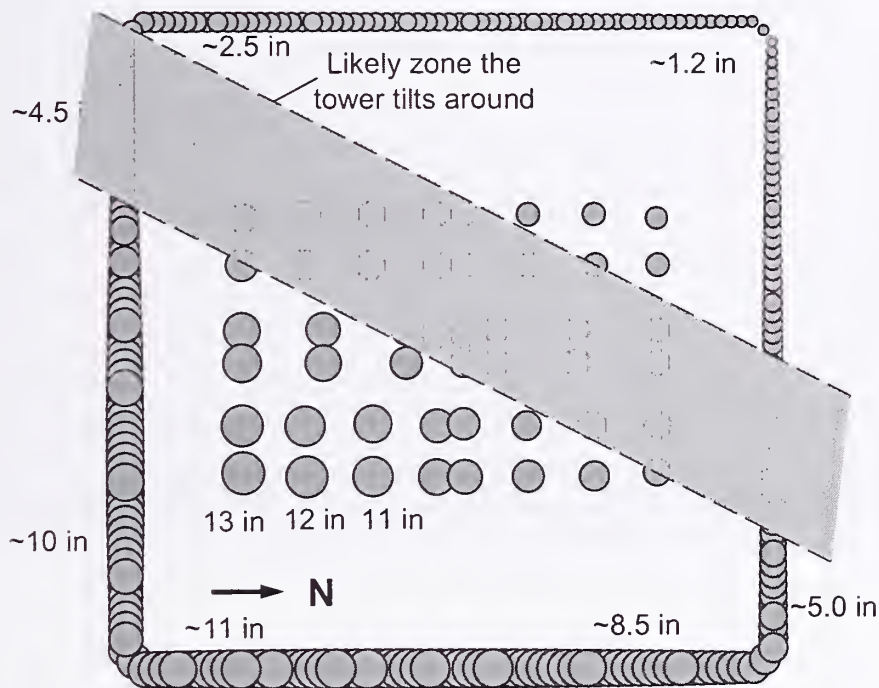


Figure 8–37. Vertical displacement at Floor 83 of WTC 2 at 43 min for Case D (note the tilt toward east and south).

**Table 8–7. Change in total column loads before and after aircraft impact.  
(Loads After Impact) – (Loads Before Impact)  
(Compression is positive).**

Row	Floor	West	East	North	South	Core
(1)	83	604	4368	-1374	227	-4007
(2)	105	674	2699	-895	1263	-3741
(3)	(2) - (1)	69	-1668	479	1035	266

**Table 8–8. Change in total column loads between 40 min and 43 min.  
(Loads at 43 min) – (Loads at 40 min)  
(Compression is positive).**

Row	Floor	West	East	North	South	Core
(1)	83	-2864	-8539	2309	2819	5596
(2)	105	-2112	-3901	23	479	5513
(3)	(2) - (1)	752	4637	-2286	-2340	-84

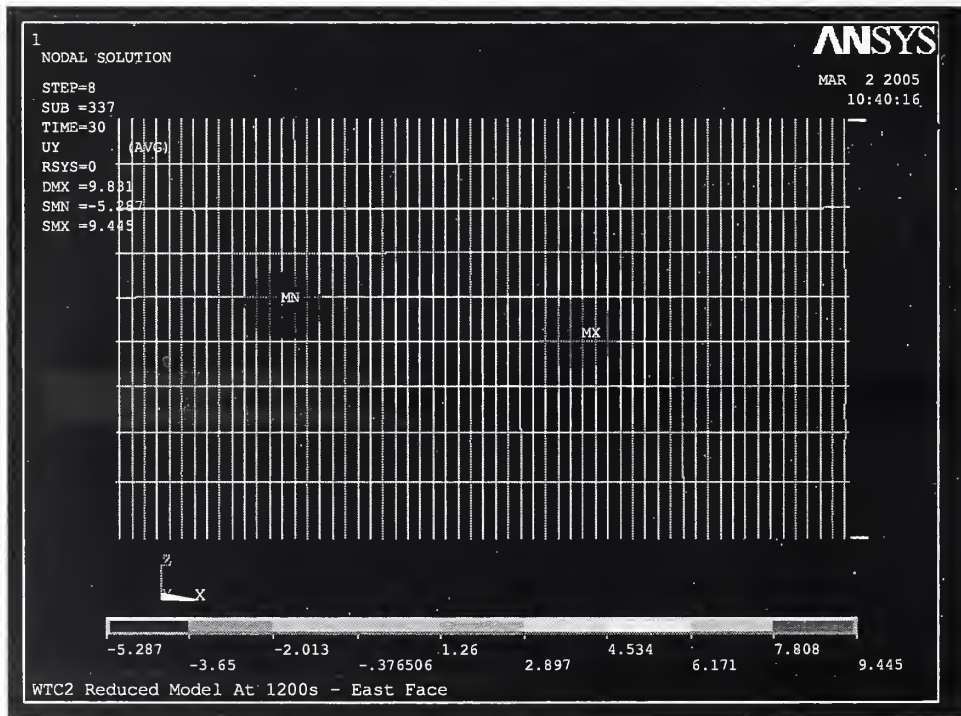


**Figure 8–38. Out-of-plane displacement of the east wall of WTC 2 at 20 min for Case D.**

At 43 min, the east wall became unstable and the inward displacement increased to 62 in., as shown in Figs. 8–39 and 8–40. The south and east wall vertical displacements increased to 11.3 in. The northwest corner of the exterior wall displaced upward about 1.0 in. to 2.0 in., as the tower tilted to the southeast around an axis passing through the southwest and northeast corners, as indicated in Fig. 8–37. The north exterior wall displaced laterally by an additional 15.2 in. to the east, and the south exterior wall displacement increased 6.7 in. to the south. The building section above the impact damage rotated about the tower axis an additional 0.10 percent at Floor 110.

The core displacements suddenly increased to 13 in. at the southeast corner of the core, as shown in Figs. 8–41 and 8–42. Loads on the core columns increased significantly, especially at the northeast corner. For instance, at Floor 83 the load in core column 1008 increased from 2,826 kip after aircraft impact (Figs. 8–33 and 8–43) to 5,317 kip at 43 min (Fig. 8–44), the load in core column 907 increased from 1,290 kip to 2,328 kip, the load in core column 805 increased from 950 kip to 1,483 kip.

Figure 8–45 shows the total displacements (deformed shape scaled by a factor of 20) above Floor 86 when the east wall buckled. The building section above the impact damage tilted to the southeast, and collapse initiated. For reference, the original undeformed tower is also shown.

When the east wall buckled, the load distribution changed significantly, due to the increased tilting of the building section above the impact damage towards the east. Figures 8–46 to 8–49 show how exterior columns loads changed in the exterior walls from before impact to when the east wall became unstable at 43 min. The exterior columns of the east wall unloaded about 200 kip on average at Floor 83. Similarly, the columns on the west face unloaded about 65 kip on average. Part of the load from the east and the west walls was redistributed to the east side of the south and the north walls. The column loads on the east side of the south wall increased from about 500 kip to 800 kip. The column loads on the east side of the north wall increased from about 250 kip to 400 kip.

Figures 8–50 and 8–51 illustrate the load redistribution among the exterior wall and core columns at Floor 83 before aircraft impact and at 43 min, respectively. The tilting of the building about an axis through the shaded area in Fig. 8–51 followed the buckling of the east wall and weakening of the core. Comparison of column loads before aircraft impact and when the east wall became unstable shows the columns unloading over the width of the east face and increasing at the east side of the south and north walls.

Figures 8–52 and 8–53 show the maximum elastic-plus-plastic-plus-creep strains in the columns between Floor 78 and Floor 83 at 20 min and 43 min, respectively. The elastic-plus-plastic strains, which were less than 0.05 percent before the aircraft impact, reached 0.60 percent in some exterior columns and 0.35 percent in some core columns after the aircraft impact, typically those adjacent to severed or heavily damaged columns. With increasing temperatures the plastic and creep strains increased, especially on the east wall and the east side of the core. When the east wall buckled, the elastic-plus-plastic strains reached their maximum of 2.2 percent in the east wall and 0.9 percent in the east side core columns. Creep strains were 1.0 percent to 2.0 percent in the east wall, about 2.0 percent to 6.0 percent in the core columns, and about 4.0 percent to 5.0 percent in the east side of the north wall.

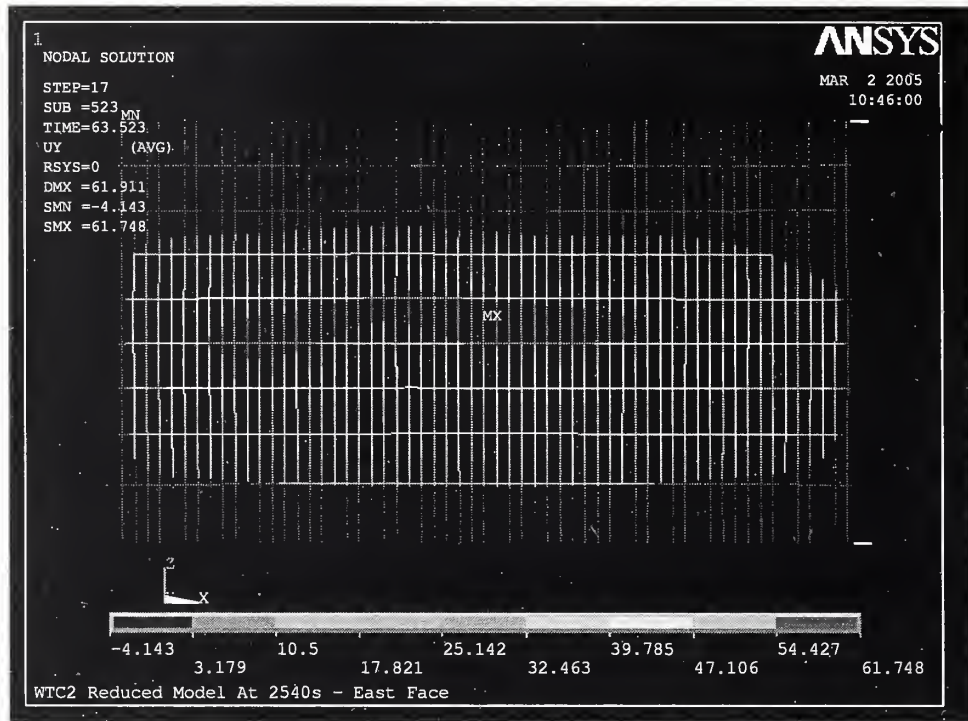


Figure 8–39. Out-of-plane displacement of the east wall of WTC 2 at 43 min for Case D.

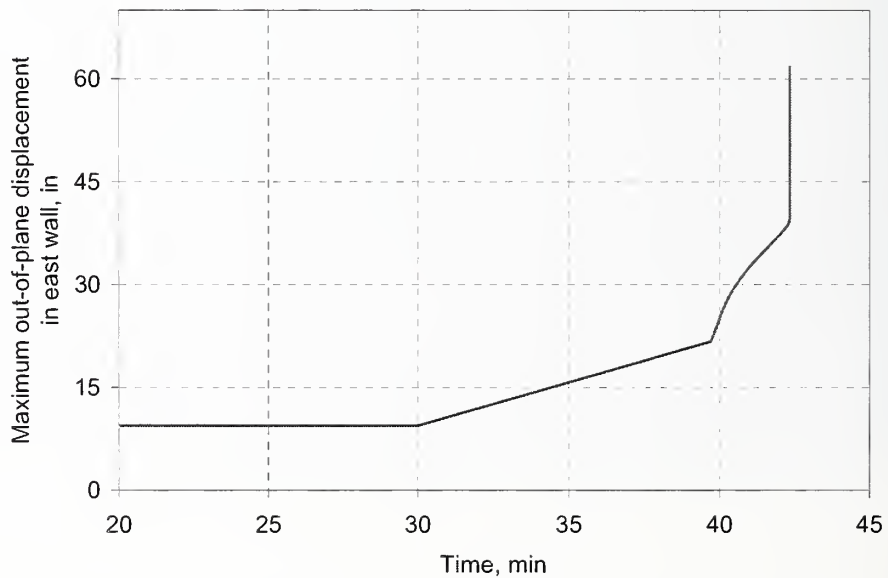


Figure 8–40. Variation of maximum out-of-plane displacement on the east wall of WTC 2 over time for Case D.

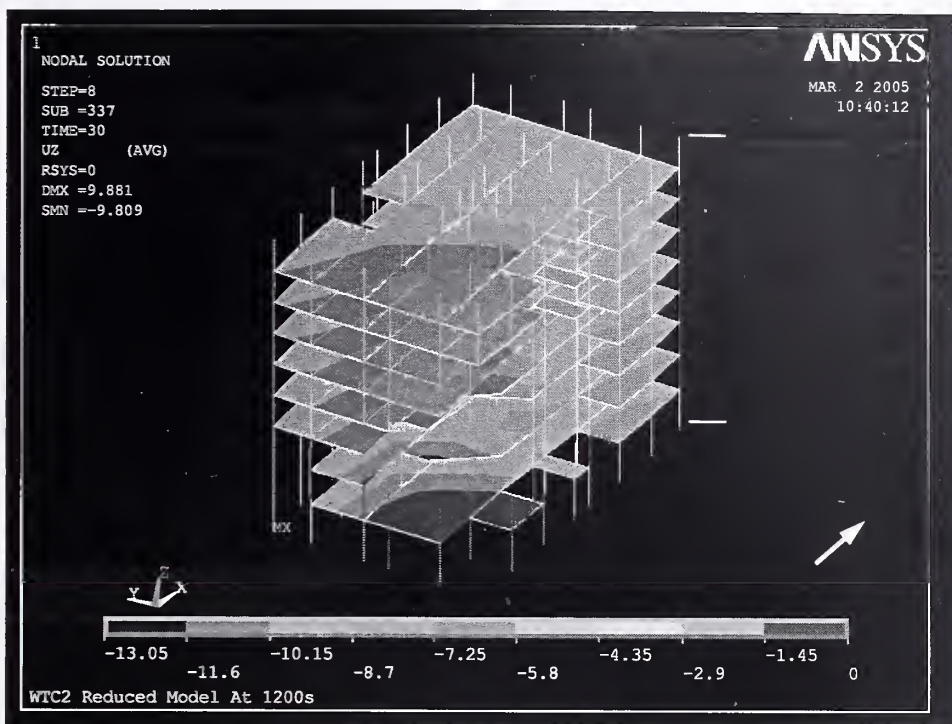


Figure 8-41. Vertical displacement of core of WTC 2 at 20 min for Case D.

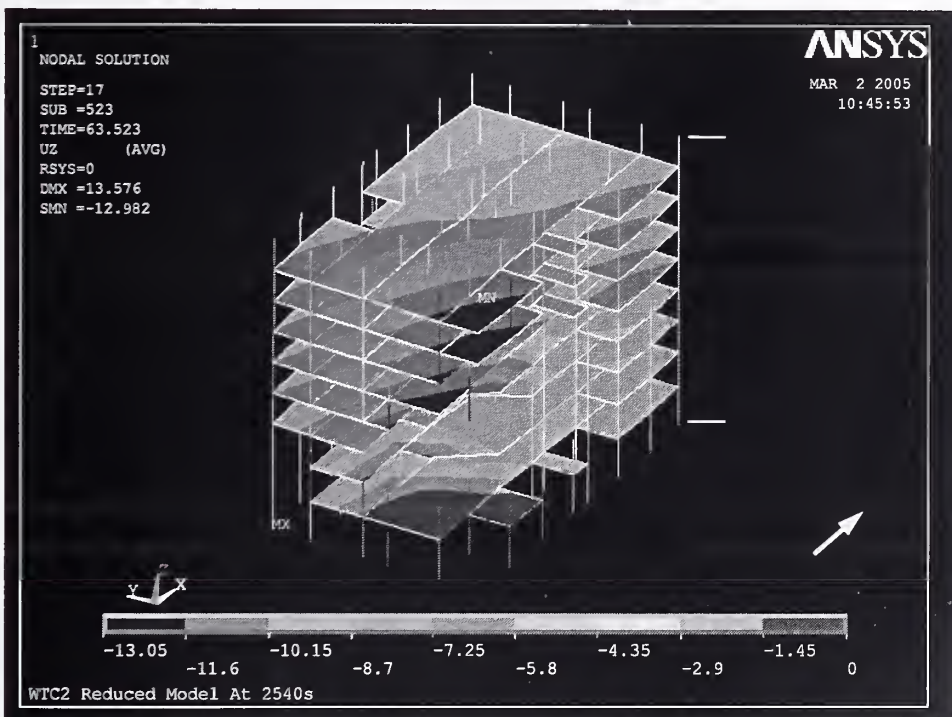


Figure 8-42. Vertical displacement of core of WTC 2 at 43 min for Case D.

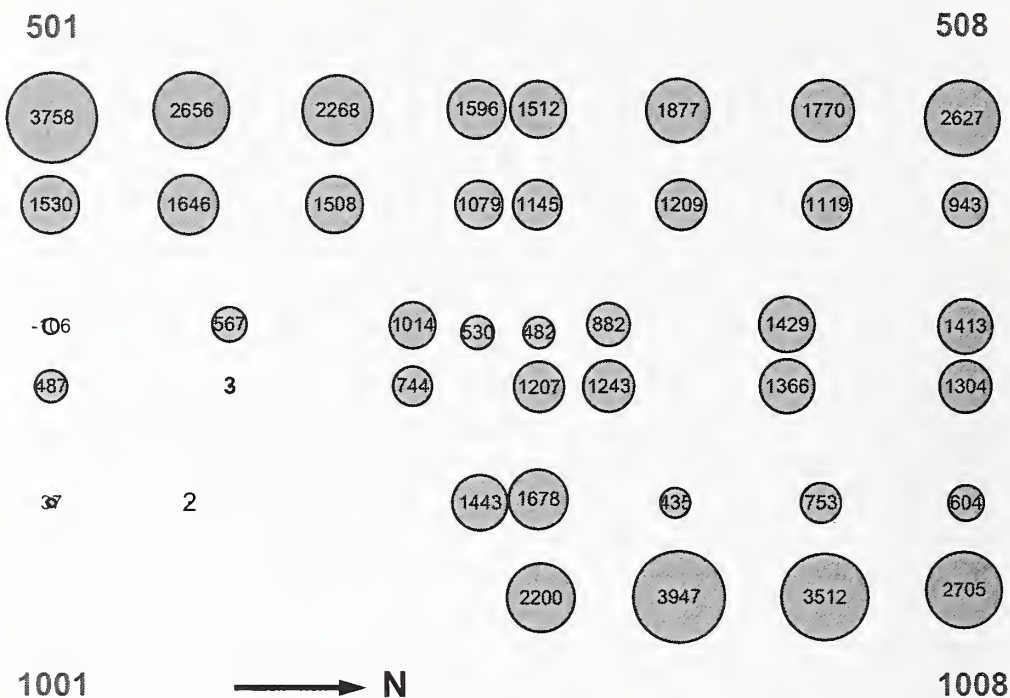


Figure 8-43. Core column loads (kip) at Floor 83 of WTC 2 at 20 min for Case D (compression is positive).

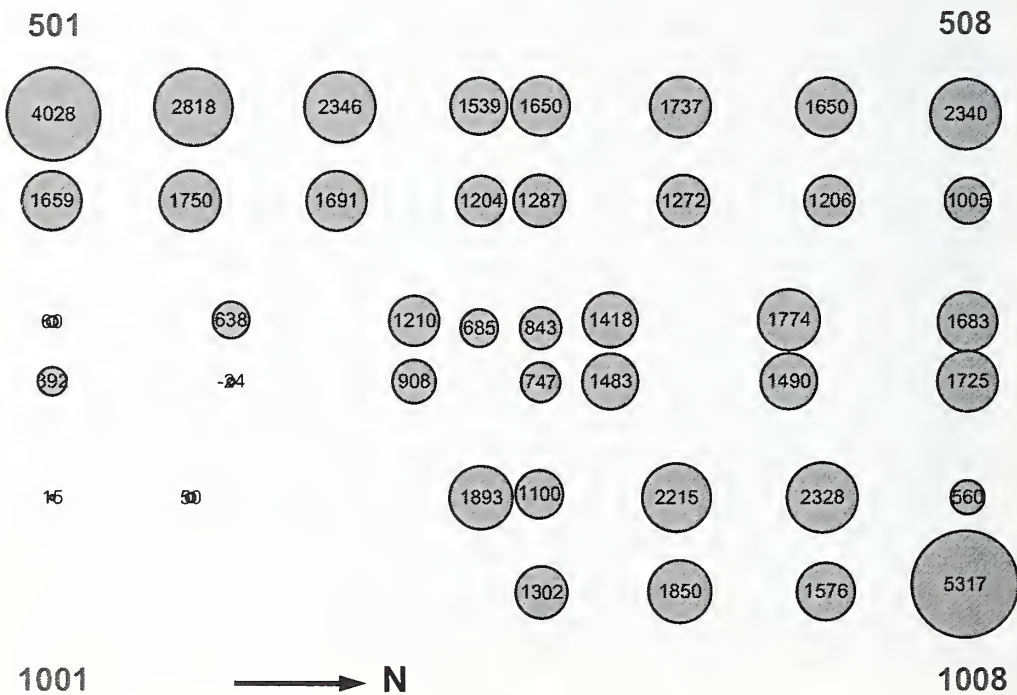


Figure 8-44. Core column loads (kip) at Floor 83 of WTC 2 at 43 min for Case D (compression is positive).

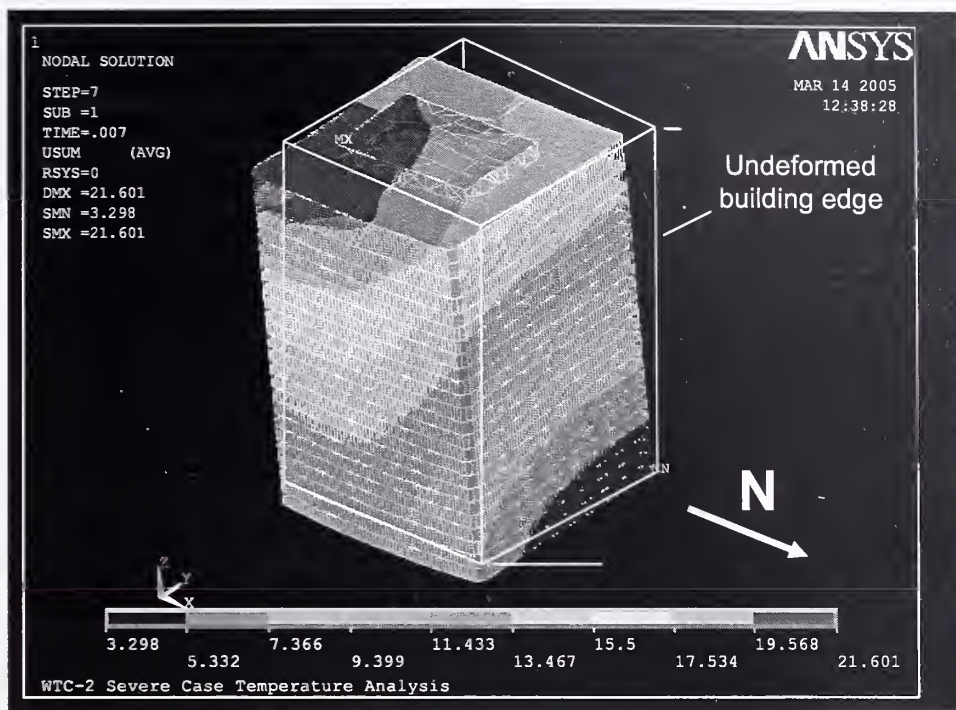


Figure 8-45. Total displacements of WTC 2 above Floor 86 at 43 min of Case D (deformed shape magnified 20 times). Note the tilt toward east and south.

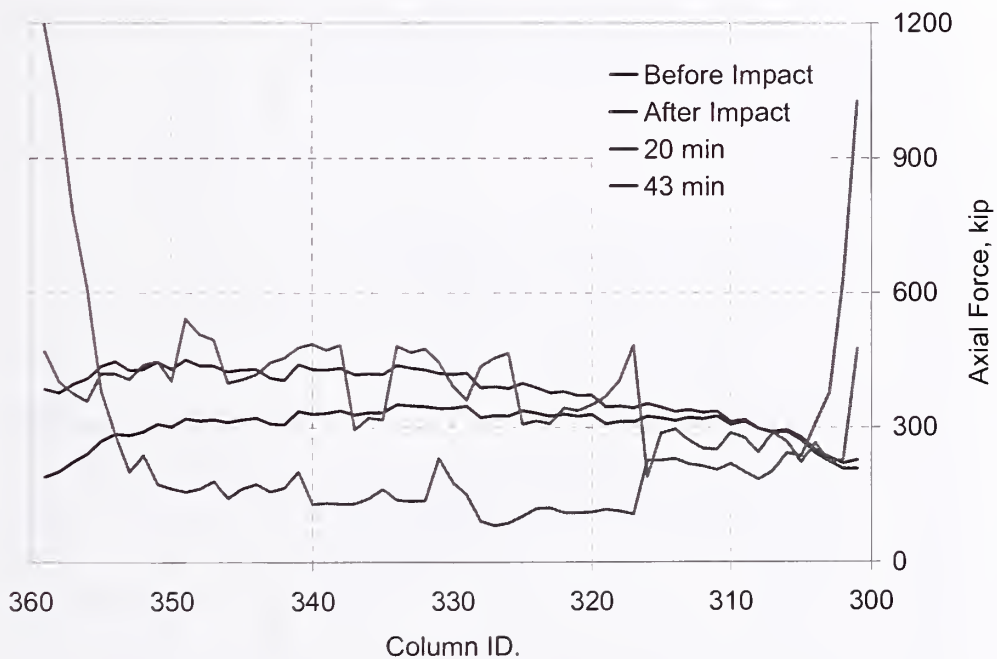
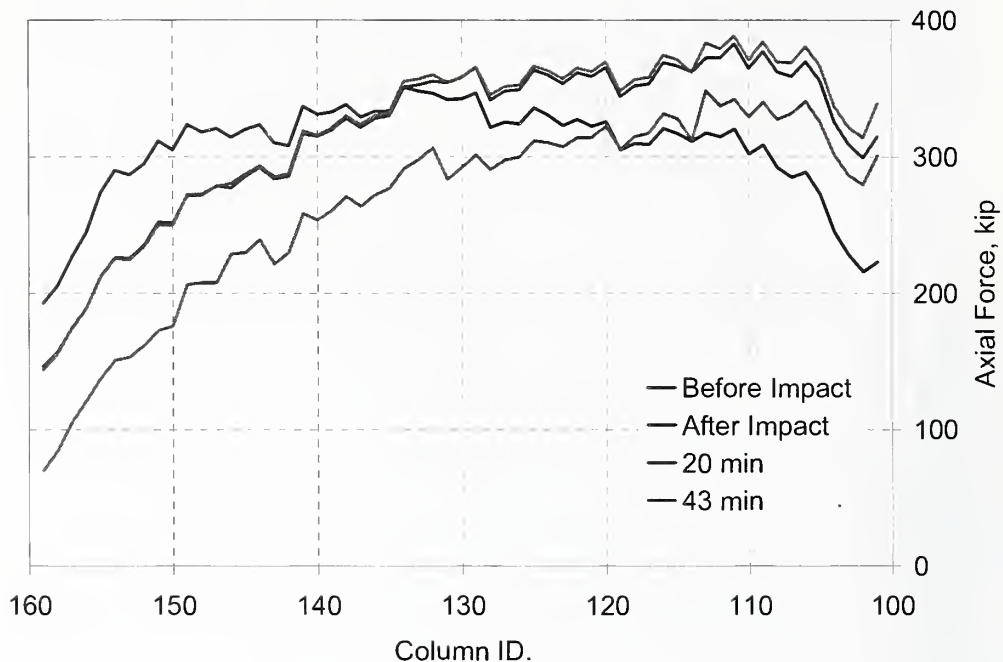
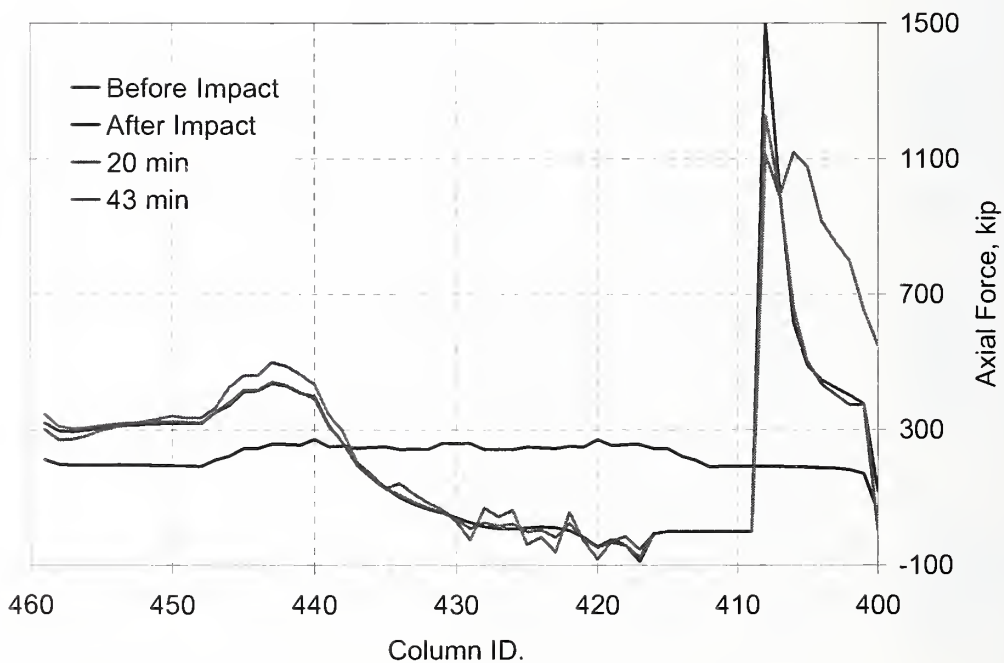


Figure 8-46. Axial force in the east wall columns at Floor 83 of WTC 2 for Case D (compression is positive).



**Figure 8–47. Axial force in the west wall columns at Floor 83 of WTC 2 for Case D (compression is positive).**



**Figure 8–48. Axial force in the south wall columns at Floor 83 of WTC 2 for Case D (compression is positive).**

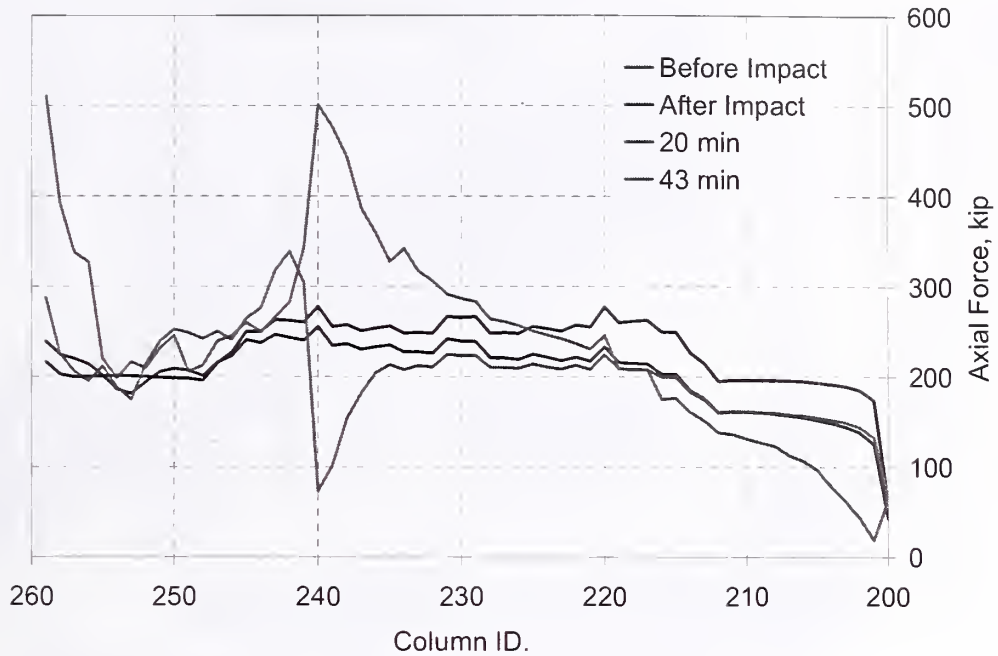


Figure 8-49. Axial force in the north wall columns at Floor 83 of WTC 2 for Case D (compression is positive).

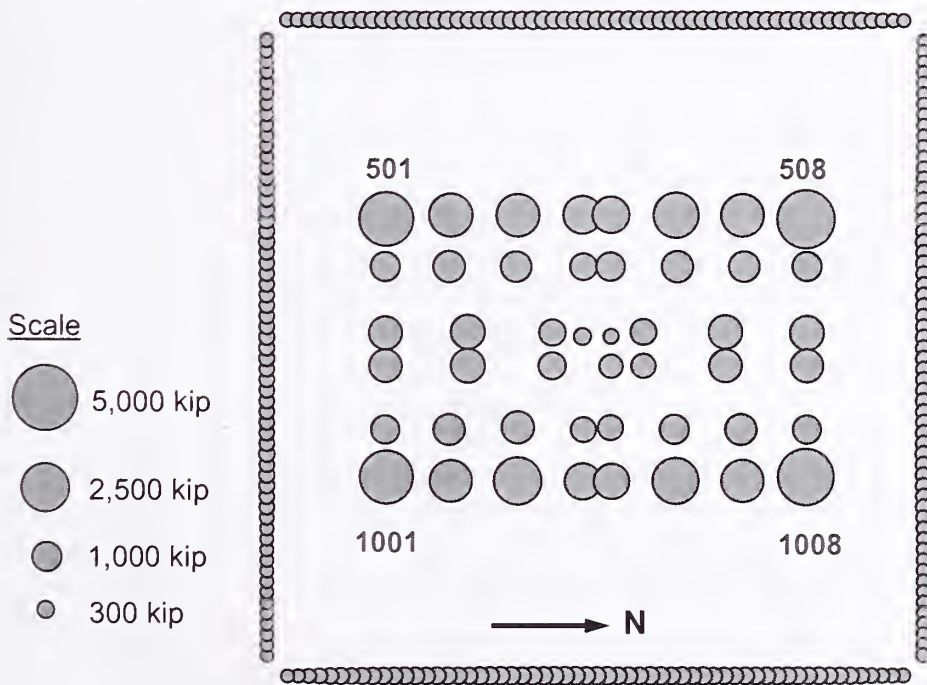


Figure 8-50. Axial force in Floor 83 columns of WTC 2 before impact for Case D (compression is positive).

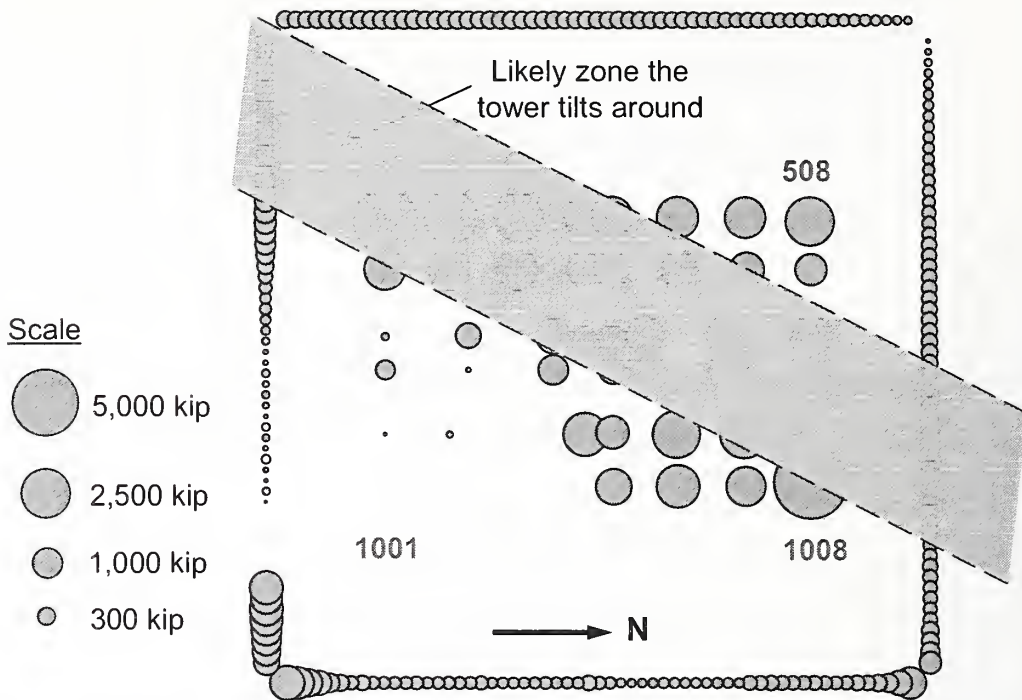


Figure 8-51. Axial force in Floor 83 columns of WTC 2 at 43 min for Case D (compression is positive).

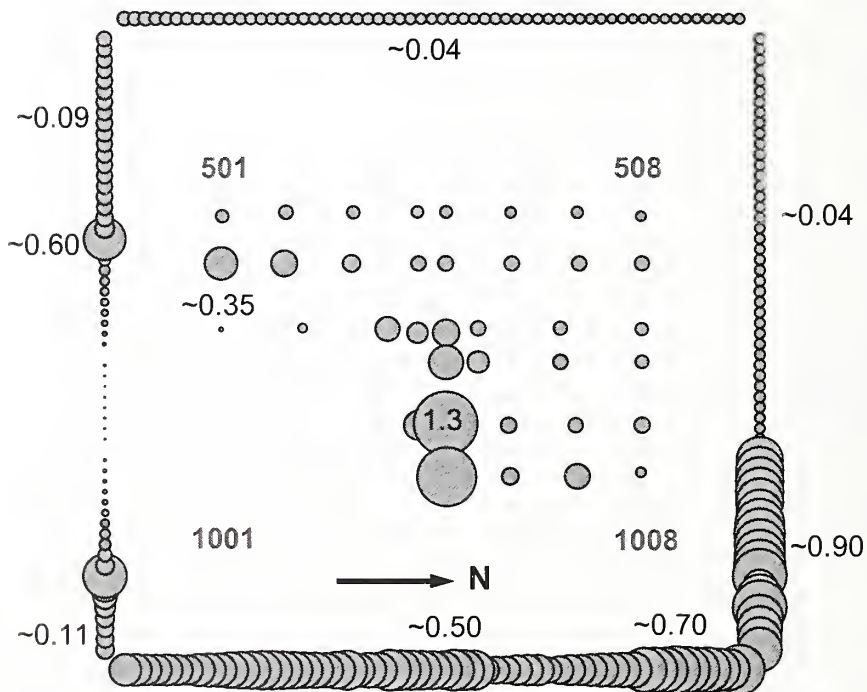
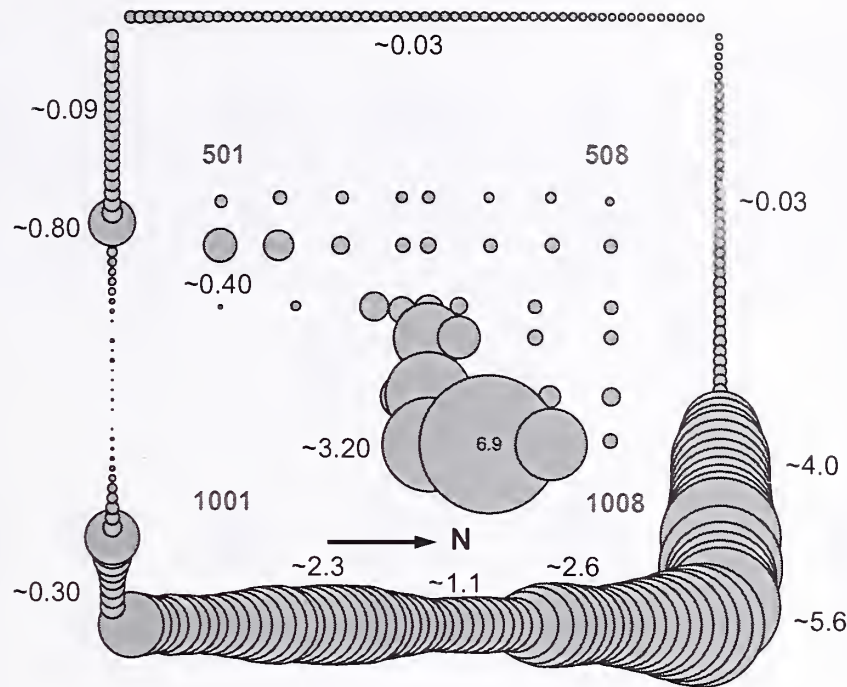


Figure 8-52. Maximum elastic-plus-plastic-plus-creep strains at 20 min for columns between Floor 78 and Floor 83 of WTC 2 for Case D (strain values are in percent).



**Figure 8–53. Maximum elastic-plus-plastic-plus-creep strains at 43 min for columns between Floor 78 and Floor 83 of WTC 2 for Case D (strain values are in percent).**

At 43 min, the core had weakened on the east side and shortened by 3.0 in. at the southeast corner. The east wall had bowed inward approximately 62 in. and unloaded to the core and the adjacent north and south walls. The inward bowing of the east wall caused failure of exterior column splices and spandrels, and induced column instability. The instability progressed horizontally across the entire east face. The east wall unloaded and redistributed its loads to the thermally weakened core through the hat truss and to the east and west walls through the spandrels. This load redistribution is shown in Tables 8–5 and 8–6. The building section above the impact zone began tilting to the east (and to the south, although to a lesser extent) as column instability progressed rapidly from the east wall along the adjacent north and south walls, and increased the gravity load on the weakened east core columns. The change in potential energy due to downward movement of building mass above the buckled columns exceeded the strain energy that could have been absorbed by the structure. Global collapse then ensued.

### 8.5.3 WTC 2 Hat Truss Members and Connections

The state of the hat truss members and the connections were checked as the global model did not include break elements to capture column and hat truss splice failures or sufficient beam elements to capture buckling of hat truss outriggers. The condition of the connections and the members in the primary load path of the hat truss was evaluated at different time intervals. The evaluation included the core column splices for tension, outriggers and supporting columns for compression, and the hat truss connections that were in the primary load path for tension.

In the WTC 2 global model, the hat truss was part of the super-element above Floor 86. The elastic model that generated the stiffness matrix for the super-element, referred to as the “top model” hereinafter, was used to determine component forces. The displacements obtained at the interface nodes between the

super-element and the nonlinear portion of the building (Floor 86) were applied to the base of the top model for each analysis step.

Figures 8–54, 8–55, and 8–56 show the loads on the core column splices at the hat truss level at different steps of the analysis. Each splice was under compressive load before the aircraft impact. After the aircraft impact, the splices at severed core column lines started to carry tensile loads. The tensile capacity of the splices was compared to tensile forces at 40 min, which was when the maximum tensile forces occurred. In calculating the tensile capacity of the connections, AISC-LRFD procedures were used.

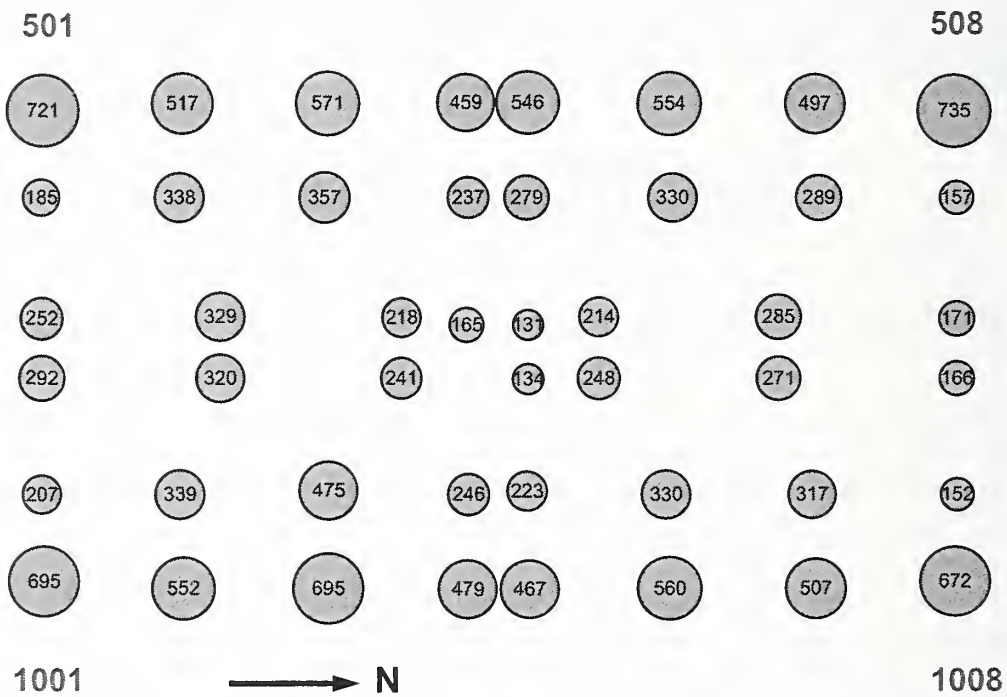


Figure 8–54. Axial force in core columns (kip) at WTC 2 Floor 105 (at hat truss level) before impact for Case D (compression is positive).

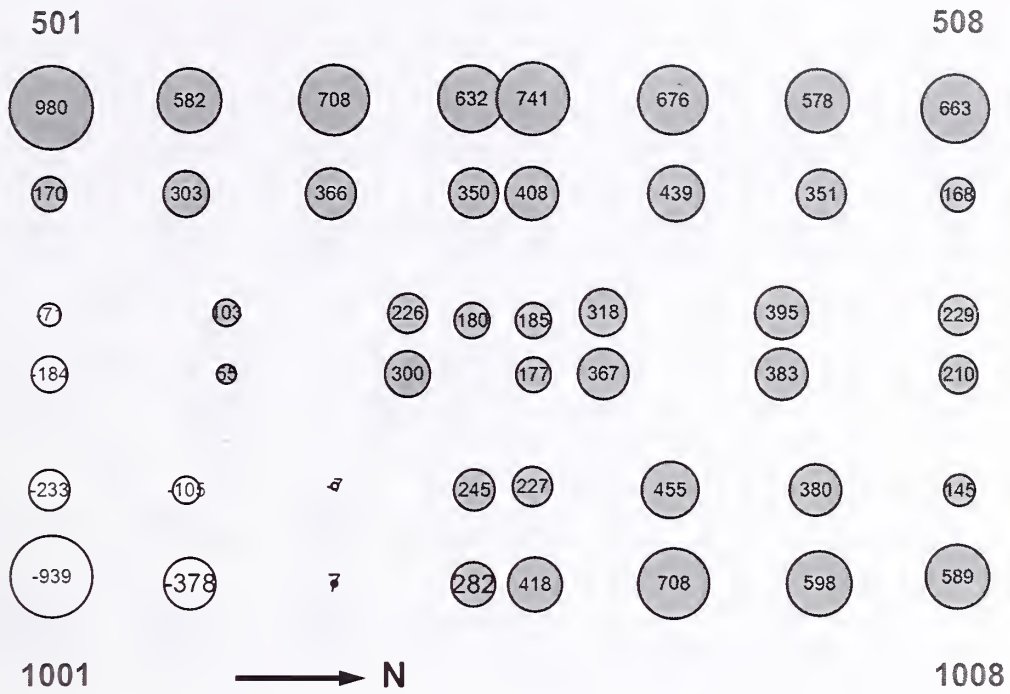
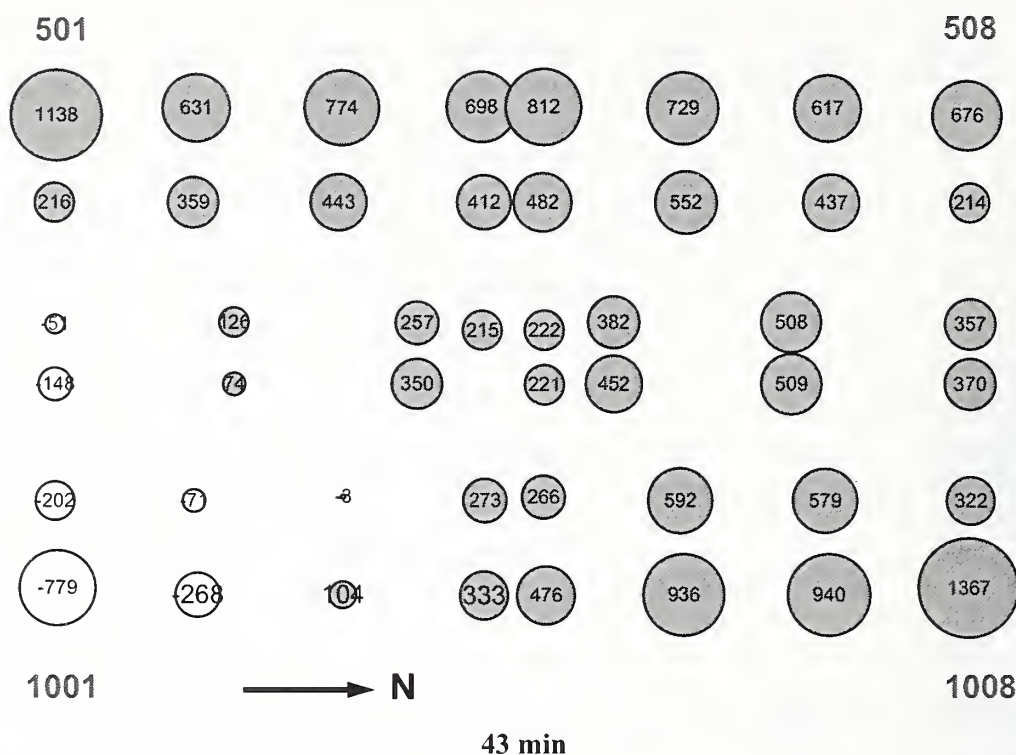


Figure 8-55. Axial force in core columns (kip) at WTC 2 Floor 105 (at hat truss level) after impact for Case D (compression is positive).



**Figure 8–56. Axial force in core columns (kip) at Floor 105 (at hat truss level) of WTC 2 for Case D conditions (compression is positive).**

The evaluation of core column splices required an iterative procedure as splice failures were not modeled in the top model. In the first iteration, the top model reached equilibrium using the interface node displacements at 40 min. Once equilibrium was reached, the columns exceeding their splice capacity were identified (in the first iteration columns 1001 and 1002 were identified) and removed from the top model. Before removing the columns, the displacement boundary conditions applied at the bottom of these column lines (at Floor 86) were replaced with the reaction forces that were obtained at the end of the first iteration. This conversion from displacement to force boundary condition allowed the remaining portion of the column lines to displace in the vertical direction when the columns were removed at Floor 105 to simulate splice failure. This iterative procedure was repeated until none of the remaining splices exceeded their tension capacity. A stable state was reached at the end of the fourth iteration. Fig. 8–57 shows the state of the core column splices at the end of the fourth iteration. Splices for columns 1001 and 1002 failed after impact, and splices for columns 701, 801, 901, 902, and 1003 failed either after impact or as the core responded to the fires.

In the global analyses, splice failures were not included in the super-element, which remained elastic throughout the analysis. However, based upon the analyses discussed below, it was concluded that the inclusion of splice failures would not have significantly affected the load redistribution in the global analysis. The core floors would have redistributed the loads in the failed columns to adjacent core columns, as occurred for columns with failed splice connections in the impact area. The adjacent columns would have then transferred the loads to the hat truss.



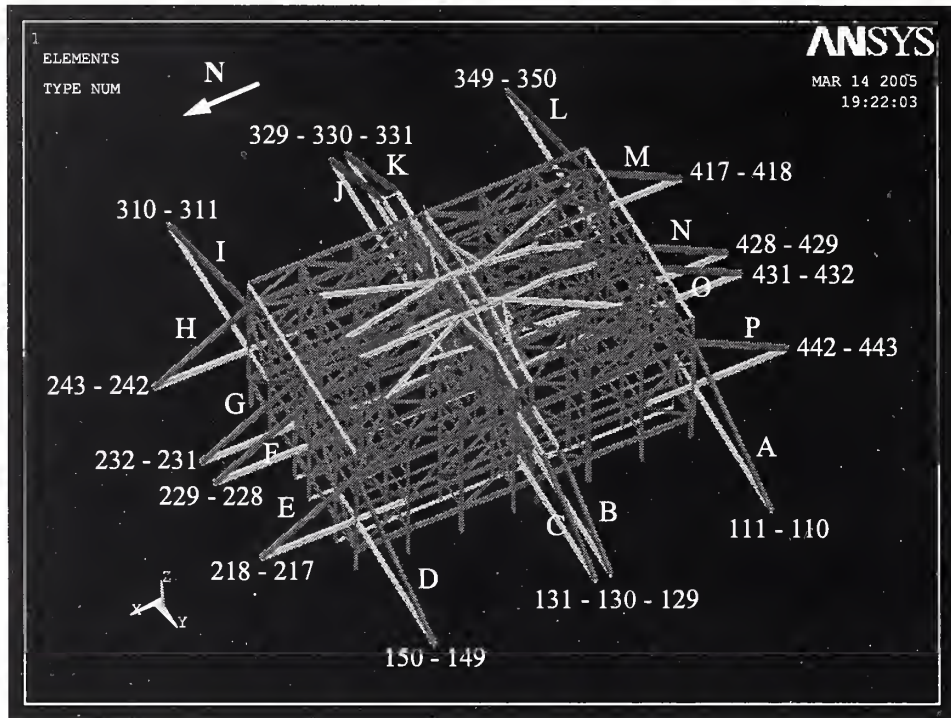


Figure 8-58. Location and IDs of outriggers and supporting columns

Table 8-9. Demand-to-capacity ratios for outriggers of WTC 2 for Case D conditions (outrigger IDs are shown in Fig. 8-3).

Outrigger ID	Bfr. Imp.	Afr. Imp.	10 min	20 min	30 min	40 min	40* min	40** min	43 min
<b>West</b>									
A	0.23	0.61	0.61	0.64	0.66	0.63	0.63	0.38	0.25
B	0.19	0.30	0.30	0.32	0.33	0.31	0.31	0.25	-0.03***
C	0.19	0.27	0.27	0.28	0.30	0.27	0.28	0.22	-0.07
D	0.21	0.18	0.18	0.19	0.21	0.18	0.20	0.19	-0.29
<b>North</b>									
E	0.29	0.11	0.10	0.10	0.13	0.14	0.17	0.09	-0.01
F	0.21	0.10	0.08	0.08	0.10	0.12	0.13	0.11	0.08
G	0.20	0.11	0.08	0.08	0.11	0.13	0.14	0.13	0.10
H	0.30	0.21	0.16	0.18	0.19	0.18	0.19	0.24	0.24
<b>East</b>									
I	0.22	0.39	0.35	0.34	0.45	0.43	0.42	0.41	-0.18
J	0.18	0.56	0.52	0.53	0.66	0.65	0.61	0.71	0.02
K	0.18	0.62	0.58	0.59	0.72	0.72	0.66	0.79	0.09
L	0.22	1.12	1.09	1.12	1.24	1.30	1.11	0.00	0.72
<b>South</b>									
M	0.30	0.68	0.64	0.64	0.70	0.75	0.52	0.72	0.87
N	0.22	0.34	0.32	0.33	0.36	0.38	0.28	0.34	0.40
O	0.22	0.30	0.28	0.30	0.32	0.33	0.27	0.31	0.33
P	0.31	0.51	0.50	0.52	0.53	0.53	0.50	0.57	0.49

\* After load redistribution due to core column splice failures.

\*\* After Outrigger L was removed.

\*\*\* Negative value indicates tension

With the identified splice failures in Columns 1001 and 1002 and adjacent core columns, the load in this outrigger would have been redistributed to other outriggers. Based on the computed load redistribution after splice failures, the demand-to-capacity ratio on Outrigger L was estimated to be reduced from 1.3 to 1.1 (Column “40\* min” in Table 8–9).

Outrigger L was removed from the top model after all the failed splices were removed to determine the effect on adjacent outriggers. Removal of the Outrigger L represented an upper bound solution as the load in the Outrigger would not have dropped down to zero. The adjacent outriggers increase in load; however, after the removal of the Outrigger L as presented in Column “40\*\* min” of Table 8–9, none of the remaining outriggers exceeded their buckling or yield capacities.

The connections within the hat truss were also checked. The hat truss connections in the primary load path were identified, and their capacities were compared to their forces. The primary load path was identified by selecting hat truss members with an absolute axial stress of 25 ksi or more at 40 min, as this was when maximum forces occurred. Only the connections that transferred tensile forces were evaluated. In calculating the capacity of the connections, the AISC-LRFD procedures were used. None of the hat truss connection capacities were exceeded. Before redistribution of load due to the column-to-hat truss splice failure, none of the hat truss connections had exceeded their capacities except for the hat truss connections associated with the 1001 core column. After the load redistribution following the splice failure, the demand on the hat truss connections for the 1001 column was less than the yield capacities of all connections. It was concluded that the hat truss was capable of transferring loads from core columns to the outriggers.

Based on this discussion, it was concluded that the hat truss transferred the majority of the loads between core and exterior wall columns, even though some column splices may have failed and one outrigger may have buckled.

## **8.6 STRUCTURAL RESPONSE OF THE WTC TOWERS TO FIRE WITHOUT IMPACT DAMAGE**

Whether the towers would have collapsed if subjected to an intense but conventional fire without aircraft impact was considered to better understand the relative roles of the impact damage and fires. This is not to imply that the fire growth and spread observed in the towers could be obtained without aircraft damage to the buildings and rapid ignition of multi-floor fires due to the dispersion of jet fuel. NIST used the observations, information, and analyses developed during the Investigation to enable the formulation of probable limits to the damage from such a fire. Since a complete analysis beyond the actual collapse times of the towers was not conducted, the findings in this section represent NIST’s best technical judgment based upon the available observations, information, and analyses.

In making the comparison, the following points were considered.

- Both WTC 1 and WTC 2 were stable after the aircraft impact. The global analyses showed that both towers had considerable reserve capacity after structural impact damage. For example, Figs. 8–9 and 8–10 show the core column demand-to-capacity ratios remained nearly the same before and after impact, except for a few columns adjacent to the severed columns. Global analysis produced similar trend for the exterior columns. This was confirmed by analysis of video footage of the post-impact vibration of WTC 2, the more

severely damaged of the two towers, which showed that the period of vibration of the building before and after impact were nearly the same, thus showing that the building had significant reserve capacity. WTC 2 oscillated with a peak amplitude that was between 30 percent and 40 percent of the tower sway under design winds and at periods nearly equal to the first two translation and torsion mode periods calculated for the undamaged structure (see NIST NCSTAR 1-2).

- Results of both the multi-workstation experiments and the simulations of the WTC fires showed that the combustibles in a given location, if undisturbed by the aircraft impact, would have been almost fully burned out in about 20 min. Note that, for the occupancies in the World Trade Center, the fuel load was estimated—and supported by fire dynamics calculations and visual observations—to be approximately 4 psf (see NIST NCSTAR 1-5).
- The fires used in the Investigation (Cases A through D), estimated from fire dynamics simulations, represented fires that were far more severe than an intense conventional fire (see NIST NCSTAR 1-5).
- In WTC 1, if fires had been allowed to continue past the time of building collapse, complete burnout would likely have occurred within a short time since the fires had already traversed around the entire floor and most of the combustibles would already have been consumed (see NIST NCSTAR 1-5). During the extended period from collapse to burnout, the steel temperatures would likely not have increased very much. The installed insulation in the fire-affected floors of this building had been upgraded to an average thickness of 2.5 in.
- In a fire simulation of WTC 2, that extended Case D for 2 hours with all windows broken during this period, the temperatures in the truss steel on the west side of the building (where the insulation was undamaged) increased for about 40 minutes before falling off rapidly as the combustibles were consumed. Results for a typical floor (floor 81) showed that temperatures of 700 °C to 760 °C were reached over approximately 15 percent of the west floor area for less than 10 minutes. Approximately 60 percent of the floor steel had temperatures between 600 °C and 700 °C for about 15 minutes. Approximately 70 percent of the floor steel had temperatures that exceeded 500 °C for about 45 min. At these temperatures, the floors would be expected to sag and then recover a portion of the sag as the steel began to cool. Based on results for Cases C and D, the temperatures of the insulated exterior and core columns would not have increased to the point where significant loss of strength or stiffness would occur during these additional 2 hours. With intact, cool core columns, any inward bowing of the west exterior wall that might occur would be readily supported by the adjacent exterior walls and core columns.
- In the simulations of Cases A through D, none of the columns and trusses for which the insulation was intact reached temperatures at which significant loss of strength occurred for the duration analyzed. The relative effects of the presence or absence of insulation on structural components, subjected to the same fire conditions, are shown in Fig. 8-59 (see NIST NCSTAR 1-5) for both adjacent trusses and exterior columns. As the plots indicate, the rate of heating was found to differ significantly depending on whether the insulation was intact or not.

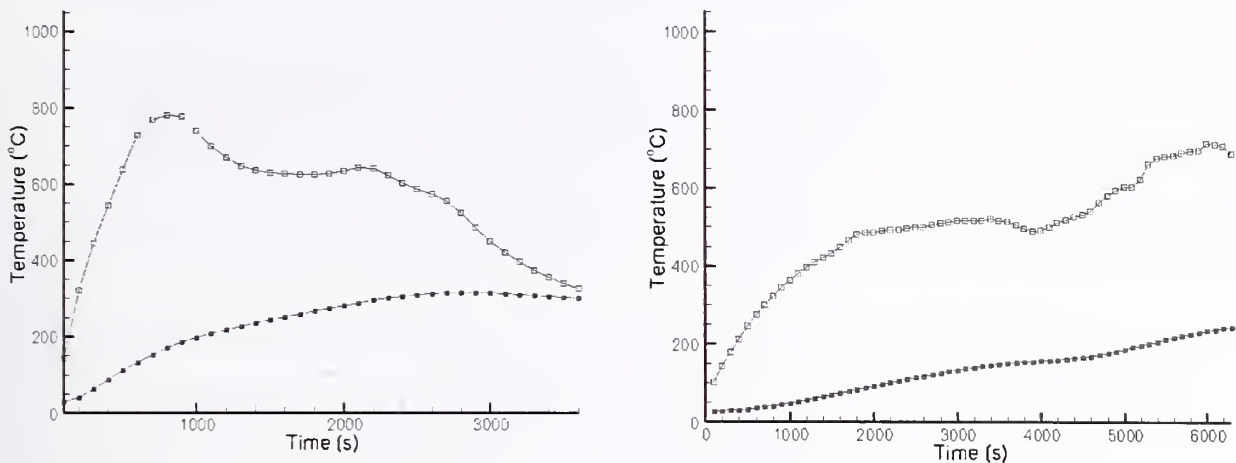


**Figure 8–59. Temperatures of two adjacent trusses (left) and two adjacent perimeter columns (right) exposed to simulated fires in WTC 1. Data plotted in blue are for structural steel components with fireproofing; data in red are for steel components without fireproofing (from NIST NCSTAR 1-5).**

- Structural computer simulations of the floor system (Chapter 7), supported by results of full-scale fire tests (NIST NCSTAR 1-5) and performance observed in standard fire tests (NIST NCSTAR 1-6B), showed that structural steel, insulated with  $\frac{3}{4}$  in. thick fireproofing, would not have reached temperatures greater than 650 °C prior to burnout of the combustibles (20 min as noted above). Simulations also showed that variations in thickness resulting from normal application, even with occasional gaps in coverage, would not have changed this result.
- The structural temperatures of core columns in WTC 1 and WTC 2 did not exceed 300 °C where the fireproofing was intact. Thermal analysis of the WTC 1 and WTC 2 floors and exterior columns indicated that the steel temperatures were generally lower than 300 °C, with a few isolated members that rarely exceeded temperatures of 400 °C for WTC 1 and 500 °C for WTC 2 (NIST NCSTAR 1-5). Under these temperatures, reductions of stiffness and strength were small and creep effects and buckling were found not to be significant (Chapters 4 and 7). Insulated floors thermally expanded and pushed outward on the exterior columns as well as sag in the full floor analyses, but the floor sag was insufficient to exert an inward pull on the exterior columns.
- Inward bowing of the exterior walls in both WTC 1 and WTC 2 was observed only on the face with the long-span floor system. In WTC 1, this was found to be the case even though equally extensive fires were observed on all faces. The impact damage to the north face reduced the area over which pull-in could occur. In WTC 2, fires were not observed on the long-span west face and were less intense on the short-span faces than on the east face.

- Inward bowing was a necessary but not sufficient condition to initiate collapse. In both WTC 1 and WTC 2, significant weakening of the core due to aircraft impact damage and thermal effects was also necessary to initiate building collapse.
- The tower structures had significant capacity to redistribute loads (a) from bowed walls to adjacent exterior walls with short-span floors via the arch action of spandrels, and (b) between the core and exterior walls via the hat truss and, to a lesser extent, the floors.

In evaluating how the undamaged towers would have performed in an intense, conventional fire, NIST considered the following factors individually and in combination:

- The temperatures that would be reached in structural steel components with intact insulation.
- The extent of the area over which high temperatures (e.g., greater than 600 °C where significant thermal weakening of the steel occurs) would be reached at any given time.
- The duration over which the high temperatures would be sustained concurrently in any given area.
- The length of the floor span (long or short) where high temperatures would be reached.
- The number of floors with areas where high temperatures would be sustained concurrently in the long-span direction.
- The potential for inward bowing of exterior walls (i.e., magnitude and extent of bowing over the width of the face and the number of floors involved) due to thermally-induced floor sagging of long-span floors and associated inward pull forces.
- The capacity of the structure to redistribute loads (e.g., via the spandrels, hat truss, and floors) if the thermal conditions were sufficiently intense to cause inward bowing of the exterior walls.

In addition, NIST considered the following known facts about the performance of the WTC tower structures in fires:

- Historical fires also provided evidence that the towers would not collapse if subjected to a major fire without accompanying impact damage. WTC 1 did not collapse during the major fire in 1975, which engulfed about 9,000 ft<sup>2</sup> on the southeast quadrant of Floor 11. The fire spread mostly via utility closets to ten floors. At the time, office spaces in the WTC towers were not sprinklered. The fire caused minimal damage to the floor system with the ½ in. specified insulation thickness applied on the trusses (four trusses were slightly distorted) and at no time was the load carrying capacity of the floor system compromised. The fire “did not damage a single primary, fireproofed element. Some top chord members (not needed for structural integrity), some bridging members (used to reduce floor tremor and the like) and some deck support angles (used only as construction elements) were buckled in the fire—all were un-fireproofed steel.” (SCHR Letter Report 1975).

- Additionally, the four Standard Fire Tests (ASTM E 119) of floor assemblies like those in the WTC towers showed that the load carrying capacity of the short span 35 ft floor system with a 0.75 in. insulation thickness was not compromised by heating for two hours at furnace temperatures with applied loads that exceeded those on September 11, 2001 by a factor of two. It took about 90 minutes of sustained heating in the furnace for temperatures to exceed 600 °C on steel truss members with either ½ in. or ¾ in. insulation thickness. The high temperature conditions in the furnace tests were at least as severe and lasting as long as the WTC fires, although the top of the slab was not heated. Although some web members buckled and the floor test assembly sagged up to 14 in. during the tests, the insulation remained intact during the tests.

From these points and observed performance, NIST concluded:

- In the absence of structural and insulation damage, a conventional fire substantially similar to or less intense than the fires encountered on September 11, 2001 likely would not have led to the collapse of a WTC tower.
- The condition of the insulation prior to aircraft impact, which was found to be mostly intact, and the insulation thickness on the WTC floor system contributed to, but did not play a governing role, in initiating collapse of the towers.
- The towers likely would not have collapsed under the combined effects of aircraft impact and the subsequent multi-floor fires encountered on September 11, 2001 if the insulation had not been widely dislodged or had been only minimally dislodged by aircraft impact.

These conclusions apply to fires that are substantially similar to or less intense than those encountered on September 11, 2001. They do not apply to a standard fire exposure or an assumed fire exposure which has (a) uniform high temperatures over an entire floor or most of a floor (note that the WTC floors were extremely large) and concurrently over multiple floors and (b) high temperatures that are sustained indefinitely or for long periods of time (greater than about 20 min at any location), and (c) combusted fire loads that are significantly greater than those considered in the analyses. They also do not apply if the capacity of the undamaged structure to redistribute loads via the spandrels, hat truss, and floors were not accounted for adequately in a full 3-dimensional simulation model of the structure.

## 8.7 SUMMARY OF STRUCTURAL RESPONSE OF THE WTC TOWERS

The structural analyses conducted of floors, isolated exterior walls and cores, and global models of WTC 1 and WTC 2 found that the collapse of the towers was due to the combined effects of structural and insulation damage from aircraft impact and the subsequent fires.

Impact damage alone did not cause collapse of the towers, as they were stable after the aircraft impact and analyses showed that they had substantial reserve capacity. The fires alone also would not have caused collapse of the towers. Without impact damage, there would not have been extensive dislodging of insulation, and the structural steel temperatures would have been generally less than 300 °C, with a few steel temperatures reaching 400 °C in WTC 1 floors and 500 °C in WTC 2 floors. The core would not have weakened, the floor sag would have been insufficient to pull inward on the exterior columns, and as a consequence the exterior walls would not have bowed inward.

Collapse occurred after the fires weakened areas of the core, floors, and exterior walls that had dislodged insulation, and the core and exterior columns were unable to support the gravity loads with their reduced capacity.

The towers would likely not have collapsed under the combined effects of aircraft impact and the subsequent multi-floor fires if the insulation had not been dislodged or had been only minimally dislodged by aircraft impact. The existing condition of the insulation prior to aircraft impact and the insulation thickness on the WTC floor system did not play a significant role in initiating collapse of the towers.

## 8.8 REFERENCES

National Oceanic and Atmospheric Administration (NOAA)/National Climatic Data Center (NCDC), (NOAA 2001a)"Automated Surface Observing System Data; Unedited Surface Weather Observations - Hourly Data, LaGuardia Airport, September 11, 2001"

National Oceanic and Atmospheric Administration (NOAA)/National Climatic Data Center (NCDC), (NOAA 2001b)"Automated Surface Observing System Data; Unedited Surface Weather Observations - Hourly Data, John F. Kennedy Airport, September 11, 2001"

National Oceanic and Atmospheric Administration (NOAA)/National Climatic Data Center (NCDC), (NOAA 2001c)"Automated Surface Observing System Data; Unedited Surface Weather Observations - Hourly Data, Newark, NJ Airport, September 11, 2001"

## Chapter 9

# PROBABLE COLLAPSE SEQUENCES

---

### 9.1 INTRODUCTION

World Trade Center (WTC) 1 and WTC 2 were subjected to aircraft impact and uncontrolled fires and experienced a series of events that required complex analyses to determine their probable collapse sequences. The analysis of these events required a formal approach to integrate multiple disciplines effectively, to discern which parameters significantly influenced the analysis methods and results, and to determine the probable sequence of events leading to the initiation of structural collapse. These methods were applied as appropriate to different scales of modeling—component, subsystem, and global scales—for the aircraft impact damage, fire dynamics, thermal, and structural response analyses.

To identify the probable collapse sequences, National Institute of Standards and Technology (NIST) adopted an approach that combined mathematical modeling, statistical-based analysis methods, laboratory experiments, and analysis of photographs and videos. The approach accounted for variations in models, input parameters, analyses, and observed events. It included the evaluation and comparison of possible collapse hypotheses based on various damage states, fire paths, and structural responses to determine the following:

- The probable sequence of events from the moment of aircraft impact until the initiation of global building collapse;
- How and why WTC 1 stood nearly twice as long as WTC 2 before collapsing (102 min for WTC 1 versus 56 min for WTC 2), although they were hit by virtually identical aircraft (Boeing 767-200ER);
- What factors, if any, could have delayed or prevented the collapse of the WTC towers.

Section 9.2 describes the methodology used to conduct the aircraft impact, fire dynamics, thermal, and structural response analyses for determining the probable collapse sequence of each tower, which is presented in Section 9.3. Section 9.4 presents a discussion and summary of the collapse sequences.

### 9.2 METHODOLOGY

To determine the probable collapse sequence for each tower, the following steps were required:

- identification of key observables, primarily from photographs and videos
- development of collapse hypotheses, which were updated periodically through the course of the investigation with the acquisition of new data and analysis results

- sensitivity studies to identify influential parameters through the application of a formal statistical approach, orthogonal factorial design (OFD)
- development and refinement of mathematical modeling—finite element analyses and computational fluid dynamics
- evaluation of analysis results against observed and expected structural behavior, with adoption of the event tree technique, and pruning and updating of the tree branches based upon comparisons with observed data

These steps were applied to the degree needed in each phase of the analyses, from aircraft impact to fire spread, thermal loads, and structural response.

### **9.2.1 Key Observed Events and Conditions**

Observations and data about the events following the aircraft impact were primarily obtained from three sources:

- Photographic and video records that had been catalogued and time stamped for the NIST Investigation (NIST NCSTAR 1-5A)
- Interviews of individuals in the towers during the event and those contacted by individuals in the towers during the event (NIST NCSTAR 1-7)
- Interviews of emergency response personnel and emergency communication records (NIST NCSTAR 1-8)

Observations were used to develop timelines and refine collapse hypotheses for each tower. Key observations were used to guide the towers' structural analysis and are summarized in the structural timelines (Chapter 6). Structural analyses were used to develop and refine understanding of the sequences of events, particularly events near or in the core that could not be observed.

Observations were classified into two groups: key observations and noted observations. Key observations were significant structural events that were explicitly addressed in or used to validate the structural analyses. Noted observations were events that may have been linked to a structural response, but their significance could not be conclusively assessed.

Observables were used in all the analyses in three ways: (1) to determine input parameters, such as the aircraft speed and direction at impact, (2) to impose time-related constraints on the analysis, such as imposing observed broken windows over time to constrain the spread of fire, or (3) to validate analysis results, such as global stability after impact and during thermal loading.

### **9.2.2 Collapse Hypotheses**

Collapse hypotheses were developed over the course of the NIST Investigation. The first hypotheses were published in the May 2003 NIST Progress Report, and were updated in the June 2004 Progress Report and October 2004 Public Meeting at NIST. The Probable Collapse Sequence for each tower was

presented at the April 2005 Public Meeting in New York City. The stages of hypothesis development are summarized as follows:

- **Possible Collapse Hypotheses** (May 2003) – not building specific; key events not identified
- **Working Collapse Hypothesis** (June 2004) – single hypothesis for both WTC towers; identified chronological sequence of major events
- **Leading Collapse Hypotheses** (October 2004) – separate hypothesis for each WTC tower; identified building-specific load redistribution paths and damage scenarios in addition to chronological sequence of major events
- **Probable Collapse Sequences** (April 2005) – refined building-specific collapse sequences with chronological sequence of major events, load redistribution paths, and damage scenarios.

Over the course of the investigation, NIST continued to investigate technical issues and modify or refine the collapse hypotheses for each tower as needed. Technical issues that were analyzed and refined during the investigation included:

- Aircraft impact damage to structural components, insulation, and partition walls.
- Dispersion of aircraft debris and damage to building contents.
- Thermal effects on core columns and floors, especially extent and movement of fires.
- Thermal effects on exterior columns, especially temperature gradients in columns.
- Extent of load redistribution within and between core columns and exterior wall columns and their reserve capacity to accommodate added gravity loads with thermal effects.
- Capacity of hat truss to accommodate load redistribution from severed columns.
- Capacity of bolted splices in the severed core columns to carry tensile loads to the hat truss.
- Relative magnitude of the load redistribution provided by the hat truss, local core floor, and the truss floor system for each tower.
- Axial/shear/bending capacity of floor connections to core and exterior columns.
- Mechanisms to propagate instability laterally in the exterior columns
- Capacity of spandrels, including splices, to transfer shear in the exterior walls.
- Role of bolted splices in the instability of exterior columns.
- Comparison and reconciliation of hypotheses with observed facts (photographs and videos, eyewitness accounts, emergency communication records).

The possible collapse hypotheses published in May 2003 were developed by NIST and considered several leading hypotheses that had been postulated publicly by experts. These are summarized in Appendix C, Table C-1. One hypothesis suggested that the load carrying core columns were weakened by the fires and failed, initiating overall building collapse without the need for any weakening or failure of the steel truss floor system. Another hypothesis suggested that significant portions of one or more floor truss systems sagged, as they were weakened by fires, pulling the exterior columns inward via the connections to initiate overall building collapse through combined compression and bending failure of the exterior columns. A variation of this hypothesis suggested that the sagging floor system failed in shear at its connections to the columns, leading to overall building collapse initiation through buckling failure of the exterior columns. Load eccentricities introduced by partially damaged floor systems could also have contributed to buckling failure of the columns.

The working collapse hypothesis published in June 2004 was developed to explain the collapse initiation of the WTC towers. The working hypothesis (summarized in Appendix C, Table C-2) identified the chronological sequence of major events as the WTC tower structures redistributed loads from one structural element to another to accommodate the aircraft impact and subsequent fire damage until no further load redistribution was possible, thus, leading to collapse. The working hypothesis was based on analysis of the available evidence and data, consideration of a range of hypotheses (including those postulated publicly by experts), and the understanding of structural and fire behavior at that time. It allowed for multiple load redistribution paths and damage scenarios for each building.

The leading collapse hypotheses for WTC 1 and WTC 2 that were presented in October 2004 are shown in Appendix C, Figs. C-3 and C-4. A separate collapse hypothesis was developed for each tower that identified load redistribution paths and damage scenarios for each major event. The leading hypotheses accounted for the WTC structural system, aircraft impact and subsequent fires, post-impact condition of insulation, the quality and properties of the structural steel and concrete, and the relative roles of the exterior and core columns and the composite floor system, including connections. The hypotheses were consistent with evidence held by NIST (at that time). They were based on the subsystem analysis described in Chapter 7.

The Probable Collapse Sequences for WTC 1 and WTC 2 were presented in April 2005 following completion of global structural response analyses and are shown in Section 9.3. The structural sequences of events were consistent with evidence held by NIST.

### 9.2.3 Mathematical Modeling – Analysis Interdependencies

Events that played a significant role in the structural performance of the towers were the aircraft impact, rapid ignition of fire on multiple floors, and the growth and spread of fire in each tower. To determine the structural response, detailed information was required on the condition of the structural system and its passive fire protection system both before and after the aircraft impact and during the ensuing fires that elevated temperatures in the structural members.

The interdependence of the various analyses is illustrated in Fig. 9-1. Reference structural models were developed before other structural models to determine the baseline performance of each tower prior to September 11, 2001. The reference models were used as a basis for the aircraft impact damage models and the structural response and failure models to ensure consistency between structural models. The

aircraft impact analysis determined damage to the exterior and the interior of the building and included the structural system, insulation, partition walls, and furnishings for each tower. The analysis also provided an estimate of the fuel dispersion in the towers. These results provided initial conditions for the fire dynamics analysis, thermal analysis, and structural analysis. The fire dynamics analysis simulated the growth and spread of fires and produced gas temperature histories for each floor subjected to fire. The fire dynamics model accounted for damage to interior partition walls and floors (which affected ventilation conditions) and the distribution of debris and fuel.

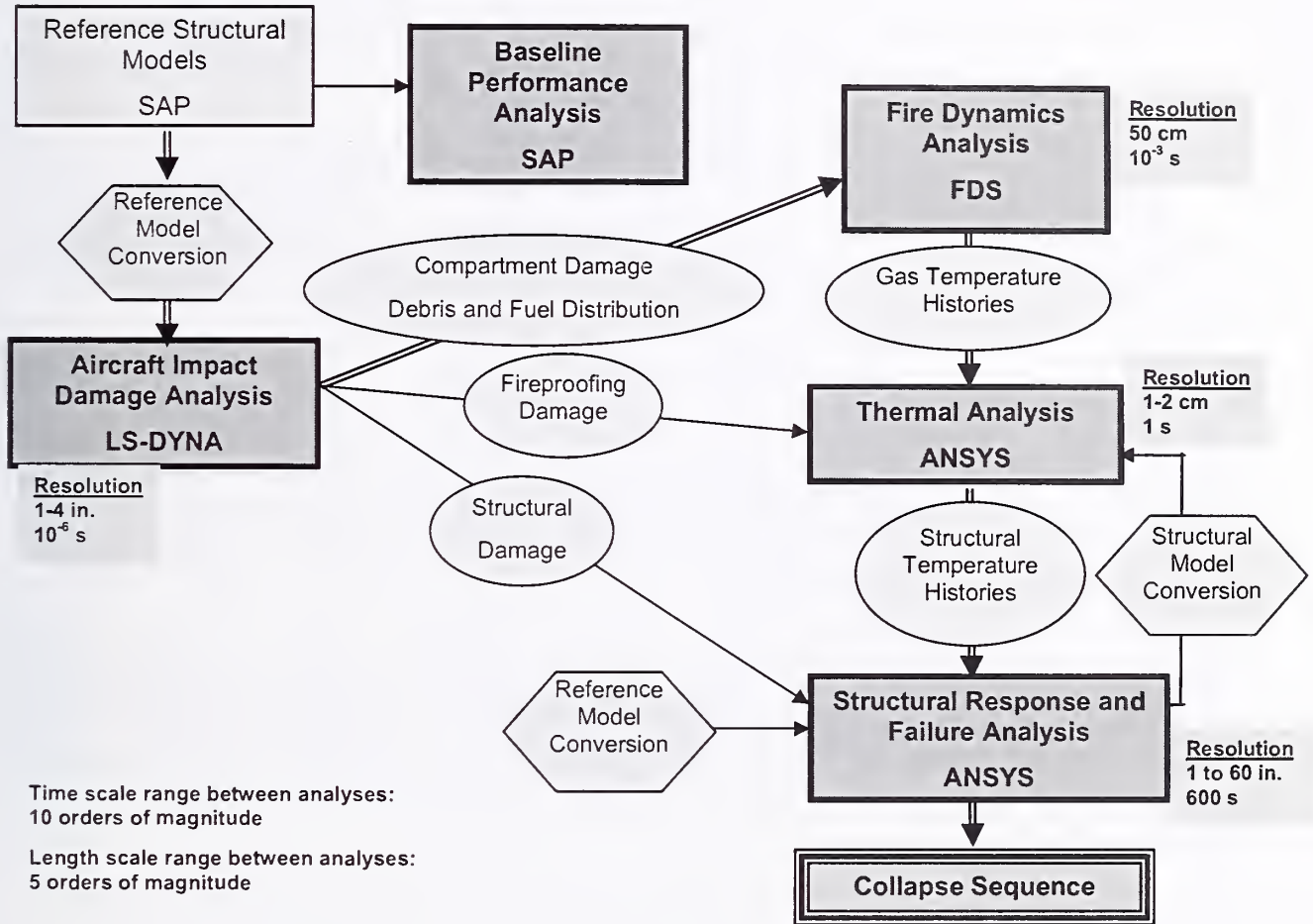


Figure 9-1. Critical analysis inter-dependencies.

The thermal analysis used a solid element heat transfer model to determine temperature histories for the various structural components accounting for the presence or dislodgement of insulation. The thermal analysis required input from the structural analysis model, fire dynamics analysis results, the analysis of damage to insulation, and temperature-dependent thermal material properties. The structural temperature histories, also referred to as thermal loads, were input to the structural analysis, along with the structural impact damage and temperature-dependent material properties, to determine the structural response of each tower.

### 9.2.4 Sensitivity Studies to Identify Influential Variables

Sensitivity studies were conducted for the aircraft impact, fire dynamics, and thermal analyses to identify the most influential parameters for component, connection, and subsystem behavior. To identify the most influential parameters, an orthogonal factorial design process was used to design analysis ‘experiments’ (Box, 1978). Numerical experiments with an orthogonal factorial design (OFD) method were conducted for detailed models of components and subsystems to identify parameters that strongly influenced the analysis results:

- Only parameters whose values were not accurately known were selected (parameters that were known with near certainty were set to the known values).
- Selected parameters were varied within a range of likely values, determined from available data and assigned three alternative values: lower value (-), central value (0), upper value (+).

The OFD approach allowed for identification of influential parameters that reduced the number of analysis runs at the global level. The influential parameters for the structural response analyses included the aircraft impact analyses through the impact damage and temperature histories that were part of the required input data. To determine structural response to damage and thermal loads, numerous component and subsystem studies were conducted that identified critical structural behavior and failure mechanisms and how they varied with temperature. Structural behaviors that were studied included restrained thermal expansion, thermal weakening of columns and floors, floor sagging and associated inward pull on exterior wall, and load redistribution through major structural subsystems. Failure mechanisms that were studied included, for example, tensile failure of core column splices and hat truss connections, column buckling, or loss of composite action in the floor system.

The influential parameters that were identified for each analysis, based on available information, were used to create three input data sets. Figure 9–2 illustrates the analysis tree with all influential parameter combinations resulting from this procedure for the three likely values, a lower value, a central value, and an upper value. It is apparent that analysis of all possible combinations required the number of analyses at each level to increase by a factor of three. The number of global structural response analyses was prohibitive with this approach.

However, computational analyses provided valuable insight into the relationship between input and output data for the aircraft impact, fire dynamics, thermal, and structural response analyses. These insights, along with the sensitivity studies, enabled significant reduction of the number of scenarios that were analyzed. Figure 9–3 shows the final pruned analysis tree, which was obtained as follows. After the aircraft impact analysis results were evaluated for the three sets of input parameters, the less severe damage case was discarded (pruned) as it did not reasonably match key observables. The base and more severe damage cases were each analyzed for fire growth and spread (FDS) and for the corresponding temperature histories of structural components (FSI). The linkage between the aircraft impact, fire dynamics, and thermal analyses for each damage case created highly correlated sets of input data and analysis results. For instance, the damage from the severe aircraft impact case provided input data for analysis of the fires corresponding to the severe impact damage, and both analyses provided input data for the thermal analysis of structural components subject to severe impact damage and the corresponding fires. The high level of correlation between the linked sets of aircraft impact, fire, and thermal analyses, as well as similar results for alternative fire conditions for the same impact damage, led to a single branch

at each successive analysis, as shown in Fig. 9-3. The temperature histories for the base and more severe cases (referred to as Case A and Case B for WTC 1 or Case C and Case D for WTC 2 elsewhere in this report) were used in the structural analysis of major subsystems—the isolated core, a full floor, and the exterior wall analyses. The results of the subsystem analyses showed that the more severe case impact damage results better matched key observables. The subsystem analysis results led to the pruning of the global structural analysis for the base case impact damage sub-tree, as shown in Fig. 9-3. Consequently, only the more severe cases (Cases B and D) were used in the global analysis of each tower.

Tables 9-1 to 9-4 list the observables used for the validation of analysis results, the significant input data, influential parameters, and significant output for each analysis.

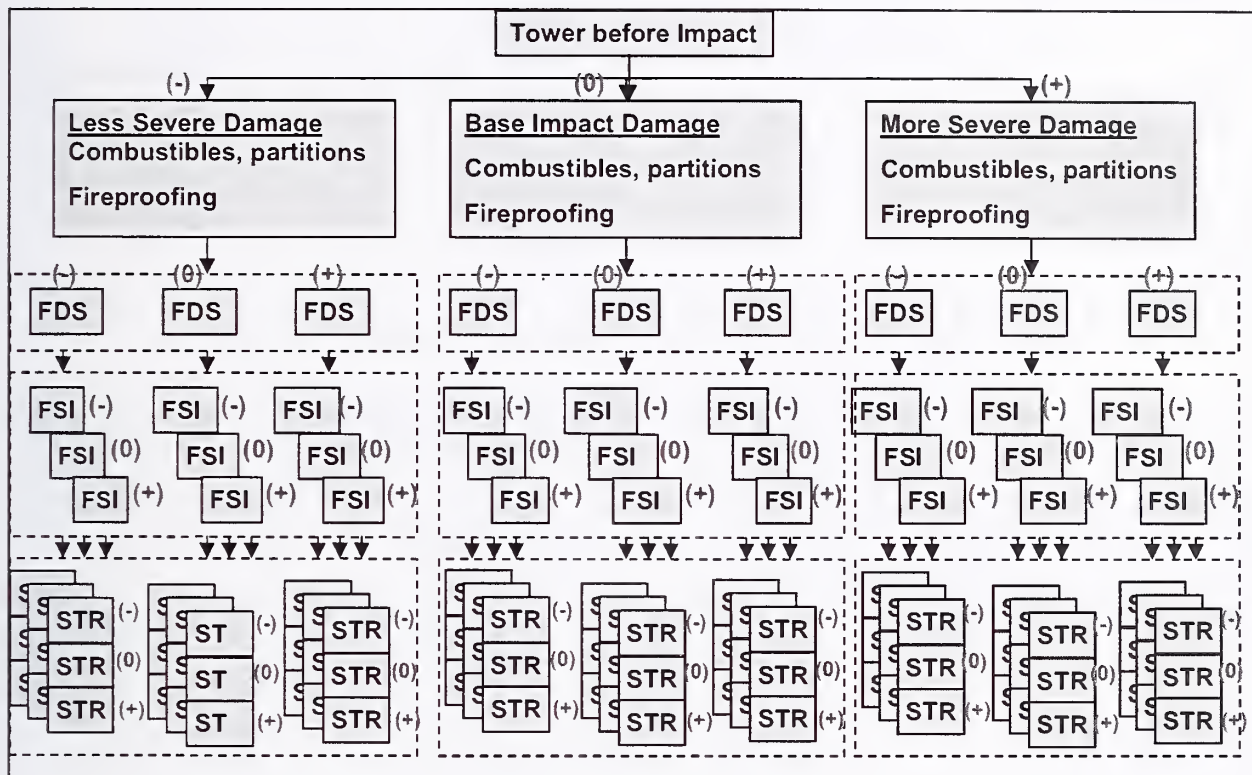


Figure 9-2. Full analysis tree for influential parameter effects.

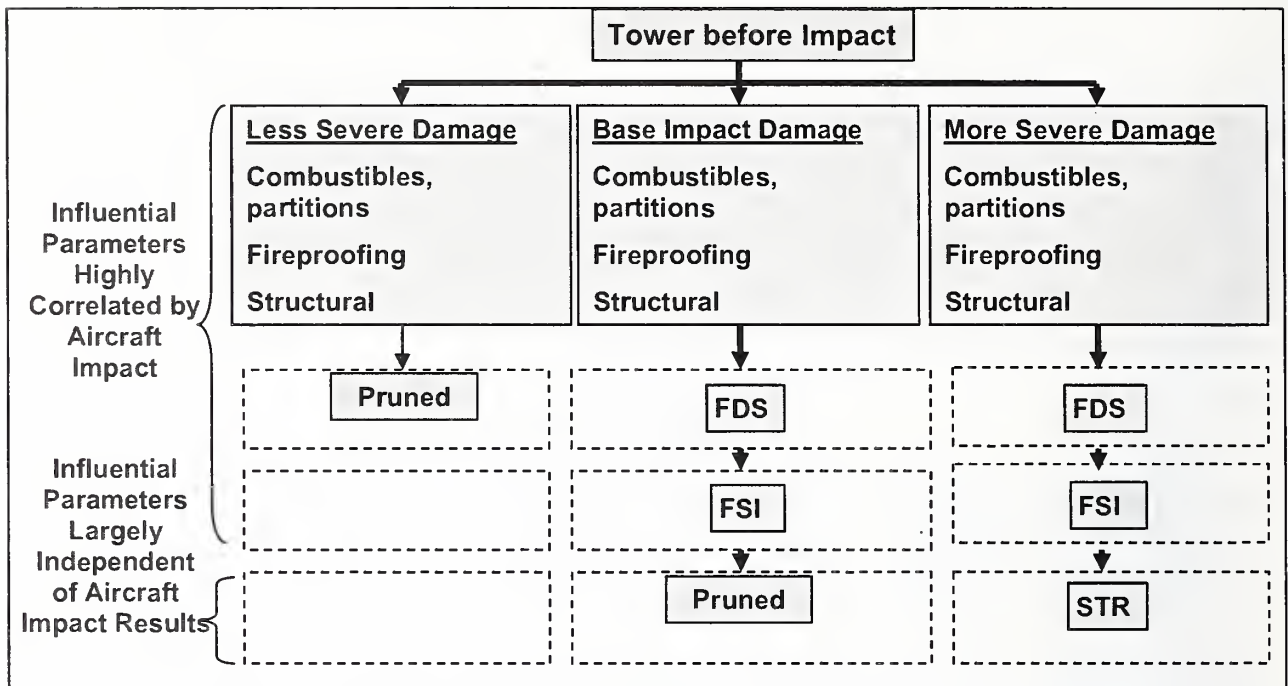


Figure 9–3. Pruned analysis tree for influential parameter effects.

Table 9–1. Aircraft impact analysis parameters.

<i>Validation Data</i>		<i>Model and Analysis</i>		
<b>Observables from Photo/Video</b>	<b>Observables from Interviews</b>	<b>Significant Input</b>	<b>Influential Parameters</b>	<b>Significant Output</b>
Impact damage to exterior wall	Stairwell damage	Structural model with service loads	Aircraft velocity	Structural damage
Engine/landing gear exit location and speed			Aircraft pitch	Debris path (insulation and partition damage)
Aircraft impact conditions for model input (velocity, location, orientation to building)			Aircraft mass	Fuel path
	Aircraft material failure strain			
	Tower steel failure strain			
	Partition strength			
		Material properties for high strain rates	Live load weight	

**Table 9–2. Fire dynamics analysis parameters.**

<i>Validation Data</i>		<i>Model and Analysis</i>		
<b>Observables from Photo/Video</b>	<b>Observables from Interviews</b>	<b>Significant Input</b>	<b>Influential Parameters</b>	<b>Significant Output</b>
Fire near windows vs location and time	None	Ventilation sources from debris damage	Average fuel density	Gas temperature histories
Smoke out windows vs location and time		Added fuel from aircraft	Distribution of intact contents vs rubble	
Window breakage vs location and time		Fuel distribution after aircraft impact	Shaft ventilation in core	
		Window openings vs time	Partition damage	
		Floor content layout		

**Table 9–3. Thermal analysis parameters.**

<i>Validation Data</i>		<i>Model and Analysis</i>		
<b>Observables from Photo/Video</b>	<b>Observables from Interviews</b>	<b>Significant Input</b>	<b>Influential Parameters</b>	<b>Significant Output</b>
None	None	Thermal models of structure	Insulation initial condition	Structural temperature histories
		Insulation initial condition	Estimated insulation damage	
		Estimated insulation damage		
		Gas temperatures		

**Table 9–4. Structural response analysis parameters.**

<i>Evidence/ Data</i>		<i>Model and Analysis</i>		
<b>Observables from Photo/Video</b>	<b>Observables from Interviews and Recordings</b>	<b>Significant Input</b>	<b>Influential Parameters</b>	<b>Significant Output</b>
Initial Stability	NYPD Aviation Unit first responder communications	Initial structural condition after impact	Pull-in force location and magnitude	Probable collapse sequence
Floors sagging at windows		Structural temperature histories	Floor disconnections	Sequence of component and subsystem failures, including instability of exterior wall
Exterior wall inward bowing and instability		Pull-in force location and magnitude	Creep strain	Global stability vs time
Tilt of building section above impact during collapse				

### 9.2.5 Evaluation of Collapse Hypotheses

Development and validation of the probable collapse sequence for each tower was shaped by evidence gathered in the investigation, including photographs and videos, design and maintenance documents, and eyewitness accounts. Photographs and videos provided knowledge about aircraft impact damage to the tower exterior walls, fire growth and spread at the building exterior, inward bowing of an exterior wall in each tower, and the direction of tilt for the building section above the impact zone as the towers collapsed. Eyewitness accounts provided some information about the interior conditions surrounding the impact areas, but the descriptions tended to be general in nature and often did not provide locations or specifics within a floor level. Figure 9–4 lists data (primarily based on photos and videos except for the metallurgical measurements) used to determine input data, impose time-related constraints, and validate analysis results for determining the probable collapse sequences.

The use of observables as a constraint had the important effect of reducing the uncertainty in the analysis results. The time and frequency of the applied constraints affected the degree to which the analysis uncertainty was reduced.

Figure 9–5 illustrates conceptually how the variance (or uncertainty) of the global stability of the towers (indicated here by the global reserve capacity RC) changed from the time of impact to the time of collapse. The shaded band qualitatively indicates the degree of uncertainty in RC at each time  $t$  after considering the analysis results and the observations made prior to  $t$ , except for collapse. The aircraft impact caused a reduction in the towers strength, but substantial reserve capacity remained afterward. The combined effect of the impact damage and fires caused a gradual reduction of the global capacity. The initial period of heating caused minimal changes in the structural capacity, but as time progressed,

various events occurred that caused a sudden or more rapid loss of global capacity. For instance, failure of critical columns from thermal weakening or inward bowing of an exterior wall may be events associated with a rapid loss of global capacity.

Based only on model predictions, the variance (or uncertainty) of the global reserve capacity grew with time. However, whenever an observable matched analysis results, it reduced the uncertainty in the analysis results. Alternatively, when the observables were used to constrain model parameters and adjust results to be consistent with observations, the variance of the global reserve capacity and the sequence of events that took place were reduced. As the structural analyses approached the time to collapse, the ability of the analyses to match the time to failure depended upon the variance in the analysis results. When considering the sequence of structural events and time to failure, it was more important to match the sequence of events as the time to collapse initiation was influenced by adjustments in influential parameters and imposition or matching of observables. As a result of using observables to constrain model parameters and analysis results, NIST believes that the probable collapse sequences that were determined are highly robust. The times to failure for the collapse sequences, however, are subject to considerable variability, particularly since they are sensitive to small changes in the magnitude of the pull-in forces.

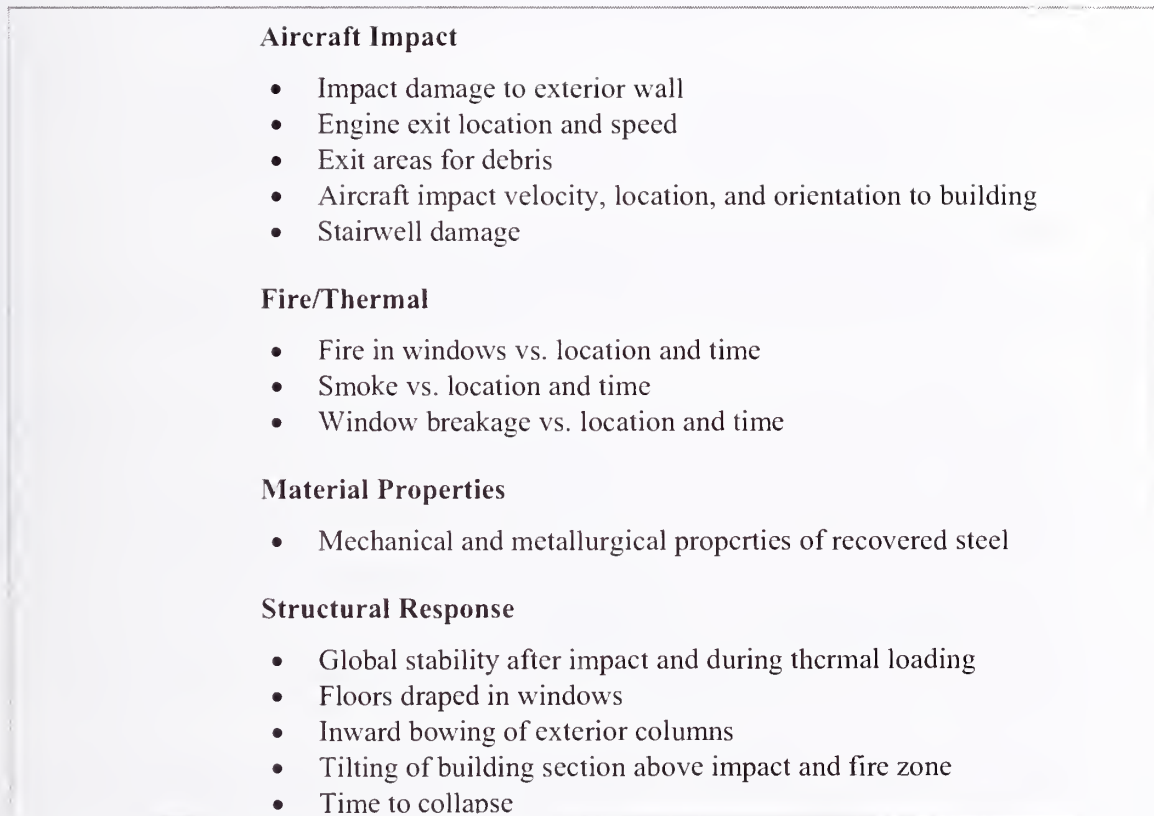


**Figure 9–4. Data used for input, constraints, and validation of probable collapse sequences.**

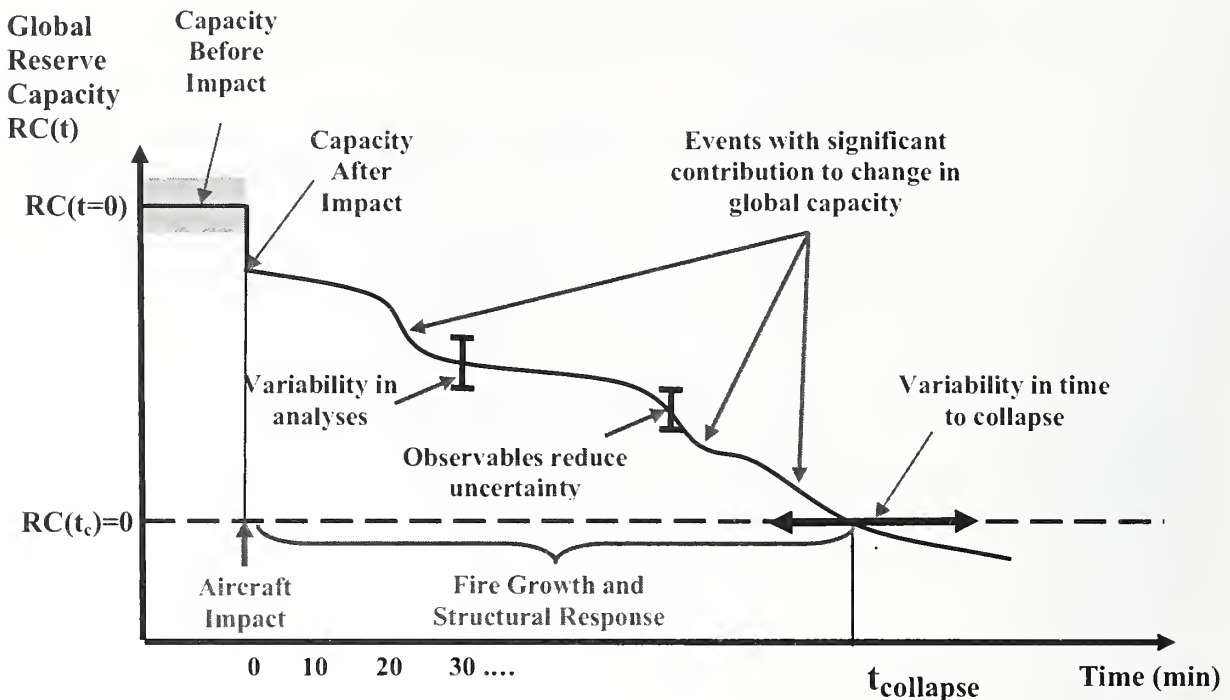


Figure 9-5. Variability in global reserve capacity using model predictions and observables for sequential analyses with imperfect information.

### 9.3 PROBABLE COLLAPSE SEQUENCES

The following four structural events that were common to both towers are part of the sequence of events described:

- **Floor sagging** was caused by elevated steel temperatures resulting from loss of insulation. Substantial sagging of the floor resulted in pull-in forces at column connections, and led to inward bowing of the exterior wall. Calculations, supported by the four Standard Fire Tests, showed that the most likely cause of floor sagging was buckling of the truss web diagonals, as shown in Fig. 9-6. In the figure, the left portion of the truss maintained flexural stiffness, but the right end lost some flexural stiffness as a result of extensive web buckling. The resultant sagging produced tensile forces in the floor system which was approximated by a combination of flexural and catenary behaviors as shown in Fig. 9-7. A floor system with tensile forces at its connections does not restrain the exterior wall from bowing inward.
- **Bowing and plastic buckling of an exterior wall** under the combined effects of elevated temperatures, redistributed gravity loads, pull-in forces from sagging floors, and loss of lateral support due to failure of truss seat connections.
- **Weakening of the core columns** (which was resisted by the hat truss) was caused by the combined effects of structural impact damage, redistributed gravity loads, elevated temperatures, plastic and creep strains, and plastic buckling of core columns.

- Redistribution of gravity loads** resulted from impact damage, restrained thermal expansion, core weakening, leaning of the tower section above the impact damage, and bowing and buckling of exterior walls. Redistribution of gravity loads between the core to the exterior walls occurred primarily through the hat truss, while load redistribution between adjacent exterior walls occurred primarily through the spandrels. Restrained thermal expansion occurred in the exterior wall when heated columns were restrained by adjacent cooler columns. Restrained thermal expansion also occurred when the core columns were restrained by the hat truss connection to the exterior wall; elongation of the core columns transferred loads from the exterior wall to the core.

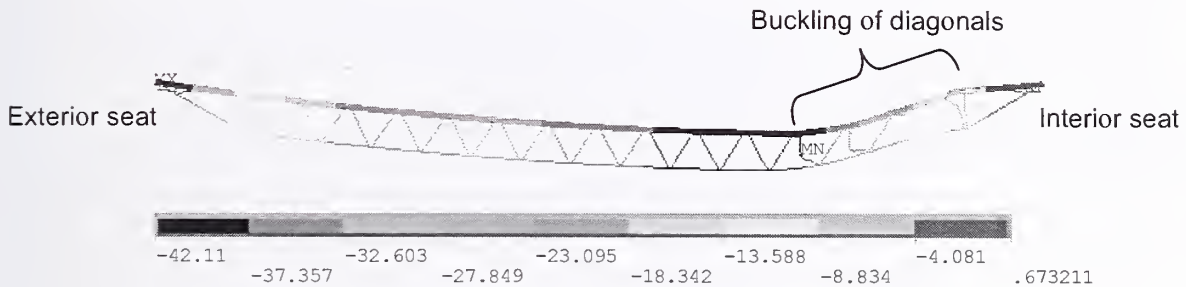


Figure 9-6. Vertical displacement contour of the detailed truss model under thermal loading.

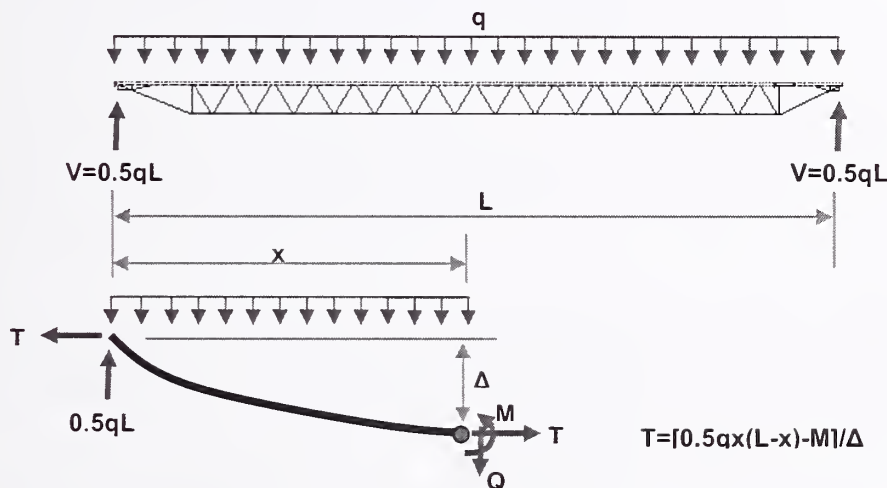


Figure 9-7. Combined flexural and catenary action in the floor system.

### 9.3.1 Probable Collapse Sequence of WTC 1

The aircraft impacted the north wall of WTC 1 at 8:46 a.m. The aircraft impact severed exterior columns and floors on the north side of the tower and into the core between Floors 93 and 98. The subsequent fires weakened structural subsystems, including the core, floors, and exterior walls. The core weakened, the floors sagged, and the south exterior wall bowed inward. At 10:28 a.m., about 102 min after the aircraft impact, WTC 1 began to collapse.

A sequence of main structural events that led to the collapse of WTC 1 starting from aircraft impact is discussed below. The WTC 1 collapse sequence consisted of five main events: aircraft impact, core weakening, floor sagging and disconnection, inward bowing of the south wall, and collapse initiation. Each event is discussed in terms of (1) the factors and sub-events that led to the event and (2) the consequential structural changes that were caused by the event. Observations for WTC 1 are presented again in Table 9–5. The probable collapse sequence is presented in Fig. 9–8.

**Table 9–5. Observations for WTC 1.**

<i>Time</i>	<i>Time from Impact</i>	<i>Observation</i>
8:46:26	0 min	WTC 1 was impacted by a Boeing 767 between Floors 93 and 99 and Columns 109 and 152. Fig 6–1 shows Columns 120 to 159.
9:25:28	39 min	Fire on west side of south wall.
9:40	69 min	No inward bowing of perimeter columns was visible
10:22:59	97 min	Inward bowing of the south perimeter wall was visible from Floor 95 to about Floor 99, with a maximum inward bowing of ~ 55 in. at Column 315 and Floor 97.
10:28:18	102 min	Smoke and debris clouds out of the north, east, and west walls on Floor 98. Fire out of windows on the north, east, west, and south walls between Floor 92 and Floor 98, and Floor 104.
10:28:20	102 min	Tower began to collapse – first exterior sign of collapse was at Floor 98. Rotation of at least 8 degrees to the south occurred before the building section began to fall vertically under gravity.
10:28:48	102 min	Remaining portion of core collapsed.

**1. Aircraft Impact Damage:**

- Aircraft impact severed a number of exterior columns on the north wall from Floor 93 and Floor 98, and the wall section above the impact zone moved downward.
- After breaching the building's exterior, the aircraft continued to penetrate into the building, severing floor framing and core columns at the north side of the core. Core columns were also damaged toward the center of the core and, to a limited extent on the south side of the core. Fireproofing was damaged from the impact area to the south exterior wall, primarily through the center of WTC 1 and at least over a third to a half of the core width.
- Aircraft impact severed a single exterior panel at the center of the south wall between floors 94 and 96.
- The impact damage to the exterior walls and to the core resulted in redistribution of severed column loads, mostly to the columns adjacent to the impact zones. The hat truss resisted the downward movement of the north wall, and rotated about the east-west axis.
- As a result of the aircraft impact damage, the north and south walls each carried about 7 percent less gravity loads after impact, and the east and west walls each carried about 7 percent more loads. The core carried about 1 percent more gravity loads after impact.

**2. Effects of Subsequent Fires and Impact Damaged Fireproofing:****A. Thermal Weakening of the Core:**

- The undamaged core columns developed high plastic and creep strains over the duration the building stood, since both temperatures and stresses were high in the core area. The plastic and creep strains exceeded thermal expansion in the core columns.
- The shortening of the core columns (due to plasticity and creep) was resisted by the hat truss, which unloaded the core over time and redistributed loads to exterior walls.
- As a result of the thermal weakening (and subsequent to impact and prior to inward bowing of the south wall), the north and south walls each carried about 10 percent more gravity loads, and the east and west walls each carried about 25 percent more loads. The core carried about 20 percent less gravity loads after thermal weakening.

**B. Thermal Weakening of the Floors:**

- Floors 95 to 99 weakened with increasing temperatures over time on the long-span floors and sagged. The floors sagged first and then contracted due to cooling on the north side; fires reached the south side later, the floors sagged, and the seat connections weakened.
- Floor sagging induced inward pull forces on the south wall columns.
- About 20 percent of the connections to the south exterior wall on floors 97 and 98 failed due to thermal weakening of the vertical supports.

**C. Thermal Weakening of the South Wall:**

- South wall columns bowed inward as they were subjected to high temperatures and inward pull forces in addition to axial loads.
- Inward bowing of the south wall columns increased with time.

**Figure 9–8. WTC 1 probable collapse sequence.**

### 3. Collapse Initiation

- The inward bowing of the south wall induced column instability, which progressed rapidly horizontally across the entire south face.
- The south wall unloaded and tried to redistribute the loads via the hat truss to the thermally weakened core and via the spandrels to the adjacent east and west walls.
- The entire section of the building above the impact zone began tilting as a rigid block (all four faces, not only the bowed and buckled south face) to the south (at least about 8°) as column instability progressed rapidly from the south wall along the adjacent east and west walls.
- The change in potential energy due to downward movement of building mass above the buckled columns exceeded the strain energy that could be absorbed by the structure. Global collapse then ensued.

**Figure 9–8. WTC 1 probable collapse sequence (cont).**

### Aircraft Impact

WTC 1 was impacted by an aircraft on the north wall. Columns 112 to 151 between Floors 94 and 98 were severed or heavily damaged on the north wall. After breaching the building's perimeter, the aircraft continued to penetrate into the building. The north office area floor system sustained severe structural damage between Columns 112 and 145 at Floors 94 to 98. Core columns were severed or heavily damaged (nine were predicted) between Floor 92 and Floor 97. The aircraft impact also severed a single exterior panel at the center of the south wall from Columns 329 to 331 between Floor 93 and Floor 96. In addition, insulation on floor framings and columns were damaged from the impact area to the south perimeter wall, primarily through the center of WTC 1 and over one-third to one-half of the core width.

Gravity loads on severed columns were redistributed mostly to columns adjacent to the impact zone. Due to the severe impact damage to the north wall, the wall section above the impact zone moved downward. The hat truss resisted the downward movement of the north wall and rotated about its east-west axis, which reduced the load on the south wall. As a result, the north and south walls each carried about 7 percent less gravity loads at Floor 98 after impact, the east and west walls each carried about 7 percent more loads, and the core carried about 1 percent more gravity loads at Floor 98 after impact, as shown in Table 9–6.

### Core Weakening

Temperatures in the core area rose quickly; therefore, the thermal expansion of the core was larger than the thermal expansion of the exterior walls in early stages of the fire, resulting in an increase in the gravity loads in the core columns until 10 min (8:56 a.m.), as shown in Table 9–6. The additional loads due to impact damage and high temperatures resulted in high plastic and creep strains in the core columns during early stages of the fire. Creep strain continued to increase until the collapse initiated. By 30 min (9:16 a.m.), the plastic-plus-creep strains exceeded thermal expansion strains. Due to high plastic and creep strains and plastic buckling of some core columns, at 100 min (10:26 a.m.), the core structure at Floor 99 had displaced downward 2.0 in. on average.

**Table 9–6. Total column loads at Floor 98 and Floor 105 of WTC 1 for Case B.**

		North		East		South		West		Core	
		Floor 98	Floor 105								
(1)	Before Impact	10,974	8,026	8,545	6,562	11,025	8,092	8,572	6,604	34,029	20,361
(2)	After Impact	10,137	7,294	9,071	7,028	10,356	7,488	9,146	7,076	34,429	20,761
(3)	10 min	9,796	6,944	8,490	6,461	9,848	6,981	8,536	6,469	36,473	22,790
(4)	20 min	10,437	7,551	9,108	7,075	9,900	7,057	9,202	7,158	34,495	20,806
(5)	30 min	10,913	8,020	10,034	7,998	10,420	7,569	9,715	7,685	32,060	18,377
(6)	40 min	11,068	8,193	10,599	8,571	11,004	8,129	10,178	8,147	30,294	16,608
(7)	50 min	11,149	8,285	10,908	8,878	11,192	8,315	10,458	8,428	29,435	15,743
(8)	60 min	11,205	8,351	11,168	9,130	11,285	8,414	10,716	8,687	28,766	15,069
(9)	70 min	11,286	8,435	11,366	9,319	11,343	8,481	10,939	8,914	28,205	14,502
(10)	80 min	11,376	8,528	11,555	9,497	11,409	8,551	11,119	9,097	27,681	13,978
(11)	90 min	10,916	8,096	11,991	9,847	9,949	7,327	11,657	9,506	28,587	14,876
(12)	100 min	10,828	8,023	12,249	10,076	9,638	7,066	11,905	9,720	28,478	14,767
(13)	(2) - (1)	-837	-732	526	466	-668	-604	574	472	400	400
(14)	(10) - (2)	1,239	1,234	2,484	2,470	1,052	1,063	1,973	2,021	-6,748	-6,783
(15)	(12) - (2)	692	730	3,178	3,048	-719	-422	2,759	2,644	-5,951	-5,993
(16)	(12) - (10)	-548	-504	694	579	-1,771	-1,485	786	623	797	790

Note : Compression is positive. Units are in kip.

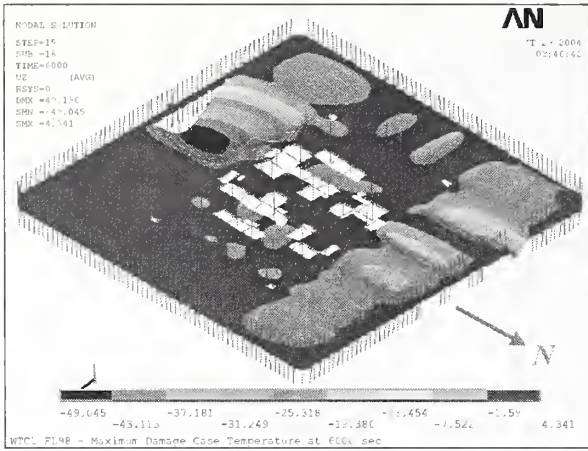
The shortening of core columns was resisted by the hat truss, which unloaded the core with time and redistributed the gravity loads from the core to the exterior walls, as can be seen in Table 9–6 at 80 min. As a result, the north, east, south, and west walls carried about 12 percent, 27 percent, 10 percent, and 22 percent more gravity loads, respectively, for Floor 98 at 80 min than the state after impact, and the core carried about 20 percent less loads. At 80 min, the unloading of the core columns was at its maximum.

### Sagging of Floors and Floor/Wall Disconnections

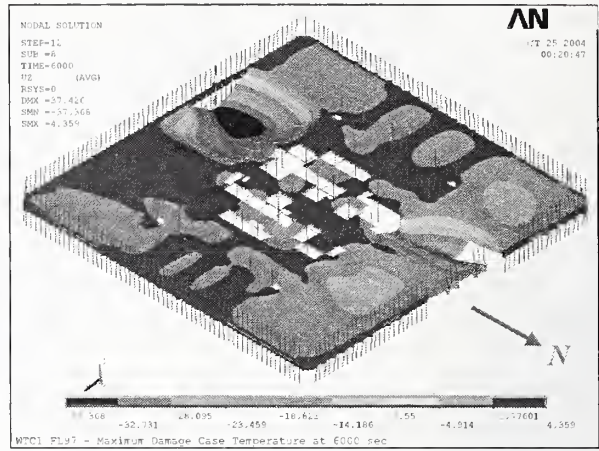
The floors thermally expanded in the early stages of the fires. However, the thermal expansion was overcome by the significant sagging of the floors, which then pulled inward on the exterior columns. Floor 95 to Floor 99 sagged due to elevated temperatures in the south floor areas with long-span trusses. While the north floors first sagged and then contracted due to cooling on the north side, the fires reached the south side later, and the south floors sagged. Figure 9–9 shows vertical displacement contours of Floor 95 to Floor 98 predicted by the full floor models at 100 min (10:26 a.m.). Floor sagging induced pull-in forces on the south wall columns over Floors 95 to 99. In addition, about 20 percent of the exterior seats of Floors 97 and 98 on the south wall failed due to their reduced vertical shear capacity, as shown in Fig. 9–10.

### Bowing of South Wall

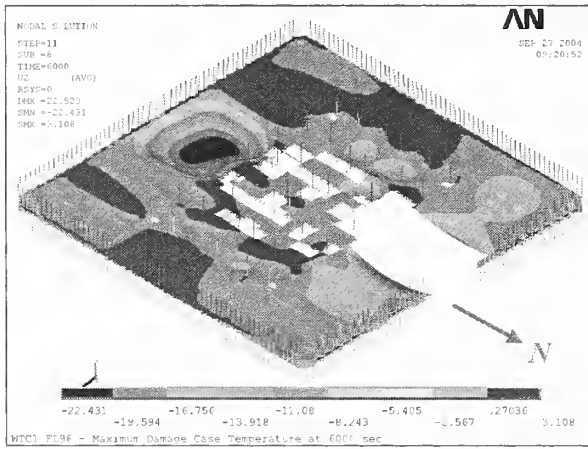
Exterior columns on the south wall bowed inward as they were subjected to high temperatures, pull-in forces from the floors (beginning at about 80 min), and additional loads redistributed from the core. The observed inward bowing of the south wall at 10:23 a.m. was 55 in. while the calculated inward bowing was 31 in., as shown in Figs. 9–11 and 9–12. Since no bowing was observed on the south wall at 9:55 a.m., the south wall was considered to begin bowing inward around 10:10 a.m. when the floors on the south side began to experience large sagging. The inward bowing of the south wall increased with time due to additional gravity loads caused by core weakening and increased temperatures on the south wall. As the floor applied inward pull to the south exterior wall at approximately 80 min, the south wall began to unload to adjacent walls and the core.



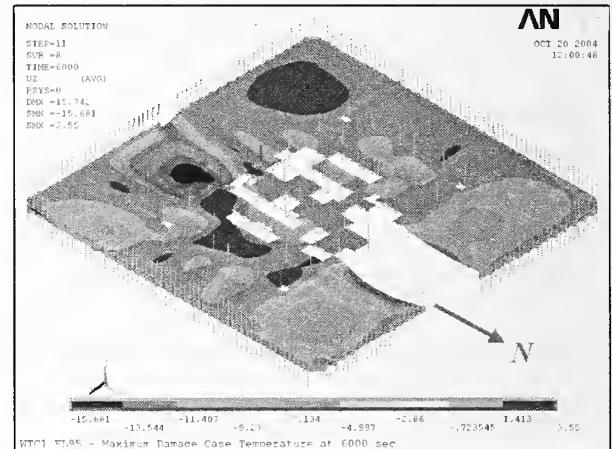
(a) Floor 98



(b) Floor 97

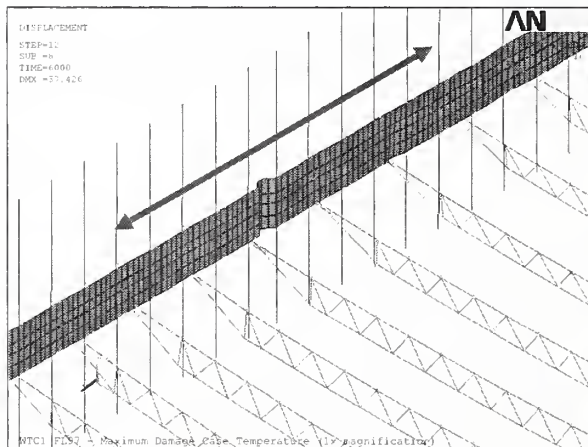


(c) Floor 96

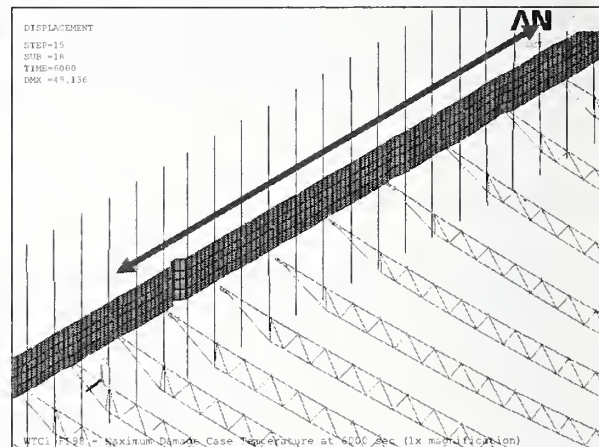


(d) Floor 95

Figure 9-9. Vertical displacement of Floors of WTC 1 for Case B' at 100 min.



(a) Floor 97



(b) Floor 98

Figure 9-10. Loss of vertical supports observed in Floor 97 and Floor 98 of WTC 1 for Case B' (1x displacement magnification).

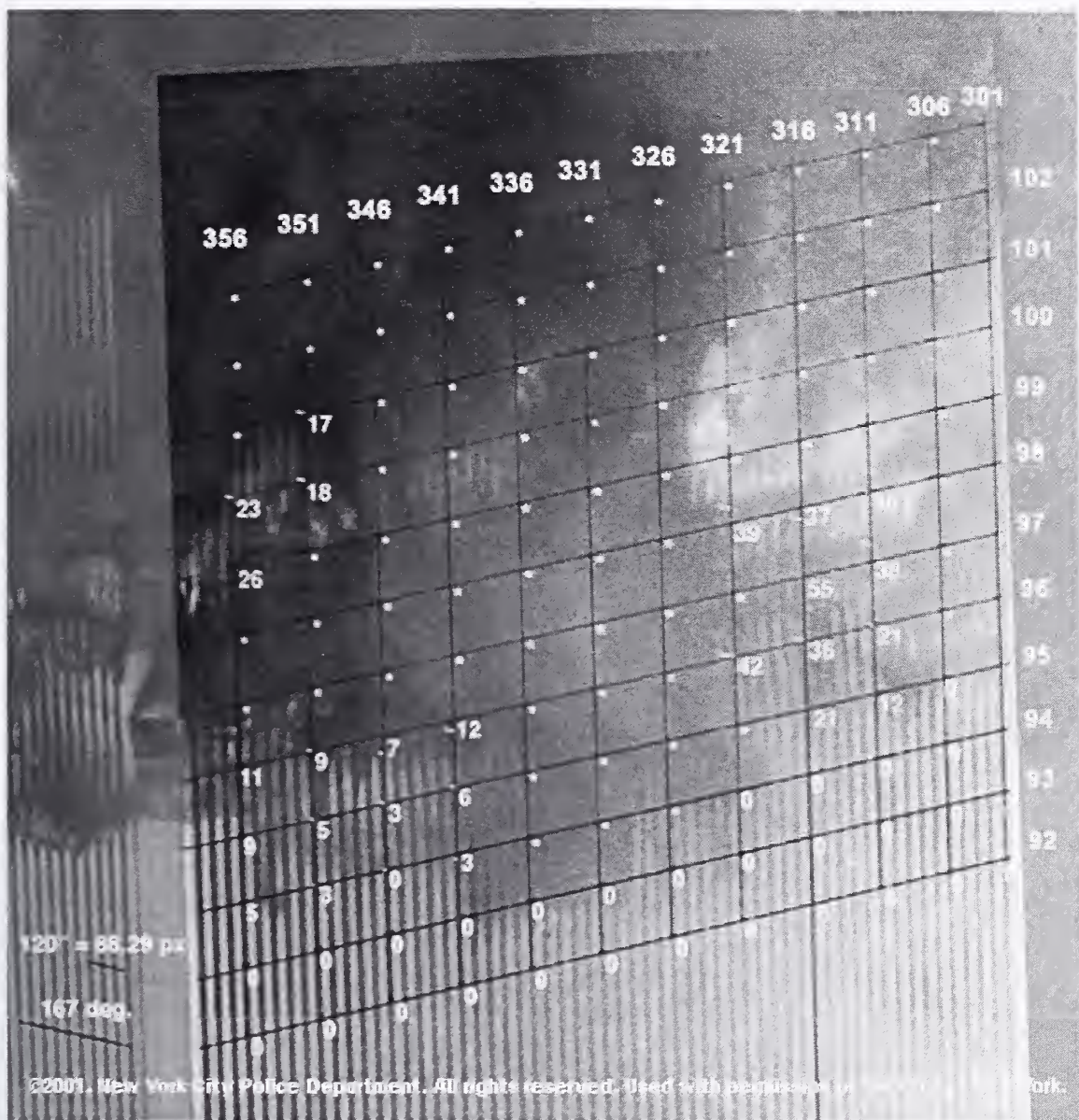


Figure 9-11. Inward bowing of the WTC 1 south wall of WTC 1 at 10:23 a.m.

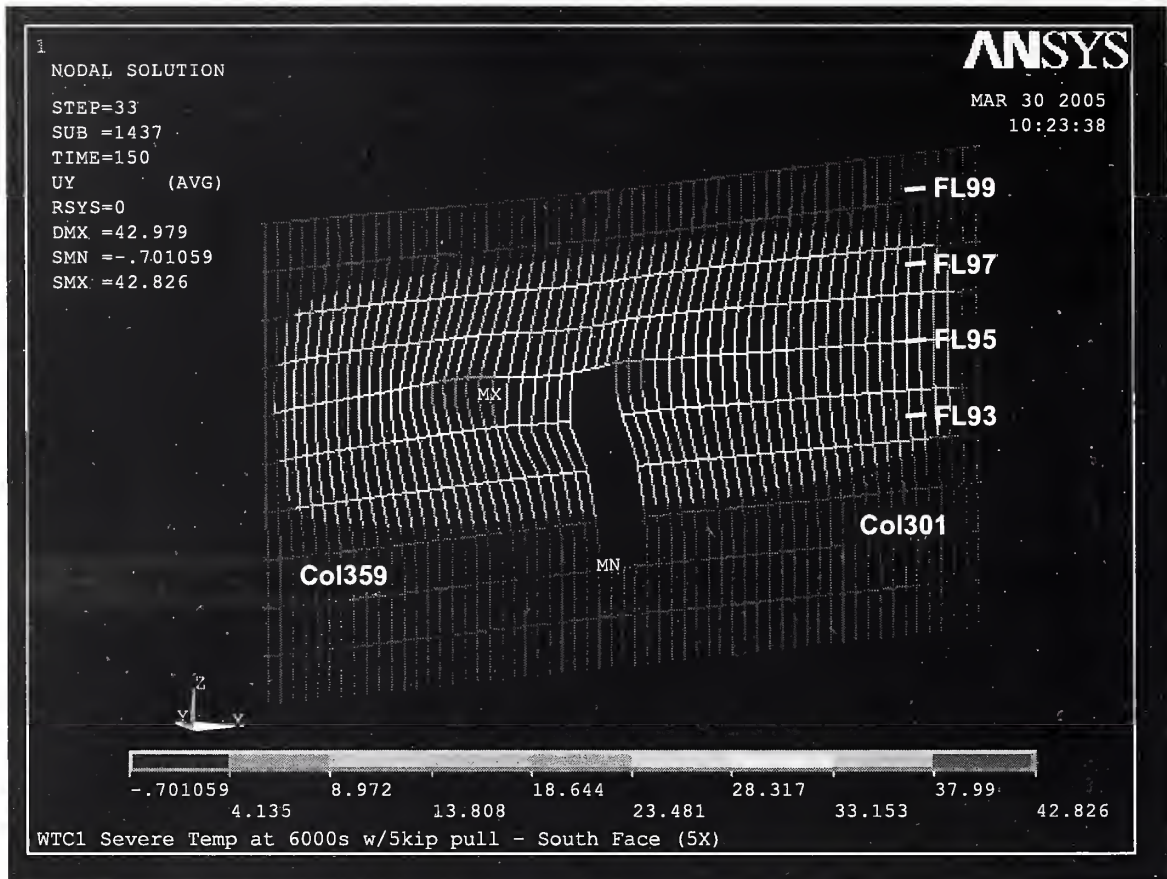


Figure 9–12. Inward bowing of south wall of WTC 1 global model with creep at 100 min for Case B with 5 kip pull-in forces (5x displacement magnification).

### Buckling of South Wall and Collapse Initiation

The inward bowing of the south wall increased as the post-buckling strength of bowed columns continued to reduce. The bowed columns increased the loads on the unbuckled columns on the south wall by shear transfer through the spandrels. Consequently, instability progressed horizontally, and when it engulfed the entire south wall, it progressed along the east and west walls. Moreover, the unloading of the south wall resulted in further redistribution of gravity loads on the south wall to the east and west walls and to the thermally weakened core via the hat truss. At 100 min, the north, east, and west walls at Floor 98 carried about 7 percent, 35 percent, and 30 percent more gravity loads than the state after impact, and the south wall and the core carried about 7 percent and 20 percent less loads, respectively. The increased loads on the east and west walls were due to their relative higher stiffness compared to the impact damaged north wall and bowed south wall. The section of the building above the impact zone began tilting to the south at least about  $8^\circ$  as column instability progressed rapidly from the south wall along the adjacent east and west walls, as shown in Fig. 9–13. The gravity loads could no longer be redistributed, nor could the remaining core and perimeter columns support the gravity loads from the floors above. The change in potential energy due to downward movement of building mass above the buckled columns exceeded the strain energy that could have been absorbed by the structure. Global collapse ensued.



Fire expelled on east face

Smoke and debris expelled on north face at Floor 98



WTC 1 building section above impact damage zone tilts to the south



Figure 9-13. Expulsion of smoke and debris at WTC 1 Floor 98 on the east, north, and west faces.

### 9.3.2 Probable Collapse Sequence of WTC 2

The aircraft impacted the south wall of WTC 2 at 9:03 a.m. The impact mostly severed columns and floors that were toward the east side of the building between Floor 78 and Floor 84. The subsequent fires were also observed on the east side of the building. At 9:59 a.m., about 56 min after the aircraft impact, the building started to collapse, with the east wall buckling inward followed by tilting of the building portion above Floor 82 toward the east and south.

The section below discusses the sequence of main structural events that led to the collapse of WTC 2 starting from aircraft impact. Each event is discussed in terms of (1) the factors and sub-events that caused the event and (2) the structural changes that were caused by the event. The probable collapse sequence consists of five main structural events: aircraft impact, sagging and disconnections of floors, inward bowing of the east exterior wall, unloading and tilting of the core, and initiation of collapse. Observations for WTC 2 are presented in Table 9–7. The probable collapse sequence is presented in Fig. 9–14.

**Table 9–7. Key observations on WTC 2.**

Time	Time from Impact (min)	Observation
9:03	0 min	WTC 2 was impacted by a Boeing 767 between Floors 77 and 85 and Columns 404 and 443.
9:23	20 min	Inward bowing of east face, maximum deflections of 10 in. at Floor 80.
9:53	50 min	Bowing in of columns, maximum deflections of 20 in. at Floor 80. East side of Floor 83 draped between Columns 310 and 342.
9:58:02		Perimeter columns bowing inward on east face.
9:58:59		WTC 2 began to collapse.
9:58:59	55 min – 56 min	Building section above the impact area tilted to the east and south. Tilting appears to take place around Floor 82. Rotation of approximately 4 to 5 deg to the south and 20 to 25 deg to the east occurred before the building section began to fall vertically.

#### Aircraft Impact

The aircraft impacted the south wall of WTC 2 and severed a significant number of exterior columns on the south wall from Floor 78 to Floor 84. The floors on the south side sustained severe structural damage between Columns 410 and 436 from Floors 79 and 83. Core columns were severed or heavily damaged (11 were predicted) between Floor 77 and Floor 84. The aircraft impact also severed two columns in the north wall. The aircraft impact caused damage to the floor framing and core columns at the southeast corner of the core. Insulation was damaged from the impact area through the east half of the core to the north and east perimeter walls. The floor truss seat connections over about one-quarter to one-half of the east side of the core were predicted to be severed by the impact analysis on Floor 80 and Floor 81. Based on the hanging object in the photographs, about one-third of the east perimeter wall floor connections on Floor 83 were assumed to be severed.

### 1. Aircraft Impact Damage:

- Aircraft impact severed a number of exterior columns on the south wall from floors 78 to 84, and the wall section above the impact zone moved downward.
- After breaching the building's exterior, the aircraft continued to penetrate into the building, severing floor framing and core columns at the southeast corner of the core. Fireproofing was damaged from the impact area through the east half of the core up to the north and east exterior walls. The floor truss seat connections over about 1/4 to 1/2 of the east side of the core were severed on floors 80 and 81 and over about 1/3 of the east exterior wall on floor 83.
- Aircraft impact severed a few columns near the east corner of the north wall between floors 80 and 82.
- The impact damage to the exterior walls resulted in redistribution of severed column loads, mostly to the columns adjacent to the impact zones. The impact damage to the core columns resulted in redistribution of severed column loads mostly to other intact core columns and the east exterior wall. The hat truss resisted the downward movement of the south wall, and rotated about the east-west axis.
- As a result of the aircraft impact damage, the core carried 6 percent less gravity loads after impact and the north face carried 10 percent less loads. The east face carried 24 percent more gravity load, while the west face and the south face carried 3 percent and 2 percent more gravity load, respectively.
- After impact, the core was leaning toward the east and south exterior walls. The exterior walls acted to restrain the core structure.

### 2. Effects of Subsequent Fires and Impact Damaged Fireproofing:

#### A. Thermal Weakening of the Core:

- Several of the undamaged core columns near the damaged and severed core columns developed high plastic and creep strains over the duration the building stood, since both temperatures and stresses were high in the core area. The plastic and creep strains exceeded thermal expansion in the core columns.
- The core continued to tilt toward the east and south due to the combination of column shortening (due to plasticity, creep, and buckling) and the failure of column splices at the hat truss in the southeast corner.
- As a result of thermal weakening (and subsequent to impact), the east wall carried about 5 percent more gravity loads and the core carried about 2 percent less loads. The other three walls carried between 0 and 3 percent less loads.

#### B. Thermal Weakening of the Floors:

- Floors 79 to 83 weakened with increasing temperatures over time on the long-span floors on the east side and sagged.
- Floor sagging induced inward pull forces on the east wall columns.
- About an additional 1/3 of the connections to the east exterior wall on floor 83 failed due to thermal weakening of the vertical supports.

#### C. Thermal weakening of the east wall:

- East wall columns bowed inward as they were subjected to high temperatures and inward pull forces in addition to axial loads.
- Inward bowing of the east wall columns increased with time.

**Figure 9–14. WTC 2 probable collapse sequence.**

### 3. Collapse Initiation

- The inward bowing of the east wall induced column instability, which progressed rapidly horizontally across the entire east face.
- The east wall unloaded and tried to redistribute the loads via the hat truss to the weakened core and via the spandrels to the adjacent north and south walls.
- The entire section of the building above the impact zone began tilting as a rigid block (all four faces; not only the bowed and buckled east face) to the east (about 7° to 8°) and south (about 3° to 4°) as column instability progressed rapidly from the east wall along the adjacent north and south walls. The building section above impact continued to rotate to the east as it began to fall downward, and rotated to at least 20 to 25 degrees.
- The change in potential energy due to downward movement of building mass above the buckled columns exceeded the strain energy that could be absorbed by the structure. Global collapse then ensued.

**Figure 9–14. WTC 2 probable collapse sequence (cont).**

As a result of the impact damage, dead and live loads carried by severed columns on the south wall and in the southeast corner of the core were redistributed to adjacent intact columns and also to the columns on the east wall (see Table 9–8). After redistribution, the total axial load on the core columns reduced by 6 percent, and the total axial load on the north wall columns reduced by 10 percent. The total axial load on the east wall columns, however, increased by 24 percent, and the total axial load on the west and south wall columns slightly increased by 2 percent to 3 percent.

Just below the hat truss level (Floor 105), analyses predicted that about seven column splices failed for columns at the southeast corner of the core. This increased the core tilting toward the southeast and also increased the vertical downward displacement of the core at the impact zone. After the failure of the core column splices, the remaining core columns transferred 73 percent of the loads released in the failing core columns to the exterior walls through the hat truss and 27 percent of the loads were transferred through the core floors.

Even though some column loads on the south wall were reduced after impact, the total load did not change, as some of the loads from the core area were redistributed to that wall through the hat truss (see Table 9–9). At the end of the load redistribution after impact, the core was leaning toward the east and south. The perimeter walls acted to restrain the core structure in the lateral direction.

### Sagging of Floors and Floor/Wall Disconnections

Thermal expansion of the floors also occurred early in the fires, but as floor temperatures increased, the floor sagged and began to pull inward on the exterior columns. As a result of the aircraft impact damage and increasing temperatures due to subsequent fires, Floor 79 through Floor 83 sagged over time. The amount of sagging was more significant at Floor 80 and Floor 81 where the truss seats on the east side of the core were failed due to aircraft impact (see Fig. 9–15). Increased temperatures also weakened the truss seats on the east exterior wall and caused additional disconnections at Floor 82 and Floor 83, which further increased the floor sag (see Fig. 9–16). Floor sagging induced pull-in forces on the east wall columns, and started shortly after impact and grew with time.

## Bowing of East Wall

The east wall columns bowed inward as a result of increasing temperatures (reduced strength and stiffness) and pull-in forces induced by sagging floors (see Figs. 9–17 and 9–18). The amount of inward bowing in the east wall steadily increased with time due to the combined effects of pull-in forces from sagging floors, increased axial loads, and a continuous increase in thermally induced plastic and creep strains (see Fig. 9–19). The load in bowed columns decreased, with some load transferring to adjacent unbowed columns, but the total column load on the east wall remained more or less constant for the duration after aircraft impact (see Fig. 9–20).

## Unloading and Tilting of Core

With increasing time and temperatures, the core columns developed high compressive plastic and creep strains, especially on the east side of the core. Plastic and creep strains started to exceed the thermal expansion strains approximately 30 min after the aircraft impact (see Fig. 9–21). High plastic and creep strains caused unloading on the east side core columns. This increased the core tilt toward the southeast and transferred more loads to the east wall. As a result, at Floor 83, the total axial load carried by the core columns were reduced by 8 percent, the east wall loads increased by 29 percent, and the north wall loads decreased by 12 percent, relative to the total loads before aircraft impact. The total loads on the south and west walls did not change significantly (see Tables 9–8 and 9–9).

## Buckling of East Wall and Collapse Initiation

With continuously increased bowing and axial loads, the east wall became unstable. The instability started at the center portion of the wall and rapidly progressed horizontally on both sides. As a result of buckling, the east wall significantly unloaded, redistributing its loads to the weakened core through the hat truss and to the east side of the south and north walls through the spandrels (see Figs. 9–22 through 9–24 and Table 9–10). Furthermore, the portion of the building above the buckled columns suddenly moved downward, and the building tilt towards the east increased.

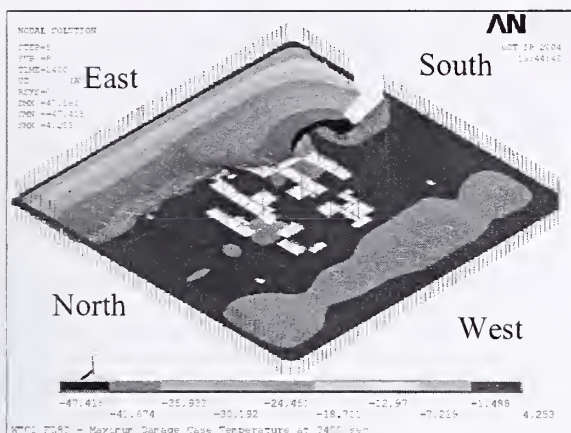
The section of the building above the impact zone began tilting to the east (about 7° to 8°) and south (about 3° to 4°) as column instability progressed from the east wall to the adjacent south and north walls. The building section above impact continued to rotate to the east as it began to fall downward, and rotated to at least 20 degrees to 25 degrees. The gravity loads could no longer be redistributed, nor could the remaining core and perimeter columns support the gravity loads from the floors above. The change in potential energy due to downward movement of the building mass above the buckled columns exceeded the strain energy that could be absorbed by the structure. The building portion above the impact zone became unstable, and building collapse ensued.

**Table 9–8. Total column loads at Floor 83 of WTC 2 for  
Case D. Compression is positive.**

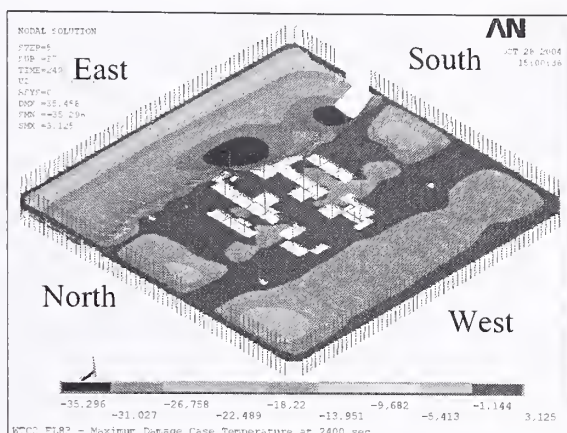
Row	Analysis Stage	West	East	North	South	Core
(1)	Before Impact	18065	18114	13567	13284	61828
(2)	After Impact	18670	22481	12193	13511	57821
(3)	10 min	18728	22226	11896	13358	58413
(4)	20 min	18914	22208	12052	13318	58124
(5)	30 min	18876	23681	11770	13365	56967
(6)	40 min	18531	23682	11906	13473	56825
(7)	43 min	15667	15143	14215	16292	62422
(8)	(2)-(1)	604	4368	-1374	227	-4007
(9)	(6)-(2)	-138	1201	-287	-38	-996
(10)	(7)-(6)	-2864	-8539	2309	2819	5596

**Table 9–9. Total column loads at Floor 105 of WTC 2 for  
Case D. Compression is positive.**

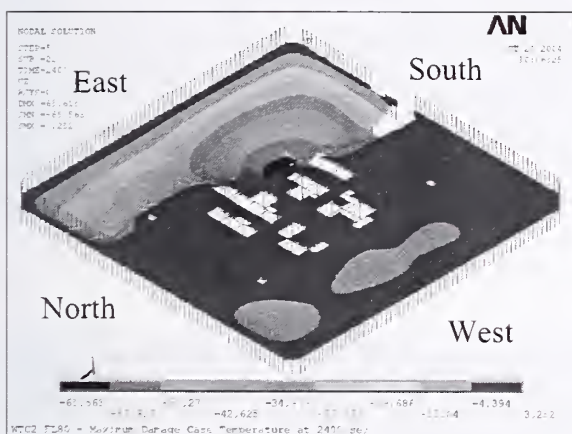
Row	Analysis Stage	West	East	North	South	Core
(1)	Before Impact	8497	8572	7382	7169	17123
(2)	After Impact	9170	11272	6487	8432	13382
(3)	10 min	9182	11061	6250	8275	13975
(4)	20 min	9279	11120	6311	8351	13682
(5)	30 min	9370	11859	6416	8553	12544
(6)	40 min	9198	11927	6524	8691	12402
(7)	43 min	7086	8026	6546	9169	17915
(8)	(2)-(1)	674	2699	-895	1263	-3741
(9)	(6)-(2)	28	656	37	259	-980
(10)	(7)-(6)	-2112	-3901	23	479	5513



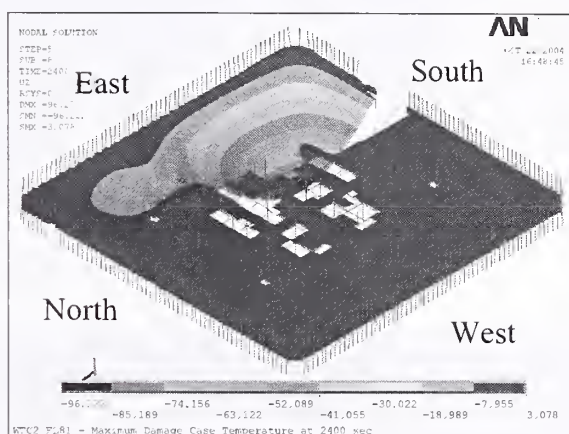
Floor 82



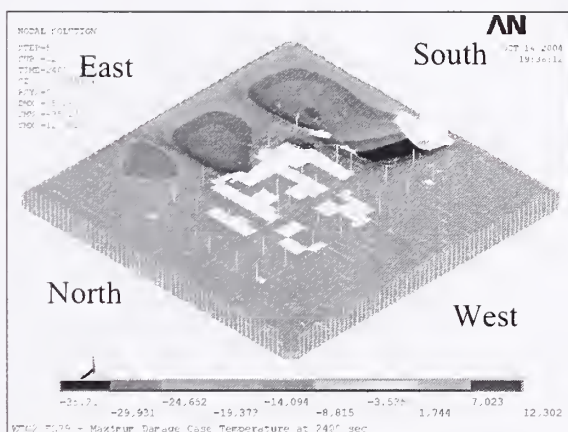
Floor 83



Floor 80

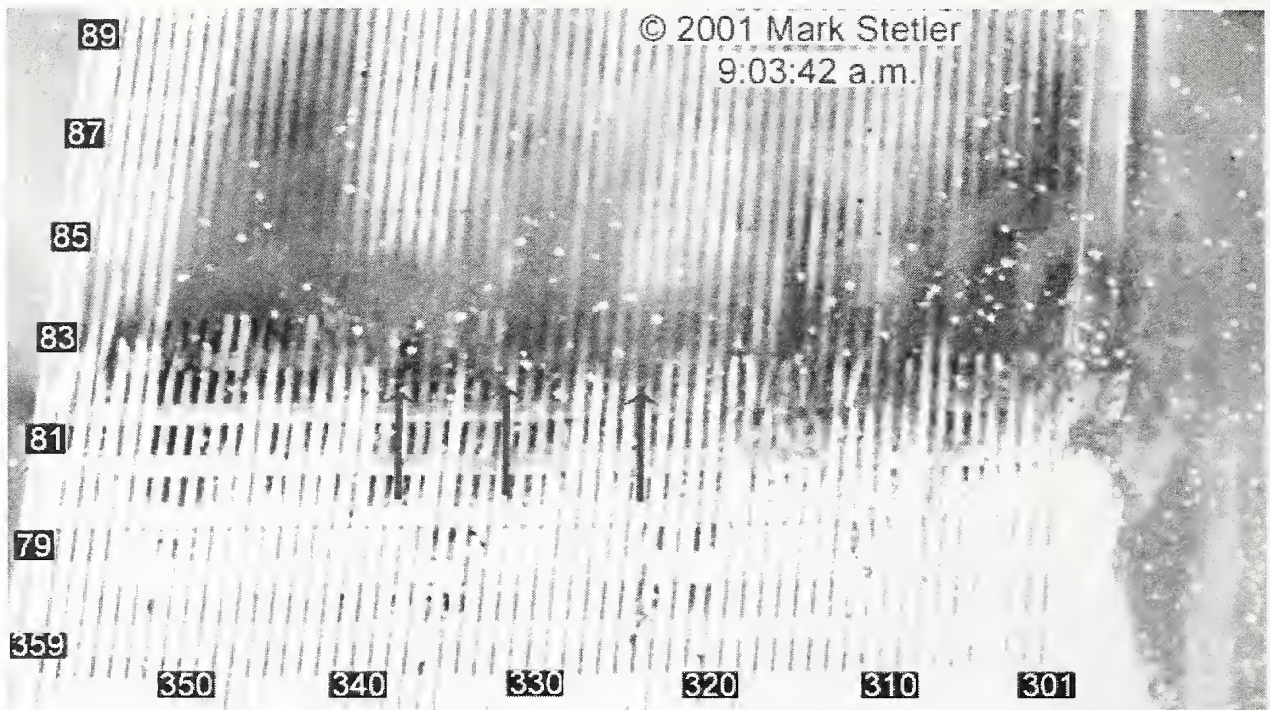


Floor 81

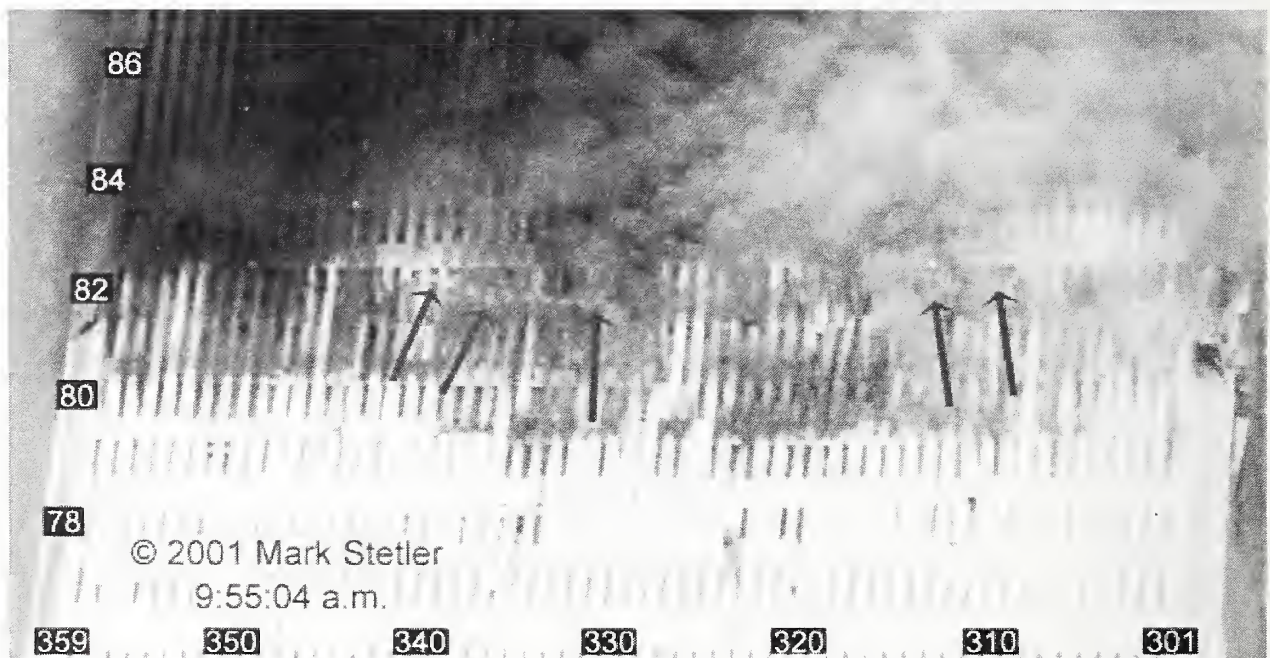


Floor 79

Figure 9-15. Vertical displacements of Floors 79 through Floor 88 of WTC 2 at 40 min (Case D).

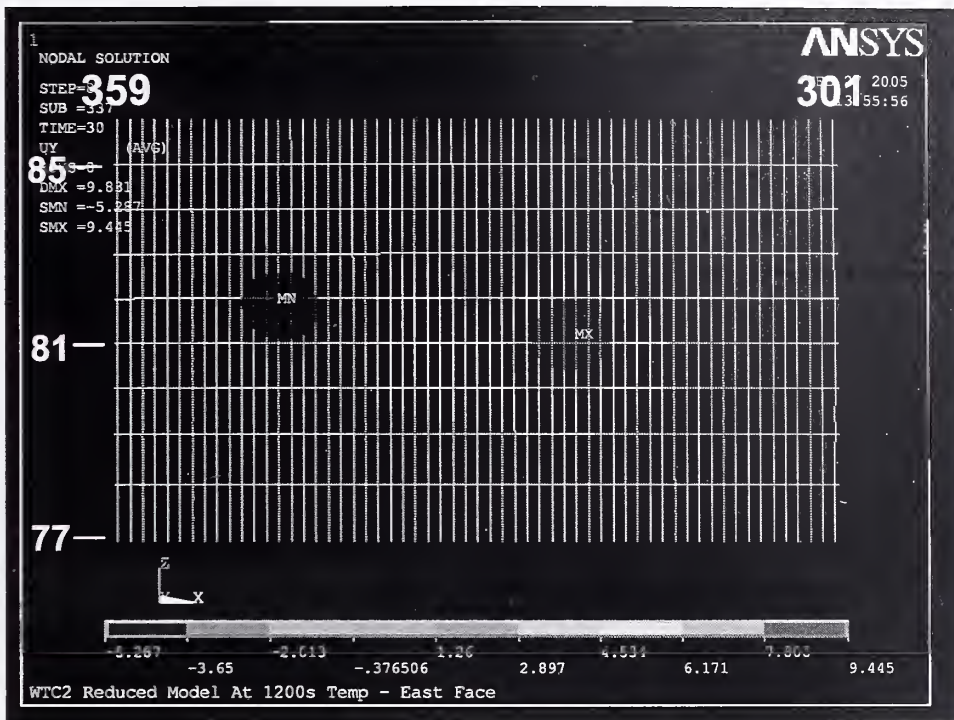


After impact damage

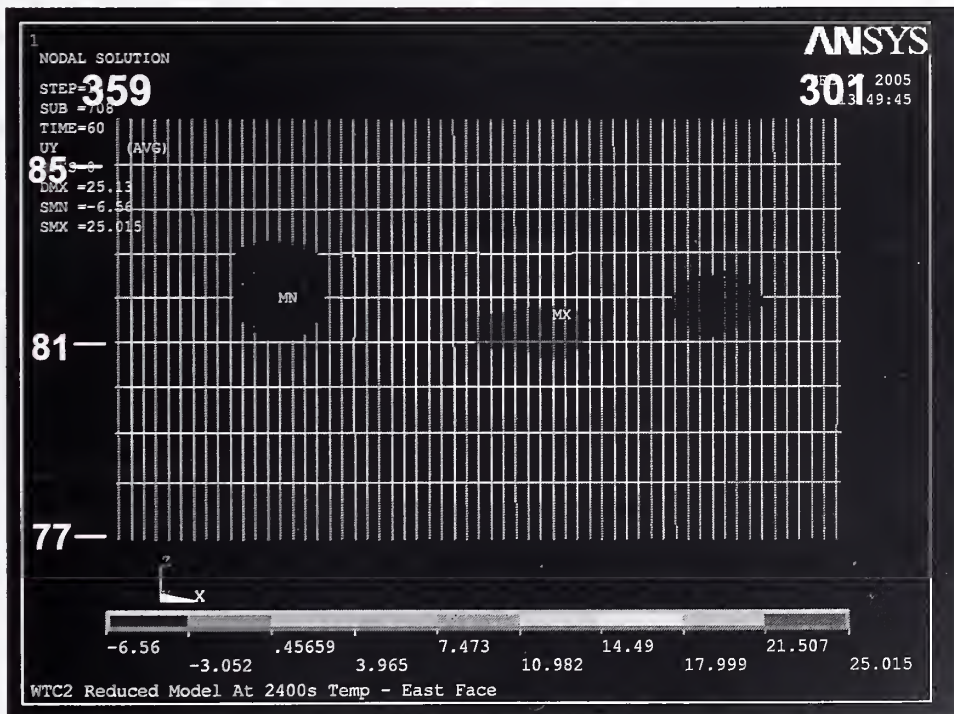


Damage a few minutes before collapse

Figure 9–16. Floor sagging observed on the east wall of WTC 2 at different stages.



At 20 minutes



At 40 minutes

Figure 9-17. Out-of-plane displacements on the east wall of WTC 2 (Case D).



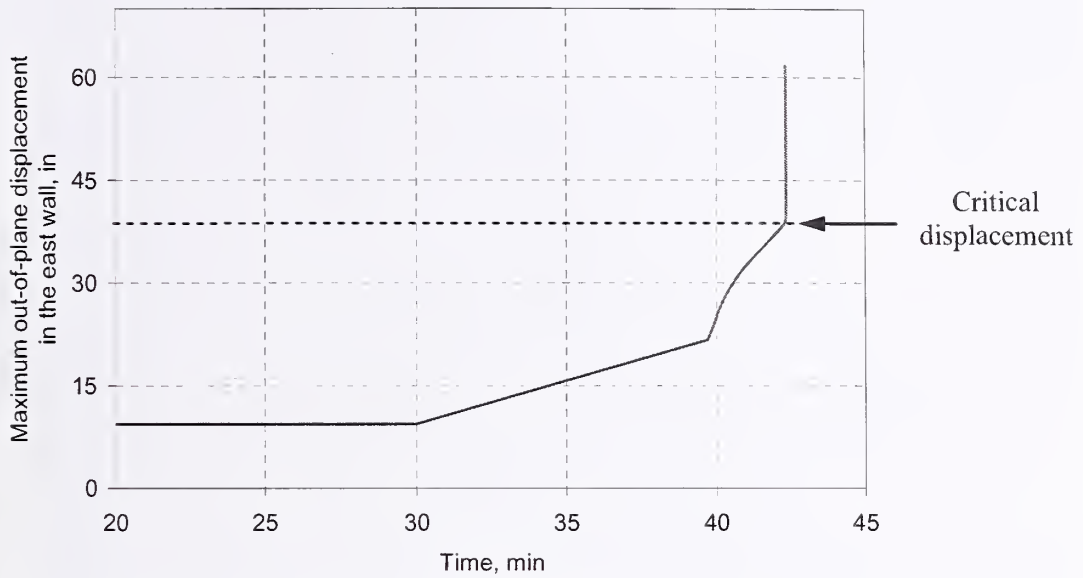


Figure 9-19. Variation of maximum out-of-plane displacement on the east wall of WTC 2 (Case D).

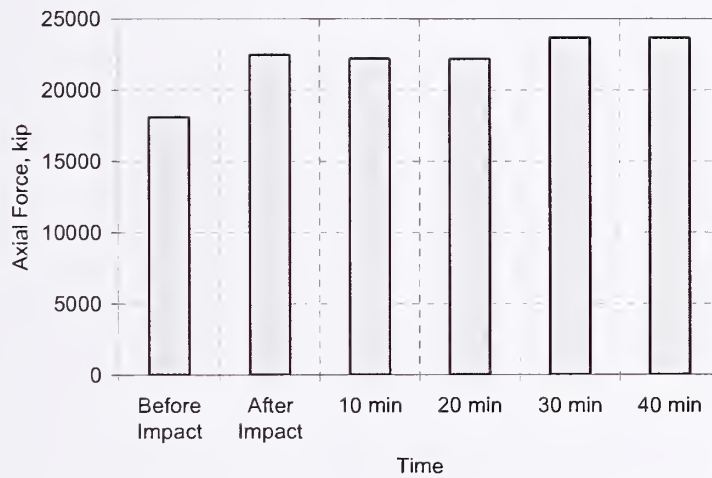


Figure 9-20. Total column loads at Floor 83 of the east wall of WTC 2 at different stages (Case D).

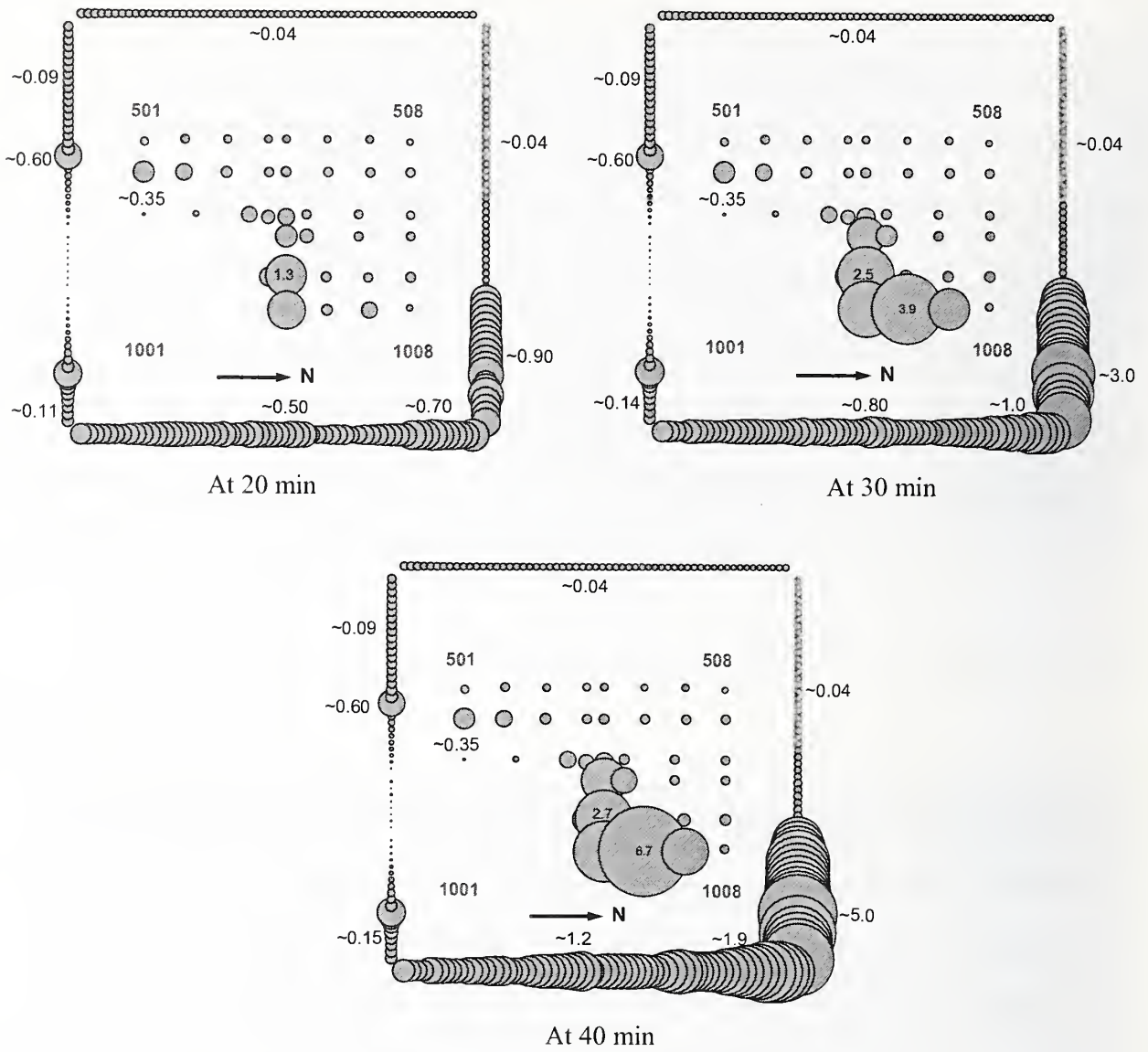


Figure 9-21. Maximum elastic + plastic + creep strains for columns between Floor 78 and Floor 83 of WTC 2 at different stages (Case D) (strain values are in percent).

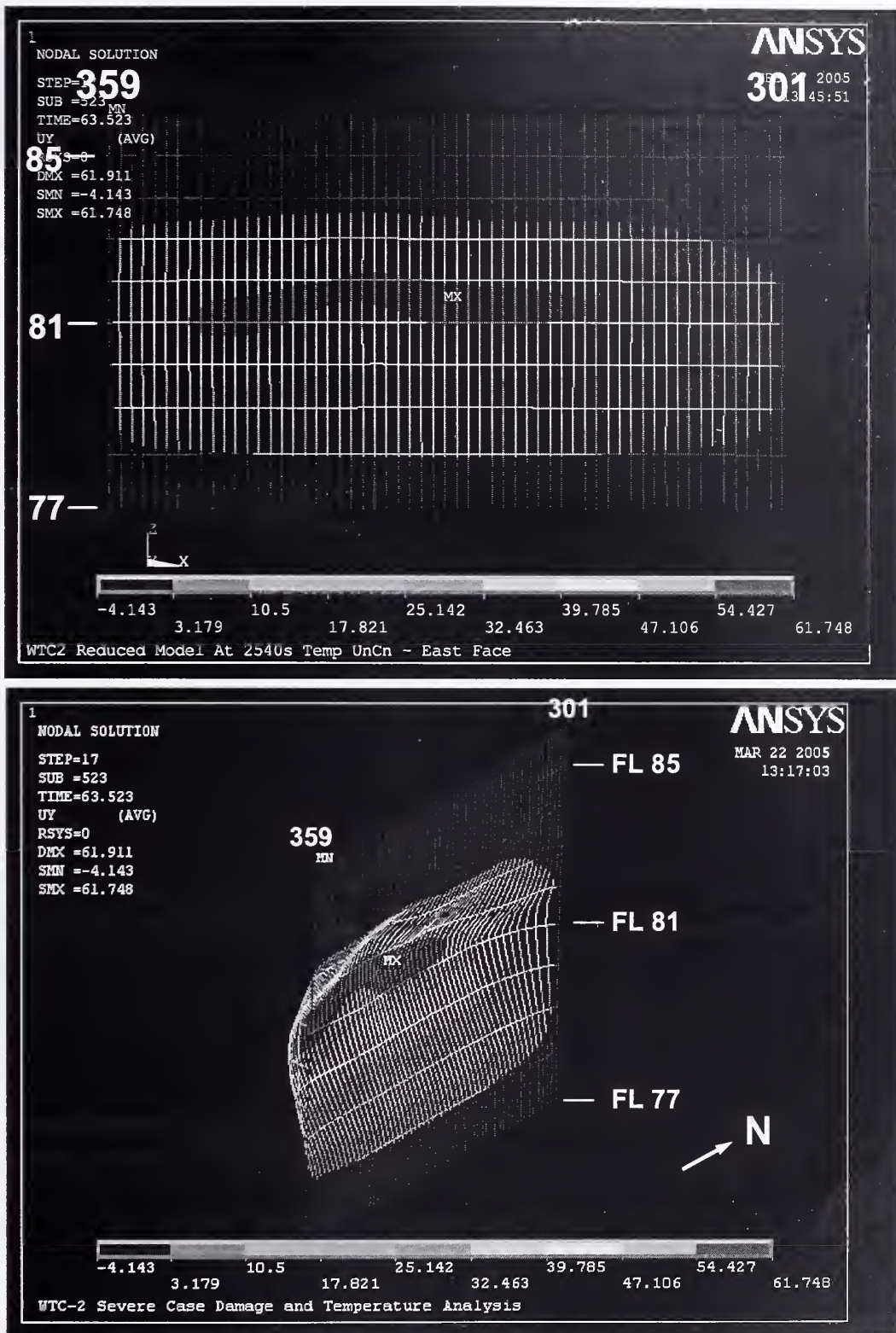
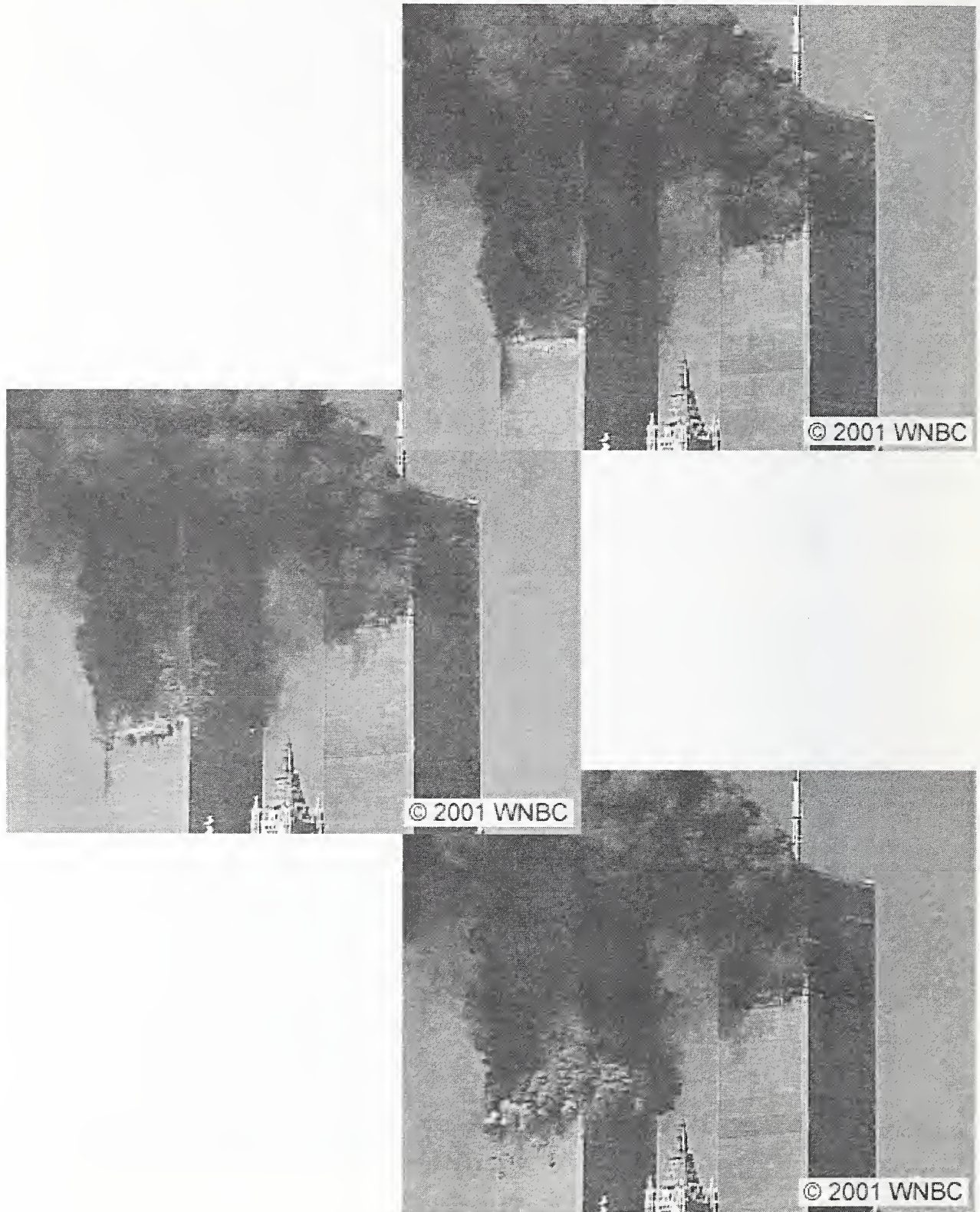


Figure 9-22. Inward bowing of the east wall of WTC 2 when buckled at 43 min for Case D (4x displacement magnification).



**Figure 9–23. Inward bending of exterior columns of the west wall of WTC 2 just before collapse.**

**Table 9–10. Change in total column loads when the east wall of WTC 2 buckles (Case D, compression is positive).**

Row	Floor	West	East	North	South	Core
(1)	83	-2864	-8539	2309	2819	5596
(2)	105	-2112	-3901	23	479	5513
(3)	(2) - (1)	752	4637	-2286	-2340	-84

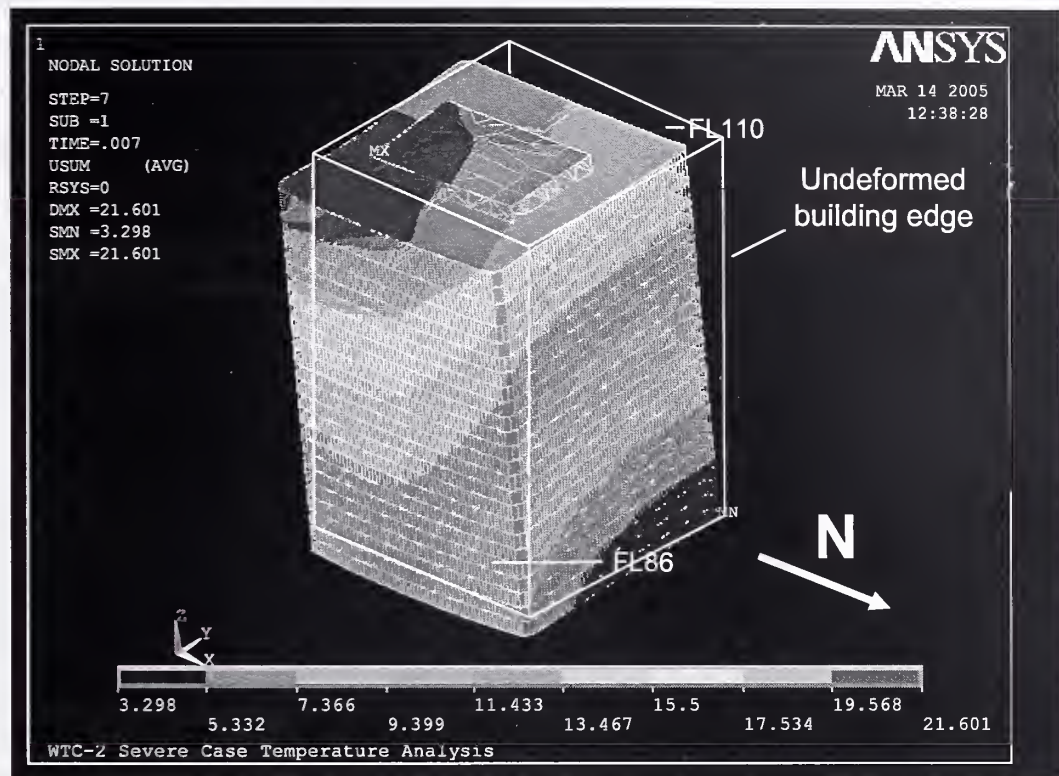


**Figure 9–24. Total displacements of WTC 2 above Floor 86 at 43 min for Case D. Note tilt toward east and south (20x displacement magnification).**

### 9.3.3 Events Following Collapse Initiation

Failure of the south wall in WTC 1 and east wall in WTC 2 caused the portion of the building above to tilt in the direction of the failed wall. The tilting was accompanied by a downward movement. The story immediately below the stories in which the columns failed was not able to arrest this initial movement as evidenced by videos from several vantage points.

The structure below the level of collapse initiation offered minimal resistance to the falling building mass at and above the impact zone. The potential energy released by the downward movement of the large building mass far exceeded the capacity of the intact structure below to absorb that through energy of deformation.

Since the stories below the level of collapse initiation provided little resistance to the tremendous energy released by the falling building mass, the building section above came down essentially in free fall, as seen in videos. As the stories below sequentially failed, the falling mass increased, further increasing the demand on the floors below, which were unable to arrest the moving mass.

The falling mass of the building compressed the air ahead of it, much like the action of a piston, forcing material, such as smoke and debris, out the windows as seen in several videos.

NIST found no corroborating evidence for alternative hypotheses suggesting that the WTC towers were brought down by controlled demolition using explosives planted prior to September 11, 2001. NIST also did not find any evidence that missiles were fired at or hit the towers. Instead, photographs and videos from several angles clearly showed that the collapse initiated at the fire and impact floors and that the collapse progressed from the initiating floors downward, until the dust clouds obscured the view.

## **9.4 DISCUSSION AND SUMMARY**

The results of structural analyses conducted in this study on components, subsystems, isolated exterior walls and cores, and global models of WTC 1 and WTC 2 showed that the collapses of the towers were initiated by the combined effects of the structural and insulation damage from aircraft impact and the subsequent intense fires.

The impact damage alone did not cause collapse of the towers, as they stood for a period of time, and collapse occurred after the fire-induced weakening of core, floor systems and exterior walls. Global analyses showed that both towers had substantial reserve capacity after the aircraft impact.

Similarly, the fires alone did not cause the collapse of the towers. In the absence of insulation damage, the weakening of the core columns and sagging of the floors sufficient to pull in on the exterior walls would not have occurred.

### **9.4.1 Structural Response to Impact Damage and Fire**

All three major subsystems played a role in the structural collapse sequence for WTC 1 and WTC 2 as described herein.

#### **Role of the Building Core**

The core columns were designed to carry the building gravity loads and were loaded to approximately 50 percent of their capacity before the aircraft impact.

The core columns were weakened significantly by the aircraft impact damage and thermal effects. Thermal effects dominated the weakening of WTC 1. As the fires moved from the north to the south side of the core, the core was weakened over time by significant creep strains on the south side of the core. Aircraft impact damage dominated the weakening of WTC 2. Immediately after impact, the vertical displacement at the southeast corner of the core increased 6 in. (from 4 in. to 10 in.). With the impact damage, the core subsystem leaned to the southeast and was supported by the south and east floors and exterior walls.

Gravity loads redistributed from the core to the exterior faces primarily through the hat truss due to aircraft impact and thermal effects. The WTC 1 core carried 1 percent less loads after impact but 20 percent less after thermal weakening. The WTC 2 core carried 6 percent less loads after impact and 2 percent less loads after thermal weakening.

Additional axial loads redistributed to the exterior columns from the core were not significant (only about 20 percent to 25 percent on average) as the exterior columns were loaded to approximately 20 percent of their capacity before the aircraft impact.

### **Role of the Building Floors**

The floors were designed to support occupancy loads and transfer them to the core and perimeter columns. They were also designed to act as horizontal diaphragms when the buildings were subject to high winds. In the collapse of the towers, the primary role of the floors was to provide inward pull forces after sagging that induced inward bowing of exterior columns (South face of WTC 1; East face of WTC 2).

The floors provided inward pull forces as they sagged significantly under thermal loads. However, the sagging floors continued to support their floor loads despite the dislodged insulation and extensive fires. Some truss seat connections with dislodged insulation at the exterior columns did fail and disconnect from the exterior wall under thermal loads. Floor disconnections increased the unsupported length of the exterior columns and distributed floor loads to adjacent truss seats. There were no inward pull forces where the floors were disconnected.

### **Role of Exterior Walls**

Column instability over an extended region of the exterior face ultimately triggered the global system collapse as the loads could not be redistributed through the hat truss to the already weakened building core. In the area of exterior column buckling, loads transferred through the spandrels to adjacent columns and adjacent exterior walls. As the exterior wall buckled (south face for WTC 1 and east face for WTC 2), the column instability propagated to adjacent faces and caused the initiation of the building collapse.

The exterior wall instability was induced by a combination of thermal weakening of the columns, inward pull forces from sagging floors, and to a much lesser degree, additional axial loads redistributed from the core.

#### **9.4.2 Structural Response to Fire Without Impact Damage**

Without insulation to delay the heating of steel components, steel temperatures began to rise upon exposure to fires. Thermal expansion occurred as temperatures increased; members restrained against thermal expansion increased in compressive load and may have caused a local or global load redistribution, depending upon the compressive load increase and extent of heating. Once steel temperatures exceeded 500 °C to 600 °C, the steel experienced significant reductions in stiffness and strength. The thermal analysis found that temperatures of floor trusses and columns with intact insulation rarely exceeded 400 °C during Case B fires (100 min long) for WTC 1 and 500 °C during Case D fires (60

min long) for WTC 2. Insulated floors thermally expanded, pushed outward on the exterior columns, and sagged in the full floor analyses, but the floor sag was insufficient to exert an inward pull on the exterior columns.

Steel members with dislodged insulation were found to have temperatures greater than 600 °C and often higher than 800 °C within 10 min to 15 min after exposure to a nearby fire. Fire exposures considerably longer than the 60 to 100 min exposure in WTC 2 and WTC 1, respectively, were required for insulated members to reach these temperatures. Reductions in modulus of elasticity, yield strength, and ultimate tensile strength of steel in the WTC towers were predicted to be 13 percent, 20 percent, and 10 percent, respectively, at 400 °C, and 35 percent, 92 percent, and 80 percent, respectively, at 700 °C. Steel loses its strength significantly at 700 °C. At these temperatures, the long-span floors were found to sag sufficiently to exert an inward pull on the exterior walls, primarily due to buckling of truss web diagonal members. In addition, creep in steel columns becomes significant when the steel temperatures are greater than 500 °C and subject to high stresses for a period of time.

Inward bowing of an exterior wall was a necessary but not sufficient condition to initiate collapse. In both WTC 1 and WTC 2, significant weakening of the core due to aircraft impact damage and thermal effects was also necessary to initiate building collapse. The tower structures had significant capacity to redistribute loads (a) from bowed walls to adjacent exterior walls with short-span floors via the arch action of spandrels, and (b) between the core and exterior walls via the hat truss and, to a lesser extent, the floors. Without the impact damage, the towers' capacity to redistribute loads would have been even greater.

As shown in the analysis results, the temperatures in steel components without insulation damage were lower for the same fire. Lower temperatures resulted in reduced creep, plasticity, and buckling. Without insulation damage, floor sagging was insufficient to exert pull-in forces on the exterior wall; the core columns maintained their stiffness and strength; and the exterior wall did not bow inward. The lack of thermally induced damage would result in negligible load redistributions, and the towers would have remained stable.

### 9.4.3 Time to collapse

The difference in the time it took for each WTC tower to collapse was due primarily to the differences in structural damage, the time it took the fires to travel from the impact area across the floors and core to critical locations, and the time it took to weaken the core and exterior columns. WTC 2 had asymmetric structural damage to the core, including the severing of a corner core column, and WTC 1 had more symmetrical damage. The fires in WTC 2 reached the east side of the building more quickly, within 10 to 20 minutes, than the 50 to 60 minutes it took the fires in WTC 1 to reach the south side.

### 9.4.4 Comparison with Other Collapse Hypotheses

Alternate analyses and collapse hypotheses were performed and reported by other studies. A comparison of NIST and other hypotheses is presented to review assumptions, methodologies, and results. The comparison includes analyses performed by

- Northwestern University,

- Weidlinger Associates, Inc. with Hughes Associates and ArupFire,
- University of Maryland at College Park and the Israel Institute of Technology,
- Edinburgh University, and
- Arup.

The NIST structural response analyses included the effects of aircraft impact damage to the structure and thermal insulation, fire growth and spread, the resulting time-varying temperatures of the structural components, and the progression of local structural failure leading up to collapse initiation. The analyses included the effects of construction sequence, thermal expansion, plastic and creep strains, temperature-dependent material properties, and relevant failure modes for structural members and connections.

With the exception of the Weidlinger-led study, the analyses for the other collapse hypotheses presented here ignored impact damage, assumed time-temperature curves for structural subsystems (i.e. floor trusses and exterior columns), and conducted analyses of components or subsystems but did not conduct global analyses of the entire structure (i.e., core, floors, exterior walls, and hat truss) that considered all of the load redistribution paths as local members and subsystems were thermally weakened over time. The Weidlinger study included impact damage and assumed time-temperature curves for structural subsystems for their global analyses of each tower.

### **Northwestern University**

The study performed by Northwestern University (Bazant 2002) was a simplified approximate analysis of the overall collapse of the WTC towers which addressed the question of why a total collapse occurred. The analysis addressed the results of prolonged heating which would have caused the columns of a single floor to lose their load carrying capacity and initiated the collapse of the building. The analysis assumed loss of thermal insulation during impact, uniform temperatures of 800 °C for a uniform column size and load across a single floor, and creep buckling and loss of load carrying capacity in over half of the columns. The analysis included evaluation of the dynamic amplification of the loads and the ability of the columns in the lower floors to dissipate the kinetic energy of the falling upper building mass through formation of plastic hinge mechanisms. The analysis found that the ratio of the kinetic energy of the upper building section dropping one floor to the deformation energy of plastic hinge rotation in the lower building columns was approximately a factor of eight.

The study by Northwestern did not address the details of impact damage, fire dynamics, or structural response of the towers. Rather, a generalized condition was assumed of heated columns, and the question of why there was total collapse was addressed. NIST agrees with the assessment of the tower's required structural capacity to absorb the released energy of the upper building section as it began to fall as an approximate lower bound. The likelihood of the falling building section aligning vertically with the columns below was small, given the observed tilting, so that the required capacity would be greater if interaction with the floors was also considered, as pointed out in the study.

## **Weidlinger Associates, Inc. with Hughes Associates and ArupFire**

The study led by Weidlinger Associates, Inc. (Abboud 2003, Post 2002a, Post 2002b, Glanz 2002) used the SAP2000 and FLEX finite element code to calculate the aircraft impact damage to both towers and their structural response to damage and elevated temperatures. FLEX is an explicit, nonlinear, large deformation transient analysis finite element code for the analysis of structures subject to blast, impact, and shock loads. The fires were evaluated by Hughes Associates and ArupFire Inc. The fires were found to be less than fully developed office fires, with gas temperatures ranging from 400 °C to 700 °C in the impact regions and well ventilated regions near the exterior walls; exterior locations with persistent fires were assumed to have 1000 °C temperatures. Based upon study of smoke plumes and fire spread, it was concluded that the floors did not fail or have a significant role in the collapse of the towers. The structural response analysis found that the impact debris dislodged thermal insulation and that the hat truss played a significant role in transferring loads between the core and exterior walls. The analysis identified the specific cause of each towers' collapse to be the failure of core columns that either lost insulation or were destroyed during the aircraft impact. WTC 2 exterior columns on the east side began to fail first and redistributed loads to the core columns until the loads could no longer be supported, due to successive failures of core columns. WTC 1 core columns began to fail first due to damage and thermal weakening and attempted to redistribute loads to the exterior walls through the hat truss. WTC 2 was found to collapse first primarily because the damage was off-center and compromised the southeast corner of the core.

NIST agrees with many of the findings by the Weidlinger Associates, Inc. led study. However, there were some differences in the modeling approach and assessment of contributing factors. The most significant difference was that the floors were not analyzed for their response to fire, so that the collapse hypothesis did not account for floor sag and its contribution to inward bowing of the exterior columns. The reason for WTC 2 collapsing before WTC 1 was attributed to the off-center damage, particularly the damage to the southeast corner core column. NIST found that in addition to the differences in impact damage between the two towers, the time it took the fires to travel from the impact area across floors and the core to critical areas, and the time it took for the core and exterior columns to become thermally weakened, also contributed to the difference in times to collapse initiation.

## **University of Maryland and Israel Institute of Technology**

The study performed by the University of Maryland and the Israel Institute of Technology (Quintiere 2002) was based upon a thermal conduction analysis of truss web members subjected to a uniform gas temperature and a structural failure analysis based on buckling of the truss web member due to a temperature-induced reduction in stiffness. Gas temperatures were estimated to be approximately 900 °C for the duration of the fires in each tower. A thermal conduction analysis of web members was conducted to estimate the temperature of the web member as a function of time and insulation thicknesses (0.75 in. and 1.5 in.). A web member with an assumed load was calculated to buckle when temperatures of about 630 °C to 770 °C were reached, due to a reduced modulus of elasticity. The time at which the insulated members reached temperatures that met the buckling criteria fell within the observed collapse time of each tower. It was noted that a bare steel web member would fail by this criteria in 10 min to 15 min, and that this time did not match the observed time to collapse initiation. Given the failure of truss web members, it was postulated (not supported by calculations) that the floors would sag and fail at their connections to the columns and that progressive collapse would ensue as the floors below also failed.

NIST findings differed from those given in this study. NIST also found that web members in the floor trusses buckled when heated sufficiently, which led to sagging of the floor, but did not find appreciable floor sagging when the truss insulation remained intact. The Maryland study suggested that the sagging floors resulted in failure of the floor to column connections; NIST analyses found that the sagging floors did not cause floor connections to fail, except at a few isolated locations, but rather produced an inward pull on the exterior walls. An inward pull of exterior columns would not occur if floor to column connections had failed. To produce the inward bowing of the exterior walls that was observed, the floors had to sag and exert an inward pull well before collapse initiated, not at the time of collapse as proposed in the Maryland study. Additionally, analysis of a floor collapsing onto a floor below, which was unlikely given the required event of all floor connections failing nearly at the same time, was not found to result in failure of the impacted floor.

### University of Edinburgh

The University of Edinburgh study (Usmani 2003, Usmani 2005) performed a nonlinear, large displacement finite analysis of a typical 2D slice of the tower structure that encompassed twelve floors around the impact level of WTC 1 using ABAQUS. However, there were also some simplifying assumptions to reduce the model complexity, such as restraining lateral movement of the floor at the core end and a pinned connection to the external columns at the other end. The truss diagonals were modeled with a single axial element and connections were not explicitly modeled. It was assumed that the core columns were relatively cool and that the collapse would initiate at the exterior columns. A generalized exponential curve represented the time-temperature relationship, and assumed temperature profiles were applied to the floors for various fire scenarios. The exterior columns were linearly ramped from ambient temperatures. The analysis found that the heated floors expanded and pushed the exterior columns outward and that the outward movement was resisted by tension in the cool floors above and below the fire floors. The analysis also found that a floor buckled at 400 °C, causing the exterior column to 'rebound', resulting in large compressive loads on the floors above and below, which in turn buckled. It was stated that the same mechanism propagated to adjacent floors until it was arrested or caused collapse. Consideration of the hat truss, its capacity for redistribution of loads between the exterior walls and core, and its role in delaying the collapse mechanism until the structure's redistribution capacity was exhausted was discussed, but no supporting analyses were presented. These results were cited as a possible fire-induced collapse mechanism for a tower without impact damage that was based on thermal expansion rather than fire-induced loss of strength and stiffness.

NIST findings also differed from the findings of the University of Edinburgh study. NIST included thermal expansion in its detailed analyses of full floor systems, and did not find that buckling of any floor system occurred. Rather, as truss web members began to buckle, the floors began to sag, which increased over time. The sudden buckling of the first floor in the Edinburgh analysis, followed by the sudden subsequent failure of floors above and below, does not match the observed inward bowing of the exterior walls which increased over time. Further, NIST found that failure of an exterior wall was necessary but not sufficient to initiate the collapse of either tower. In both WTC 1 and WTC 2, significant weakening of the core due to aircraft impact damage and thermal effects was also necessary to initiate building collapse.

## Arup

The study by Arup (Lane 2005) was conducted to determine if the WTC towers had any collapse mechanisms specific to their structural system features. Based upon information available through presentations, studies included 2D analysis of a twelve-floor slice of the exterior column and floors to the core, a twelve-floor slice across the entire tower (from exterior column to exterior columns), and 3D quarter floor, half floor, and quarter-floor seven-story section models. None of the models included the hat truss; all of the models included individual floor trusses and the floor slabs. Temperatures from the fires for structural members were assumed, where the floor trusses reached 800 °C in a “very short time”, the exterior columns and spandrels heated linearly to 400 °C by 3600 s. Slab temperatures were not reported. Three floors were heated to 800 °C, the floors sagged and the exterior wall section was pulled inward. The inward bowing of the exterior wall was considered to be a collapse mechanism for the towers. Arup stated that the behavior was calculated for the duration of the fire with no user intervention and without inclusion of any aircraft impact damage, including damage to thermal insulation.

The description of Arup analyses is based on presentations since no published reports by Arup were available prior to the release of this report. The study by Arup found that the composite truss floors sagged as they were heated and pulled inward on the exterior wall, similar to the findings by NIST. However, the NIST analyses did not find uniform temperatures across an entire floor nor simultaneously on multiple floors, as assumed in the Arup analyses. Further, NIST did not find any insulated truss members reaching temperatures of 800 °C prior to the collapse of either tower. NIST thermal analyses showed that steel temperatures in areas where the insulation remained intact rarely exceeded 400 °C in WTC 1 and 500 °C in WTC 2. The Arup 3D seven-floor model did not include load transfer mechanisms, including the hat truss, the core, and sufficient portions of the exterior wall to provide the arching action observed in the impact faces. NIST found that failure of an exterior wall was necessary but not sufficient to initiate the collapse of either tower. In both WTC 1 and WTC 2, significant weakening of the core due to aircraft impact damage and thermal effects and redistribution of loads between the core and exterior wall were found to be necessary to initiate building collapse.

### 9.4.5 Factors that Affected Performance

From the collective knowledge and insights gained through the Investigation of the collapse of the WTC towers, the following factors were identified that affected performance of both towers on September 11, 2001:

- The closely spaced columns, along with deep short spandrels, allowed a redistribution of loads as a result of aircraft impact damage to the exterior wall.
- Because there was effectively no wind on the morning of September 11, 2001, the capacity of the exterior wall provided to accommodate design wind loads was available to carry redistributed gravity loads.
- The large dimensional size of the WTC towers helped the buildings withstand the aircraft impact.
- The composite floor system with primary and bridging trusses forming a 2-way grid, and the two layers of welded wire fabric in the slab, acted to bridge over damaged areas without

propagation of collapse from areas of aircraft impact damage to other locations, thereby avoiding larger scale floor collapse upon impact.

- The hat truss played a major role in the post-impact performance of the building. This was accomplished through redistribution of the loads from the significant weakening of the core, due to aircraft impact damage and subsequent thermal effects, by redistributing loads from the damaged core columns to adjacent intact columns and, ultimately, by redistributing loads to the exterior walls from the thermally weakened core columns that lost their ability to support the buildings' weight.
- The buildings would likely not have collapsed under the combined effects of aircraft impact and the subsequent jet-fuel ignited multi-floor fires, if the insulation had not been dislodged or had been only minimally dislodged by aircraft impact. The existing condition of the insulation prior to aircraft impact and the insulation thickness on the WTC floor system did not play a significant role in initiating collapse on September 11, 2001.

## 9.5 REFERENCES

Zdenek Bazant and Yong Zhou (2002), *Why Did the World Trade Center Collapse?—Simple Analysis*, Journal of Engineering Mechanics, Vol. 128, No. 1

Abboud, Najib et.al., (2003), Anatomy of a disaster: A structural investigation of the World Trade Center collapses, Proceedings of the Third Congress Forensic Engineering, San Diego, CA, United States, Oct 19-21 2003, p 360-370

Nadine Post (2002a), Report Ties WTC Collapses to Column Failures, Engineering News Record, McGraw Hill Construction, 10/25/2002

Nadine Post (2002b), Study Absolves Twin Tower Trusses, Fireproofing, Engineering News Record, McGraw Hill Construction, 11/04/2002

James Glanz and Eric Lipton (2002), In Data Trove, A Graphic Look at Towers' Fall, The New York Times, October 29, 2002

J.G. Quintiere, M. di Marzio, and R. Becker (2002), A suggested cause of the fire-induced collapse of the World Trade Towers, Fire Safety Journal, Vol. 37, Issue 7, October 2002, p 707-716.

A.S. Usmani, Y.C. Chung, and J.L. Torero (2003), How did the WTC towers collapse: a new theory, Fire Safety Journal, vol 38, Issue 6, October 2003, p 501-533.

A.S. Usmani (2005), Stability of the World Trade Center Twin Towers Structural Frame in Multiple Floor Fires, Journal of Engineering Mechanics, Vol. 131, No. 6, Jun 2005, p 654-657.

B. Lane (2005), Comments on structural fire response and collapse analysis, Presentation given at the Technical Conference on the Federal Building and Fire Safety Investigation of the World Trade Center (WTC) Disaster, National Institute of Standards and Technology (NIST), Gaithersburg, Maryland, September 13-15, 2005, <http://wtc.nist.gov>

This page intentionally left blank.

## Chapter 10

### FINDINGS

---

There were many facets to the work reported herein. First, the thickness of the passive fire protection was established from recorded measurements and interpretation of photographs of the originally applied SFRM. This information was used, along with statistical analysis and thermal structural analyses, to establish the thickness of passive fire protection (insulation or fireproofing) to be used in finite element thermal analyses. Next, standard fire resistance tests were conducted to establish the appropriate classification (fire resistance rating) of the original design of the WTC floor system and structural performance of the floor system in standard fires for insight into performance in actual fires. Characterization of the temperatures of the structural components, determined from simulated WTC fires, allowed the calculation of the performance of major subsystems constituting the structural system of the towers. In turn, insights obtained from these analyses were used to formulate and execute global analyses to analyze the collapse sequence of each tower. The structural analyses results were guided, and where possible validated, by observations made from the review of thousands of photographs and video recordings. This chapter reports the findings resulting from these efforts to characterize the conditions of the WTC towers before the attacks, their weakening due to the aircraft impacts, their subsequent response to the growth and spread of fires, and the progression of local failure that ultimately led to the total collapse of both towers.

#### 10.1 PASSIVE FIRE PROTECTION

The passive fire protection applied to the steel structural components in the WTC towers was investigated to provide information on the in-place condition of the thermal insulation before and after the aircraft impact. The specified and “as applied” thicknesses, the variability in thickness, the condition of the insulation over a 30-year service life, and the effects that the variability and condition have on the structural behavior of insulated steel members were studied. The rationale behind the selection of the effective thickness of thermal insulation for use in thermal analyses was presented. Additionally, the procedures and practices used to provide the passive fire protection for the floor system of the WTC tower structures was documented.

#### 10.2 BUILDING CODE REQUIREMENTS FOR STRUCTURAL FIRE RESISTANCE

**Finding 1:** The WTC towers were classified as Class 1B, as defined by the 1968 New York City Building Code. This classification required a 3 h fire rating for columns and 2 h for floors. The towers could have been classified as Class 1A since both Class 1A and 1B permitted buildings of unlimited height. Class 1A required a 4 h fire resistance rating for columns and a 3 h rating for floors. In 1969, The Port Authority of New York and New Jersey (PANYNJ) specified 0.5 in. fireproofing for all beams, spandrels, and trusses, to maintain the Class 1-A Fire Rating of the New York City Building Code. A condition assessment conducted in 2000 reported that the WTC towers were classified as Class-1B—noncombustible, fire-protected, and retrofitted with sprinklers consistent with Local Law 5/1973.

## 10.2.1 Selection of Fire Resistive Materials

**Finding 2:** The passive fire protection for the floor trusses was specified to be 0.5 in. of BLAZE-SHIELD Type D, although the technical basis for the selection of this product and required thickness value is not known. After applying the Type D sprayed fire resistive materials to the lower 40 floors of WTC 1, the BLAZE-SHIELD insulating material was switched to Type D/CF (reported to meet or exceed the insulating properties of Type D) which did not contain asbestos. In 1995, the Port Authority conducted a study to establish the fireproofing requirements for the floor trusses in areas undergoing major tenant renovation. The thickness required to achieve a 2 h fire rating was determined to be 1.5 in. using the BLAZE-SHIELD II product. At the time of the WTC disaster, fireproofing had been upgraded on a number of floors in the WTC towers: 18 floors in WTC 1, including all of the floors affected by the aircraft impact and fires, and 13 floors in WTC 2, although none that were directly affected by the aircraft impact and fires.

## 10.2.2 Equivalent thickness of SFRM

**Finding 3:** Based on analyses of SFRM thickness measurements and interpretation of photographs showing the condition of the originally applied material, the average thickness of the original thermal insulation on the floor trusses was estimated to be 0.75 in. with a standard deviation of 0.3 in. (coefficient of variation of 0.40). The average thickness of the upgraded thermal insulation was estimated to be 2.5 in. with a standard deviation of 0.6 in. (coefficient of variation of 0.24). Based on finite-element simulations, it was concluded that the original passive fire protection on the floor trusses was thermally equivalent to a uniform thickness of 0.6 in., and the upgraded insulation was thermally equivalent to a uniform thickness of 2.2 in. These values were used in the thermal analyses for determining temperature histories of structural components.

**Finding 4:** No information was available on in-place conditions of the thermal protection on the exterior columns and spandrel beams, and little information was available on the conditions of fire resistive material on core beams and columns. For thermal analyses of the towers, the SFRM on these elements was taken to have uniform thicknesses equal to the specified thickness. This assumption was supported by the observation that measured average thickness tended to be *greater* than the specified thickness while, due to variability, the effective thickness tended to be *less* than the average uniform thickness. The specified thickness values were 0.5 in. for beams and spandrels, 2.06 in. (2 1/16 in.) for columns lighter than 14WF228, and 1.19 in. (1 3/16 in.) for columns equal to or heavier than 14WF228.

**Finding 5:** The adhesive strength of BLAZE-SHIELD DC/F to primed steel was found to be a third to a half of the adhesive strength to steel that had not been coated with primer paint. The SFRM products used in the WTC towers were applied to steel components with primer paint.

## 10.3 FIRE RESISTANCE TESTS

Four Standard Fire Tests (ASTM E 119) were conducted on floor assemblies constructed to duplicate, as closely as practical, the floor system used in the WTC towers. Full scale tests with a 35 ft span and having 3/4 in. thick SFRM were tested, one in the restrained test condition and the other in the unrestrained test condition. Tests of half-scale specimens, which spanned approximately 17 ft, were conducted using SFRM conditions simulating the “as specified” condition (0.5 in. thick SFRM) and the “as-applied”

condition (0.75 in. thick SFRM). The following findings are based on this series of four tests and a comparison of their results.

### 10.3.1 Structural Performance

**Finding 6:** Test assemblies, representative of the WTC floor system, exposed to the Standard Fire Test (ASTM E 119) conditions resulted in extensive spalling on the underside of the floor slab, thermal damage to the bridging trusses, and buckling of compression diagonals and vertical struts of the main trusses.

**Finding 7:** All four tests demonstrated that the floor assemblies were capable of sagging without failure. The unrestrained test, which had two 0.875 in. bolts fastening the main truss to the truss seats, did not sag sufficiently to bear on the bolts. In the three restrained tests the main truss ends were welded to the truss seats to provide the required restraint. The magnitude of the sagging observed in the tests was consistent with that computed from finite element structural analyses. No evidence of knuckle failure was seen in the tests.

**Finding 8:** All four test assemblies supported their full design load under standard fire conditions for two hours without failure.

### 10.3.2 Fire Resistance Ratings

**Finding 9:** The 1968 New York City (NYC) building code—the code that the WTC towers were intended but not required to meet when they were built—required a 2 h fire rating for the floor system.

**Finding 10:** The restrained duplicated floor system obtained a fire resistance rating of 1.5 h while the unrestrained floor system achieved a 2 h rating. This finding was unexpected since the unrestrained rating is typically less than the restrained rating.

**Finding 11:** The test of the 17 ft specimen with as-applied SFRM did not produce the same rating as the 35 ft test specimen, giving 2 h and 1.5 h, respectively. In both cases, the rating was established on the basis of temperatures of the unexposed surface (top of concrete slab) and not on the ability of the specimen to support the load.

**Finding 12:** The 45 min rating for the standard 17 ft test with the specified 0.5 in. SFRM did not meet the 2 h requirement of the 1968 NYC Building Code. This test had no SFRM on the bridging trusses nor on the underside of the metal deck.

**Finding 13:** The 2 h rating for the standard 17 ft test with the as-applied average 0.75 in. SFRM met the 2 h requirement of the 1968 NYC Building Code. This test had half the SFRM thickness on the bridging trusses (0.375 in.) and overspray on the underside of the metal deck.

**Finding 14:** The difference in test results for the two 17 ft specimens is due primarily to the concrete slab performance (spalling and cracking) and the presence or lack of SFRM overspray on the metal deck and not due to the SFRM thickness on the trusses. Differences in the degree of concrete spalling were possibly due to differences in moisture content and the slab cracking.

## 10.4 RESPONSE OF STRUCTURAL COMPONENTS

The response of the structural components and their connections for the tenant floors and exterior walls was examined with detailed structural models. Results of the floor and exterior wall component and connection analyses identified structural behaviors and failure modes that were required for inclusion in the global analyses.

### 10.4.1 Floor System

**Finding 15:** The interior truss seats had a greater vertical shear capacity than the exterior truss seats. The controlling failure mode for vertical shear was weld fracture. However, the vertical load at the truss connection of approximately 16 kip had to increase by a factor of two to six to reach failure (weld fracture) for temperatures near 600 °C to 700 °C.

**Finding 16:** Detailed structural analysis of a single truss section of the composite floor system subjected to elevated uniform temperatures was found to initially push out on the exterior columns as a result of the concrete slab thermal expansion and then pull inward as the web diagonals buckled and the truss sag increased. The magnitude of the pull-in force was found to depend highly on the stiffness of the exterior box column which, in turn, depended on expansion of floors above and below.

**Finding 17:** Detailed analysis of the knuckles (shear connectors in the floor system for composite action) through test simulation and detailed truss analysis found that failure of the knuckles in the floor system was unlikely. This finding was also supported by the lack of any knuckle failures in the four standard fire resistance tests (ASTM E 119) of the floor truss assemblies with twice the floor load that was on the WTC floors.

### 10.4.2 Exterior Wall System

**Finding 18:** Large inelastic deformations and buckling of the spandrels at elevated temperatures were predicted, but were found not to significantly affect the stability of the exterior columns. Partial separations of the spandrel splices were also predicted at elevated temperatures, but were found not to significantly affect the stability of the exterior columns.

**Finding 19:** Analyses of bolted splices in the exterior columns found that the splice may slide or open when the exterior columns are bowing and subject to large lateral deflections. No column splice bolts were predicted to have failed.

**Finding 20:** An exterior wall section (9 columns wide and 9 floors high) was found to bow inward when the floor connections applied an inward pull force. For the condition where three sequential floors were disconnected, there was no bowing of the columns for five different elevated temperature conditions. When the column section with three disconnected floors was subjected to increased axial column loads, the wall section bowed outward over the unsupported column length.

## 10.5 FIRE PROTECTION AND PARTITION DAMAGE DUE TO AIRCRAFT IMPACT

The aircraft impact of the WTC towers caused extensive damage to the buildings' exteriors, penetrated into the interiors causing further damage to the structural systems, dislodged insulation, and ignited multi-floor fires. The structural damage to each tower resulting from the aircraft impact was estimated using a transient finite element analysis. Results of this analysis were used to predict damage to the structure, fireproofing, and partition walls in the path of the debris field.

**Finding 21:** For WTC 1, partitions were damaged and fireproofing was dislodged by direct debris impact over five floors (Floors 94, 95, 96, 97, and 98) and included most of the north floor areas in front of the core, the core, and central regions of the south floor areas, and on some floors, extended to the south wall. For WTC 2, partitions were damaged and fireproofing was dislodged by direct debris impact over six floors (Floors 78, 79, 80, 81, 82, and 83) and included the south floor area in front of the core, the central and east regions of the core, and most of the east floor area, and extended to the north wall.

**Finding 22:** The fireproofing damage estimates were conservative as they ignored possibly damaged and dislodged fireproofing in a much larger region that was not in the direct path of the debris but was subject to strong vibrations during and after the aircraft impact. A robust criteria to generate a coherent pattern of vibration-induced dislodging could not be established to estimate the larger region of damaged fireproofing.

## 10.6 OBSERVATIONS AND TIMELINE

Thousands of photographs and hours of video records were reviewed for insights into the structural performance of the towers. A timeline of significant events that characterized the weakening and eventual collapse of the WTC towers was developed with the photographs and videos that were time-stamped. Quantitative information, such as the amount of inward bowing observed on the exterior walls of the buildings, was extracted from key photographs through image enhancement and scaled measurements. Key observations and the timelines were used to guide the global collapse analyses.

### 10.6.1 WTC 1

**Finding 23:** Inward bowing of the south exterior wall was first observed at 10:23 a.m. The bowing appeared to extend between Floors 94 and 100 and Columns 305 and 359. The maximum bowing was estimated from images to be 55 in.±6 in. at Floor 97 on the east side of the south face of WTC 1. The central area in available images was obscured by smoke. The extent of fires observed on all faces of WTC 1 was similar, although somewhat more extensive on the east and west faces (where short span floors were located) and similarly extensive on the north and south faces (where long span floors were located). Inward bowing was observed only on the south face. The north face had extensive aircraft impact damage, and the damaged floors were not capable of imposing inward pull forces on the north face.

**Finding 24:** The time to collapse initiation was 102 minutes from the aircraft impact (8:46:30 a.m. until 10:28:22 a.m.).

**Finding 25:** From exterior observations, tilting of the building section appeared to take place near Floor 98. Column buckling was then observed to progress rapidly across the east and west faces.

**Finding 26:** The WTC 1 building section above the impact and fire area tilted to the south as the structural collapse initiated. The tilt was toward the side of the building that had the long span floors. Video records taken from east and west viewpoints showed that the upper building section tilted to the south. Video records taken from a north viewpoint showed no discernable east or west component in the tilt. A tilt to the south of at least 8 degrees occurred before dust clouds obscured the view and the building section began to fall downward.

## 10.6.2 WTC 2

**Finding 27:** On the east face and north face of WTC 2, draped objects were observed through the windows of floor 82 on the east face and floors 81 to 83 on the north face near the northeast corner. The draped objects appeared to be hanging floors. The drape of these objects was observed to increase with time and extend across approximately half of the east face.

**Finding 28:** Inward bowing of the east wall was first observed at 9:21 a.m. The inward bowing was approximately 10 in.±1 in. at Floor 80 and extended between Floors 78 and 83 and Columns 304 and 344. The remaining portion of the face to the south of Column 344 was not included in the image. The bowing appeared to extend over a large fraction of the east face and to be greatest near the center of the face. Fires were more extensive along the east face (where long span floors were located) and at the east side of the north and south faces (where short span floors were located). Fires were not observed on the west face (where long span floors were located). Inward bowing was observed only on the east face. The south face had extensive aircraft impact damage, and the damaged floors were not capable of imposing inward pull forces on the south face. There was no impact damage or fire on the west floors to cause pull-in forces on the west face.

**Finding 29:** An increase of the inward bowing of the east wall was observed at 9:53 a.m. The inward bowing appeared to extend between Floors 78 and 84 and Columns 305 and 341. The remaining portion of the face to the south of Column 344 was not included in the image. The maximum bowing was estimated from images to be 20 in.±1 in. at Floor 80 on the east face of WTC 1.

**Finding 30:** The time to collapse initiation was 56 minutes after aircraft impact (9:02:59 a.m. to 9:58:59 a.m.).

**Finding 31:** From exterior observations, tilt of the building section above the impact and fire area appeared to take place near Floor 82. Column buckling was then seen to progress across the north face.

**Finding 32:** The building section above the impact and fire area tilted to the east and south at the onset of structural collapse. The tilt occurred toward the east side with the long span floors. Estimates made from photographs indicate that there was approximately a 3 degree to 4 degree tilt to the south and a 7 degree to 8 degree tilt to the east prior to significant downward movement of the upper portion of the building. The tilt to the south did not increase any further as the upper building section began to fall, but the tilt to the east continued, reaching 20 degrees to 25 degrees before dust clouds obscured the view.

## 10.7 STRUCTURAL RESPONSE OF MAJOR TOWER SUBSYSTEMS

Prior to conducting the analysis of the global structural response of each tower, major structural subsystems were analyzed to provide insight into their behavior within the WTC global system. The three major structural subsystems, the core framing, a single exterior wall, and full tenant floors, were analyzed separately for their response to impact damage and fire. The hat truss was not analyzed separately as its structural behavior did not require significant simplification in the global analysis. The component analyses provided a foundation for these large, nonlinear analyses with highly redundant load paths, and they enabled a significant reduction in finite element model complexity and size. The major subsystem models used final estimates of impact damage and elevated temperatures determined from the aircraft impact analysis and the fire dynamics and thermal analyses.

### 10.7.1 Isolated Core Subsystem

**Finding 33:** The WTC 1 isolated core subsystem analysis found that the core structure was most weakened from impact and thermal effects at the center of the south side of the core. Smaller displacements occurred in the global model due to the constraints of the hat truss and floors.

**Finding 34:** The WTC 2 isolated core subsystem analysis found that the core structure was unstable for the estimated structural damage to core columns. The core was most weakened from impact and thermal effects at the southeast corner and along the east side of the core. Larger displacements occurred in the global model as the isolated core model had lateral restraints imposed that were somewhat stiffer than in the global model.

### 10.7.2 Full Floor Subsystem

**Finding 35:** Floor sagging was caused primarily by either buckling of truss web diagonals or disconnection of truss seats at the exterior wall or the core perimeter. Except for the truss seat failures near the southeast corner of the core in WTC 2 following the aircraft impact, web buckling or truss seat failure was caused primarily by elevated temperatures of the structural components.

**Finding 36:** Analysis results from both the detailed truss model and the full floor models found that the floors began to exert inward pull forces when floor sagging exceeded approximately 25 in. for the 60 ft floor span.

**Finding 37:** Sagging at the floor edge was due to loss of vertical support at the truss seats. The loss of vertical support was caused in most cases by the reduction in vertical shear capacity of the truss seats due to elevated steel temperatures.

### 10.7.3 Isolated Exterior Wall Subsystem

**Finding 38:** Inward pull forces were required to produce inward bowing that was consistent with displacements measured from photographs. The inward pull was caused by sagging of the floors. Heating of the inside face of the exterior columns also contributed to inward bowing.

**Finding 39:** The observed inward bowing of the exterior wall indicated that most of the floor connections were intact to cause the observed bowing.

**Finding 40:** The floors that were identified through analysis to be affected by the fires and the dislodged insulation matched well with the floors that were observed to have participated in the inward bowing of the exterior walls.

**Finding 41:** The extent of floor sagging required at each floor was greater than that predicted by the full floor models. The estimates of the extent of sagging at each floor were governed by the combined effects of insulation damage and fire; insulation damage estimates were limited to areas subject to direct debris impact. Other sources of floor and insulation damage from the aircraft impact and fires (e.g., insulation damage due to shock and subsequent vibrations as a result of aircraft impact or concrete slab cracking and spalling as a result of thermal effects) were not included in the floor models.

## **10.8 STRUCTURAL RESPONSE TO AIRCRAFT IMPACT DAMAGE AND FIRE**

Global analysis of WTC 1 and WTC 2 used final estimates of impact damage and elevated temperatures to determine the structural response and sequence of component and subsystem failures that led to collapse initiation.

### **10.8.1 General Findings**

**Finding 42:** The structural analyses of WTC 1 and WTC 2 found that the collapse of the towers was due to the combined effects of structural and insulation damage from aircraft impact and the subsequent fires on the core, floor systems, and exterior walls. The towers collapsed when the weakened core and exterior columns could no longer redistribute or support the building loads with their reduced load carrying capacity.

**Finding 43:** Impact damage alone did not cause collapse of the towers, as they were stable after the aircraft impact. Global analyses showed that both towers had substantial reserve capacity after the aircraft impact.

**Finding 44:** The multi-floor fires alone did not cause collapse of the towers. Without impact damage to the insulation, the structural steel temperatures would have been generally less than 200 °C to 300 °C, with a few isolated locations of structural steel temperatures exceeding 400 °C in WTC 1 floors and 500 °C in WTC 2 floors. The core would not have weakened, the floor sag would have been insufficient to pull inward on the exterior columns, and the exterior walls would not have bowed inward.

**Finding 45:** The towers would likely not have collapsed under the combined effects of aircraft impact and the subsequent multi-floor fires if the insulation had not been dislodged or had been only minimally dislodged by aircraft impact. Had insulation not been dislodged by the debris field, temperature rise of structural components would likely have been insufficient to induce global collapse. Structural components that became thermally weakened were generally determined by impact of the debris field. The existing condition of the insulation prior to aircraft impact and the insulation thickness on the WTC floor system did not play a role in initiating collapse of the towers.

**Finding 46:** Creep strain was significant in the core and exterior columns over the 56 min to 102 min period of fire exposure in columns with temperatures greater than 500 °C to 600 °C and high stress. Columns with creep strains of sufficient magnitude to cause column shortening played a significant role in the collapse initiation.

**Finding 47:** The faces of the buildings that exhibited inward bowing were associated with the long span direction of the floor system. The primary direction of tilting at collapse initiation for WTC 1 and WTC 2 was in the direction of the bowed faces.

### 10.8.2 Performance with Intact Fire Protection

**Finding 48:** A detailed thermal-structural analysis, which did not include slab delamination/spalling effects, showed that a full collapse of the WTC floor system would not occur even with a number of failed trusses or connections.

**Finding 49:** Most of the horizontal and vertical capacity of the floor connections to the exterior and core columns significantly exceeded the demand under design load conditions.

## 10.9 PROBABLE COLLAPSE SEQUENCES

The results of structural analyses conducted in this study on components, subsystems, isolated exterior walls and cores, and global models of WTC 1 and WTC 2 showed that the collapses of the towers were initiated due to the combined effects of the structural and insulation damage from aircraft impact and the subsequent intense fires. The probable collapse sequences for WTC 1 and WTC 2 are based upon the collective consideration of structural analyses, statistical based methods, observations, and laboratory testing.

### 10.9.1 Role of the Building Core

**Finding 50:** The core columns were weakened significantly by the aircraft impact damage and thermal effects. Thermal effects dominated the weakening of WTC 1. As the fires moved from the north to the south side of the core, following the debris damage path, the core was weakened over time by significant creep strains on the south side of the core. Aircraft impact damage dominated the weakening of WTC 2. Immediately after impact, the vertical displacement at the southeast corner of the core increased 6 in. (from 4 in. to 10 in.). With the impact damage, the core subsystem leaned to the southeast and was supported by the south and east floors and exterior walls.

**Finding 51:** As the core was weakened from aircraft impact and thermal effects, it redistributed loads to the exterior walls primarily through the hat truss. Additional axial loads redistributed to the exterior columns from the core were not significant (only about 20 percent to 25 percent on average) as the exterior columns were loaded to approximately 20 percent of their capacity before the aircraft impact.

### 10.9.2 Role of the Building Floors

**Finding 52:** The primary role of the floors in the collapse of the towers was to provide inward pull forces that induced inward bowing of exterior columns (south face of WTC 1; east face of WTC 2).

**Finding 53:** Sagging floors continued to support floor loads as they pulled inward on the exterior columns. There would have been no inward pull forces if the floors truss seats had failed and disconnected.

### 10.9.3 Role of Exterior Frame-Tube

**Finding 54:** Column instability over an extended region of the exterior face ultimately triggered the global system failure as the loads could not be redistributed through the hat truss to the already weakened building core. In the area of exterior column buckling, load transferred through the spandrels to adjacent columns and adjacent exterior walls. As the exterior wall buckled (south face for WTC 1 and east face for WTC 2), the column instability propagated to adjacent faces and caused the initiation of the building collapse.

**Finding 55:** The exterior wall instability was induced by a combination of thermal weakening of the columns, inward pull forces from sagging floors, and to a lesser degree, additional axial loads redistributed from the core.

### 10.9.4 Probable Collapse Sequences

**Finding 56:** Although the north face of WTC 1 had extensive impact damage, thermal weakening of the core columns on the south side of the core and inward bowing of the south face caused the building to tilt to the south at collapse initiation. The extent of fires observed on all faces of WTC 1 was similar, although somewhat more extensive on the east and west faces (where short span floors were located) and somewhat less extensive on the north and south faces (where long span floors were located). Thermal weakening of exterior columns with floor sagging (which induced inward pull and occurred on the south side) caused inward bowing of the south face and tilting in the south direction.

**Finding 57:** Although the south face of WTC 2 had extensive impact damage, thermal weakening of the core columns on the east side of the core and inward bowing of the east face caused the building to tilt more to the east and less to the south at collapse initiation. Fires were more extensive along the east face and at the east side of the north and south faces. Thermal weakening of exterior columns with floor sagging (which induced inward pull and occurred on the east side) caused inward bowing of the east face and primary tilting in that direction (with additional southward tilting due to the aircraft impact damage).

**Finding 58:** The time it took for each WTC tower to collapse was due primarily to the differences in structural damage, the time it took the fires to travel from the impact area across the floors and core to critical locations, and the time it took to weaken the core and exterior columns. WTC 2 had asymmetric structural damage to the core, including the severing of a corner core column, and WTC 1 had more symmetrical damage. The fires in WTC 2 reached the east side of the building more quickly, within 10 min to 20 min, than the 50 min to 60 min it took the fires in WTC 1 to reach the south side.

**Finding 59:** NIST found no corroborating evidence for alternative hypotheses suggesting that the WTC towers were brought down by controlled demolition using explosives planted prior to September 11, 2001. NIST also did not find any evidence that missiles were fired at or hit the towers. Instead, photographs and videos from several angles clearly showed that the collapse initiated at the fire and

impact floors and that the collapse progressed from the initiating floors downward, until the dust clouds obscured the view.

This page intentionally left blank.

# Appendix A

## SUMMARY OF AIRCRAFT IMPACT DAMAGE FOR INITIAL CASES 1 TO 4

### WTC 1 CASE A<sub>i</sub> – THERMAL INSULATION AND PARTITION DAMAGE FOR OCCUPANCY FLOOR

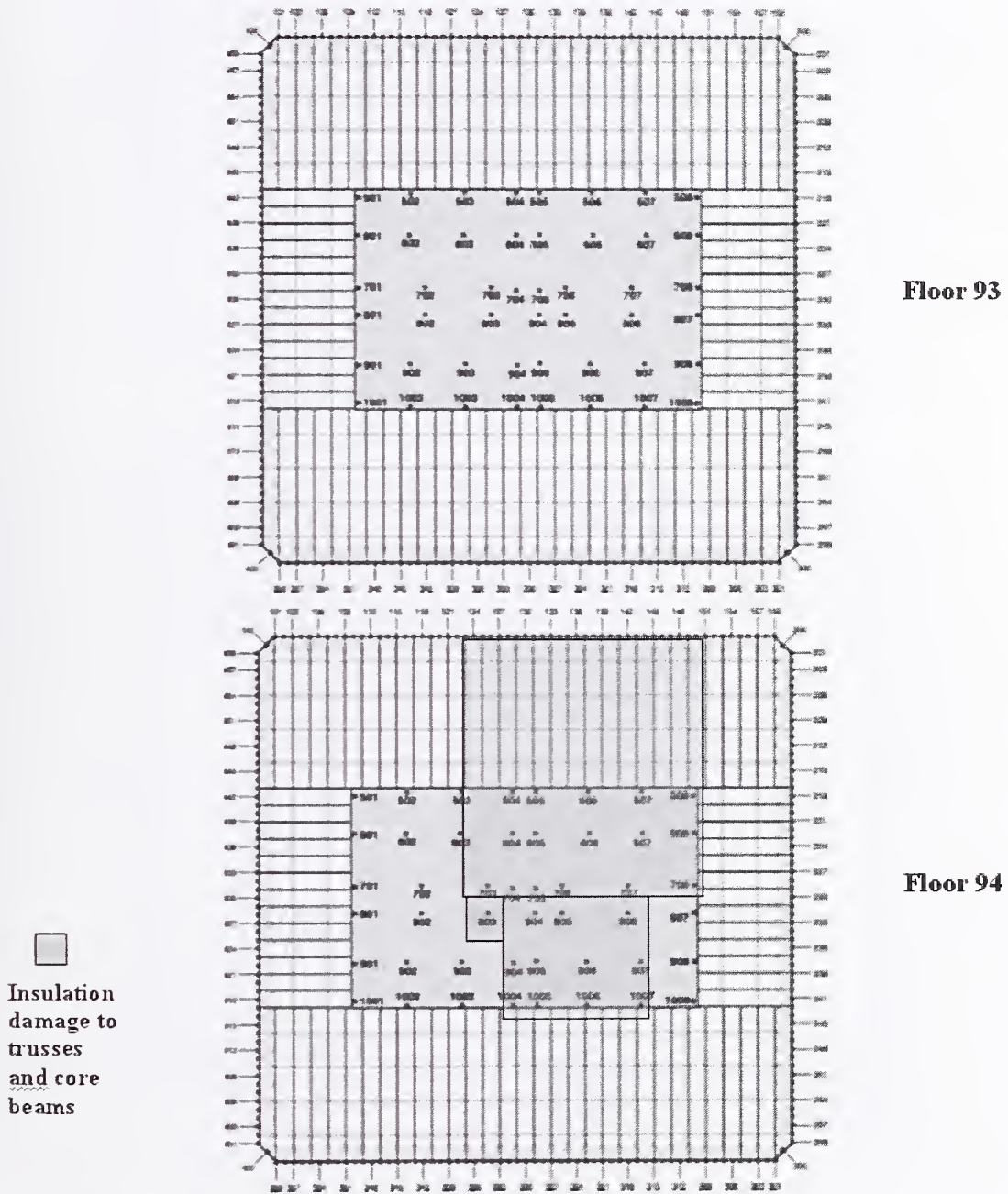


Figure A-1. WTC 1 Case A<sub>i</sub> aircraft impact damage to Structural Floor 93 and 94.

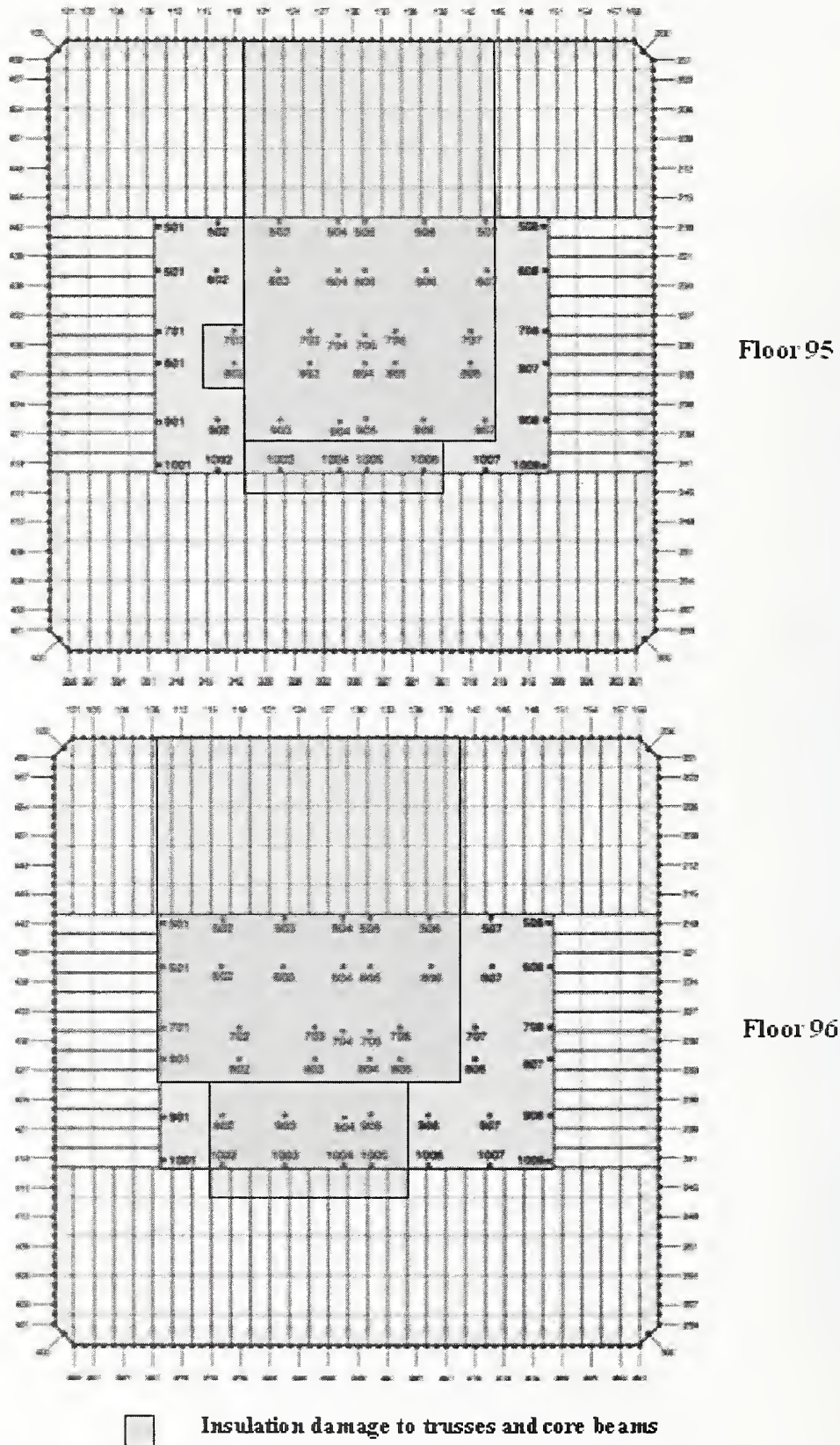


Figure A-2. WTC 1 Case A<sub>1</sub> aircraft impact damage to Structural Floors 95 and 96.



WTC 1 CASE A<sub>1</sub> – DAMAGE FOR STRUCTURAL FLOOR

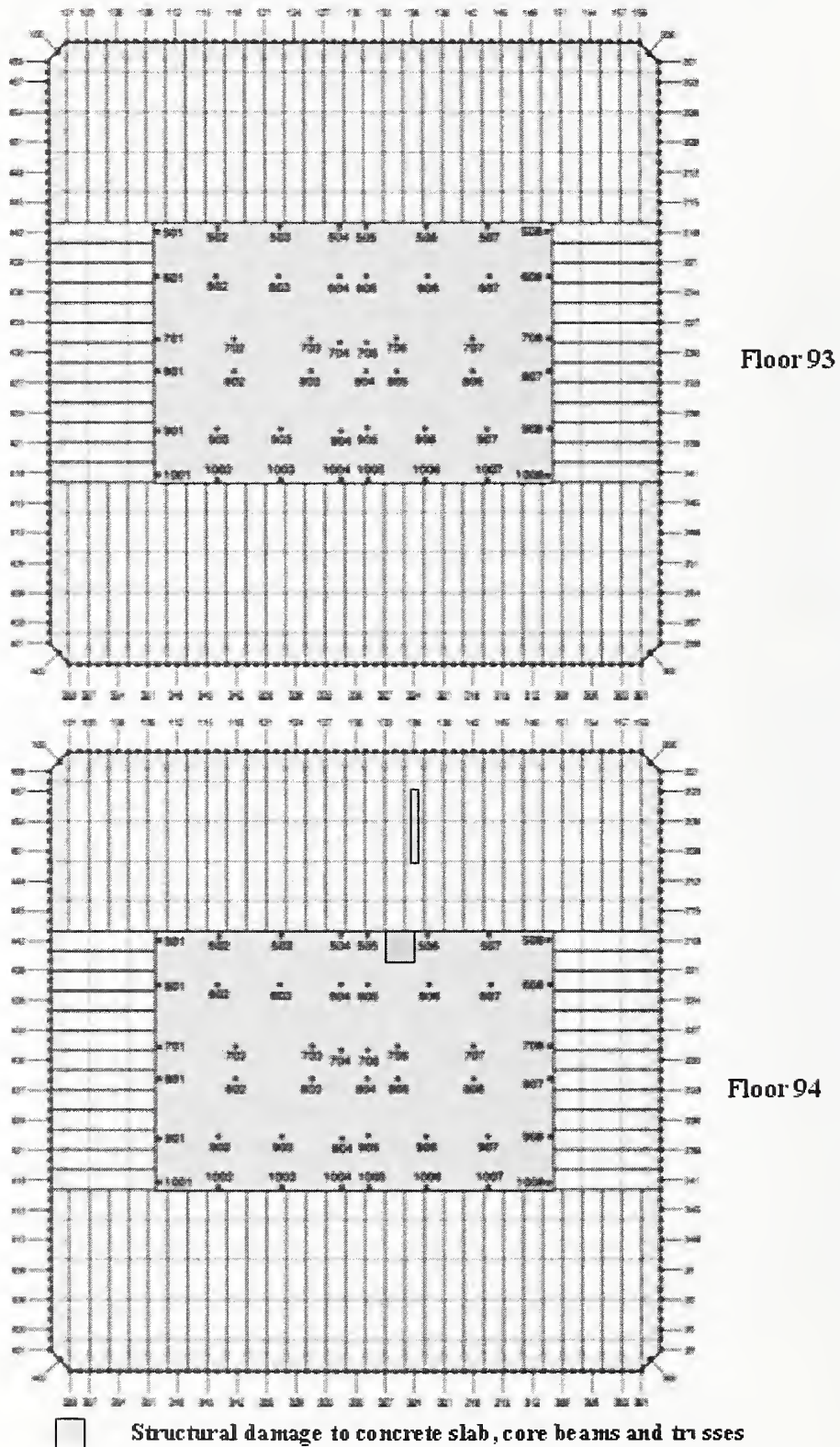


Figure A-4. WTC 1 Case A<sub>1</sub> aircraft impact damage to Structural Floor 93 and 94.



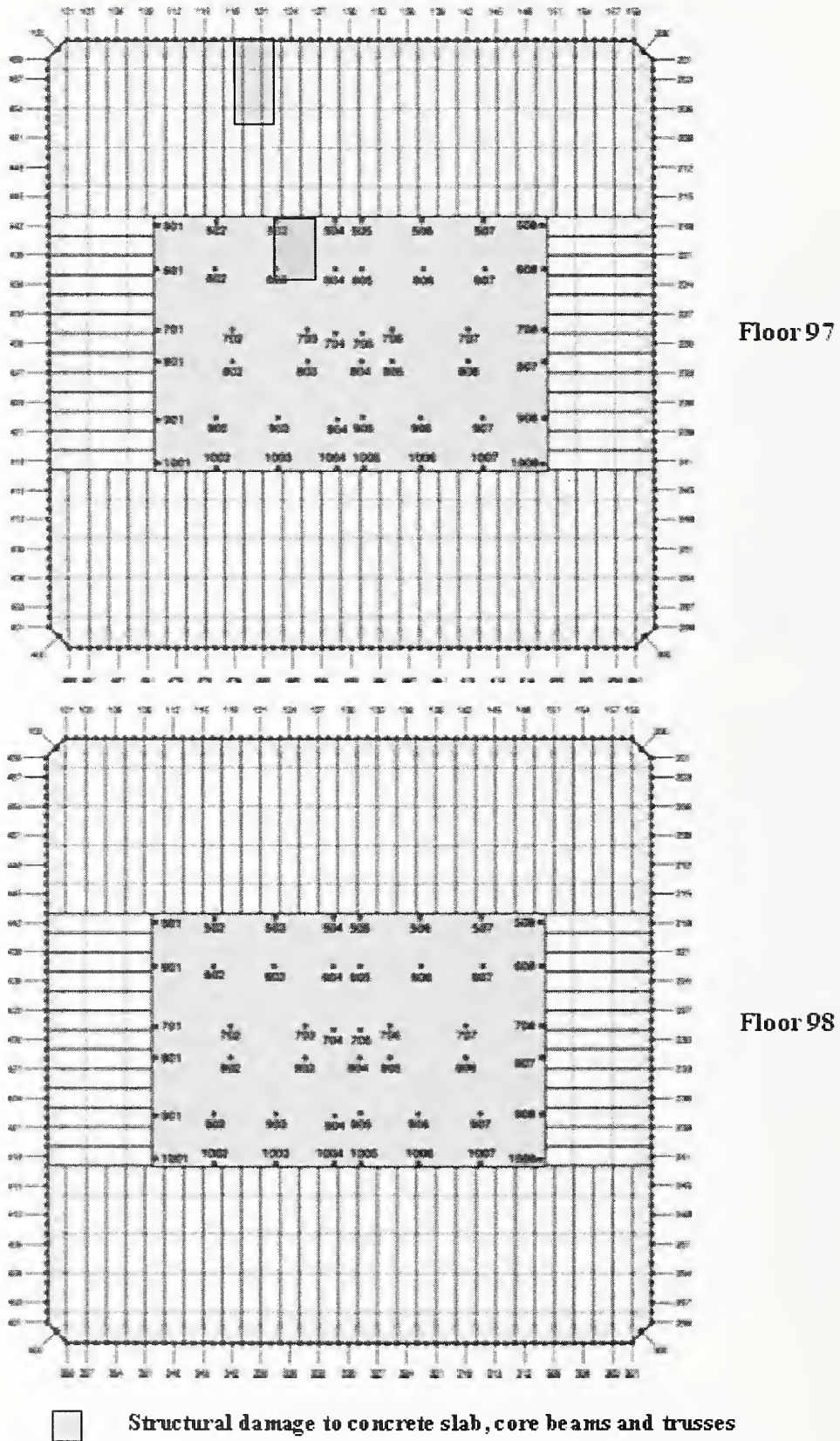


Figure A-6. WTC 1 Case A; aircraft impact damage to Structural Floors 97 and 98.

**WTC 1 CASE B<sub>1</sub> – THERMAL INSULATION AND PARTITION DAMAGE FOR OCCUPANCY FLOOR**

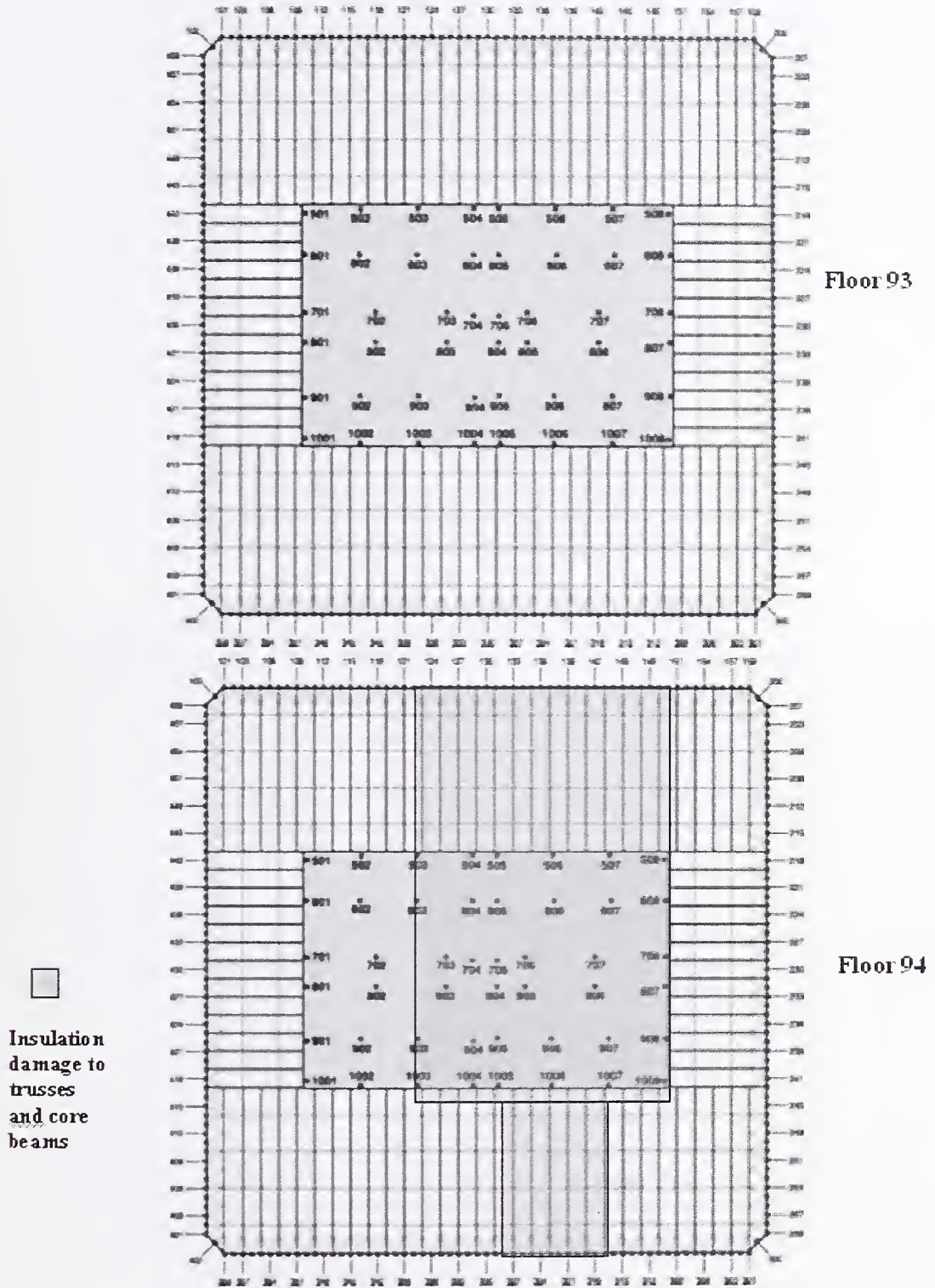


Figure A-7. WTC 1 Case B<sub>1</sub> aircraft impact damage to Structural Floor 93 and 94.

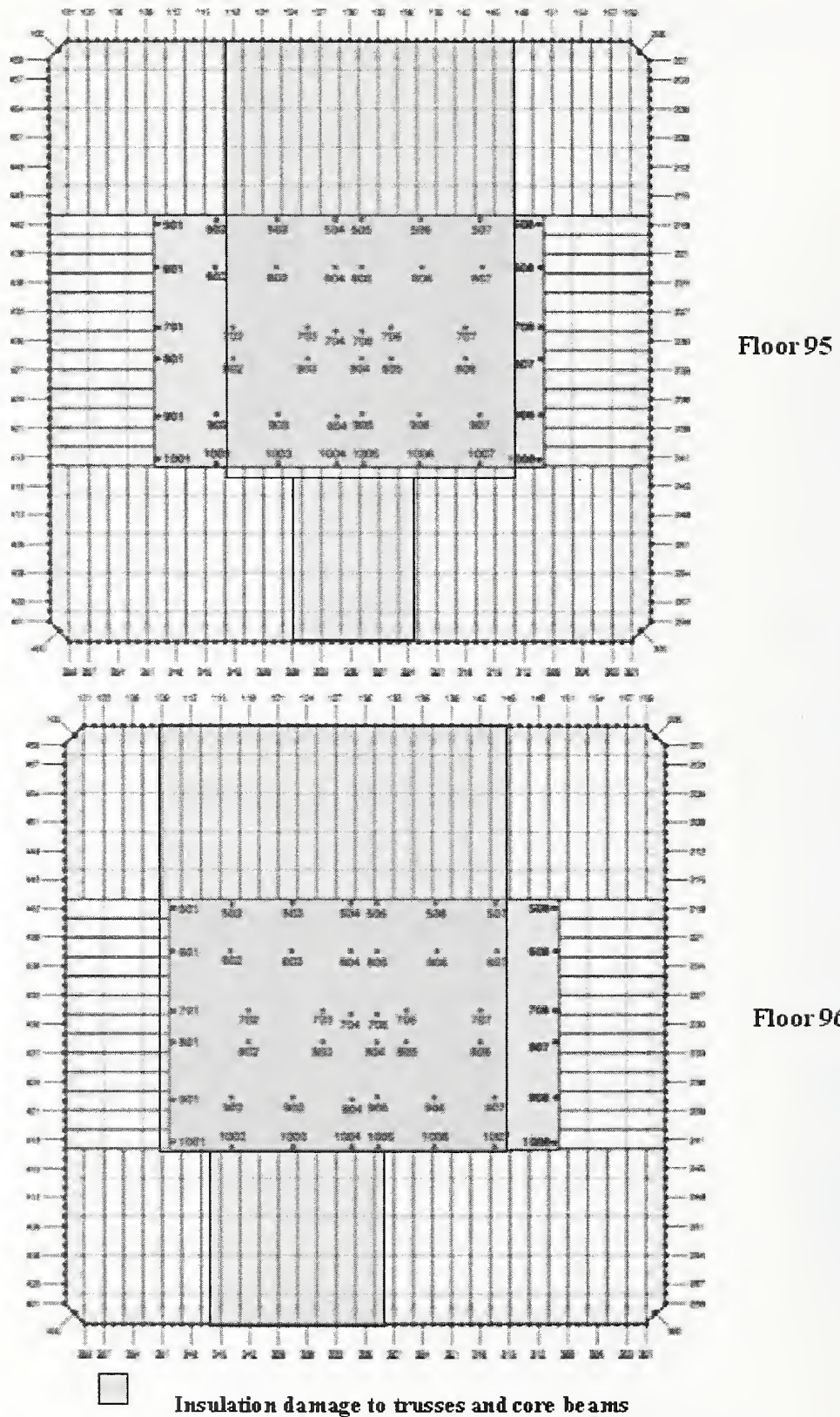


Figure A-8. WTC 1 Case B<sub>1</sub> aircraft impact damage to Structural Floors 95 and 96.

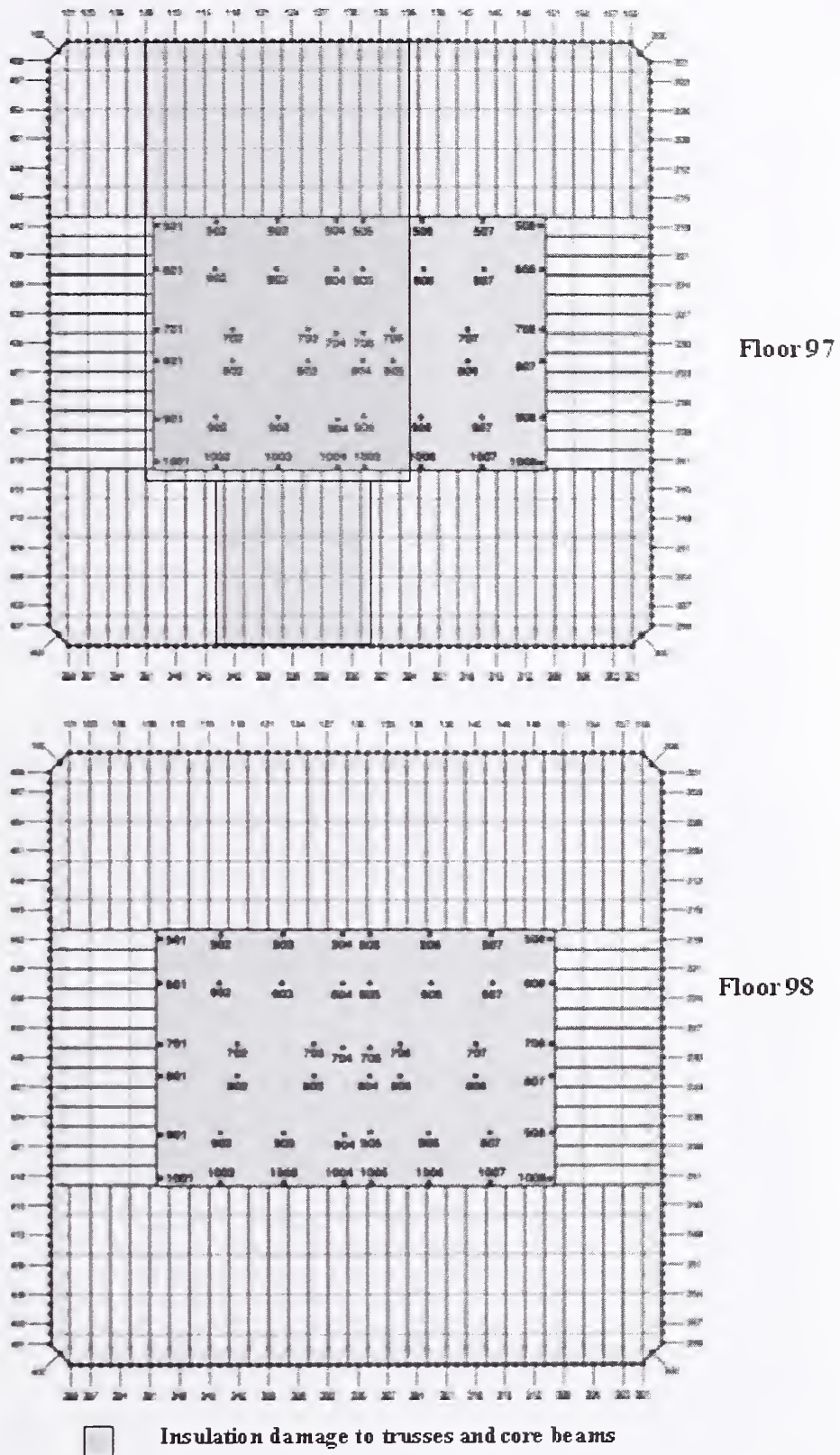


Figure A-9. WTC 1 Case B; aircraft impact damage to Structural Floors 97 and 98.

### WTC 1 CASE B<sub>1</sub> – DAMAGE FOR STRUCTURAL FLOOR

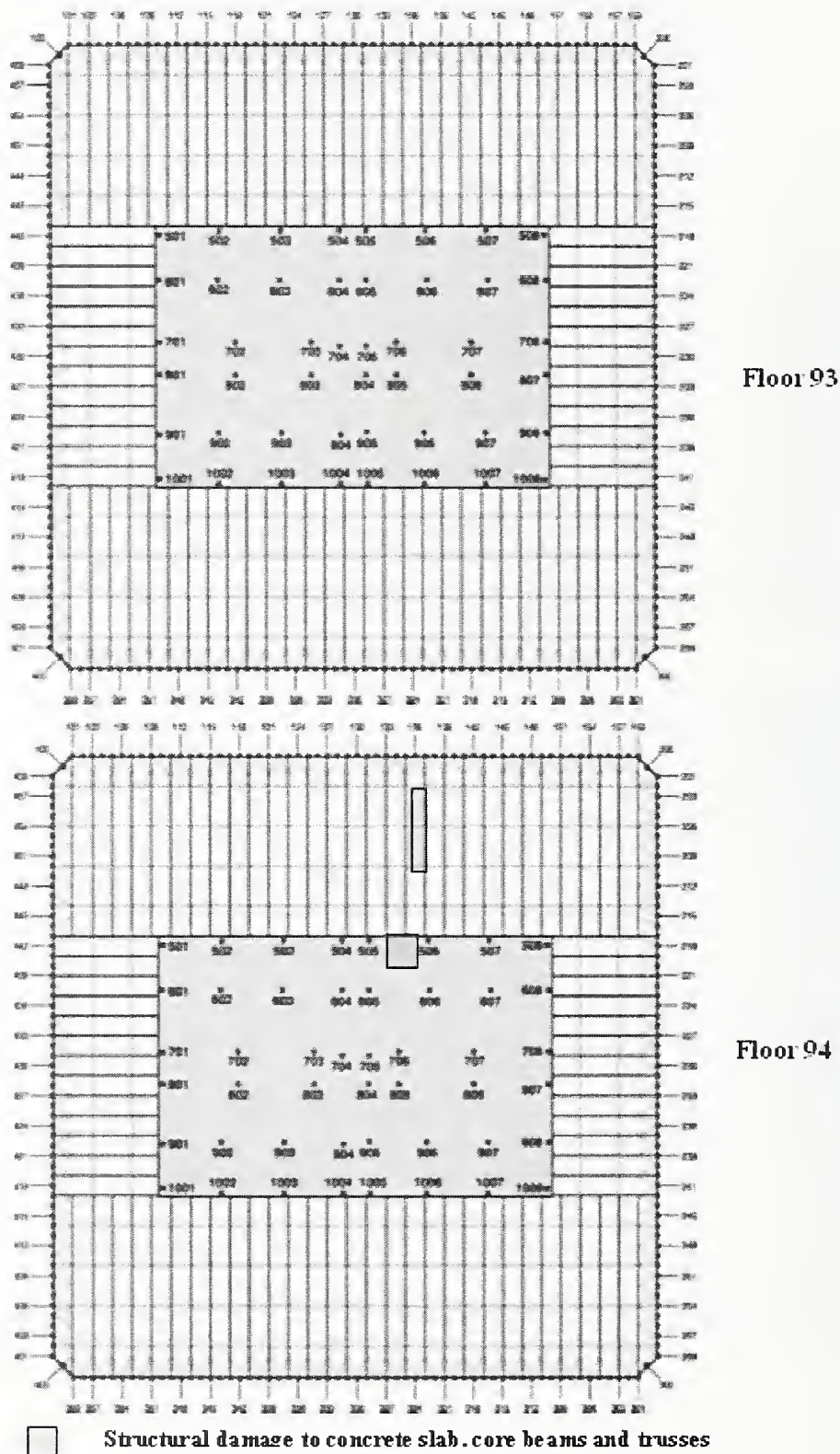


Figure A-10. WTC 1 Case B<sub>1</sub> aircraft impact damage to Structural Floor 93 and 94.

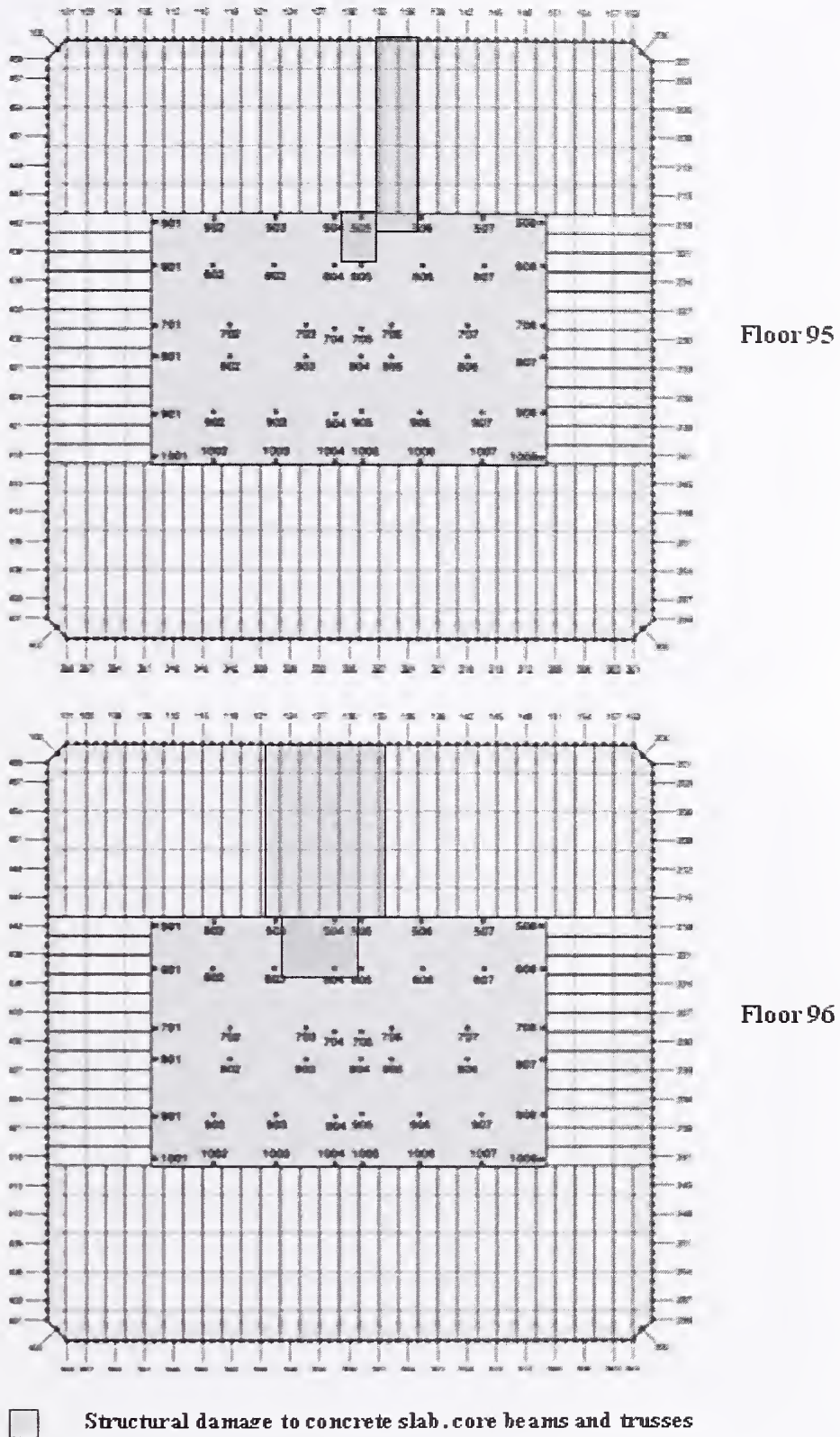
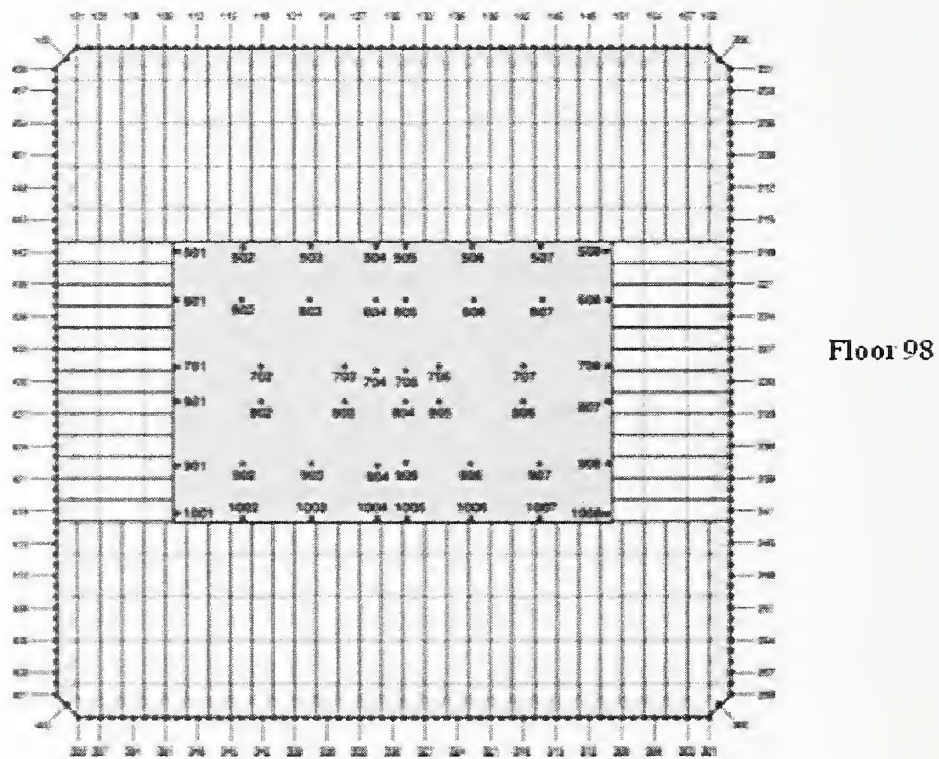
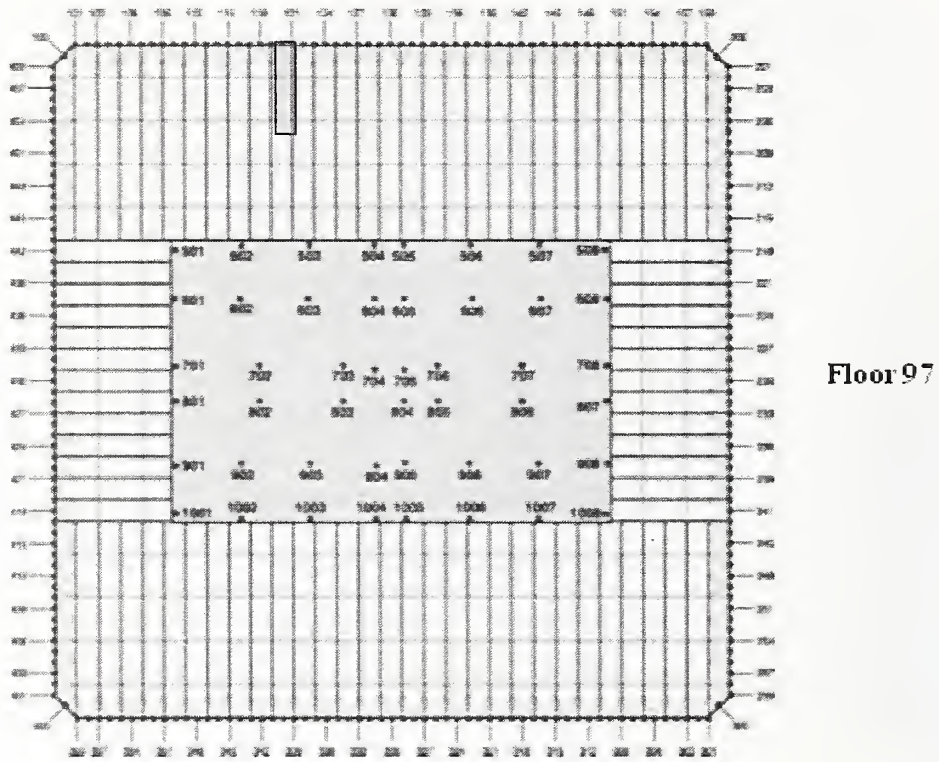


Figure A-11. WTC 1 Case B<sub>i</sub> aircraft impact damage to Structural Floors 95 and 96.



Structural damage to concrete slab, core beams and trusses

Figure A-12. WTC 1 Case B<sub>i</sub> aircraft impact damage to Structural Floors 97 and 98.

### WTC 2 CASE C<sub>1</sub> – THERMAL INSULATION AND OCCUPANCY DAMAGE FOR OCCUPANCY FLOOR

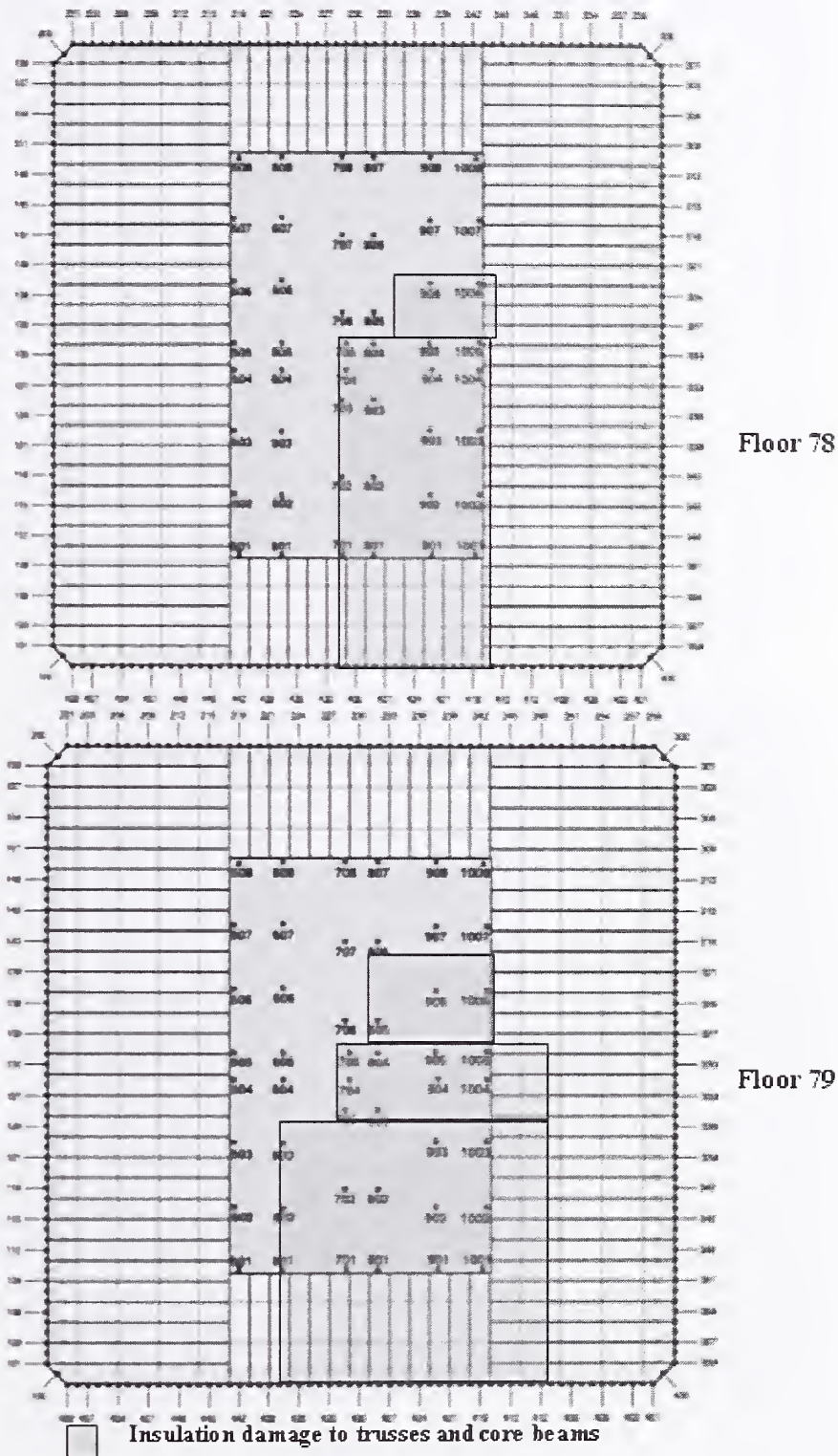


Figure A-13. WTC 2 Case C<sub>1</sub> aircraft impact damage to Structural Floors 78 and 79.

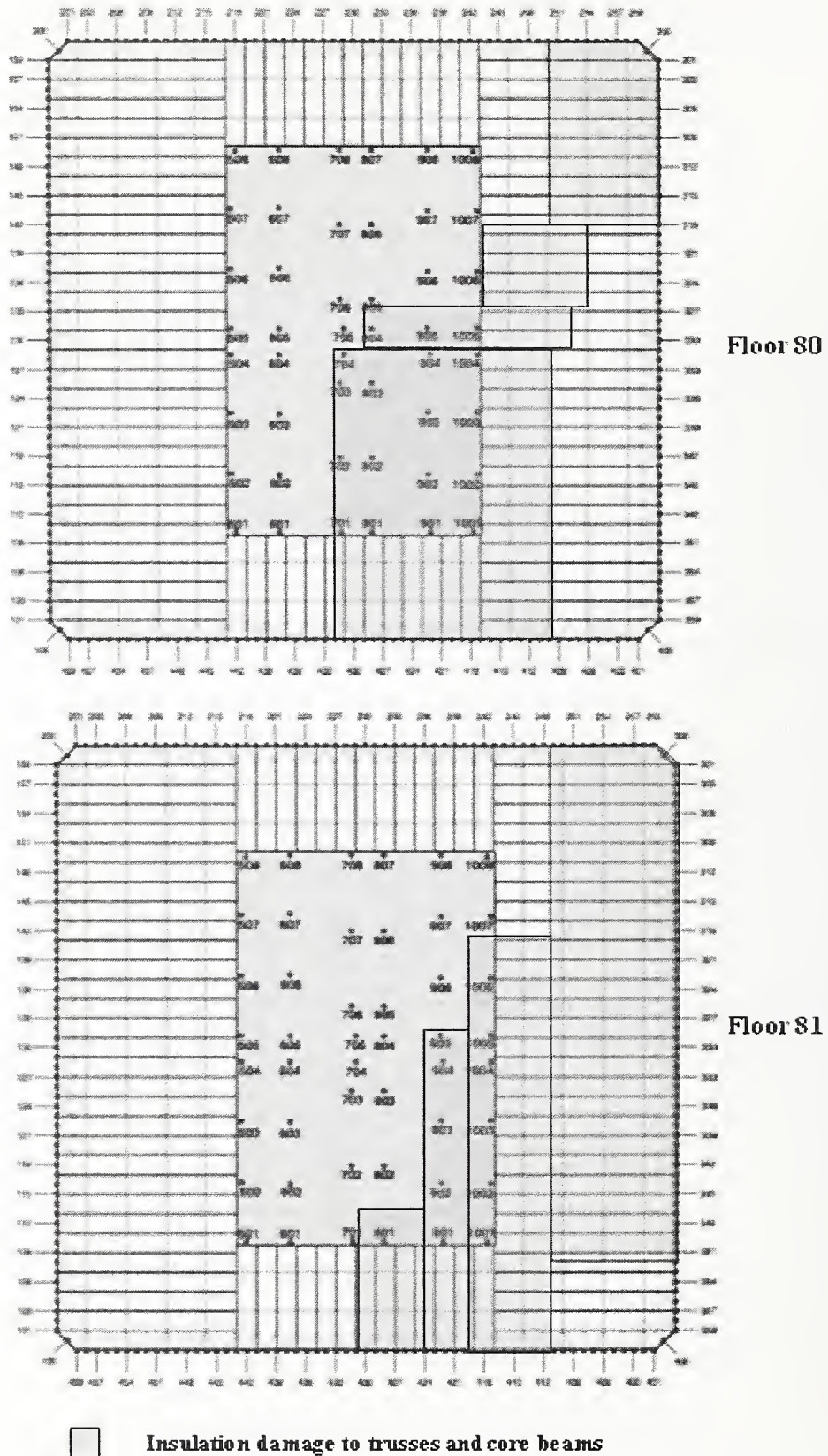


Figure A-14. WTC 2 Case C; aircraft impact damage to Structural Floors 80 and 81.

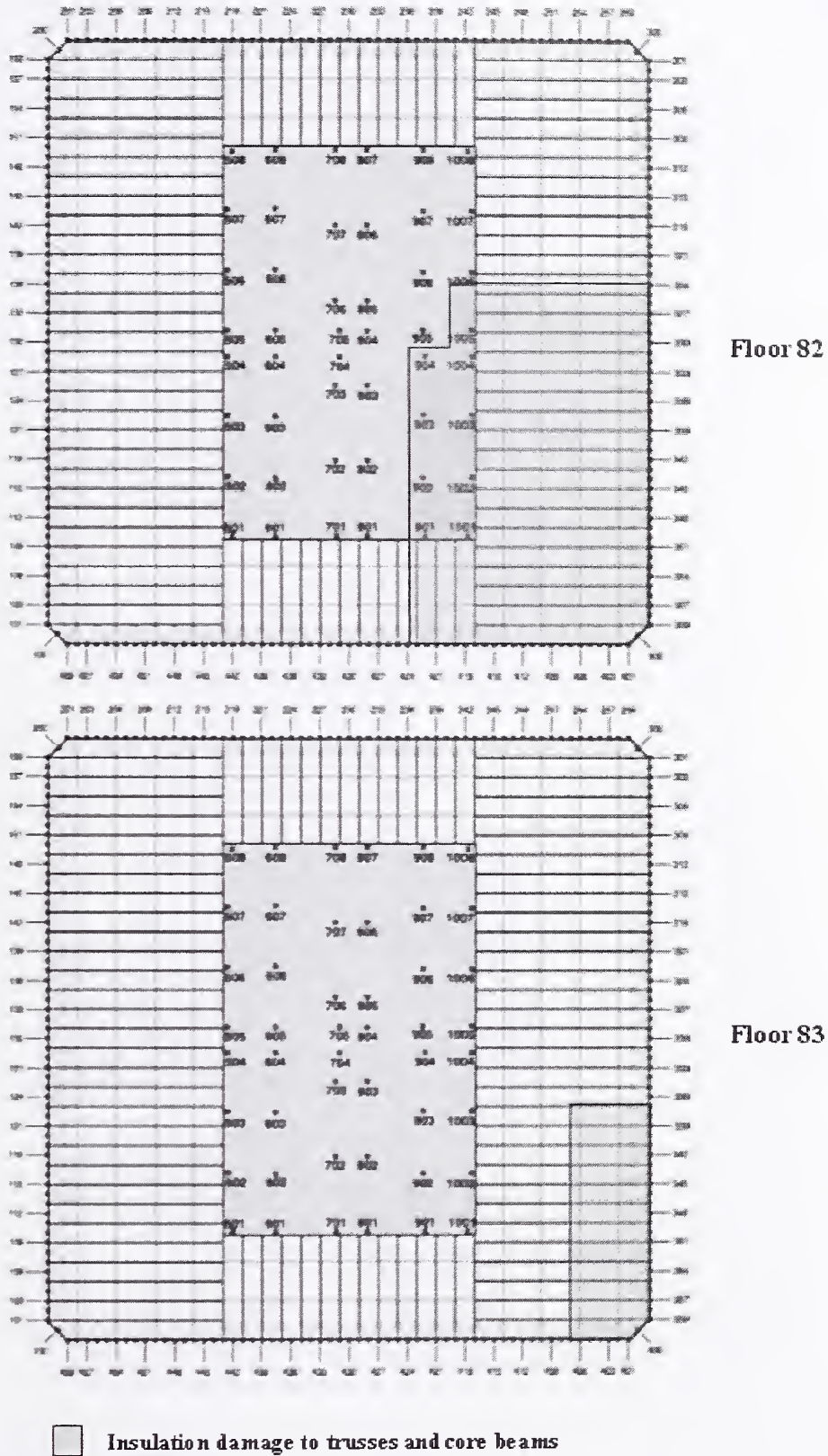


Figure A-15. WTC 2 Case C<sub>i</sub> aircraft impact damage to Structural Floors 82 and 83.

### WTC 2 CASE C<sub>1</sub> – DAMAGE FOR STRUCTURAL FLOOR

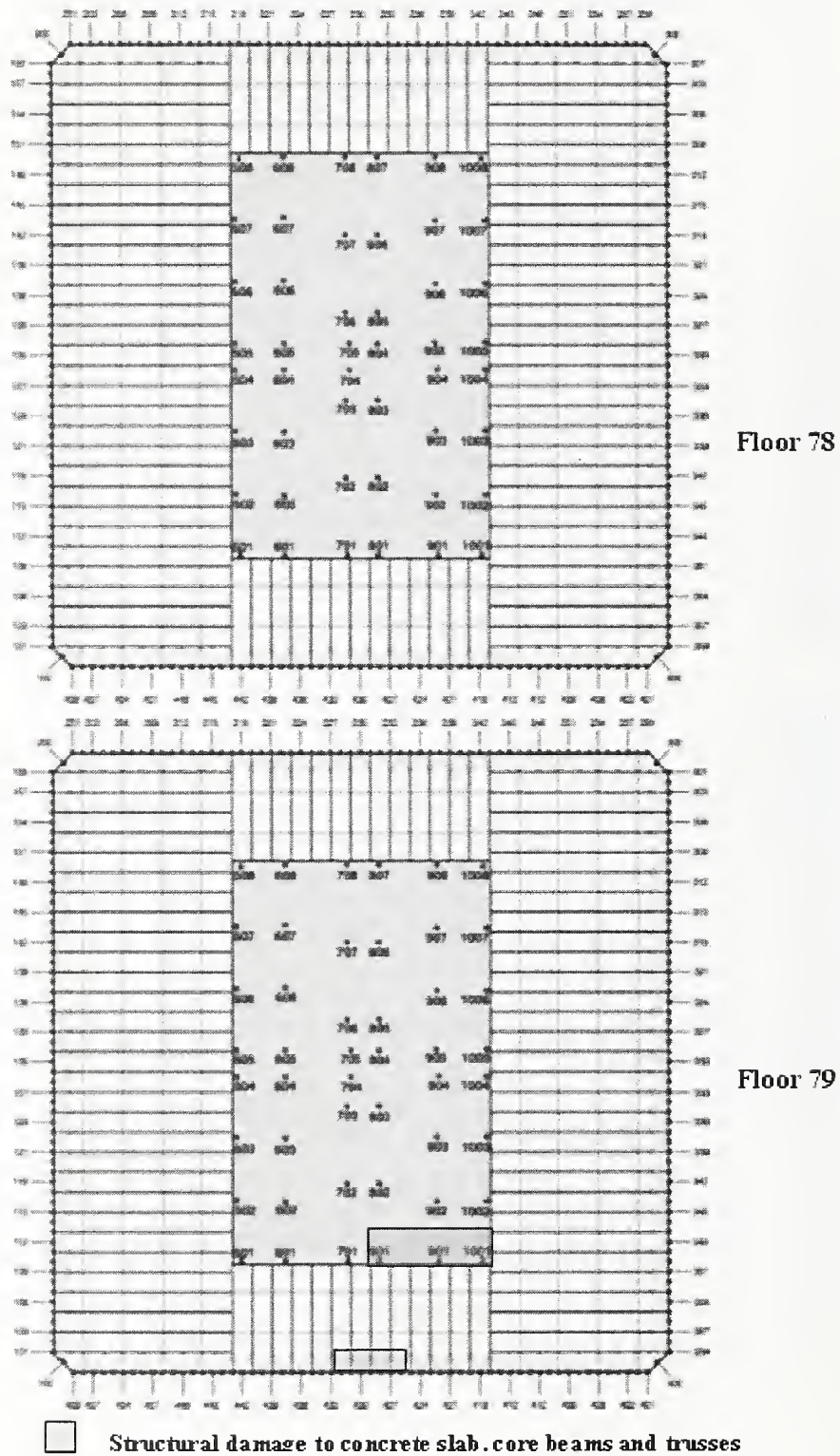
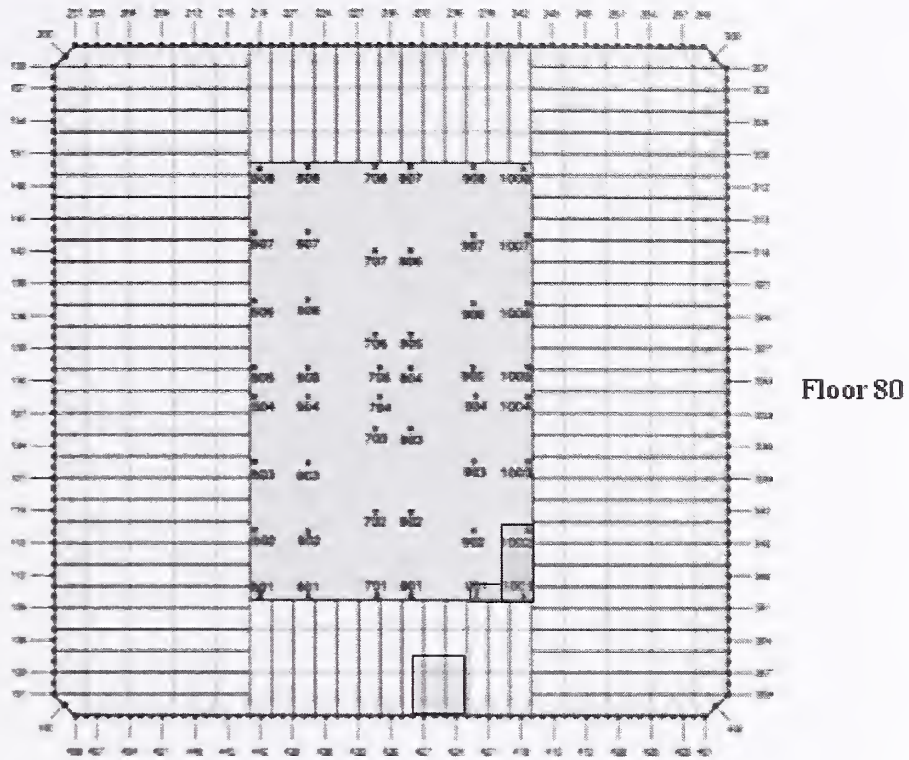
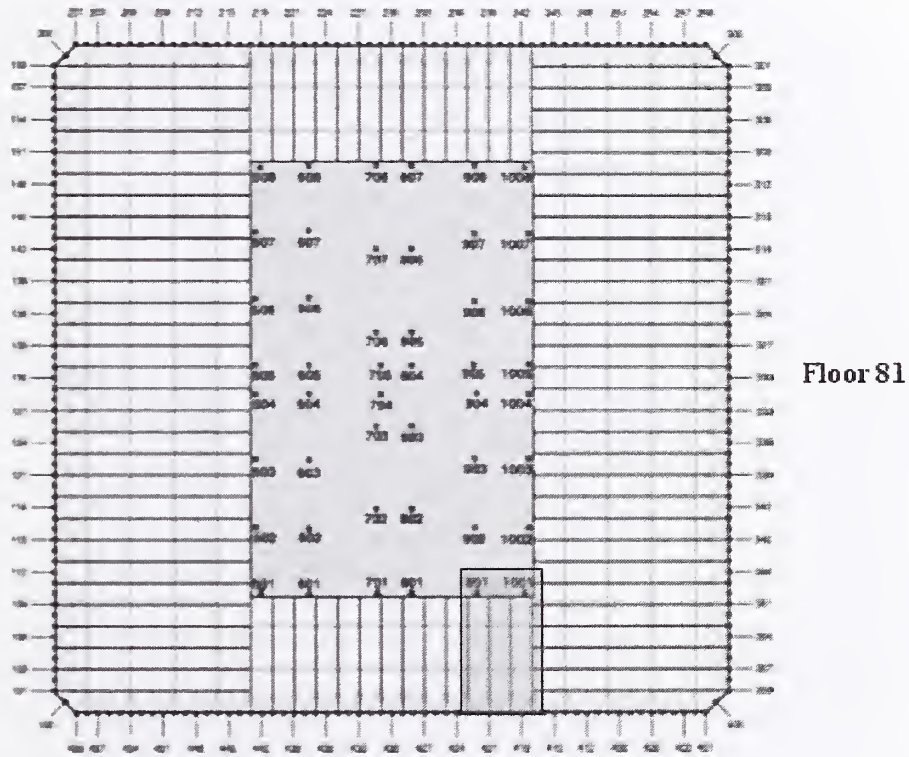


Figure A-16. WTC 2 Case C<sub>1</sub> aircraft impact damage to Structural Floors 78 and 79.



Floor 80



Floor 81


 Structural damage to concrete slab, core beams and trusses

Figure A-17. WTC 2 Case C; aircraft impact damage to Structural Floors 80 and 81.

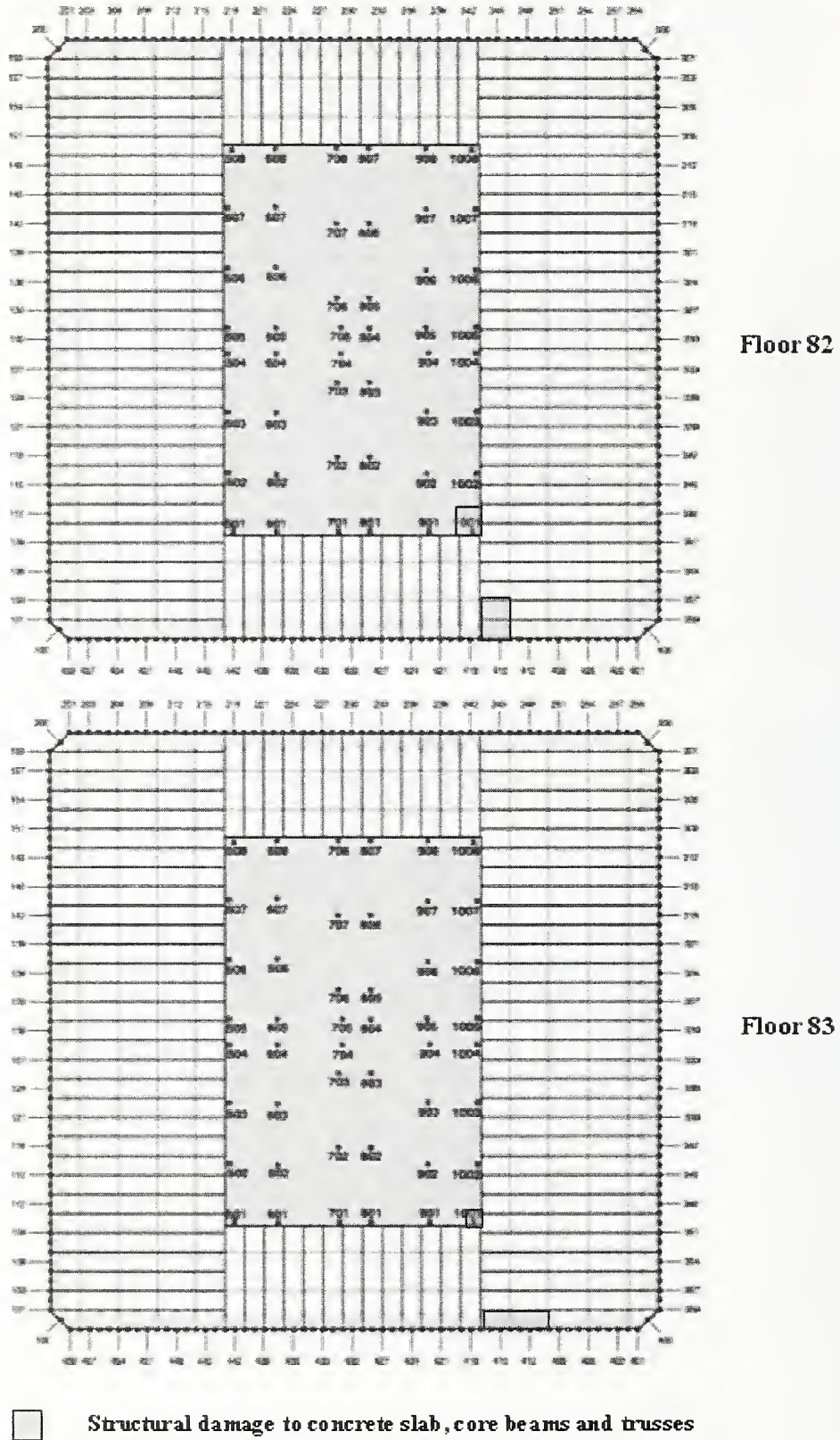


Figure A-18. WTC 2 Case C; aircraft impact damage to Structural Floors 82 and 83.

### WTC 2 CASE D<sub>1</sub> – THERMAL INSULATION AND PARTITION DAMAGE FOR OCCUPANCY FLOOR

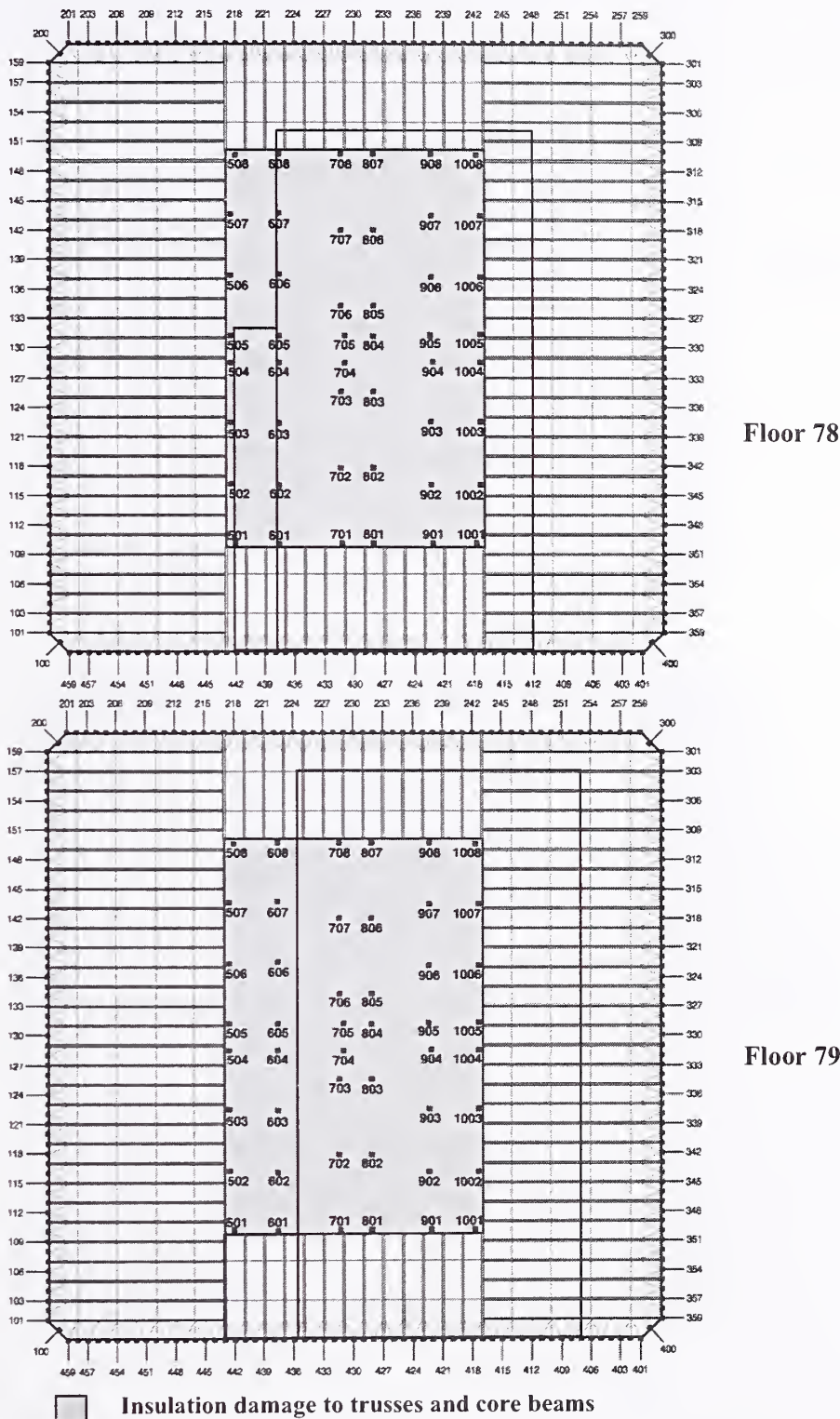


Figure A-19. WTC 2 Case D<sub>1</sub> aircraft impact damage to Structural Floors 78 and 79.

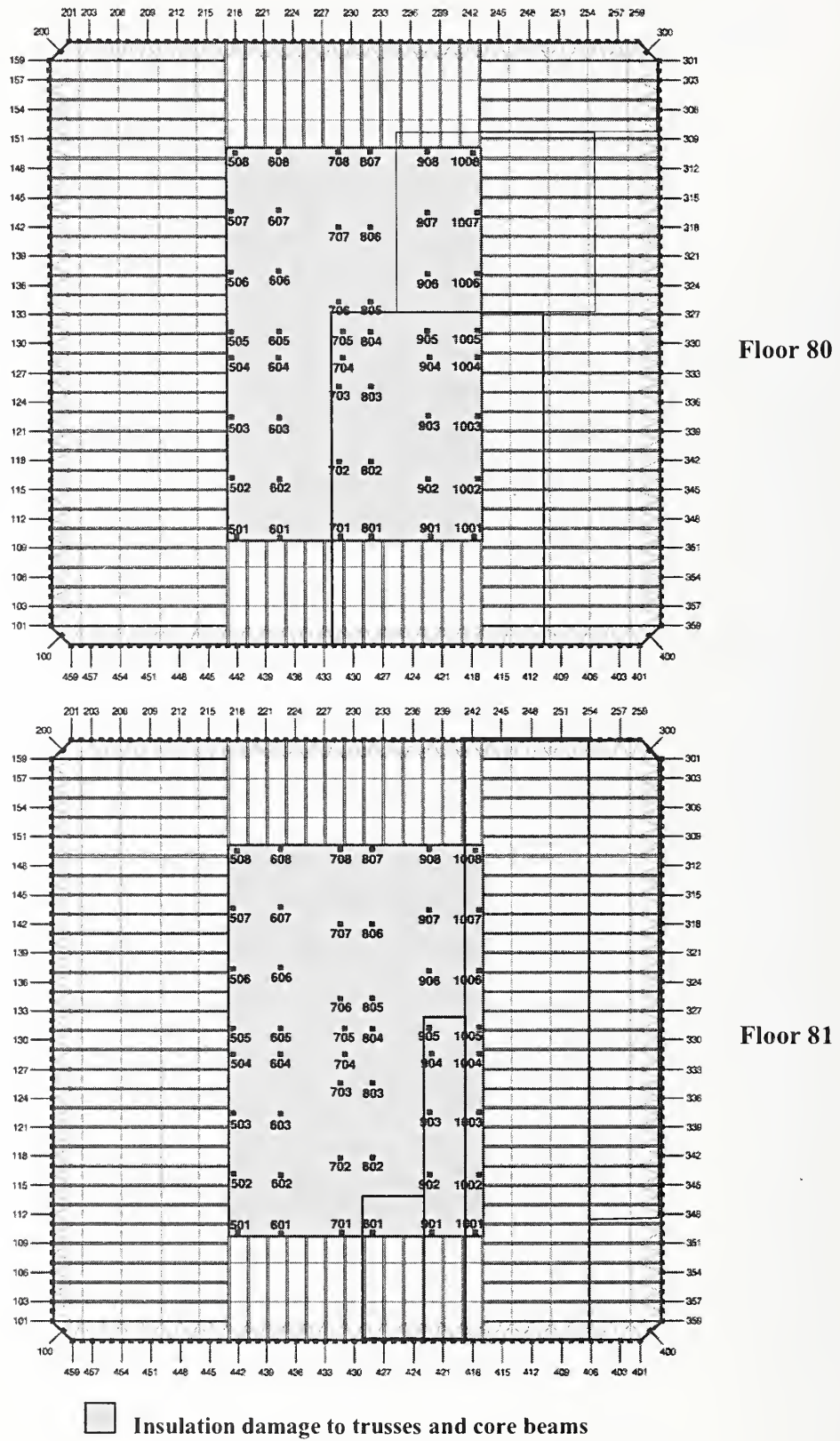


Figure A-20. WTC 2 Case D; aircraft impact damage to Structural Floors 80 and 81.

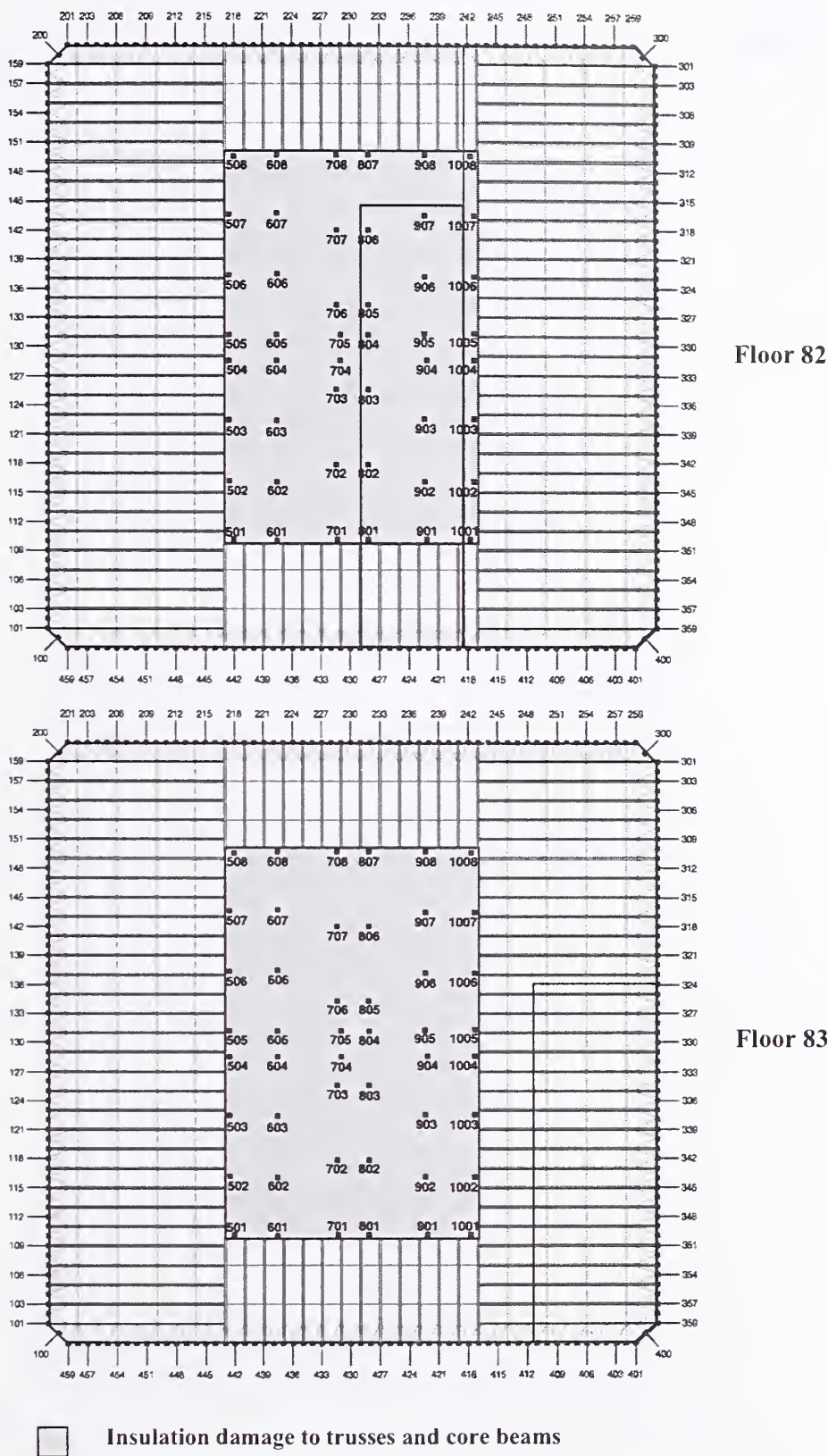


Figure A-21. WTC 2 Case D; aircraft impact damage to Structural Floors 82 and 83.

### WTC 2 CASE D<sub>1</sub> – DAMAGE FOR STRUCTURAL FLOOR

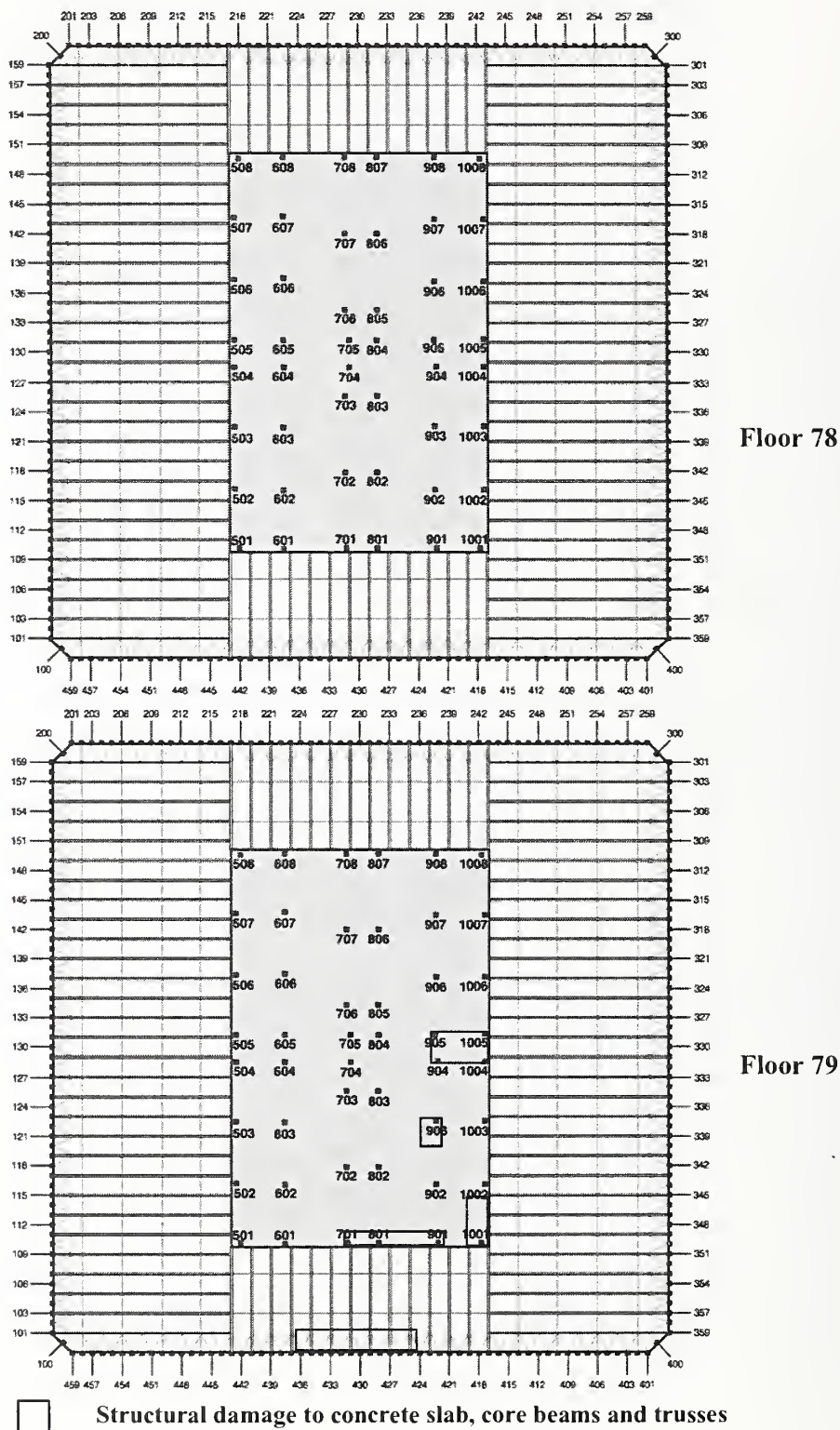


Figure A-22. WTC 2 Case D<sub>1</sub> aircraft impact damage to Structural Floors 78 and 79.

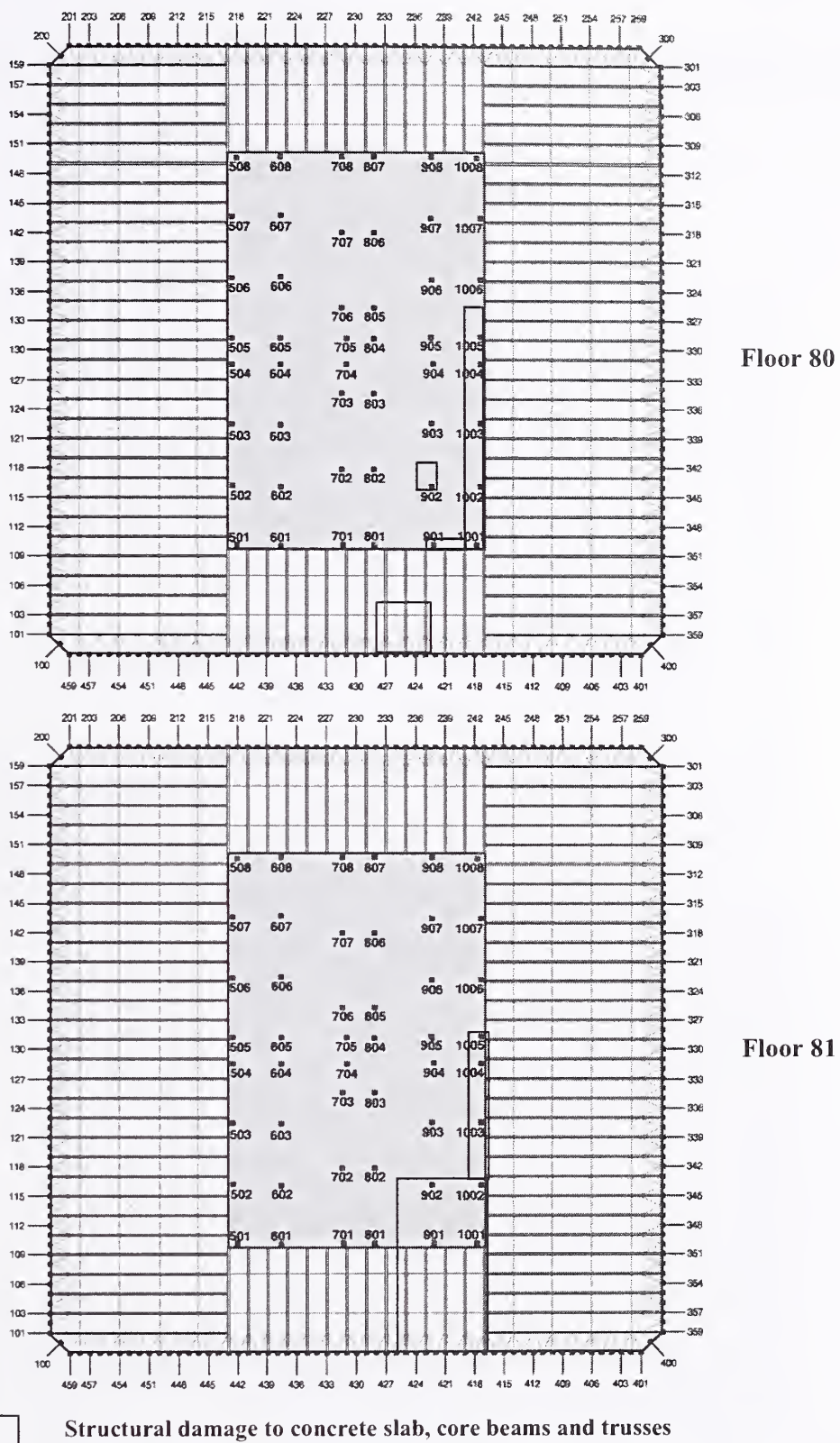
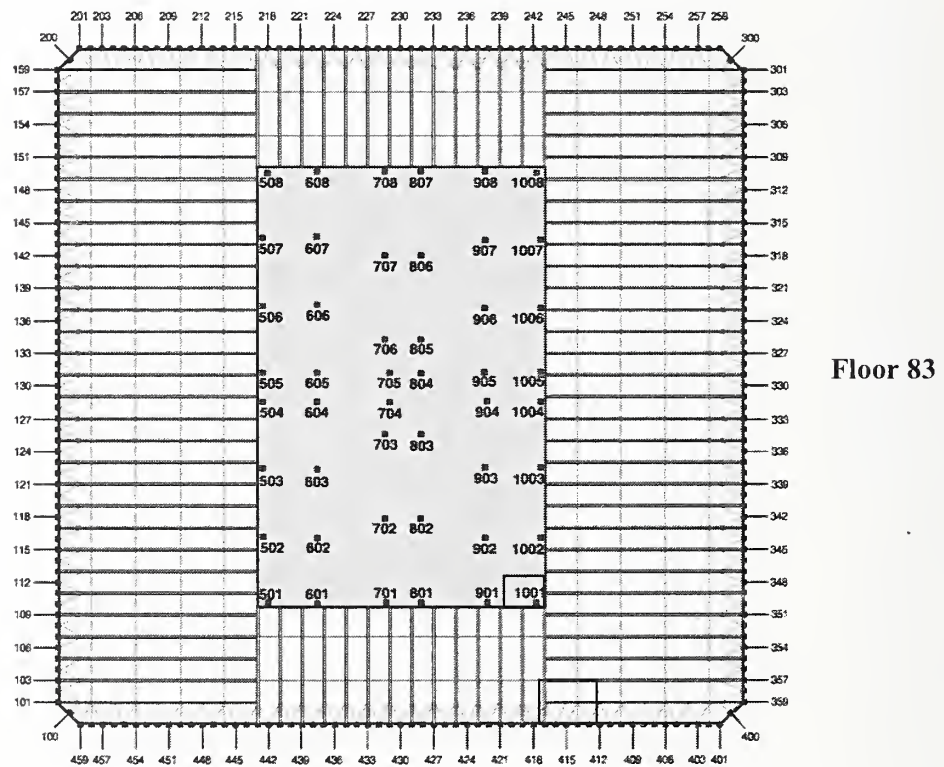
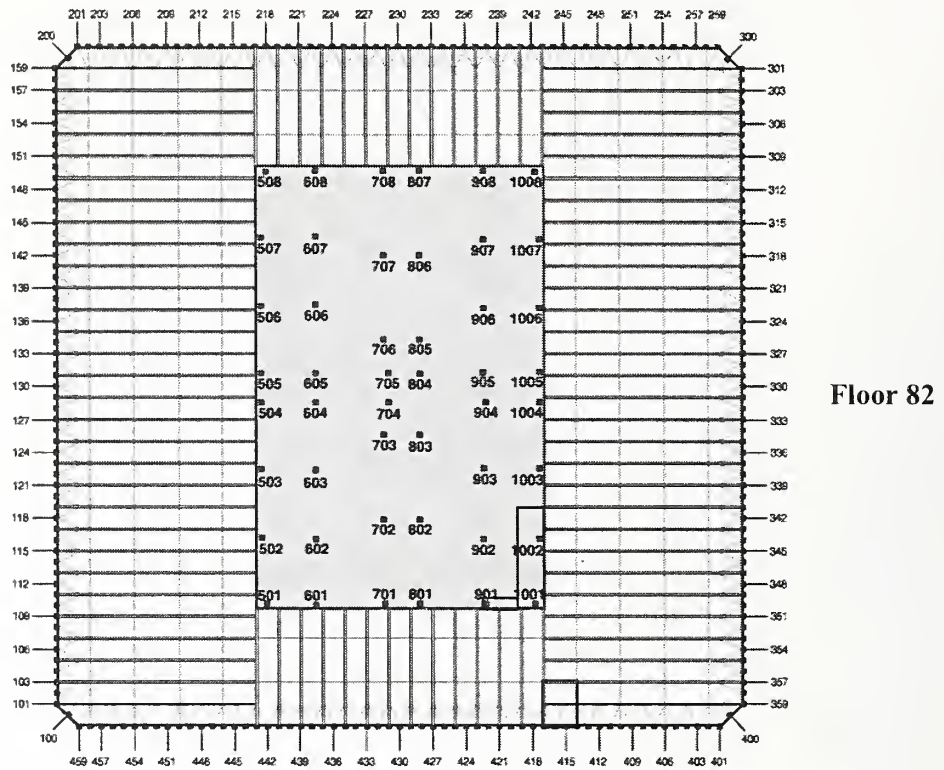


Figure A-23. WTC 2 Case D; aircraft impact damage to Structural Floors 80 and 81.



 Structural damage to concrete slab, core beams and trusses

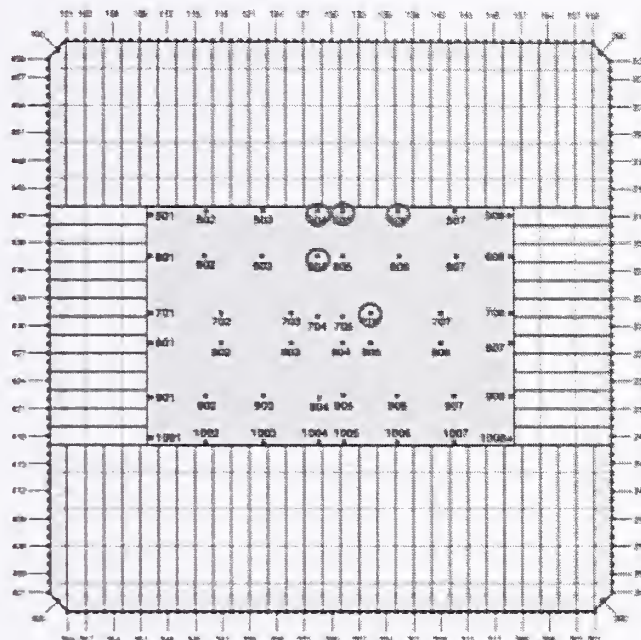
Figure A-24. WTC 2 Case D; aircraft impact damage to Structural Floors 82 and 83.

# Appendix B

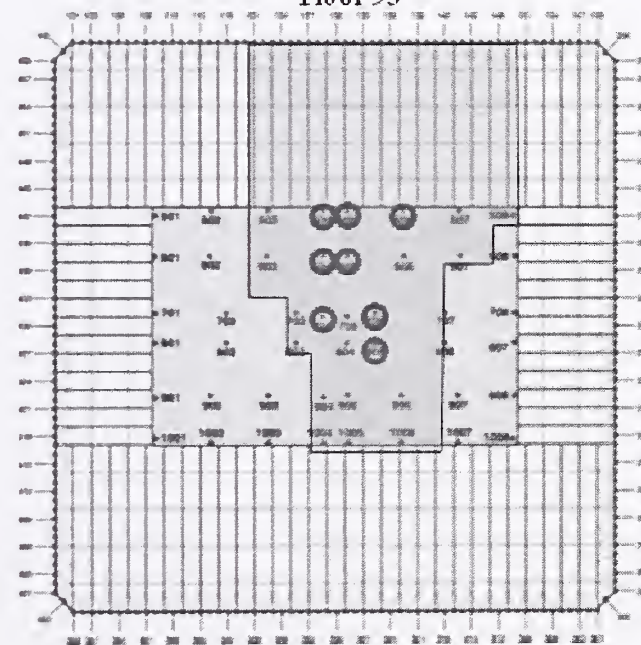
## SUMMARY OF AIRCRAFT IMPACT DAMAGE FOR FINAL CASES A TO D

### WTC 1 CASE A - OCCUPANCY FLOOR GRAPHICS

- Severe Floor Damage
- Floor insulation
- Column Damage
- Severe
- Heavy damage
- Moderate damage
- Light damage



Floor 93



Floor 94

Figure B-1. WTC 1 Case A aircraft impact damage to Occupancy Floors 93 and 94.

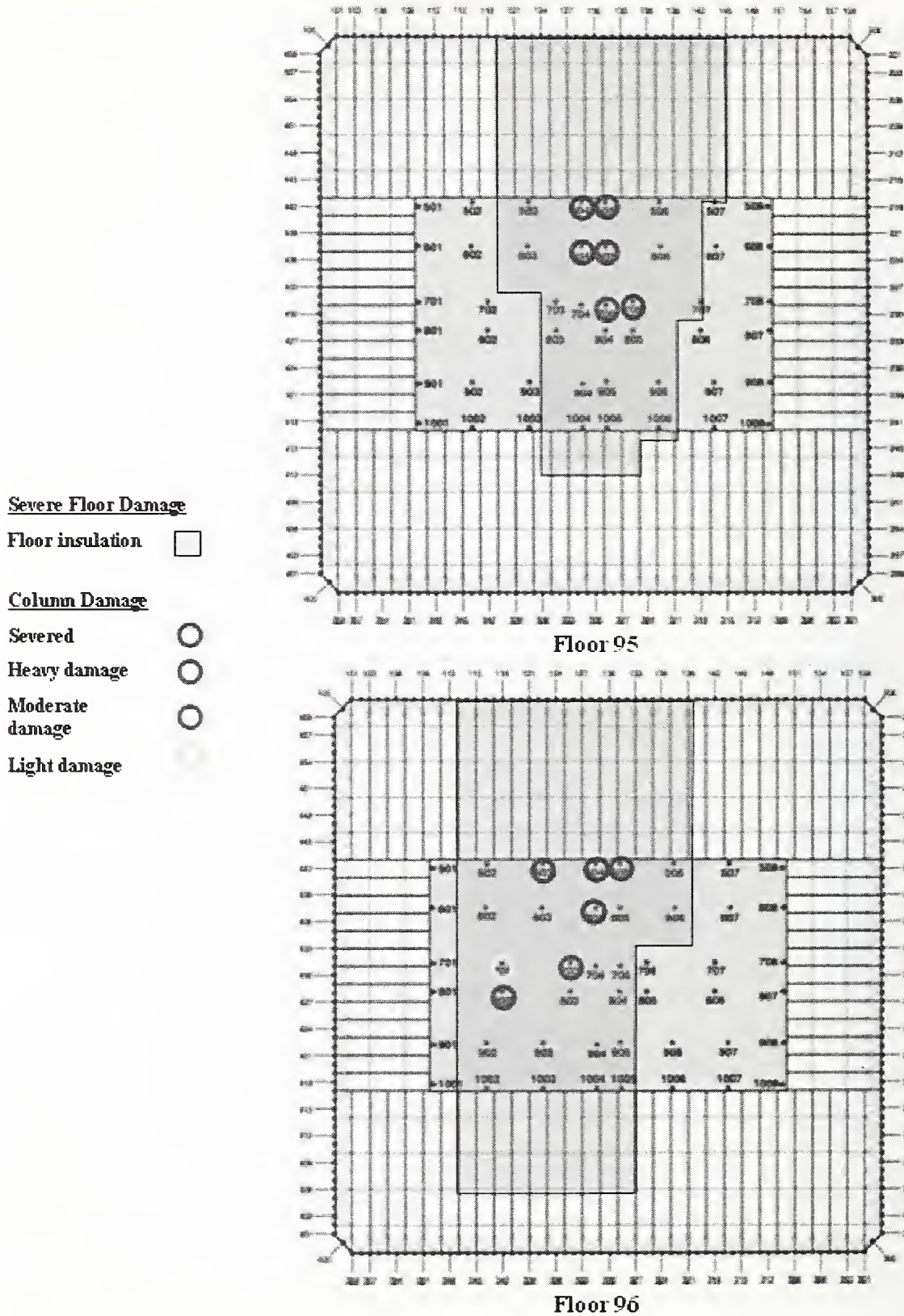


Figure B-2. WTC 1 Case A aircraft impact damage to Occupancy Floors 95 and 96.

Severe Floor Damage

Floor insulation

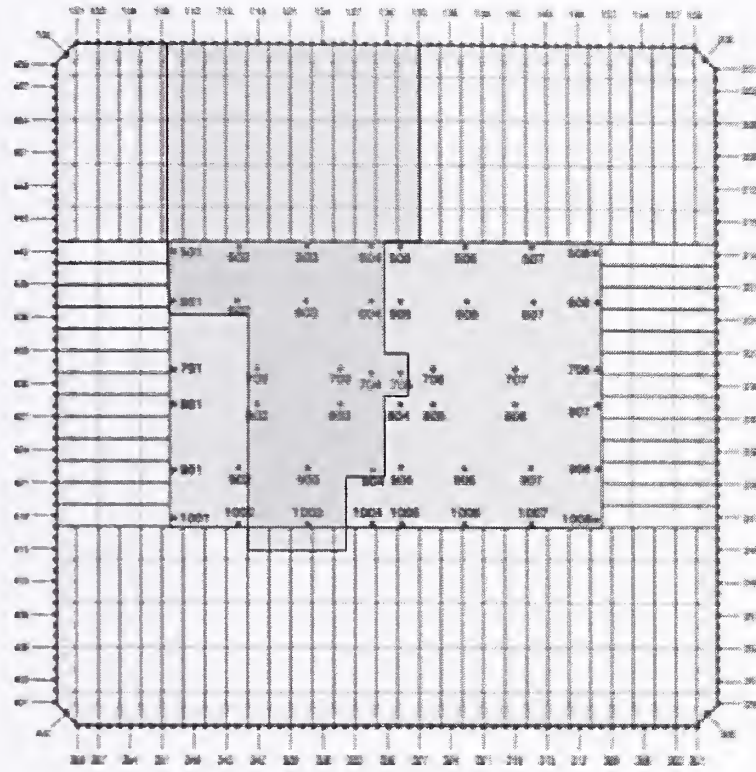
Column Damage

Severed

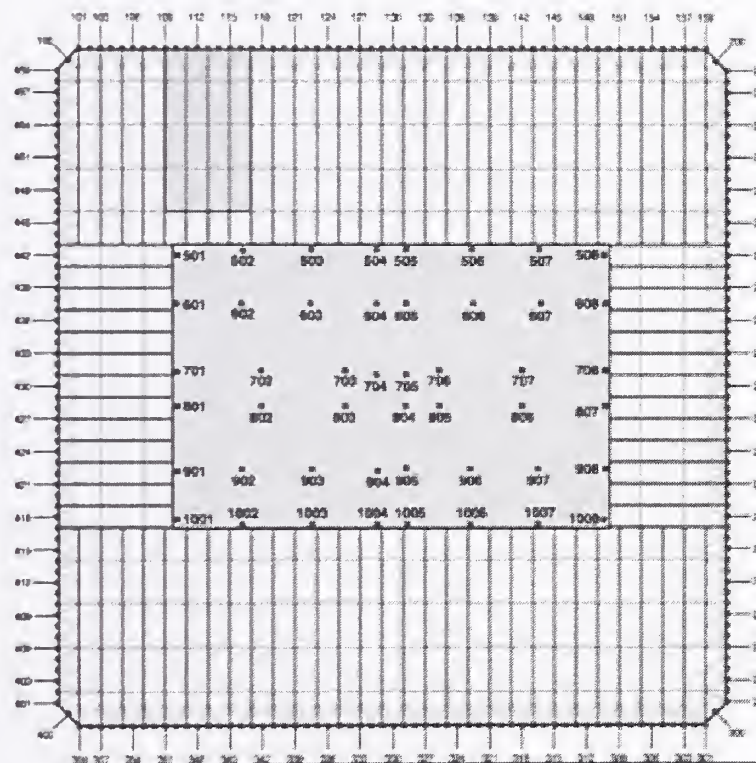
Heavy damage

Moderate damage

Light damage



Floor 97



Floor 98

Figure B-3. WTC 1 Case A aircraft impact damage to Occupancy Floors 97 and 98.

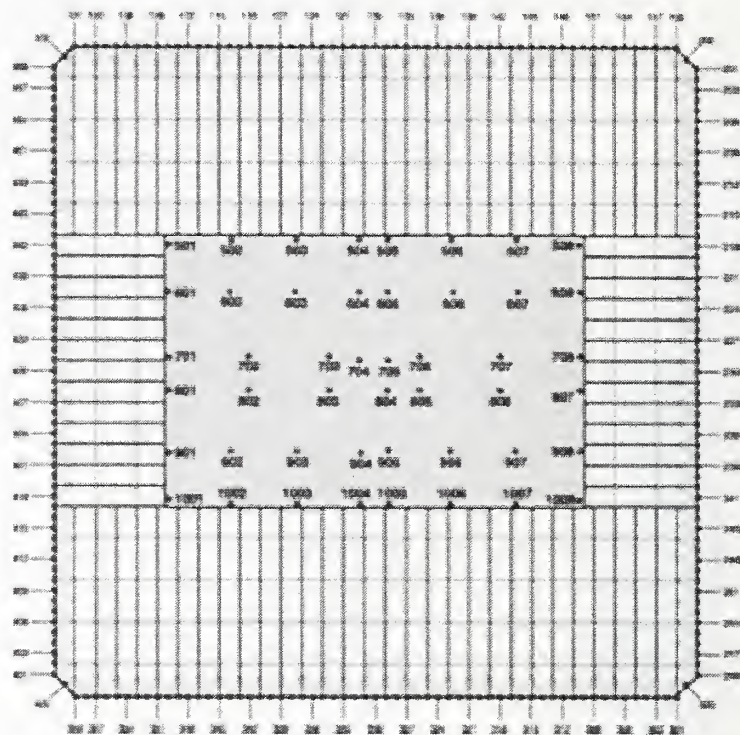
## WTC 1 CASE A - STRUCTURAL FLOOR GRAPHICS

Severe Floor Damage

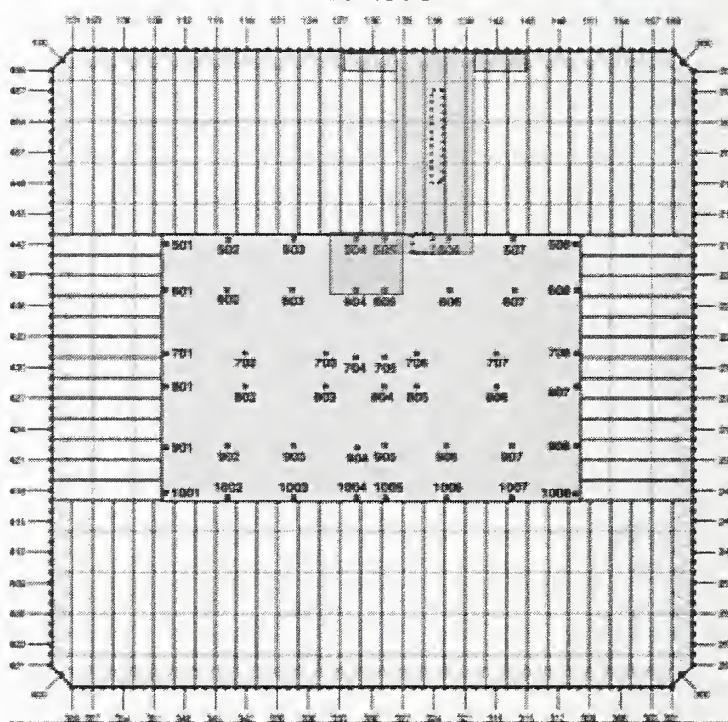
Floor system structural damage



Floor system removed



Floor 93



Floor 94

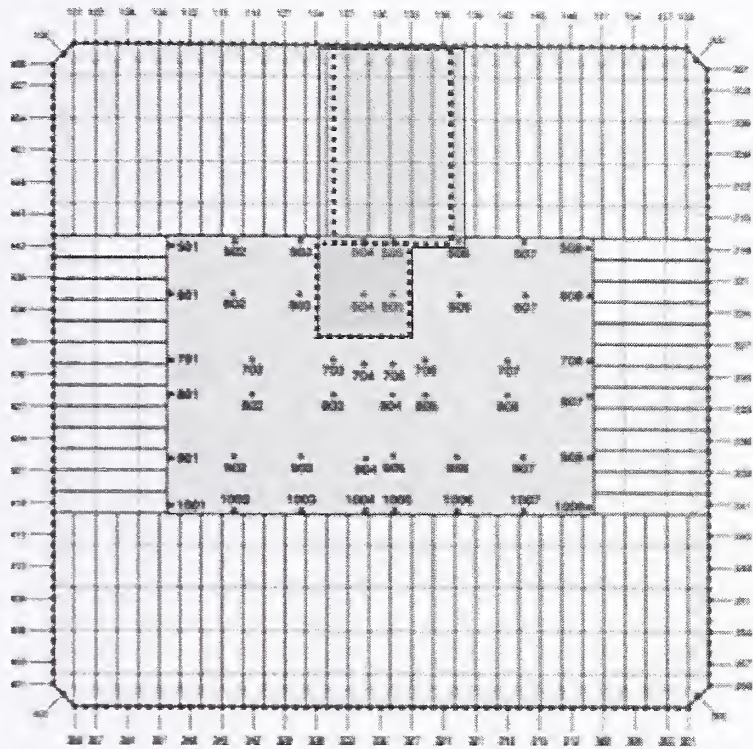
Figure B-4. WTC 1 Case A aircraft impact damage to Structural Floors 93 and 94.

Severe Floor Damage

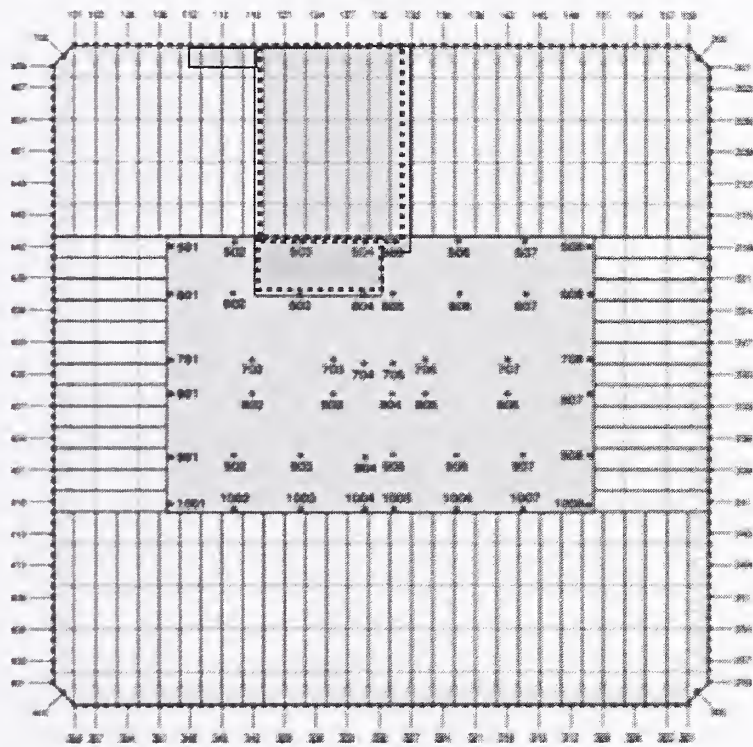
Floor system structural damage



Floor system removed



Floor 95



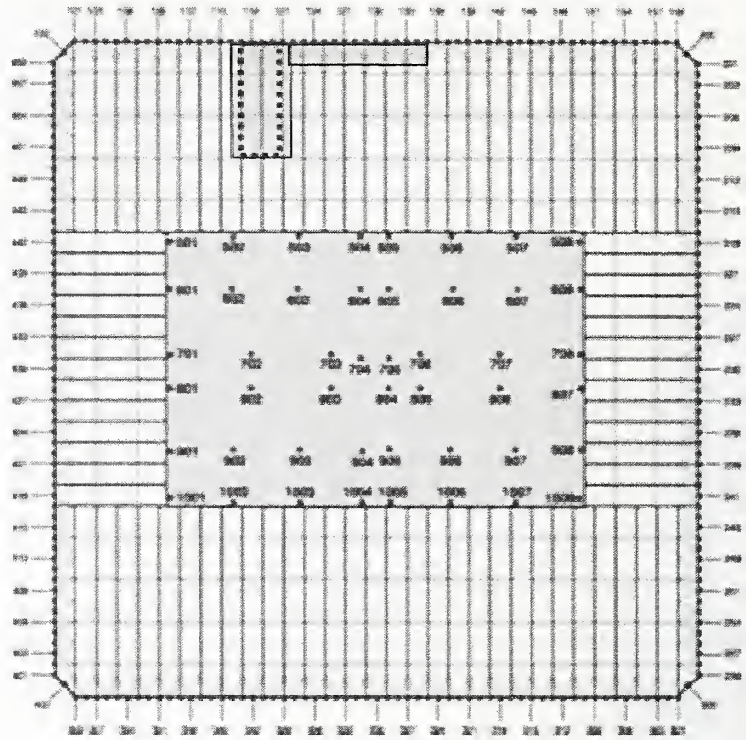
Floor 96

Figure B-5. WTC 1 Case A aircraft impact damage to Structural Floors 95 and 96.

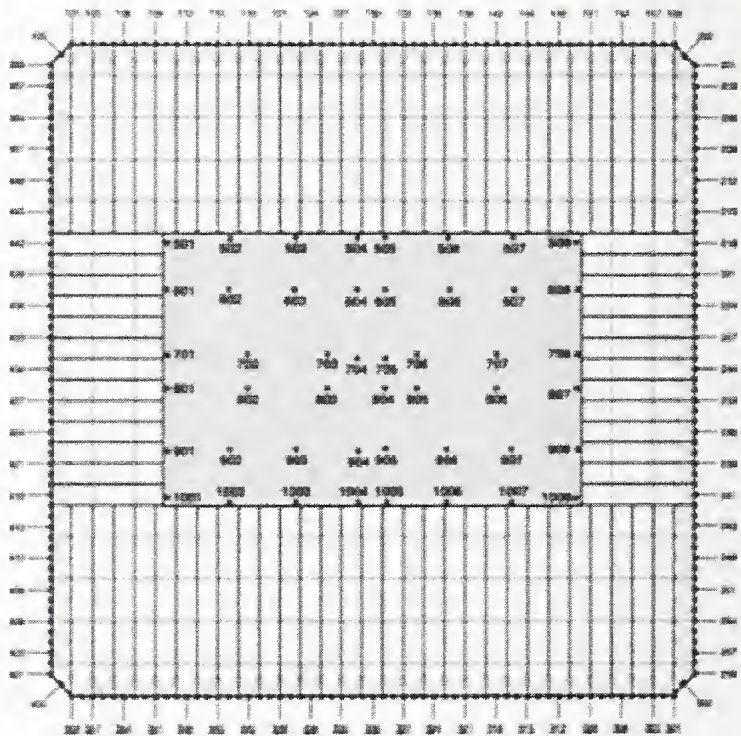
**Severe Floor Damage**

**Floor system structural damage**

**Floor system removed**



**Floor 97**



**Floor 98**

**Figure B-6. WTC 1 Case A aircraft impact damage to Structural Floors 97 and 98.**

WTC 1 CASE B - OCCUPANCY FLOOR GRAPHICS

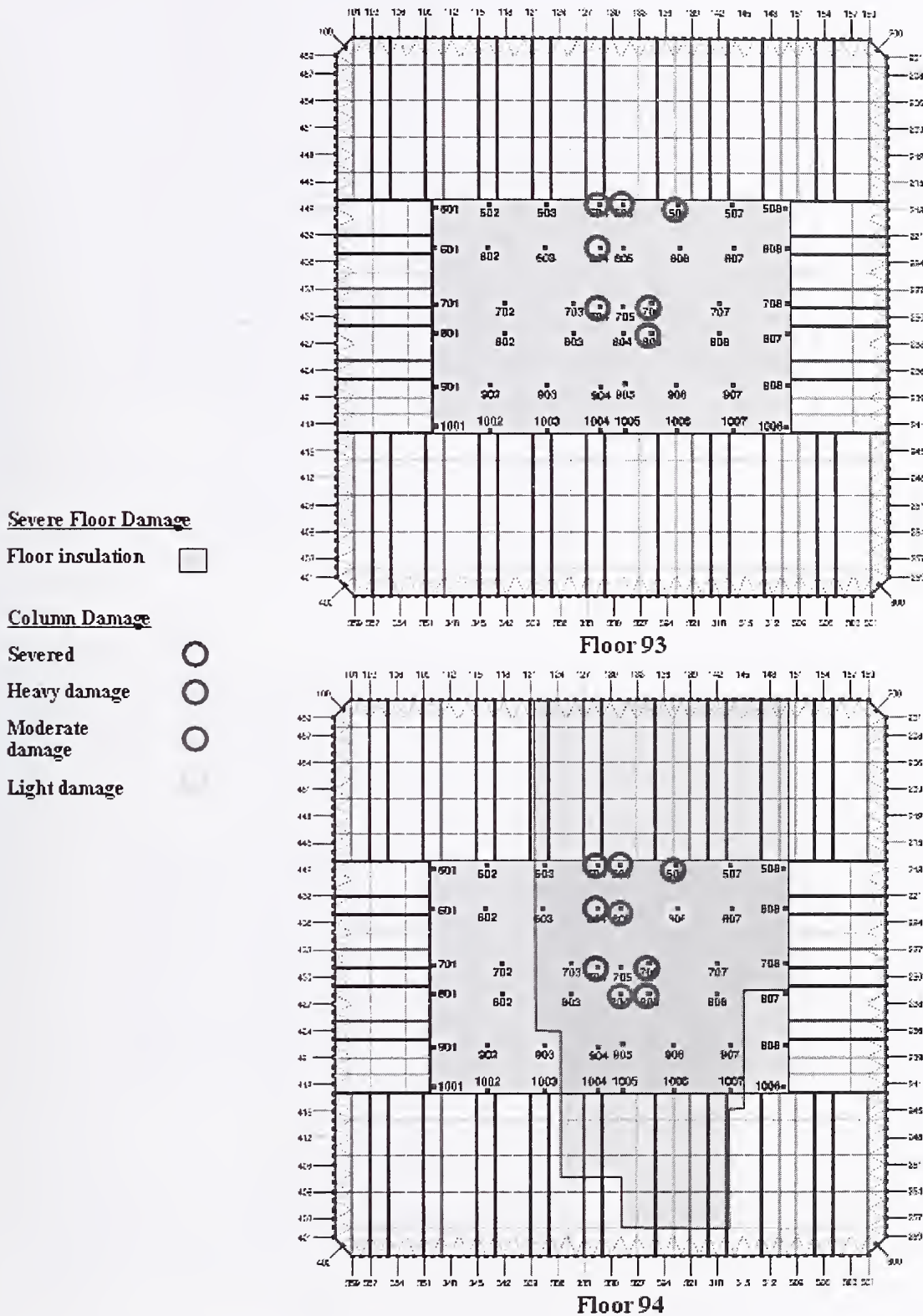


Figure B-7. WTC 1 Case B aircraft impact damage to Occupancy Floors 93 and 94.

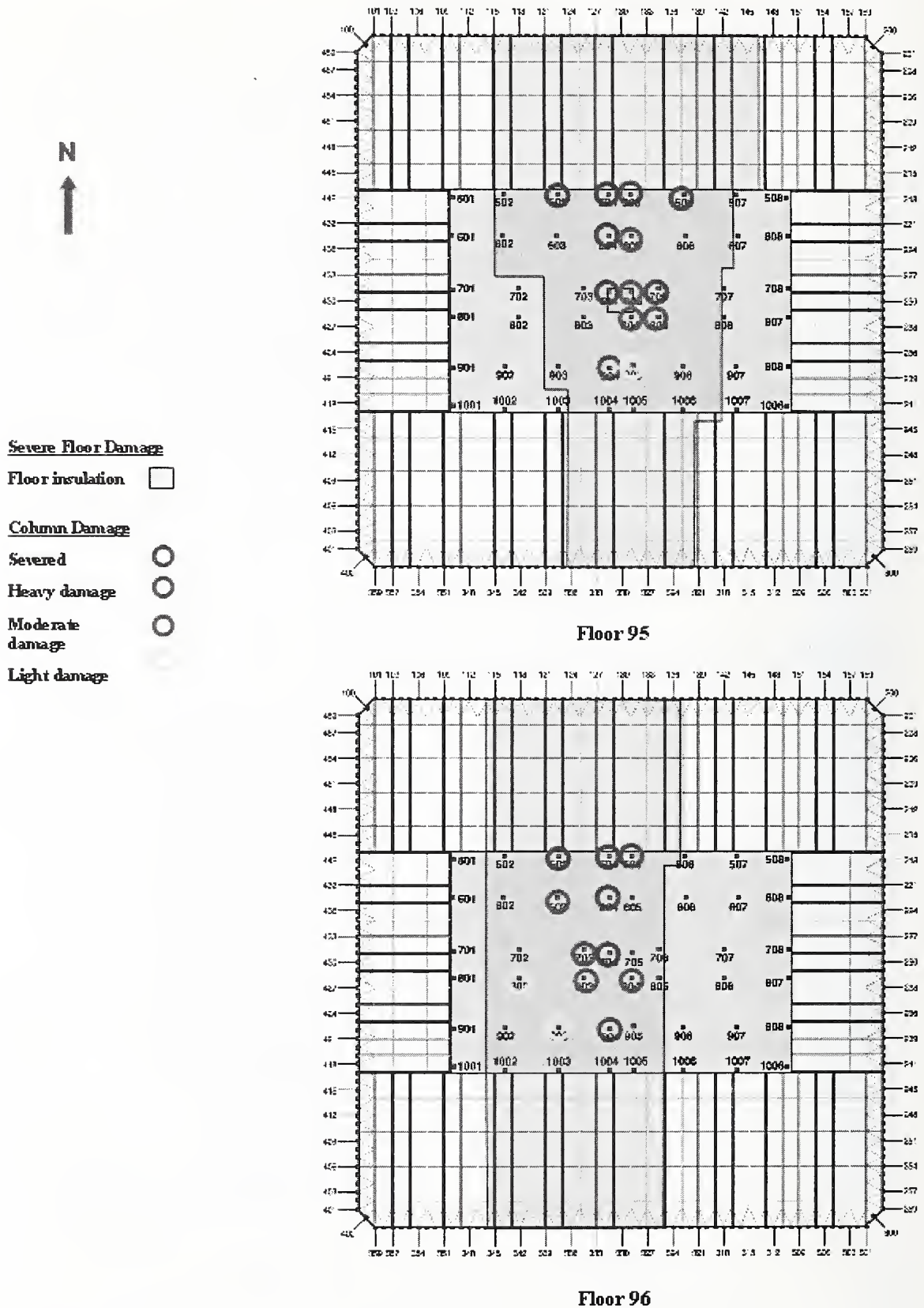


Figure B-8. WTC 1 Case B aircraft impact damage to Occupancy Floors 95 and 96.

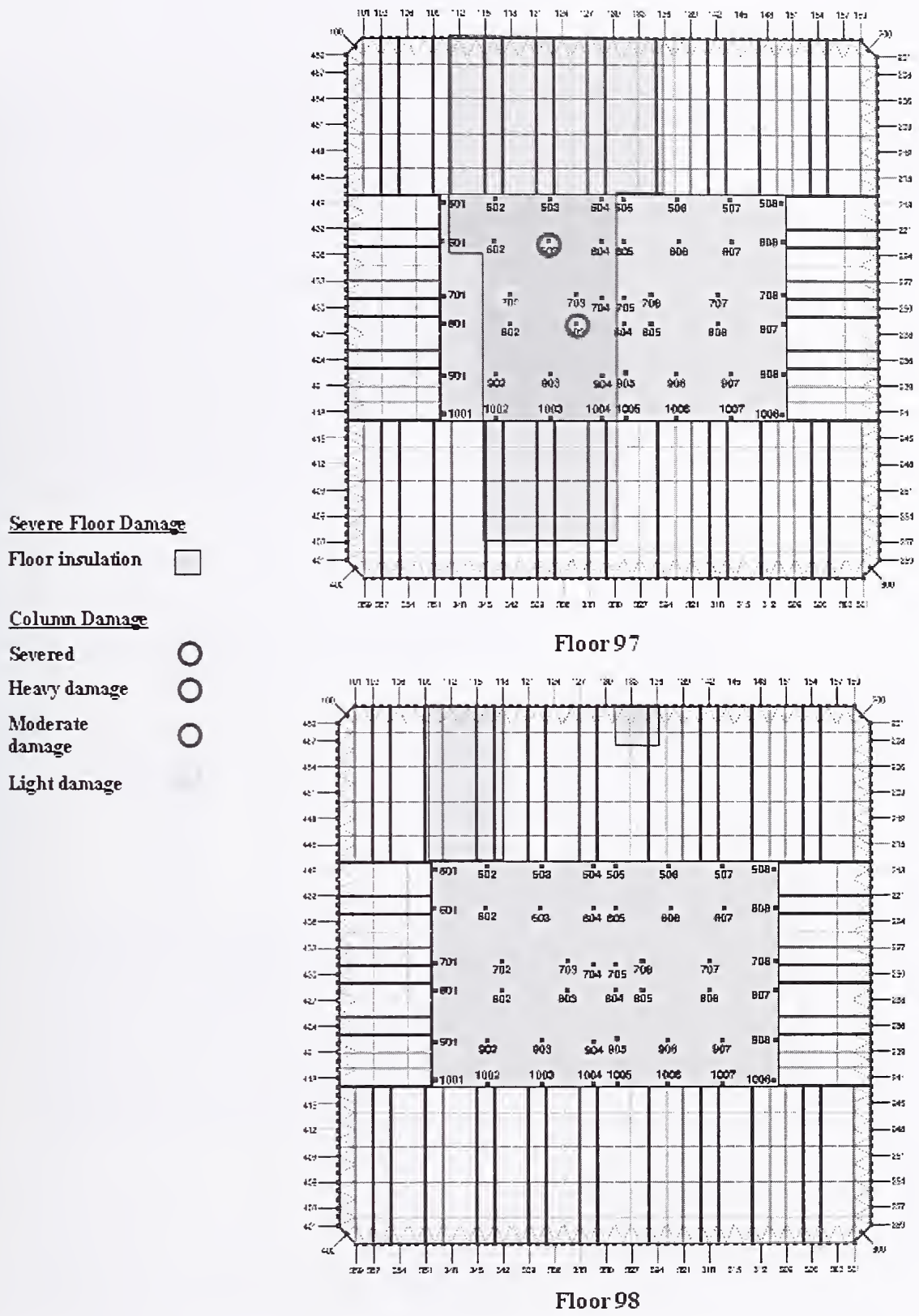


Figure B-9. WTC 1 Case B aircraft impact damage to Occupancy Floors 97 and 98.

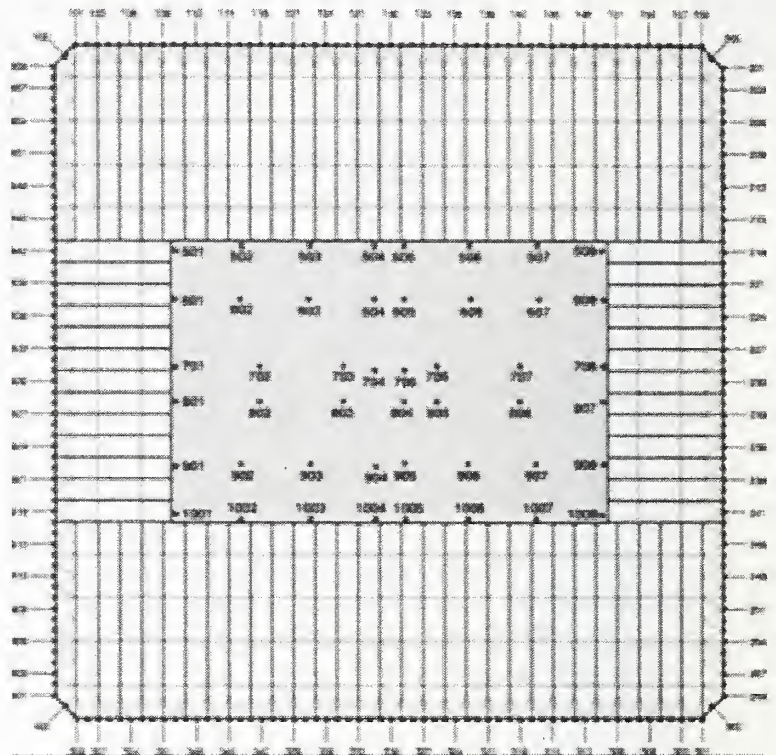
## WTC 1 CASE B - STRUCTURAL FLOOR GRAPHICS

Severe Floor Damage

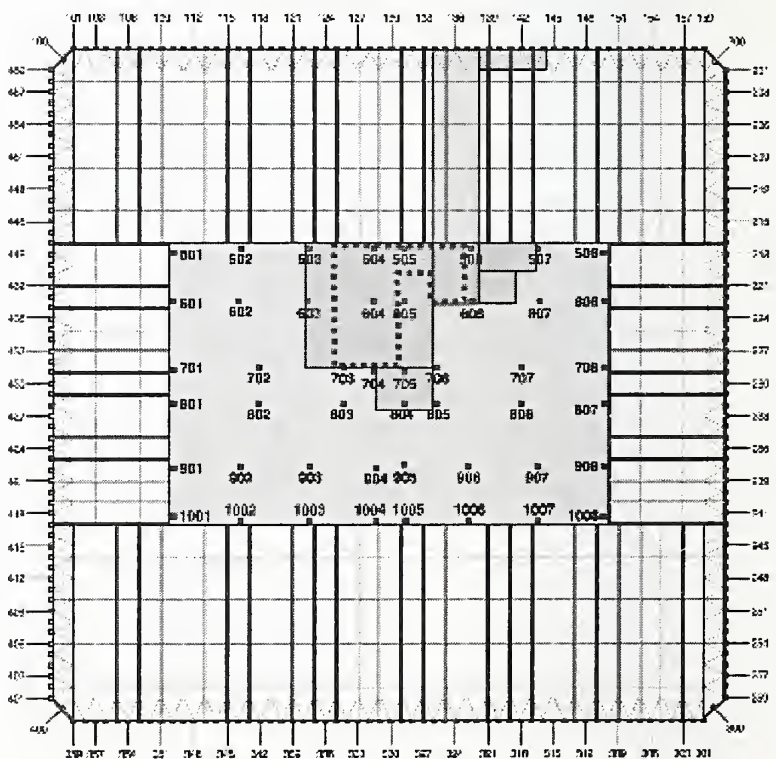
Floor system structural damage



Floor system removed



Floor 93



Floor 94

Figure B-10. WTC 1 Case B aircraft impact damage to Structural Floors 93 and 94.

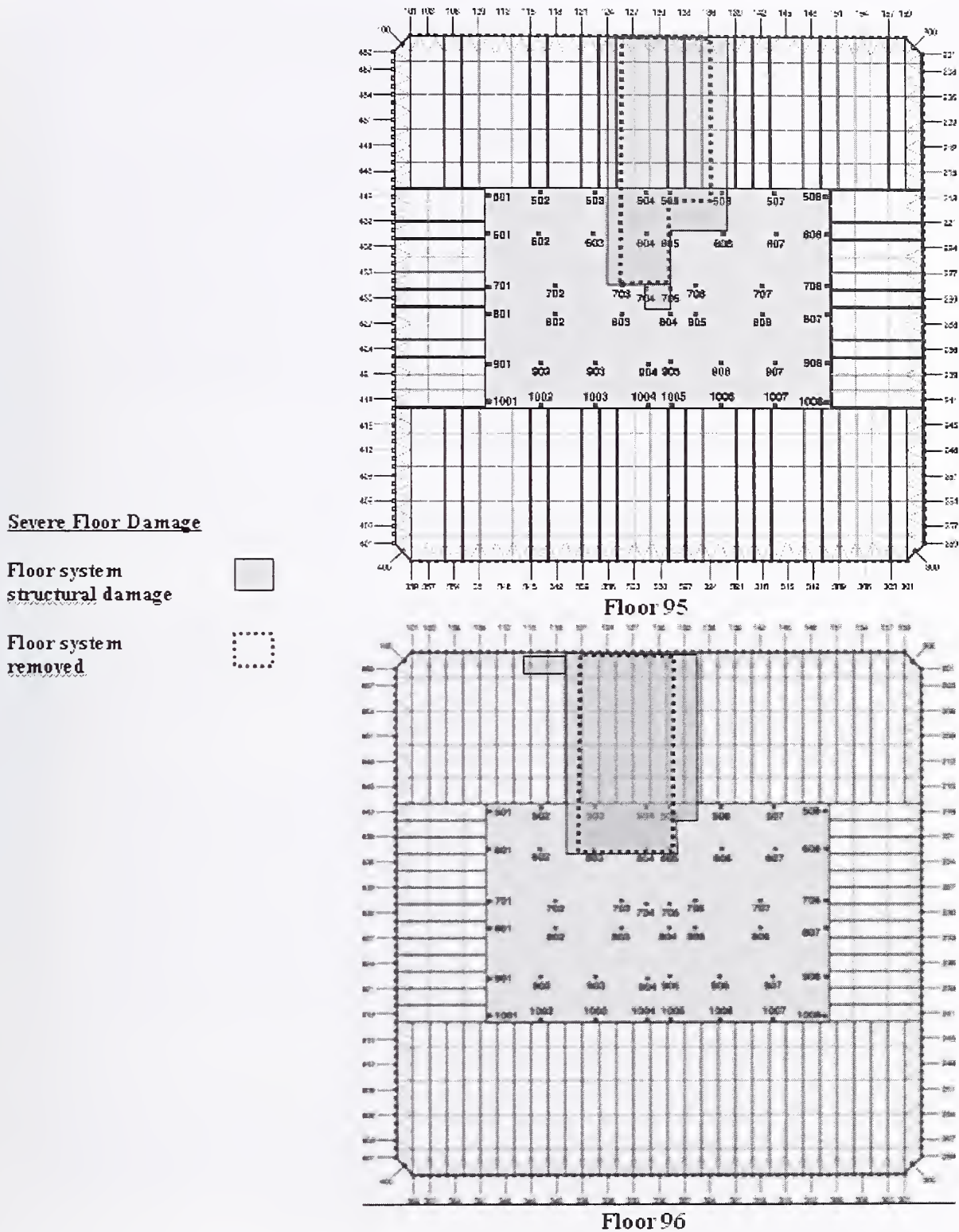


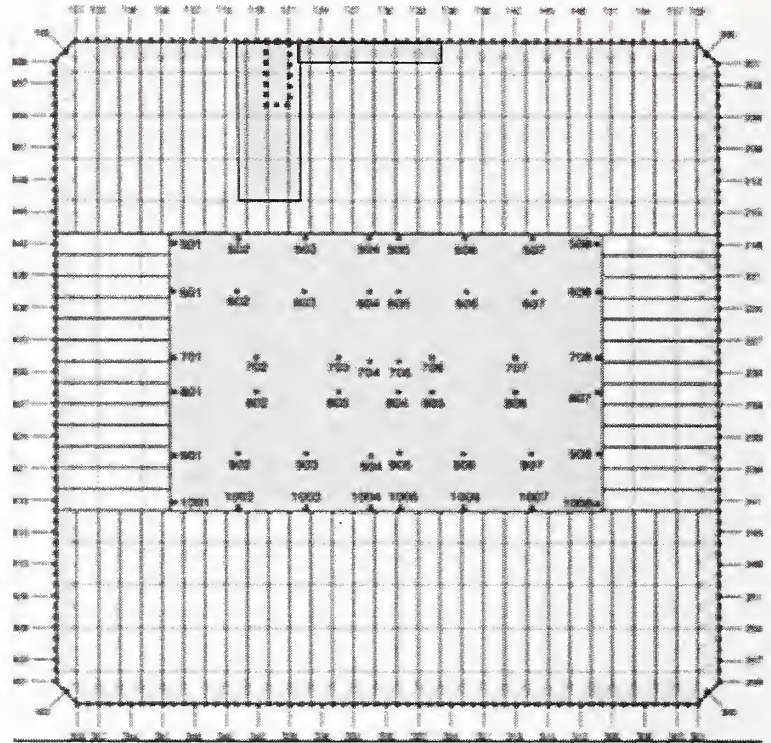
Figure B-11. WTC 1 Case B aircraft impact damage to Structural Floors 95 and 96.

**Severe Floor Damage**

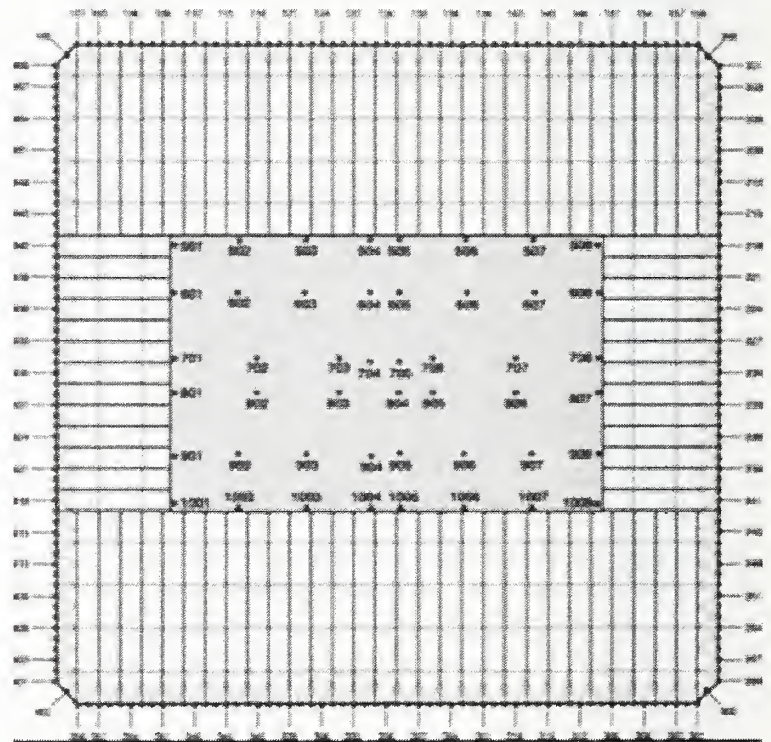
**Floor system structural damage**



**Floor system removed**



**Floor 97**



**Floor 98**

**Figure B-12. WTC 1 Case B aircraft impact damage to Structural Floors 97 and 98.**

WTC 2 CASE C – OCCUPANCY FLOOR GRAPHICS

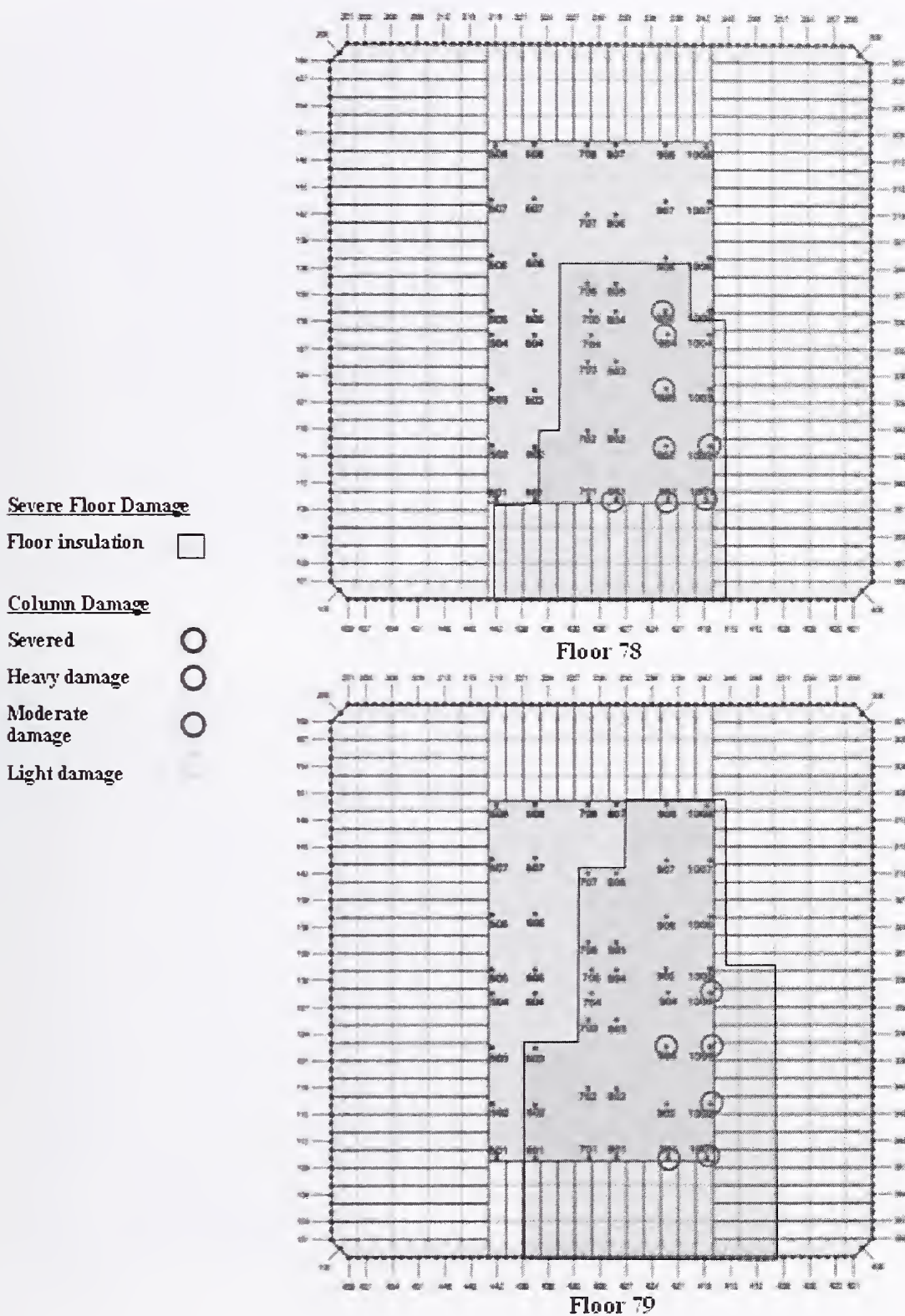


Figure B-13. WTC 2 Case C aircraft impact damage to Occupancy Floors 78 and 79.

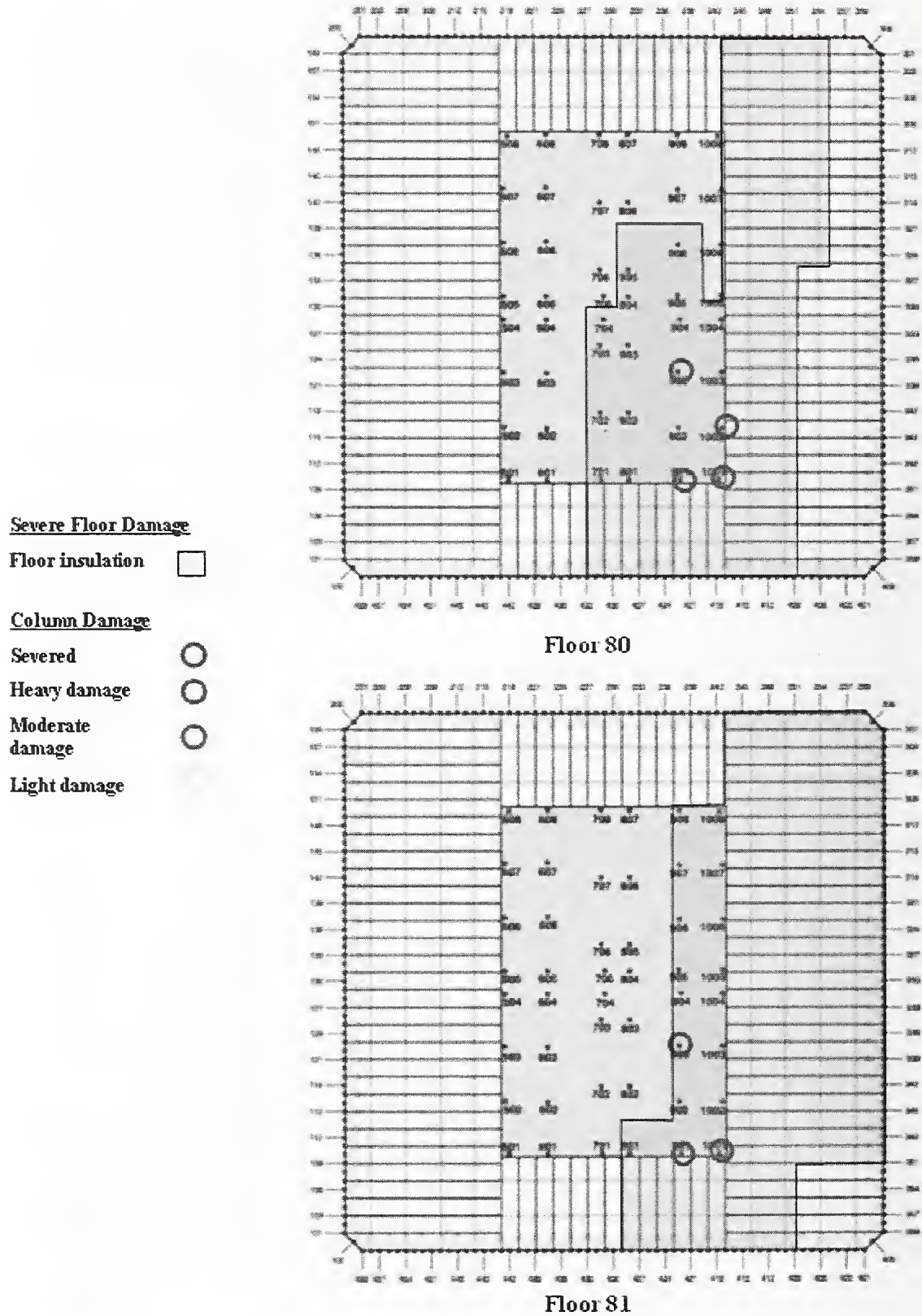


Figure B-14. WTC 2 Case C aircraft impact damage to Occupancy Floors 80 and 81.

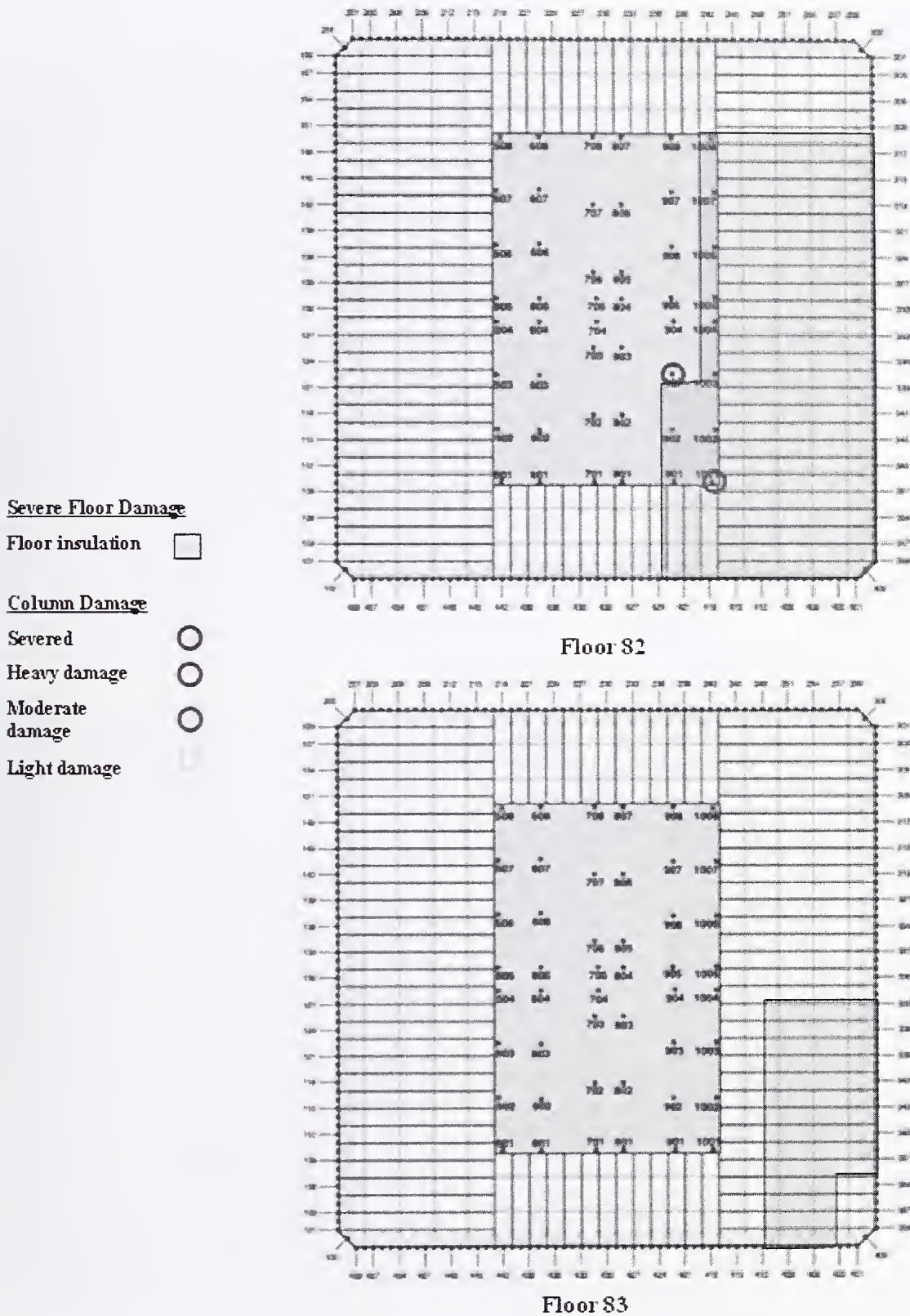


Figure B-15. WTC 2 Case C aircraft impact damage to Occupancy Floors 82 and 83.

## WTC 2 CASE C – STRUCTURAL FLOOR GRAPHICS

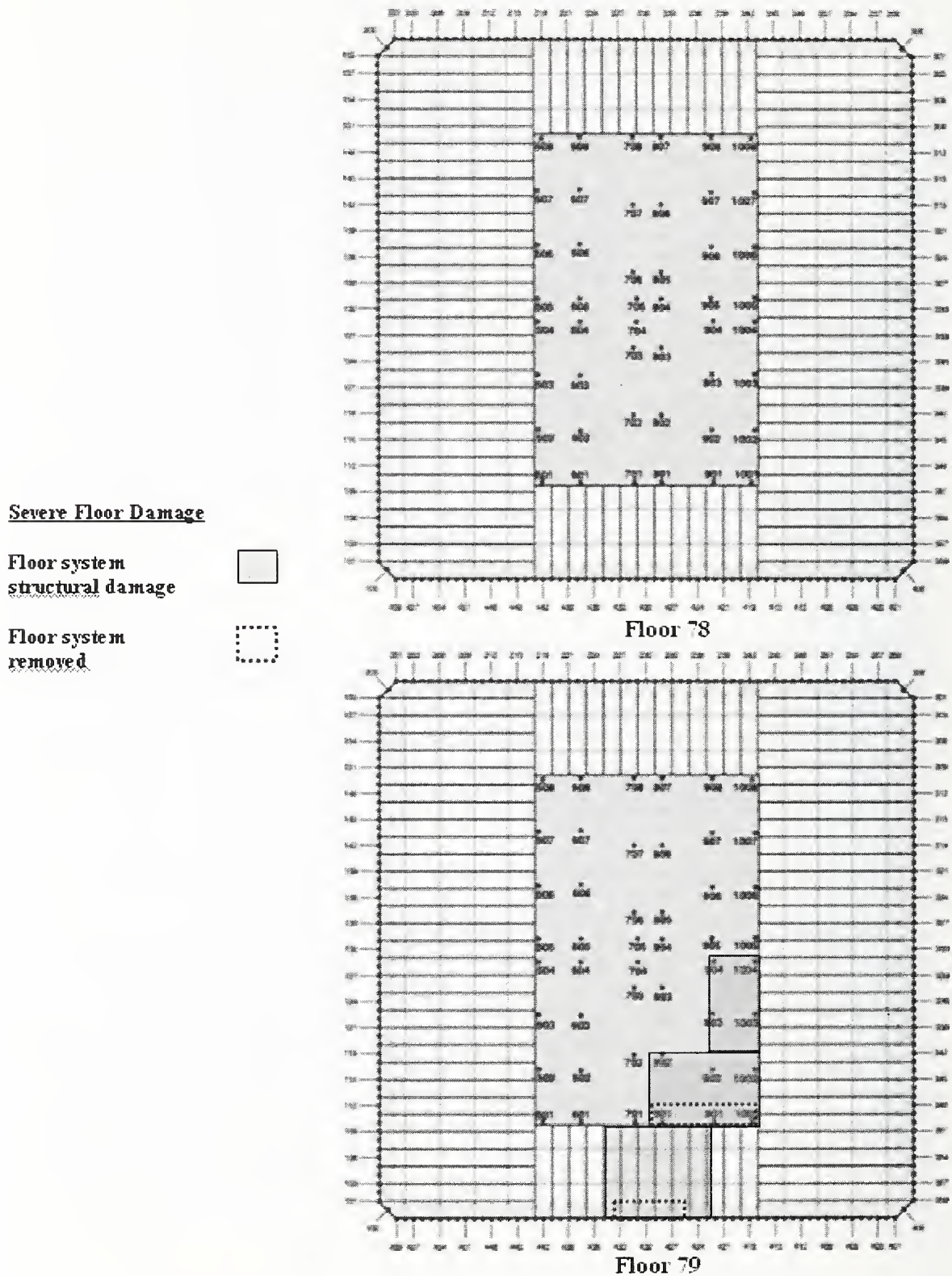


Figure B-16. WTC 2 Case C aircraft impact damage to Structural Floors 78 and 79.

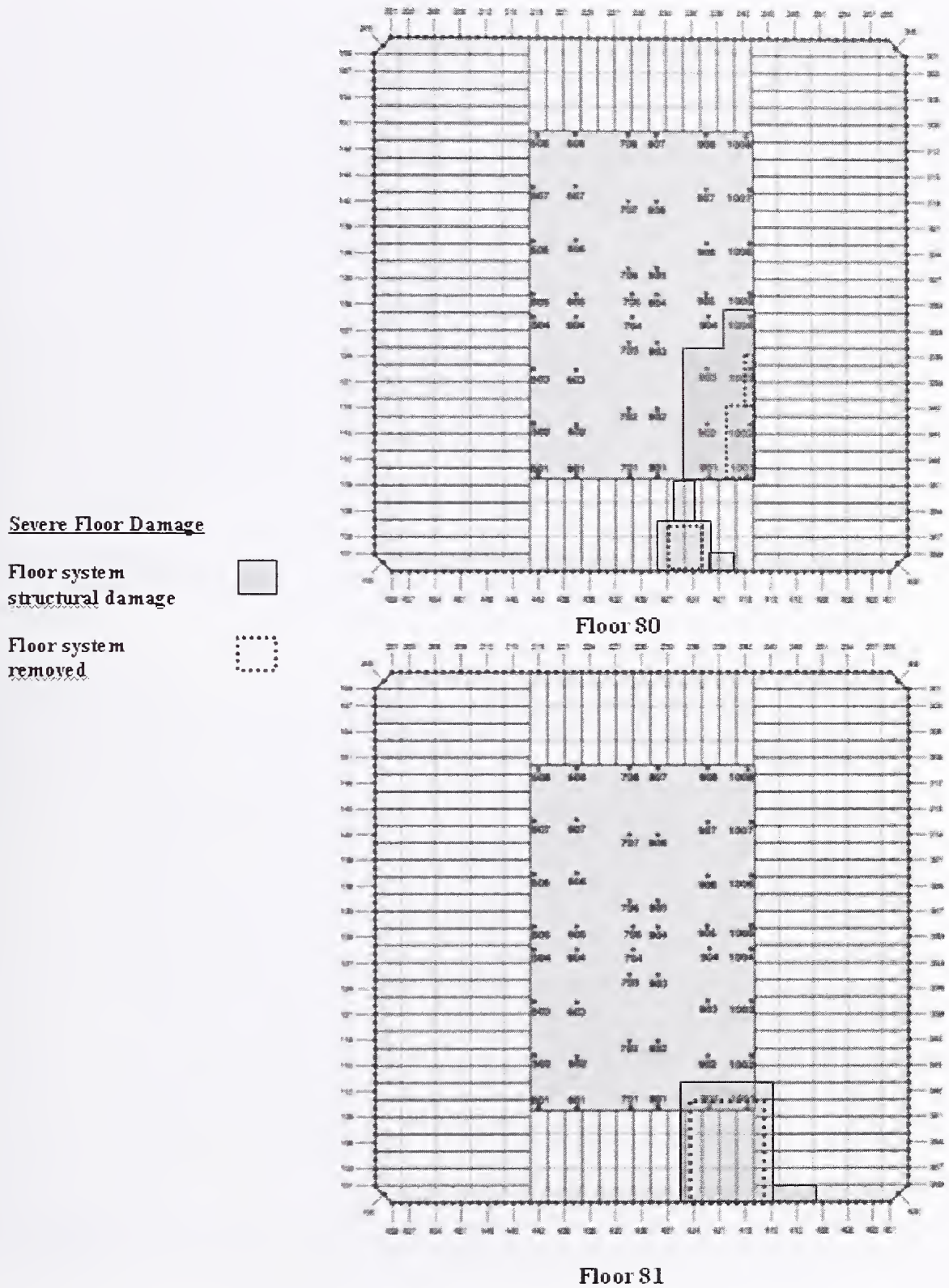
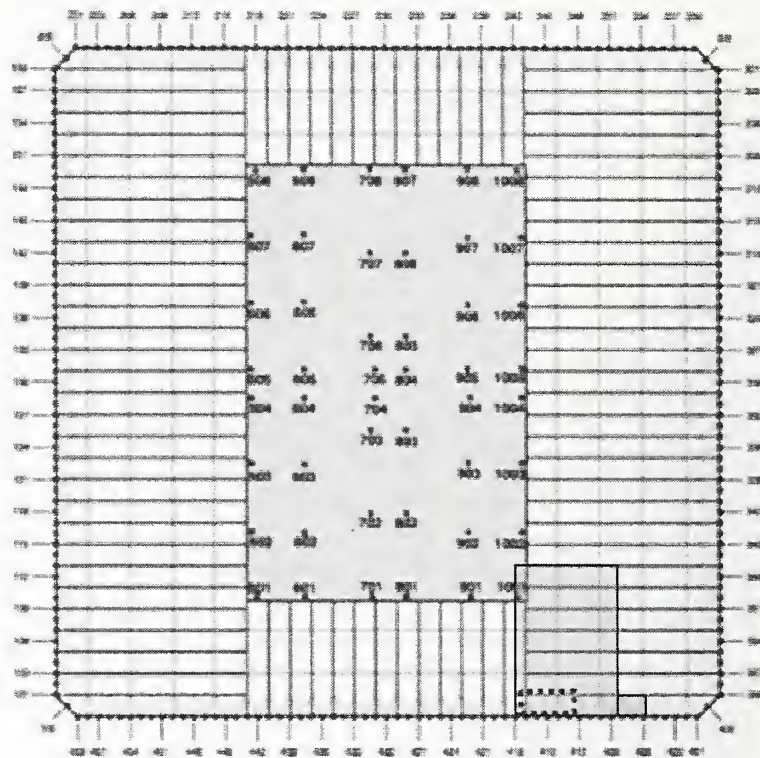


Figure B-17. WTC 2 Case C aircraft impact damage to Structural Floors 80 and 81.

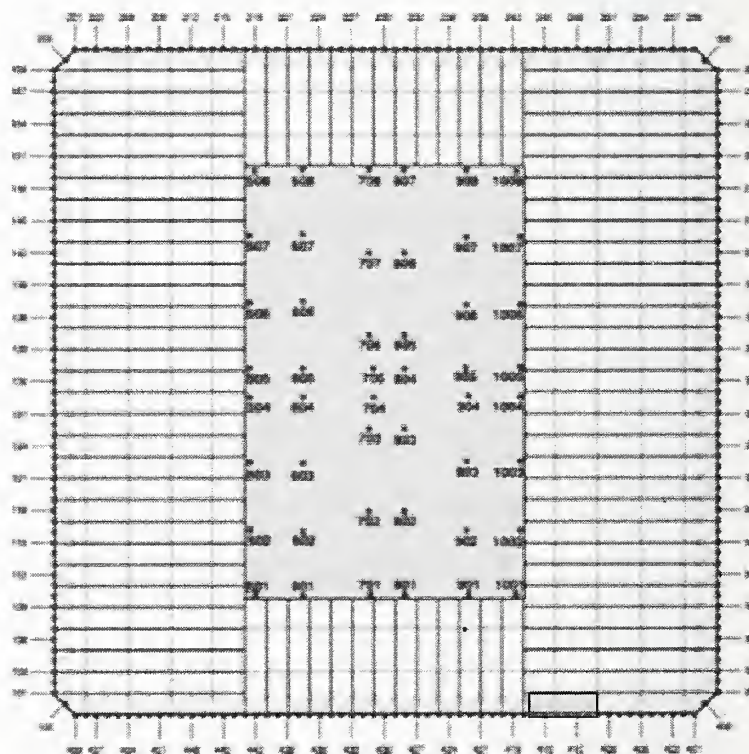
**Severe Floor Damage**

**Floor system structural damage**

**Floor system removed**



**Floor 82**



**Floor 83**

**Figure B-18. WTC 2 Case C aircraft impact damage to Structural Floors 82 and 83.**

### WTC 2 CASE D – OCCUPANCY FLOOR GRAPHICS

Severe Floor Damage

Floor insulation

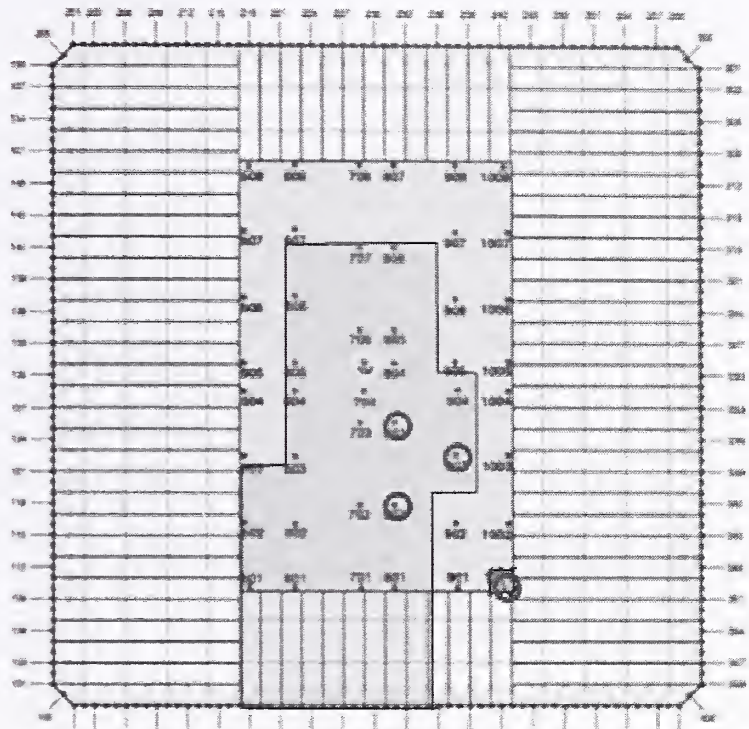
Column Damage

Severed

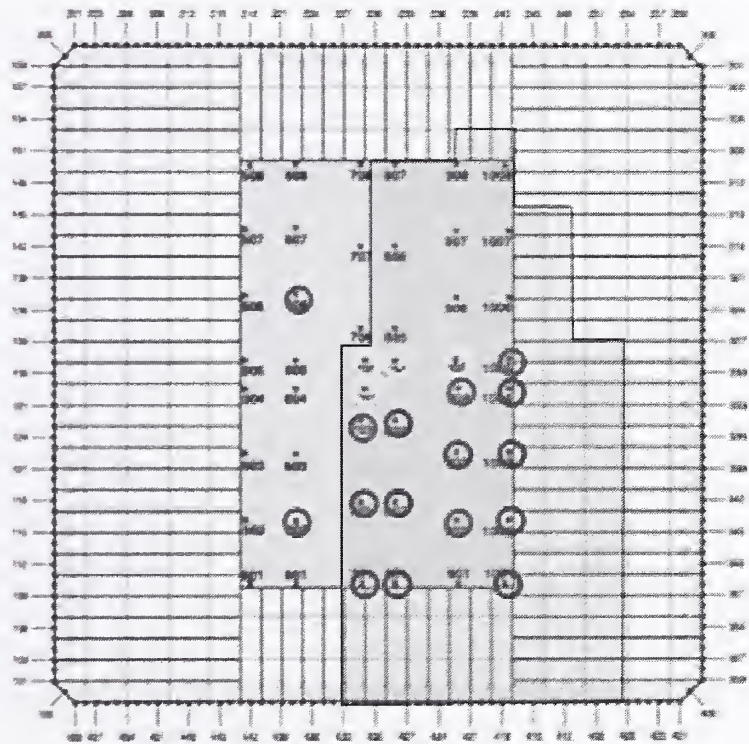
Heavy damage

Moderate damage

Light damage



Floor 78



Floor 79

Figure B-19. WTC 2 Case D aircraft impact damage to Occupancy Floors 78 and 79.

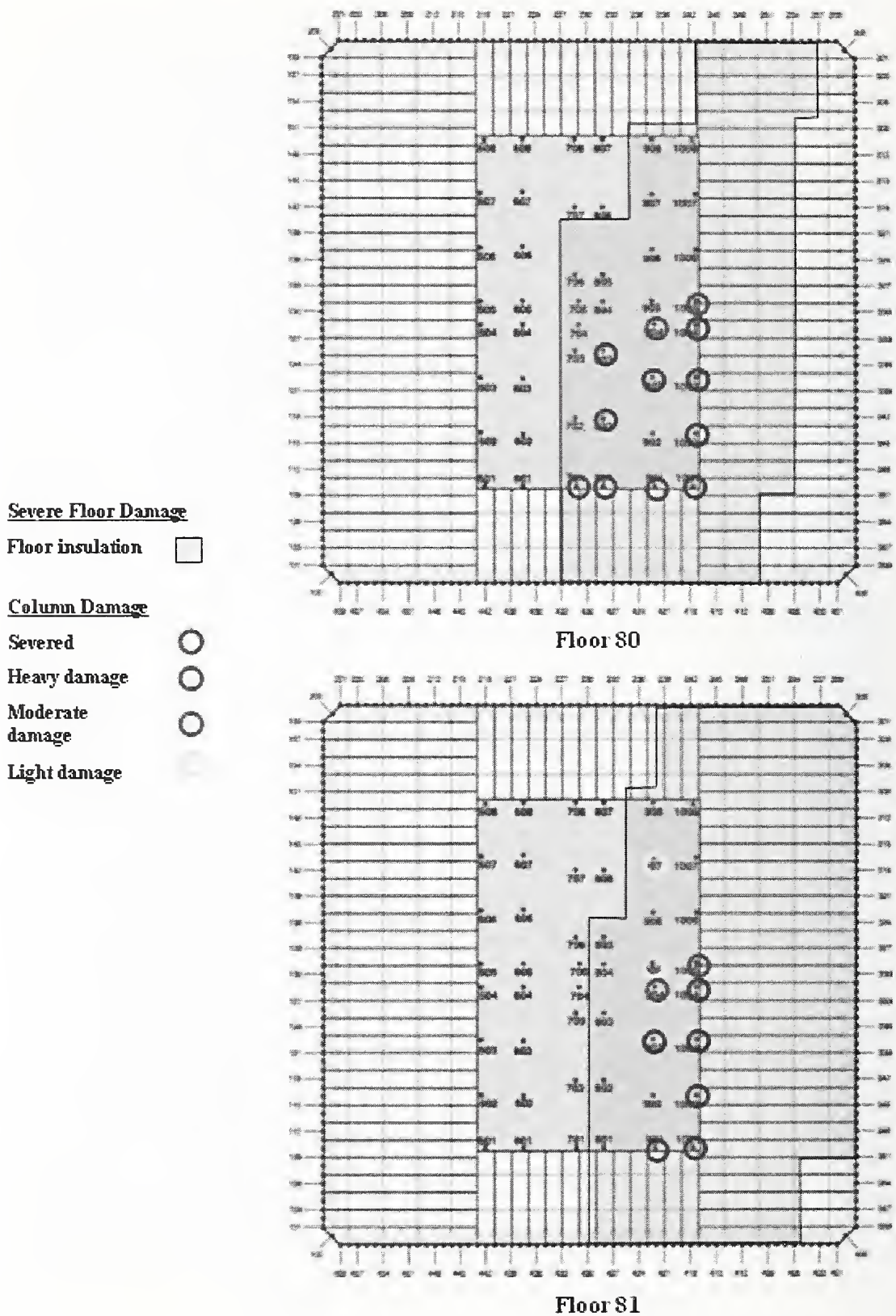


Figure B-20. WTC 2 Case D aircraft impact damage to Occupancy Floors 80 and 81.

Severe Floor Damage

Floor insulation

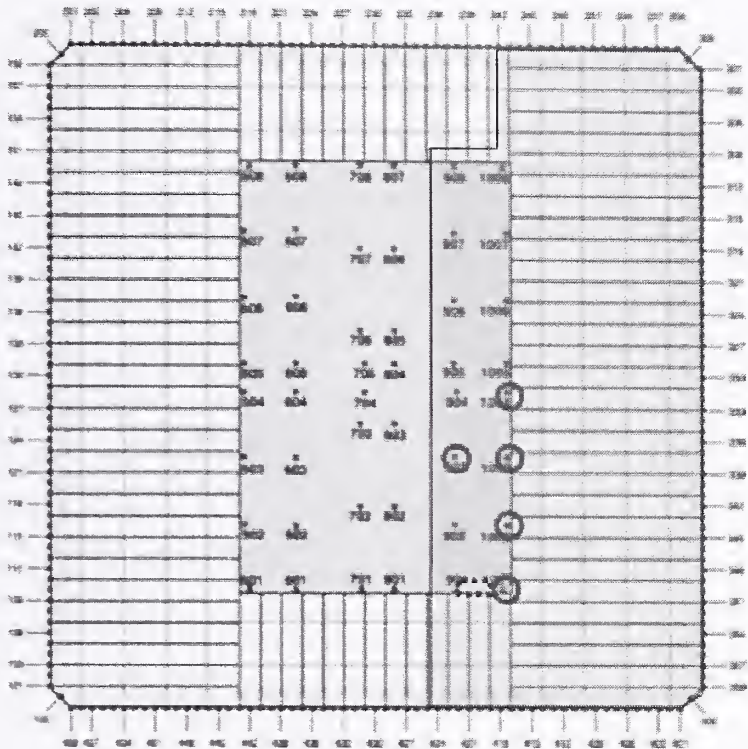
Column Damage

Severed

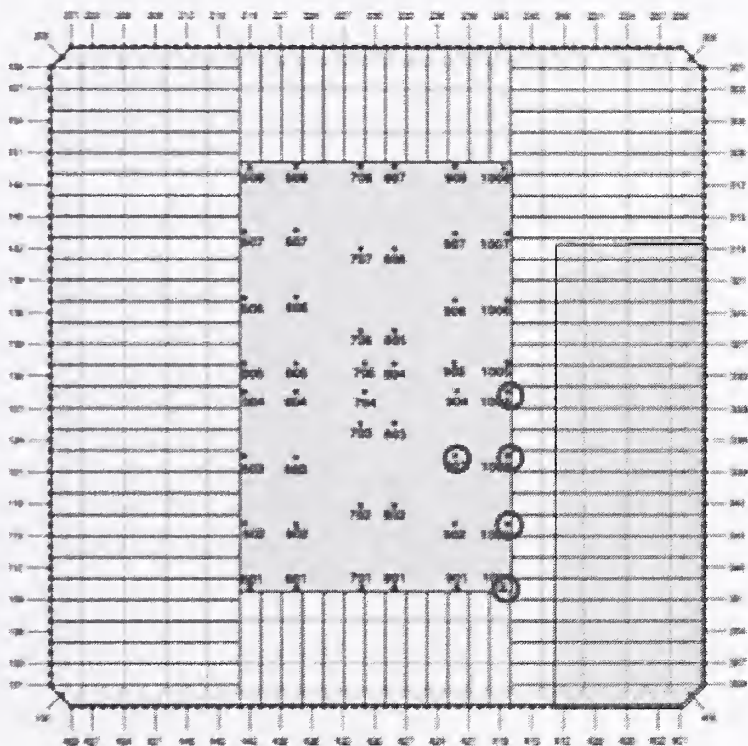
Heavy damage

Moderate damage

Light damage



Floor 82



Floor 83

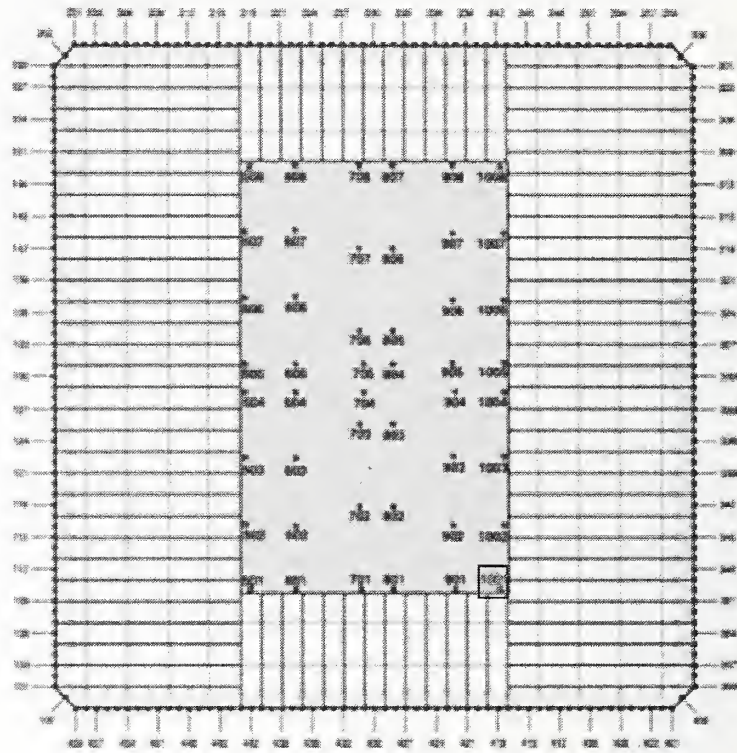
Figure B-21. WTC 2 Case D aircraft impact damage to Occupancy Floors 82 and 83.

### WTC 2 CASE D – STRUCTURAL FLOOR GRAPHICS

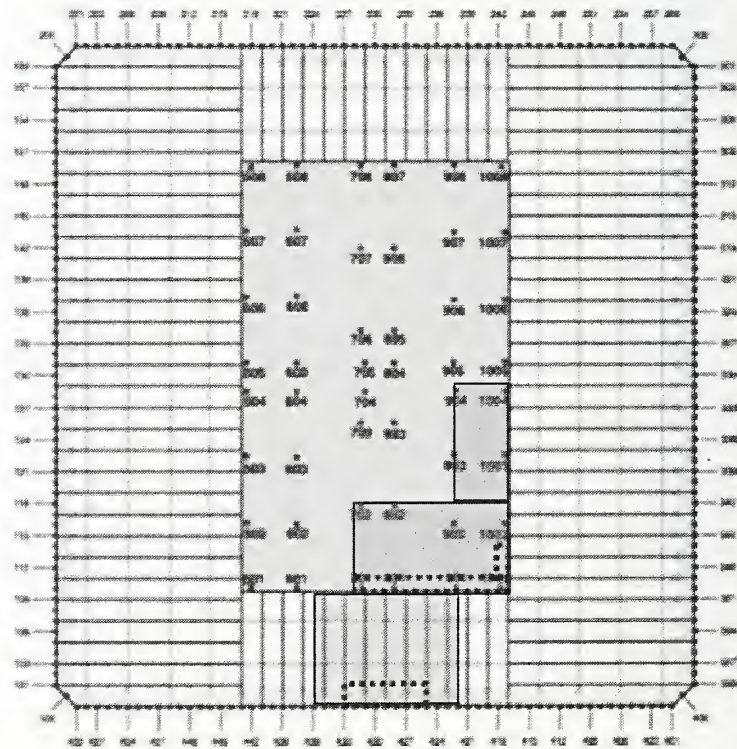
**Severe Floor Damage**

**Floor system structural damage**

**Floor system removed**



**Floor 78**



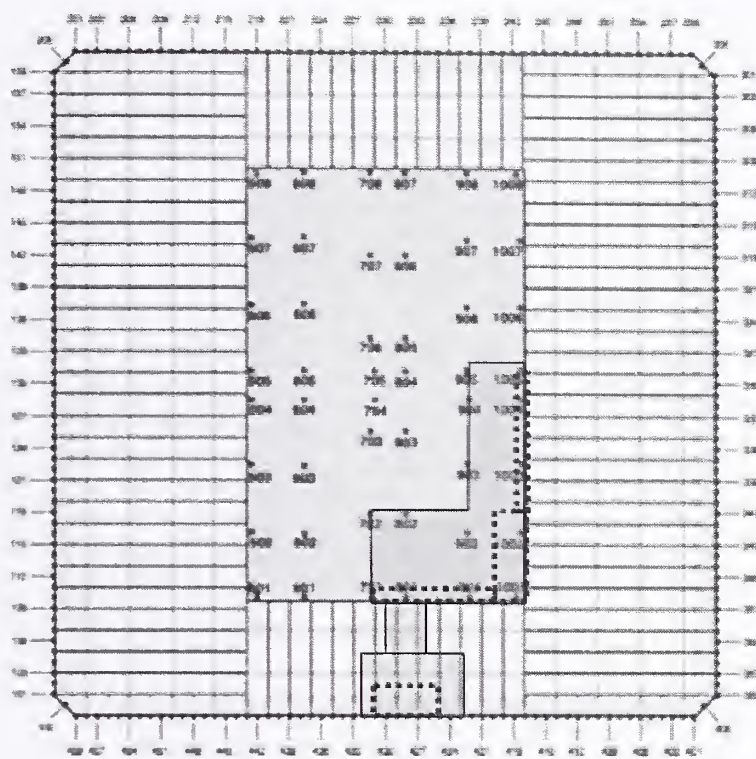
**Floor 79**

**Figure B–22. WTC 2 Case D aircraft impact damage to Structural Floors 78 and 79.**

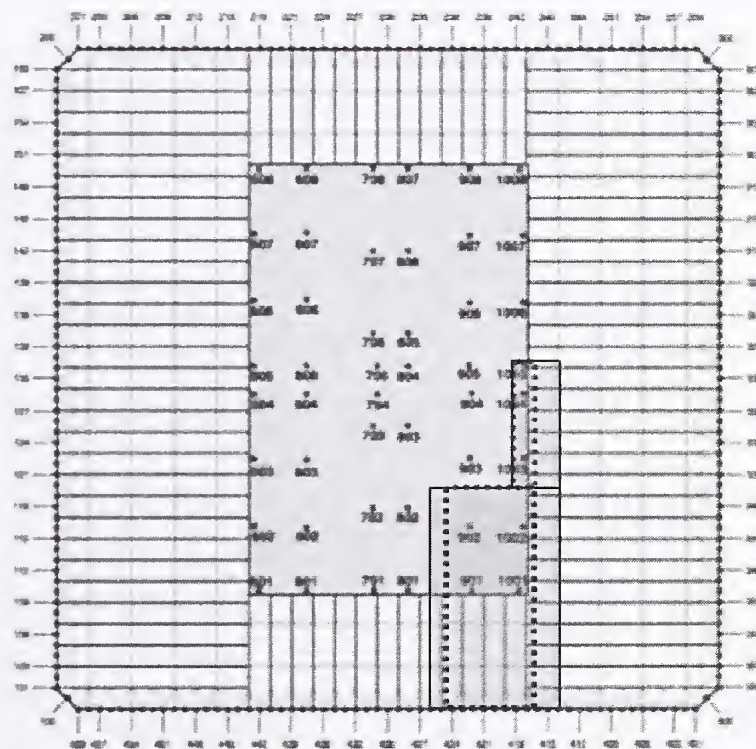
**Severe Floor Damage**

**Floor system structural damage**

**Floor system removed**



**Floor 80**



**Floor 81**

**Figure B-23. WTC 2 Case D aircraft impact damage to Structural Floors 80 and 81.**

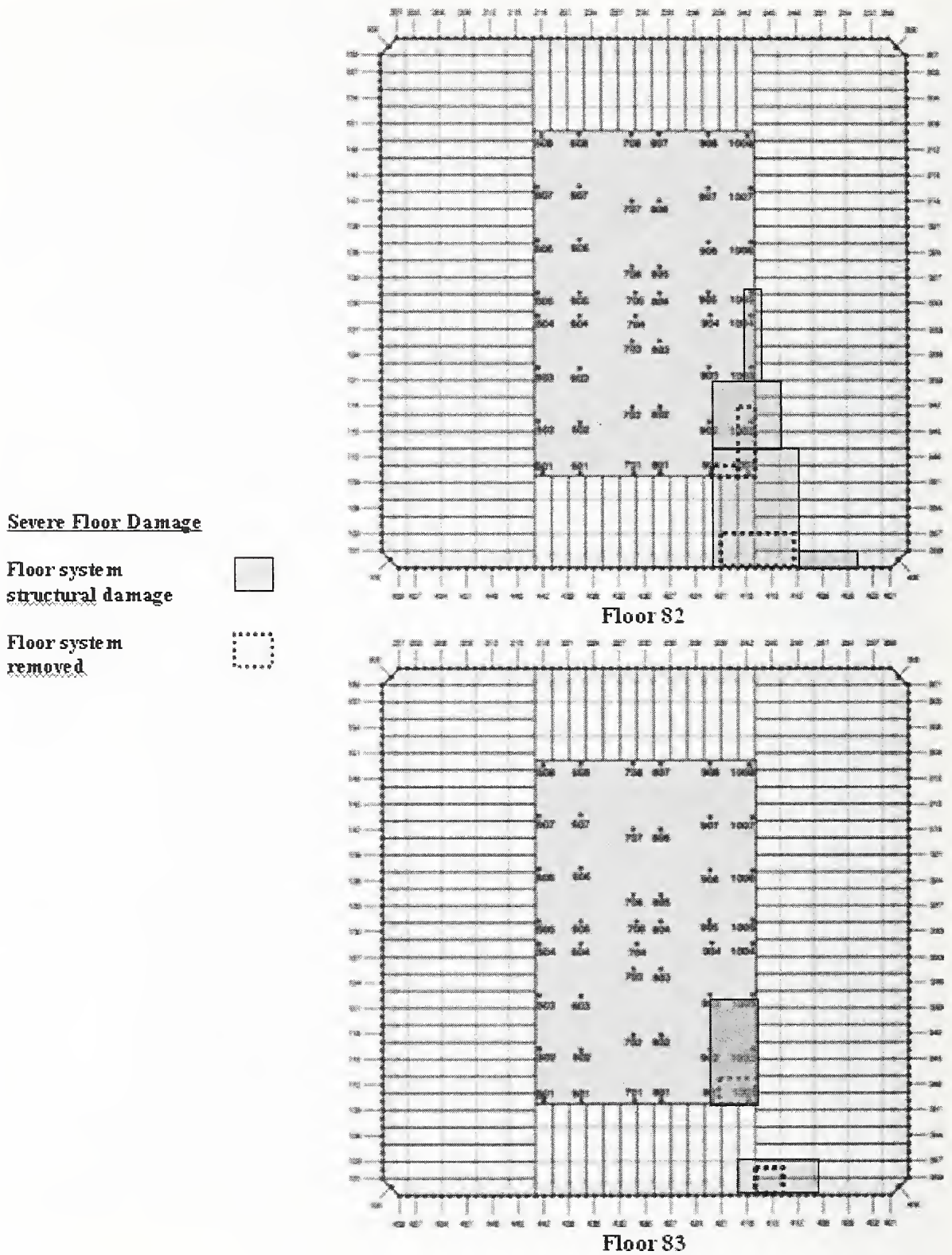


Figure B-24. WTC 2 Case D aircraft impact damage to Structural Floors 82 and 83.



